DETERMINING THE ROLE OF ENDOTHELIAL PROGENITOR CELLS IN POST-NATAL NEOVASCULARIZATION

A Dissertation
Presented to
The Academic Faculty

by

Scott T. Robinson

In Partial Fulfillment
of the Requirements for the Degree
Doctor in Philosophy in the
Wallace H. Coulter Department of Biomedical Engineering

Georgia Institute of Technology
December 2010

DETERMINING THE ROLE OF ENDOTHELIAL PROGENITOR CELLS IN POST-NATAL NEOVASCULARIZATION

Approved by:

Dr. W. Robert Taylor, M.D., Ph.D.,
Advisor
School of Medicine
Emory University

Dr. Robert M. Nerem, PhD
School of Biomedical Engineering
Emory University

Dr. T.J. Murphy, PhD
School of Medicine
Georgia Institute of Technology

Dr. David R. Archer, Ph.D.
School of Medicine
Emory University

Dr. Barbara D. Boyan, Ph.D.
School of Biomedical Engineering
Georgia Institute of Technology

Date Approved: May 17, 2010

ACKNOWLEDGEMENTS

Giving proper due to all those who have contributed to my thesis work, as well as my professional and personal development during my time in graduate school, would double the length of this document. As those who were involved with this project are well aware, the challenges that had to be overcome for completion of this thesis were formidable.

Were it not for my fantastically supportive advisor and thesis committee, I probably would not have reached the finish. The advice I have received from all of my committee members, both scientifically and otherwise, has been invaluable, and for this I cannot thank them enough.

I would like to first thank my advisor, Bob Taylor, for all of the support he has given me during my tenure in his lab. I truly could not have asked for a better mentor. Throughout the seven year ordeal that has been my thesis project, Bob has offered his unwavering support and continually shown confidence in me, even when my self confidence was lacking. In addition to the endless advice, both personal and professional, that he has provided in our "therapy sessions", Bob's ability to balance a successful career in academia with an even more successful family life is something I truly aspire to obtain. Bob has been a phenomenal boss, mentor, and friend, whose daily interactions with I will miss greatly.

In addition to Bob's mentorship, I have received an enormous amount of support from my thesis committee. Dr. Barbara Boyan has consistently been the voice of reason in our committee meetings. Two years ago she first suggested that I should "hurry up and

graduate", and has pushed me to do so ever since. Dr. TJ Murphy converted me from a mechanical engineer to a molecular biologist during my first summer in Atlanta. In the year I spent working in TJ's lab constructing retroviruses, I developed a vast skill set that was the basis for all of the work I have done since. Dr. David Archer has been a continual source of support throughout graduate school. Not only has his scientific advice been invaluable, but at one point he even started performing mouse surgeries for me in an attempt to jump-start my project. Although I don't have any data indicating the frequency with which graduate students outsource their experiments to faculty members, I suspect this occurrence is a rarity. For Dr. Archer's generosity, I am sincerely grateful. Dr. Bob Nerem has provided me with a number of opportunities while at Georgia Tech, the most memorable of which was a three month collaborative stint at REMEDI in Galway, Ireland. I am extremely appreciative of Dr. Nerem's support, which was unwavering even when I presented him with a $1500 bill for a damaged rental car.

During the course of my thesis there were numerous occasions where the science had to deteriorated to a point that I no longer wanted to continue the work. Despite those all-to-frequent occasions, I was ALWAYS eager to come to lab. This was largely due to the fantastic members of the Taylor lab, who were continuous pillars of support and made life enjoyable even when science wasn't. Daiana Weiss was a teacher and helper for all things animal. From a personal standpoint, Daiana also played a significant role in finalizing my marriage, by helping translate a letter to my wife's family asking for permission to wed their daughter. Diane Sutcliff kept me company whenever I was on the second floor, and permitted the unburdening of many problems by lending an ear for endless gripe sessions. Giji Joesph has been my buddy in room 326 for nearly five years.

Not only was she instrumental in everything histology-related that I ever did, but our time together and many conversations about family and friends has forged a bond of friendship that won't soon be forgotten. Natalia Landazuri was an extraordinary mentor to me during her time in the lab. Her knowledge and experience were instrumental to this project and my development as a scientist. There have also been several incidences where Natalia could have justifiably killed me, but because of her patience and kindness she did not. I legitimately owe her my life. Ebony Washington has been my colleague and friend at the bench next door for most of my time in the Taylor lab. Together we have suffered through the insufferable psychosis of scientific research, and her friendship has made the journey enjoyable. Although she probably doesn't think so, she will graduate soon. Sarah Knight, a more recent addition to the lab, definitely added a touch of class to room 326 as only a Brit can do. Sarah also has been kind enough to provide her husband, Paul Marvar, for numerous biking trips. Cristina Flores worked with me for one summer as part of an undergraduate research project. During her time in the lab she became a proficient cloning machine, and her efforts isolating several promoters was invaluable to this thesis.

There are also several past members of the Taylor lab whose contributions should be acknowledged. Matt Whalin was an MD/PhD student who served as a resource to everyone in the lab… for just about everything. He was a walking copy of the unabridged "Protocols in Molecular Biology". Nick Willet, or "Young Nicholas", as he is sometimes known, began life in the lab as my mentee, but quickly assumed the role as my mentor. Despite my best efforts, Young Nicholas blossomed into an outstanding scientist, whose productivity is truly remarkable given his incredibly laid back approach. Katie Rafferty and I started graduate school together, both joining the Taylor lab at the same time. I had

the pleasure of occupying the bench space directly across from Katie for 4 years. The friendship that developed and our combined ingenuity permitted what was easily my proudest achievement in graduate school: the founding of the Disciples of Cheesus. Craig Duvall also deserves some acknowledgement. The good Dr. Duvall, perhaps more than anyone, contributed to my delinquency during graduate school. During his time in and after Atlanta, Craig and I spent many hours biking, at the Chophouse, Peachtree Tavern, and Waffle House, and discussing science. Now that Craig has successfully established his own lab, I suspect that he may one day be my employer.

Several more recent additions to the Taylor lab have also served as a source of entertainment and distraction during my time in Cardiology, and leave me confident that the fun will continue in my absence. Ian Campbell provides a continuum of witty banter, beer brewing knowledge, and amusing T-shirts. Brian Clark also joined the lab a few years ago, and his prowess in the lab is only surpassed by his prowess on the baseball diamond. Although Rachel Ransom has since moved on to start medical school, she deserves special recognition as the only person to carefully read my thesis from start to finish (myself included). Rachel was an invaluable editor, and I wish her the best of luck toward a successful career in medicine. I personally recruited Rebecca Levit to join the Taylor lab and take over my thesis work. She then saved both of us years of frustration and discontinued my project. Despite the limited amount of time when our tenures overlapped, Rebecca has proven her value as the Southeast's leading expert on Australian water fowl. In addition to those mentioned above, there are a number of other graduate students, post-doctoral students and cardiology fellows who have passed through the Taylor Lab during my time there; Roberto Hodara, Alicia Lyle, Juan Valasquez, Divya

Gupta, Michelle Consolini, Greg Booth, Elethia Woolfolk, Aaran Fan, Patrick Cowhan, Dardo Ferrara, Tony Nelson and many others.

When I first began work on this project, I learned many basic molecular biology techniques in Dr. TJ Murphy's lab. Chad Kitchen, in particular, showed extraordinary patients while teaching a lug like me to pipette. I also want to thank the good people of REMEDI for accommodating me while participating in an international research collaboration with NUI Galway in Galway, Ireland for three months. Institute directors Frank Barry and Tim O'Brien, as well as Thomas Ritter, Udo Greiser, and, of course, Garry Duffy, all saw to it that I had a unique and memorable experience while in Ireland.

As a student in the BME program, I was fortunate to learn from and collaborate with the extraordinary faculty within our department at Georgia Tech and Emory Universities. On numerous occasions throughout graduate school I was also provided assistance by the incredible BME support staff, including Sally Garrish, Beth Bullock, Sandra Wilson, and Steve Marzec. An apology is also due to Shannon Sullivan, for my inability to complete paperwork on time. The directors and staff of the MD/PhD program have also provided invaluable support throughout graduate school. The faculty and staff of the Cardiology Division should also be acknowledged for their assistance throughout my time in the Taylor lab. The collegial environment on the third floor of WMB will be missed greatly.

In addition to the aforementioned intellectual influences, there are a number of other individuals, in both the BME community and Atlanta in general, who provided much needed social relief from the academic rigors of PhD training. To preserve space

and protect the innocent, I will simply thank the many friends in Atlanta who made the extracurricular moments of graduate school so enjoyable.

I would also like to thank my family for their unwavering support over the past few years. My parents, Peter and Debbie Robinson, brothers James and Geoff, grandparents Bob and Mitzi Robinson and Gran and Gordo Thomas, and my Serbian family Steva, Irene and their children Alexander and Katarina, offered their unlimited encouragement over the past seven years, despite the fact that I'm fairly certain they had no idea what I was doing.

Lastly, I would like to thank my wife, Adina, and our one and a half dogs, Albi and Maple. Adina has been a continuous source of emotional support during my time in graduate school, all while launching a successful academic career of her own. Her ability to put up with me, especially over the last several months, is remarkable. She is the ideal wife, partner, and colleague.

TABLE OF CONTENTS

	Page
ACKNOWLEDGEMENTS	iii
LIST OF TABLES	xiv
LIST OF FIGURES	xv
LIST OF ABBREVIATIONS	xvii
SUMMARY	xxi
CHAPTER 1: SPECIFIC AIMS	1
Introduction	1
Aim 1	3
Aim 2	3
Aim 3	4
Innovation and Signficance	4
CHAPTER 2: BACKGROUND AND LITERATURE REVIEW	6
Endothelial Progenitor Cells	6
Initial Discovery and Role in Blood Vessel Growth	8
Culturing of EPCs	11
Circulating EPCs	15
Evidence Against a Bone Marrow-Derived Endothelial Cell	17
Pro-Angiogenic Monocytes	19
Clinical EPC Studies	24
Apoptosis and Bax	27
Genetic Ablation Studies	31

Background Summary 33

CHAPTER 3: TWO MOUSE MODELS FOR ENDOTHELIAL PROGENITOR CELL DEPLETION 35

Introduction 35

Methods 38

Animals 38

Generation of Retroviral Plasmids 38

Generation of Transgenic IED Mice 40

Retroviral Production 40

Bone Marrow Isolation and Transduction 41

Cell Lines and Culture 42

Retroviral Titration 42

qRT-PCR 43

TUNEL Stain 43

Luciferase Assay 44

Chemiluminescence Imaging 44

Results 45

A Retroviral Bone Marrow Transduction Approach For Eliminating EPCs 45

Feasibility of a Bone Marrow Transduction Strategy 46

An *In Vitro* System for Assessment of Retroviral Function 50

Attempted *In Vitro* Validation of RED/REF 51

Retroviral Integration 53

A Transgenic Bone Marrow Transplantation Approach to Eliminating EPCs 56

Functional Assessment of CrIED Transgene *Ex Vivo* 58

Luciferase Activity *In Vivo* 60

Induction of Cre Activity and Absence of Apoptotic Cell Death 64

Discussion 65

CHAPTER 4: DELETION OF THE BH3 DOMAIN INHIBITS APOPTOTIC ACTIVITY OF BAX 72

Introduction 72

Methods 74

Plasmid Construction and Propagation 74

Cell Lines and Culture 75

Transfection 76

Imaging 77

Western Blot 77

qRT-PCR 78

Nuclear Fragmentation 78

Flow Cytometry 79

Annexin V Stain 79

YO-PRO-I Stain 79

MTT Assay 80

Results 80

Generation of ΔN-Bax Constructs 80

Expression of ΔN-Bax Induces Changes in HEK-293 Cell Morphology 81

Frequency and Intensity of EGFP Flourescence in Cells Expressing EGFP:ΔN-Bax 82

Transfection Efficiency Is Unaffected by DNA Concentration 83

EGFP: ΔN-Bax Protein Forms Extra-Nuclear Aggregates 84

Temporal Expression of EGFP:ΔN-Bax 86

EGFP:ΔN-Bax Expression Leads to Changes in Nuclear Morphology 89

Detection of ΔN-Bax In Transfected Cells 90

ΔN-Bax Does Not Induce Apoptosis 92

Discussion 96

CHAPTER 5: A RETROVIRAL-MEDIATED STRATEGY FOR FLOURESCENT LABELING OF BONE MARROW SUBPOPULATIONS 103

Introduction 103

Methods 106

Animals 106

Generation of Retroviral Plasmids 107

Retroviral Production 109

Bone Marrow Isolation and Transduction 109

Bone Marrow Transplants 110

Cell Lines and Culture 110

Flow Cytometry 111

In Vivo Matrigel Plug Assay 111

Histology 112

Results 112

Design of SINrv:tdT constructs 112

Retroviral Promoter Activity in MS1 Cells 114

Enrichment of tdTomato-Positive Cells with FACS 117

Detection of Flourescently Labeled Cells *In Vivo* 117

Retorviral Bone Marrow Transduction Strategy 119

tdTomato Expression Following Bone Marrow Transduction 120

Specificity of Retroviral Promoters *In Vivo* 122

CD14 Expression in Peripheral Blood Following Bone Marrow Transplantation 122

Chracterization of Progenitor Cell Markers on Genetically Labelled Cells 128

Discussion 132

CHAPTER 6: SUMMARY AND FUTURE CONSIDERATIONS 137

Specific Aims I and II 137

ΔN-Bax in Apoptosis 139

Specific Aim III 140

Limitations 142

Future Directions 145

APPENDIX A: BONE MARROW TRANSDUCTION PROTOCOL 153

APPENDIX B: PCR AND CLONING OLIGONUCLEOTIDES 156

REFERENCES 157

LIST OF TABLES

Page

Table 3.1: Estimated Viral Load of Vectors 57
Table 5.1: Total tdTomato Expression In Peripheral Blood From SINrv:X-tdT/BMT mice 121
Table 5.2: Comparison of Staining and tdTomato Expression 124
Table 5.3: Summary of Flow Cytometry On Peripheral Blood From SINrv:X-tdT/BMT mice 129

LIST OF FIGURES

Page

Figure 2.1: Different Mechanisms of Blood Vessel Growth 7
Figure 2.2: Intrinsic and Extrinsic Apoptosis Pathways 28
Figure 2.3: The Bcl-2 Family Members 30
Figure 3.1: General Strategy for EPC Depletion 37
Figure 3.2: Strategy for Retrovirus-Induced Bone Marrow-derived Endothelial Cell Ablation 47
Figure 3.3: Comparison of BOSC23 and Phoenix Amph Packaging Cell Lines 48
Figure 3.4: Effect of LSC on Transduction Efficiency 48
Figure 3.5: Optimized Transduction Protocol 50
Figure 3.6: Evaluation of Cell Lines For Use In Assessing Construct Function 52
Figure 3.7: Ineffectiveness of REF and RED Constructs 54
Figure 3.8: Reduced Capacity for Genomic Integration of REF and REF3 56
Figure 3.9: General CrIED Transgenic Strategy 58
Figure 3.10: Characterization of iMAECs From CrIED Mice 60
Figure 3.11: Sensitivity of CrIED-derived iMAECs to 4-Hydroxytamoxifen 61
Figure 3.12: Chemiluminescence of CrIED Mice 62
Figure 3.13: Luciferase Activity In Tissue Lysates. 63
Figure 3.14: Apoptosis In CrIED Tissue Following Tamoxifen Treatment 66
Figure 3.15: Tamoxife-induced Cre Activity In CAGCre^{TM} Mice 67
Figure 4.1: Plasmids Containing ΔN-Bax Sequence. 81
Figure 4.2: Cell Morphology Following EGFP:ΔN-Bax Expression 83
Figure 4.3: Flourescence of Cells Expressing EGFP:ΔN-Bax or EGFP 85
Figure 4.4: Confocal Imaging of Transfected Cells 87
Figure 4.5: Timecourse of Flourescence Following Transfection 88
Figure 4.6: Nuclear Fragmentation of Transfected Cells 91
Figure 4.7: Detection of ΔN-Bax mRNA and Protein In Transfected Cells 93
Figure 4.8: Apoptosis following transfection with pΔN-Bax-N1 95
Figure 4.9: Structure of Bax 100
Figure 5.1: SINrv Construct Design 113
Figure 5.2: Validation of Retroviral Constructs *In Vitro* 115
Figure 5.3: Promoter Characterization In MS1 Cells 116
Figure 5.4: tdTomato Enrichment With FACS 118
Figure 5.5: *In vivo* Monitoring of tdTomato Expression. 118
Figure 5.6: Bone Marrow Labeling Strategy 119
Figure 5.7: Validation of Bone Marrow Transplant Strategy 121
Figure 5.8: Express of tdTomato In Transduced Bone Marrow Colonies 121
Figure 5.9: Intracellular VEGF Staining of Peripheral Blood From SINrv:VEGF-tdT/BMT Mice 124
Figure 5.10: Intracellular eNOS Staining of Peripheral Blood From SINrv:VEGF-tdT/BMT Mice 125

Figure 5.11: Flow Cytometric Analysis of CD14 Expression In Peripheral Blood From SINrv:X-tdT/BMT Mice 126
Figure 5.12: Quantification of CD14 Expression in BMT-Peripheral Blood 127
Figure 5.13: PB-MNCs Are Fully Reconstituted Following Retroviral Transduction 128
Figure 5.14: Characterization of tdTomato Positive Cells In PB From SINrv:X-tdT/BMT mice 130-131

LIST OF ABBREVIATIONS

AMI	Acute Myocardial Infarction
Apaf-1	Apoptosis Protease Activating Factor-1
bFGF	Basic Fibroblast Growth Factor
Bax	Bcl-2 Associate Protein X
BCA	Bicinchoninic Acid
Bcl2	B-cell Lymphoma 2
BH	Bcl-2 Homology
BM	Bone Marrow
BM-MNC	Bone Marrow-Mononuclear Cell
BMT	Bone Marrow Transplant
BMTT	Bone Marrow Transduction and Transplantation
CAG	CMV Early Enhancer/Chicken Beta Actin
CCR2	Chemokine Receptor 2
CD	Cluster of Differentiation
cDNA	Complementary Deoxyribonucleic Acid
CEC	Circulating Endothelial Cell
CFU	Colony Forming Unit
CFU-EC	Colony Forming Unit-Endothelial Cell
CFU-	Colony Forming Uni
CMV	Cytomegalovirus
CrIED	Cre Inducible Endothelial Cell Death (Transgenic mouse)
CVD	Cardiovascular Disease

DISC	Death Inducing Signaling Complex
DNA	Deoxyribonucleic Acid
DR	Death Receptor
DT	Diphtheria Toxin
DTR	Diphtheria Toxin Receptor
EC	Endothelial Cell
EGFP	Enhanced Green Fluorescent Protein
eNOS	Endothelial Nitric Oxide Synthase
EPC	Endothelial Progenitor Cell
FACS	Fluorescence-Activated Cell Sorting
FADD	Fas-associated Protein With Death Domain
FasL	Fas Ligand
FcγR	Fc Gamma Recepter
Flk1	Fetal Liver Kinase 1 (VEGFR2)
G-CSF	Granulocyte-Colony Stimulating Factor
GM-CSF	Granulocyte Macrophage-Colony Stimulating Factor
GMP	Good Manufacturing Practice
HAEC	Human Aortic Endothelial Cell
HMEC-1	Human Microvascular Endothelial Cell 1
HSV-TK	Herpes Simplex Virus-Tyrosin Kinase
HSC	Hematopoietic Stem Cell
HUVEC	Human Umbilical Vein Endothelial Cell
IED	Inducible Endothelial Cell Death (Transgenic mouse)

IL3	Interleukin 3
IL11	Interleukin 11
iMAEC	Immortalized Mouse Aortic Endothelial Cells
KDR	Kinase Insert Domain Receptor (VEGFR2)
LDL	Low Density Lipoprotein
LVEF	Left Ventricular Ejection Fraction
MCS	Multiple Cloning Site
MMLV	Murine Moloney Leukemia Virus
MMP-9	Matrix Metalloproteinase 9
MOM	Mitochondrial Outer Membrane
mRNA	Messenger Ribonucleaic Acid
mSCF	Mouse Stem Cell Factor
OEC	Outgrowth Endothelial Cell
PAD	Peripheral Artery Disease
PB	Peripheral Blood
PB-MNC	Peripheral Blood-Mononuclear Cell
PCR	Polymerase Chain Reaction
Poly-A	Poly-adenylation Sequence
qRT-PCR	Quantitative Real Time-Polymerase Chain Reaction
REC	Retrovirus For Expression of Cre
RED	Retrovirus for Endothelial cell Death
REF	Retrovirus for Endothelial cell Fluorescence
REF3	Retrovirus for Endothelial cell Fluorescence version 3

Sca1	Stem Cell Antigen 1
SINrv	Self Inactivating Retrovirus
SVEC4-10	SV40 Immortalized Endothelial Cells
tdT	Tandem Dimer Tomato Protein
TEM	Tie2 Expressing Monocyte
Tie1	Tyrosine Kinase With Immunoglobulin-like and EGF-like Domains 1
Tie2	Tyrosine Kinase With Immunoglobulin-like and EGF-like Domains 2
TM	Transmembrane
TNFα	Tumor Necrosis Factor α
TRAIL	Tumor Necrosis Factor-Related Apoptosis Inducing Ligand
TUNEL	Terminal Deoxynucleotidyl Transferase dUTP Nick End Labeling
VE Cadherin	Vascular Endothelial Cadherin
VEGF	Vascular Endothelial Growth Factor
VEGFR2	Vascular Endothelial Growth Factor Receptor 2
VL	Vascular Leukocyte
WT	Wild Type

SUMMARY

Endothelial Progenitor Cells (EPCs) were first identified from human blood samples as a population of circulating mononuclear cells capable of displaying a mature endothelial cell phenotype in culture. Subsequent studies established that EPCs arise from the bone marrow (BM) and incorporate into the endothelium at sites of blood vessel growth, suggesting a potential role for these cells in neovascularization. Furthermore, a decline in EPC number correlates to multiple vascular pathologies, indicating that EPC counts could serve as a biomarker of cardiovascular disease. Unfortunately, due to the variability in techniques used for EPC isolation and identification, considerable heterogeneity exists within the population of cells commonly defined as EPCs. In order for the clinical potential of EPCs to be fully realized, thorough characterization of the BM-derived cell populations involved in neovascularization is required.

The *objective* of our study was to determine the functional significance of circulating EPCs in postnatal vascular growth and repair. Two separate strategies were employed to achieve this objective. In the first, we attempted to generate a mouse whose pool of bone marrow-derived endothelial precursors was drastically reduced or eliminated. Our *overall approach* was to deliver a "suicide" gene, under control of an endothelial cell-specific promoter, to bone marrow cells for use in bone marrow transplantation (BMT) experiments. Mice receiving BMTs would therefore lack the ability to deliver viable BM-derived EPCs to sites of neovascularization. Our *central hypothesis* for this study was that a reduction in EPC viability would hinder endogenous vascular repair mechanisms, thereby exacerbating cardiovascular disease. In the second

strategy, we attempted to identify novel progenitor cell populations based on the transcriptional regulation of pro-angiogenic genes. Our *overall approach* was to transduce BM with a retrovirus containing a fluorescent reporter gene under control of pro-angiogenic promoters for use in transplantation experiments. Our *central hypothesis* for this study was that unique populations of BM-derived cells could be identified by expression of the fluorescent reporter gene directed by the Vascular Endothelial Growth Factor (VEGF), endothelial Nitric Oxide Synthase (eNOS) and Vascular Endothelial (VE) Cadherin promoters.

The BMT strategy utilized to address our first hypothesis was unsuccessful due to the use of a truncated form of the pro-apoptotic Bax as our suicide gene. A plasmid encoding GFP fused to a truncated Bax fragment (ΔN-Bax, consisting of amino acids 112-192 of the full length protein) was used in transfection experiments to assess ΔN-Bax function. The GFP:ΔN-Bax fusion protein formed distinct extranuclear aggregates (presumably due to mitochondrial translocation) but did not induce apoptosis in transfected cells. The ΔN-Bax fragment also did not induce cell death when targeted to endothelial cells with retoviral-mediated gene delivery or in a transgenic mouse setting.

To address our second hypothesis, we generated retroviral vectors containing the fluorescent tdTomato reporter gene under control of the VEGF, eNOS and VE Cadherin promoters. Significant fluorescence was detected in cultured endothelial cells and *ex vivo*-expanded BM cells. Following transplantation of transduced BM cells into lethally irradiated recipient mice, we were able to identify circulating populations of tdTomato-positive cells using flow cytometry. With these results we have identified novel subpopulations of circulating BM-derived cells which may play a significant role in post-

natal neovascularization in mice. Therefore, results acquired from these studies could lead to improved cell therapy techniques for treatment of vascular disease.

CHAPTER 1

SPECIFIC AIMS

Introduction

Since their initial discovery in 1997, controversy has surrounded Bone Marrow (BM)-derived Endothelial Progenitor Cells (EPCs) and their role in the repair and regeneration of the vasculature. Based on their apparent ability to incorporate into the endothelium at sites of blood vessel growth (1), EPCs were immediately identified as a cell source for the vascularization of tissue engineered constructs and for vaso-regenerative therapy for treatment of conditions such as Acute Myocardial Infarction (AMI). Mounting evidence also suggests that EPC number and function are a strong indicator of overall cardiovascular health, and their reduction in number is a potential biomarker for atherosclerosis (2).

Despite the therapeutic and diagnostic potential of EPCs, several recent studies found that bone marrow (BM)-derived cells did not integrate into the endothelium in a number of different animal models of neovascularization (3; 4). These reports suggested that BM cells were recruited to sites of neovascularization and stimulated growth via a paracrine effect rather than differentiating into mature endothelial cells. The conflicting data regarding the incorporation of EPCs into the endothelium has lead to considerable controversy over the functional role of EPCs in vascular growth. As a result of this controversy, no consensus has been reached on the contributions of BM-derived cells during neovascularization.

Before EPCs can be employed in a clinical setting, their functional role in endogenous vessel growth and repair must be definitively elucidated. The *objective* of

our study was to determine the functional significance of circulating EPCs in postnatal vascular growth and repair.

Two separate strategies were employed to achieve this objective. In the first, we attempted to generate a mouse whose pool of bone marrow-derived endothelial precursors was drastically reduced or eliminated. Our *overall approach* was to deliver a "suicide" gene, under control of an endothelial cell-specific promoter, to murine BM cells for use in BM Transplantation (BMT) experiments. Mice receiving BMTs would therefore lack the ability to deliver viable BM-derived EPCs to sites of neovascularization. Our *central hypothesis* for this study was that a reduction in EPC viability would hinder endogenous vascular repair mechanisms, thereby exacerbating cardiovascular disease. Specific Aims I and II outline our attempts at generating a mouse model of EPC depletion.

In the second strategy, we attempted to identify novel progenitor cell populations based on the transcriptional activity of pro-angiogenic genes. Our *overall approach* was to transduce murine bone marrow with a retrovirus containing a fluorescent reporter gene under the control of multiple promoters previously implicated in neovascularization. Transduced cells are then transplanted into lethally irradiated recipient animals, where detection of fluorescence allows identification of BM-derived progenitor populations in both the circulation and tissues. Our *central hypothesis* for this study was that unique populations of BM-derived cells could be identified and isolated by transcriptional activation of a fluorescent reporter gene from the Vascular Endothelial Growth Factor (VEGF), endothelial Nitric Oxide Synthase (eNOS) and Vascular Endothelial (VE) Cadherin promoters.

To test these hypotheses, the following specific aims were proposed:

AIM I

Specific Aim 1: Develop a retroviral construct to induce endothelial specific cell death *in vitro*.

Our *working hypothesis* was that a retroviral construct, containing a suicide gene under direction of an endothelial cell-specific promoter, would induce death only in endothelial cells. To this end, we designed a Retrovirus for Endothelial cell Death (RED) in which a truncated form of the pro-apoptotic gene Bax was directed by the murine VE Cadherin promoter. To assess construct efficacy, RED was transduced into endothelial cells and fibroblasts *in vitro.* Construct function was evaluated with microscopy, flow cytometry, western blot, and quantitative Reverse Transcription-Polymerase Chain Reaction (qRT-PCR).

AIM II

Specific Aim 2: Generate a transgenic mouse model to induce endothelial specific cell death *in vivo*.

Our *working hypothesis* was that a transgenic mouse, containing the RED construct, would allow us to temporally regulate endothelial cell apoptosis in a tamoxifen inducible system. To achieve this aim, we generated a Cre-Inducible Endothelial cell Death (CrIED) mouse containing the RED construct described in Aim I. Histology, chemiluminescence imaging, western blot, and qRT-PCR were used to evaluate the transgene function.

AIM III

Specific Aim 3: Fluorescently label subpopulations of bone marrow cells using retroviral-mediated gene transfer.

Our *working hypothesis* was that pro-angiogenic bone marrow cells could be identified using retroviral-mediated gene transfer of promoter/reporter constructs. We developed retroviral constructs containing the VE Cadherin, eNOS, and VEGF promoters driving expression of the tdTomato gene. To evaluate construct efficacy, retroviral mediated gene transfer was used to genetically label endothelial cells *in vitro*. Bone marrow cells were then transduced and used in a transplantation model to identify and characterize the cell subpopulations *in vivo* with flow cytometry.

Innovation and Significance

The strategy proposed in Specific Aims I and II would have offered valuable insight into EPC biology by resolving the functional contributions of bone marrow-derived endothelial cells in vascular growth and repair. Unfortunately, we were unable to successfully implement these approaches, and as a result the potential impact of this project was not fully realized.

The work in Specific Aim III is innovative because it describes a straightforward but effective method for labeling unique populations of bone marrow-derived cells in mice. Current methods for labeling of bone marrow cells involve the development of transgenic mice, but this process is prohibitively expensive and time consuming. Our approach allows the genetic tagging of many different bone marrow cell types at a

fraction of the cost of generating transgenic mouse strains, and in a considerably shorter time frame. Furthermore, our approach can be applied to any strain, transgenic, or knockout mouse permitting studies of multiple pathologies without the need for complicated breeding strategies.

This work is significant because it allows tracing of previously undefined bone marrow-derived cell types in a setting of neovascularization. Circulating peripheral blood (PB) cells are typically identified almost exclusively by surface marker expression. Here, however, we demonstrate the ability to identify circulating cells based on gene expression that implies *function* (i.e. VEGF secretion, nitric oxide production). Furthermore, this approach permits the imaging of live cells based on the expression of intracellular protein expression. Intracellular protein labeling typically requires membrane permeabilization, preventing use of the cells following antibody staining. Promoter-specific expression of tdTomato permits identification and isolation of live eNOS or VEGF-expressing cells without the need for permeabilization, enabling use of the cells for transplantation studies following isolation.

In conclusion, we were unable to generate a mouse model with a depleted pool of endothelial progenitor cells. However, we were able to identify several previously uncharacterized populations of bone marrow cells that could potentially be involved in neovascularization, and in doing so developed a new methodology for the identification and isolation of bone marrow subpopulations.

CHAPTER 2

BACKGROUND AND LITERATURE REVIEW

Endothelial Progenitor Cells

In their report that first identified a circulating endothelial progenitor cell (EPC), Asahara et al. (1) described a peripheral blood cell that presumably arose from the bone marrow, yet was also capable of displaying characteristics of mature endothelium. This monumental study immediately challenged the prevailing paradigm of post-natal neovascularization (5). Previously, it was assumed that blood vessel growth was the result of two distinct processes: angiogenesis and arteriogenesis. Angiogenesis consists of the generation of new blood vessels from the existing endothelial cells through sprouting or intussusception, is directed by growth factors such as VEGF and basic Fibroblast Growth Factor (bFGF) (Figure 2.1), and is frequently observed in response to hypoxia. The presence of a Hypoxia Response Element (HRE) within the VEGF promoter results in Hypoxia Inducible Factor 1-α (HIF-1α) regulated gene expression, so that VEGF-induced angiogenesis is often a consequence of tissue ischemia (6). Arteriogenesis involves the expansion of preexisting collateral vessels due to an increase in blood flow, and is presumably initiated by changes in shear stress experienced by the endothelium (7) (Figure 2.1).

The work by Asahara et al.(1) suggested a third mechanism of blood vessel growth, in which circulating BM-derived cells lead to the formation of *de novo* blood vessels. This process has been referred to as post-natal vasculogenesis, and it bears similarity to the formation of blood vessels from primitive hemangioblasts during embryonic vasculogenesis (Figure 2.1). The notion of vasculogenesis in the adult, as

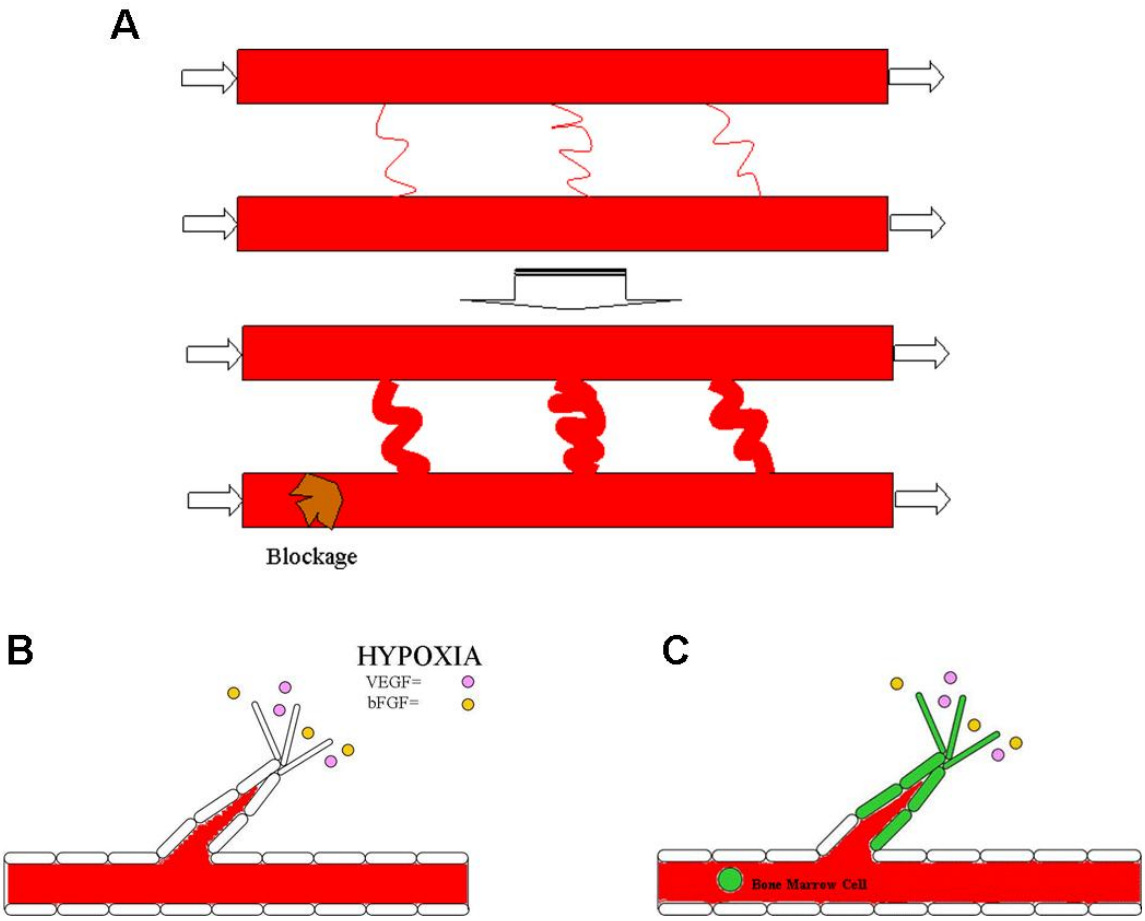

Figure 2.1: The different mechanisms of blood vessel growth. A) Arteriogenesis involves the expansion of preexisting collateral vessels due to changes in physical forces experienced by endothelial cells as a result in increase in flow. B) Angiogenesis is the sprouting of blood vessels from the existing endothelial cells in response to growth factors generated in hypoxic tissue. C) Vasculogenesis involves the *de novo* formation of blood vessels from circulating endothelial progenitor cells (EPCs), in a process similar to that seen in embryonic development.

suggested by Asahara et al.(1), encouraged a plethora of subsequent studies examining the origin and functional involvement of EPCs in various settings of neovascularization. Unfortunately, the lack of a consensus definition for an EPC has led to a variety of methodologies for isolation and characterization of the cells. This in turn has led to conflicting reports regarding quantification of EPC number as well as the functional attributes of these cells. Despite various claims linking the putative EPC to certain

subpopulations of circulating peripheral blood mononuclear cells (PB-MNCs) based on the expression of surface markers, at present no single definitive marker for identification of an EPC exists. Consequently, EPCs described as described throughout the literature may be separate, distinct cell types, necessitating cautionary interpretation when comparing findings (9).

Initial Discovery and Role in Blood Vessel Growth

In their pioneering work identifying the EPC, Asahara et al. (1) enriched human peripheral blood samples for either CD34+ or Flk-1 (VEGFR-2) mononuclear cells, which were then plated in an endothelial growth medium (1). The markers CD34 and VEGFR-2 were used for enrichment due to their expression in both hematopoietic stem cells and endothelial cells; the simultaneous expression of both markers could potentially indicate biphenotypic fate. Within 3 days, a subset of the PB-MNCs enriched for CD34 or VEGFR-2 became adherent and obtained an endothelial-like spindle shape. After 7 days in culture, characterization of the surface markers on the cultured cells revealed a mature endothelial phenotype. Injection of the CD34 or Flk-1 enriched cells into the ischemic limb of a nude mouse resulted in incorporation into the endothelial layer of blood vessels at sites of neovascularization, thus suggesting that *ex vivo* expanded cells were circulating endothelial precursors. It should be noted that the purity of CD34 and Flk-1 cells was 20% or less for each antigen, making it impossible to distinguish if the CD34 or Flk-1 cells directly gave rise to the endothelial-like colonies seen in culture

Prior to the discovery of EPCs, Circulating Endothelial Cells (CECs) were observed in a number of pathologic settings (10). However, CECs, although isolated from

blood in a manner similar to EPCs, presumably originate from mature blood vessels. Frequently identified by the endothelial marker CD146 (11), CECs are thought to be cells "sloughed off" of the native endothelium. In contrast to the origins of CECs, Asahara et al. (12) used a series of elegant bone marrow transplantation experiments to establish that some cells that contribute to neovessel formation originate in the bone marrow. To distinguish donor cells from recipient cells, donor BM from Flk1-LacZ or Tie2-LacZ transgenic mice was transplanted into lethally irradiated nude mice recipients. Donor-derived cells were then detected in a setting of tumor angiogenesis, wound healing, and hind limb ischemia (12), establishing the bone marrow-origins of Flk1 or Tie2 expressing cells in mice.

The origination of EPCs in the bone marrow was also explored independently by Shi, et al.(13) in a BMT model in dogs. Endothelial-like cells were generated *ex vivo* from CD34+ cells isolated from PB samples. Genotyping of the cells revealed that they were of donor origin. Following bone marrow transplantation, cells that adhered to the intimal surface of implanted Dacron grafts were CD34 + and determined to be of bone marrow origin (13), leading the authors to conclude that the donor-derived cells seen in culture were the same as those populating the grafts. It should be noted that the cultured "EPCs" isolated by Shi, et al. (13) were derived from a nonadherent fraction of peripheral blood cells following 3 rounds of adherence depletion. This method of isolation is differs from that described by Asahara, et al. (1), in which EPCs were obtained from an *adherent* population of PB cells.

In an attempt to isolate EPCs in mice, Takahashi, et al. (14) cultured mouse Sca1+ cells in conditions similar to those described by Asahara, et al. (1) for isolation of

human EPCs. As was seen in human PB-MNC samples, mouse Sca1+ cells also formed an endothelial-like adherent cell population in culture. The relationship between the endothelial-like cells seen in culture and the bone marrow cells involved in neovascularization was then pursued more thoroughly. Treatment of mice with GM-CSF led to an overall increase in neovascularization in both the ischemic hind limb and in a corneal micropocket assay. This functional increase in neovascularization correlated to an increased number of circulating mouse EPCs which were identified as Sca1+ cells in the PB (14). However, from these data it is unclear if the Sca1+ cells or their progeny were directly involved in the formation of new blood vessels.

Other markers besides Sca1+ have also been used to identify EPCs in mice. An increase in the number of circulating CD34+, Flk-1+ and VE Cadherin+ cells was observed following treatment with VEGF (15), establishing a correlation between the number of circulating cells and the increase in blood vessel formation following VEGF-induced angiogenesis. However, none of these studies were able to confirm that cells identified as circulating EPCs were the same as those isolated in culture or those BM-derived cells found in nascent blood vessels. Although a strong correlation was observed in each case, causality was never established.

A number of clinical trials using PB-MNC populations in the hopes of utilizing EPCs for cell therapy have begun to explore the therapeutic potential of different BM-derived cell populations for treatment of peripheral limb ischemia (16) and AMI (17). Endothelial progenitor cell number, as defined by either the number of EPC colony forming cells or the number of circulating PB-MNCs expressing various combinations of surface markers, has also been used as a biomarker of overall cardiovascular health.

Vasa, et al. (18) found that EPC number, as assessed by both number of adherent endothelial-like colonies derived from PB-MNCs after 5 days and number of circulating CD34+/KDR+ cells, inversely correlated to the number of risk factors for coronary artery disease (19). Colony number and CD34+/KDR+ cells also increased within one week of initiating statin therapy (18). These data demonstrate that EPC number may be an additional metric to assess efficacy of various treatments for cardiovascular disease (CVD).

Using a 48 hour pre-plate method to remove adherent cells, Hill, et al. (2) further established a link between CVD and EPC number by demonstrating an inverse correlation between EPC number and Framingham risk score. Hill, et al. (2) went on to establish an inverse correlation with EPC number and vascular *function*, as determined by flow-mediated brachial reactivity, in a cohort of healthy patients (2).

Culturing of EPCs

The studies outlined above are significant for a number of reasons. First, they provide evidence for a previously undefined mechanism of endogenous blood vessel growth (post-natal vasculogenesis) in addition to the established mechanisms of angiogenesis and arteriogenesis. Second, the existence of a circulating cell that naturally augments the process of angiogenesis offers a convenient source for cell therapy strategies. Finally, EPCs are a novel biomarker of vascular health, both as an indicator of disease and a metric of therapeutic efficacy for treatment of CVD. However, careful examination of the methodologies underlying each of these studies reveals considerable

variation in cell isolation techniques. In each case, although the cells examined are referred to as EPCs, in reality they may be remarkably different cell types.

The original EPC, as described by Asahara, et al.(1) was isolated from a CD34-enriched PB-MNC population that adhered to fibronectin, and exhibited an endothelial-like phenotype in 7 days. The EPC described by Vasa, et al. (18) was also derived from an adherent population of PB-MNCs, but was characterized after just 4 days in culture. In order to remove any macrophages and contaminating mature endothelial cells, Hill, et al. (2) added a single 48 hour pre-plate step for removal of adherent cells, followed by a replate and 7 day culture of the non-adherent cells. Shi, et al. (13) enriched PB-MNCs for CD34+ cells and then performed 3 pre-plate steps to remove adherent cells before replating the non-adherent cells. Each of these studies, despite utilizing different culture techniques, generated cells resembling an endothelial cell *ex vivo*. Unfortunately, subsequent studies built upon these early disparate and varied approaches, so that at present there is no consensus as to how one should definitively isolate and quantify EPCs.

Recently, several reports have explored the subtle differences between cells derived from the different EPC culture techniques. In an effort to determine the origin of EPCs in humans, Lin, et al (20) obtained PB samples from gender-mismatched bone marrow transplant recipients so that donor marrow-derived cells could be distinguished from recipient cells by *in situ* hybridization of the Y-chromosome. Through *ex vivo* expansion of PB-MNCs from the BMT recipients, Lin, et al. (20) identified two distinct populations of circulating endothelial cells in peripheral blood. The first was an early adherent cell type of recipient origin (i.e. not from the bone marrow) that exhibited an

endothelial phenotype. However, these early endothelial cells showed a limited proliferative capacity and were soon outgrown by a second highly proliferative endothelial cell of *donor* origin. The authors suggested that the early-circulating ECs were from mature vessel walls, while the late-circulating ECs arose and differentiated from the bone marrow.

The two cell types are frequently referred to as early EPCs (7 day culture) and "late" or Outgrowth Endothelial Cells (OECs, 21 day culture). Molecular characterization of "early" EPCs from adherent PB-MNCs has revealed that they are of monocytic origin, as evidenced by CD14 expression (21). In contrast, the OEC population does not express CD14, and was shown to originate from a CD14 *negative* population of cells (21). The OECs are functionally more representative of endothelial cells, as only the OECs form tubular structures in matrigel and integrate into a monolayer of Human Umbilical Vein Endothelial Cells (HUVECs). The OECs also exhibit a phenotype more typical of a true endothelial cell compared to the early EPC, although injection of either cell type results in enhanced neovascularization in the ischemic hind limb of nude mice (22). Interestingly, transplantation of a mixed population of both early EPCs and OECs results in and even *greater* improvement in recovery from hind limb ischemia than transplant of either cell type alone (23). Although early EPCs are unable to acquire a mature endothelial phenotype, the angiogenic potential of these cells is evident by their production of the pro-angiogenic cytokines VEGF and IL-8 (22). Early EPCs were also shown to enhance tube formation in a transwell fibroblast-co-culture experiment, establishing a pro-angiogenic phenotype capable of augmenting vessel formation (24).

In addition to the phenotypic differences between early EPCs and OECs, phenotypic heterogeneity has been observed even within the early EPC population alone. Examination of the clonogenic potential of late EPCs by single cell replating of the primary EPC colonies identified a small subset of cells within the early EPC population capable of proliferating and expanding upon further passage. Plated umbilical cord blood (CB), and additional source of EPCs, showed a 15-fold higher number of high-passage proliferative cells compared to PB samples, suggesting CB may serve as a highly enriched cell source for regenerative therapies (25).

Although EPCs presumably arise from the bone marrow, the variation seen in phenotype among the different groups of EPCs may indicate different sites of origin. Ingram, et al. (26) observed a highly proliferative subpopulation of cells within HUVEC and Human Aortic Endothelial Cell (HAEC) cultures, suggesting that the vessel wall itself may be a niche where proliferative EPCs reside. Zengin, et al. (27) examined excised aortic segments and observed a highly proliferative and migratory endothelial-like cell in *ex vivo* culture assays that originated at the medial-adventitial border of the blood vessel. The expression of CD34 on these cells, and the location within the blood vessel wall, preclude them from being classified as mature endothelial cells. Others have postulated that EPCs exist as a pool of cells within the native endothelium either derived from the endothelium itself, or as bone marrow cells translocated to a secondary niche within the mature endothelium (28).

Yoder, et al. (29) observed that the endothelial cell colony forming units (CFU-EC) first described by Hill, et al. (2) expressed both the leukocyte antigen CD45 and the monocytic identifier CD14, indicating that the CFU-ECs were of hematopoietic origin.

This was in contrast to the analysis of OECs, which were largely CD14 negative (29). Limited dilution and replating of single cells from the CFU-ECs also demonstrated that the cells were unable to form secondary CFU-ECs. However, some of the replated CFU-ECs were capable of forming HSC-like colonies (29). These data suggest that CFU-ECs, although capable of expressing some endothelial markers, are more closely related to a hematopoietic progenitor than an endothelial cell.

In summary, several different methods for *ex vivo* culturing of PB-MNCs have been used to identify colonies which are commonly referred to as EPCs. However, there are marked differences in phenotype between the populations of cells obtained using these different techniques. Cells generated from each of the culture methods show some capacity to enhance angiogenesis, but it is unclear which, if any, of the cultured EPCs are capable of forming true endothelial cells. Furthermore, it is unclear if any cells derived from the different EPC cultures are involved in endogenous neovascularization, as causality between the *ex vivo* and *in viv*o data has yet be established.

Circulating EPCs

EPCs were first identified based on their ability to display an endothelial cell-like phenotype in culture. The *ex vivo* approach for identification is problematic because it necessitates a retrospective analysis of the entire PB-MNC population of cells. For their effective use in cell therapy, it is necessary to *prospectively* identify EPCs. Unfortunately, no unique surface marker or group of markers exists that permits the unequivocal identification and purification of an EPC population.

Asahara, et al. (1) hypothesized that CD34 and Flk-1 (VEGF Receptor-2 or VEGFR2) could be used to identify an adult hemangioblast (i.e. cell capable of giving rise to both hematopoietic and endothelial cells) with angiogenic capacity. The authors reasoned that both of these markers were present on embryonic hemangioblasts, and that the same expression profile may be recapitulated in the adult bone marrow. Single cell clonogenic culture assays have supported this hypothesis, demonstrating that a limited number of CD34+/VEGFR2+ cells in chord blood are capable of forming both endothelial and hematopoietic stem cells (30). Gehling, et al. (31) expanded upon this idea by identifying a subset of CD34+ cells that were also positive for CD133 (AC133) (31). CD133 enriched cells formed both an adherent (EC-like) and non-adherent (HSC-like) cell population in culture, and led to increased tumor size when co-injected into Severe Combined ImmunoDeficiency (SCID) mice with A549 cells. Cells containing a combination of all three markers (CD133+/CD34+/VEGFR2+) have been described as a non-adherent precursor capable of obtaining an endothelial phenotype in culture (32), and may be derived from a CD34 negative(but CD133+/VEGFR2+) population (33).

The combination of some or all of the markers CD133, CD34, and VEGFR2 has been widely used for the prospective identification of circulating EPCs. The number of circulating CD133+/CD34+/VEGFR2+ cells were shown to increase in response to exercise (34; 35; 36) or G-CSF treatment (37), and were elevated in patients with non-small cell lung cancer (38) and immediately following AMI (39). Patients who smoked (40), or suffered from hypercholestoremia (41) or obesity (42) had reduced numbers of circulating EPCs, as defined by coexpression of CD133, CD34 and VEGFR-2. However, while the number of circulating CD34+/CD133+/VEGFR2+ cells may serve as an

indicator of vascular health and may be relevant to blood vessel function, it is unclear if these cells truly give rise to endothelial cells in a setting of neovascularization. Case, et al. (43) demonstrated that the CD34+/CD133+/VEGFR2+ cells did *not* form endothelial colonies in culture and, unlike mature endothelial cells, did not form tubular structures in a matrigel tube forming assay. Instead, CD34+/CD133+/VEGFR2+ cells readily formed HSC colonies, suggesting that they are actually a hematopoietic precursor. Interestingly, a CD34+/CD45- population ably formed endothelial-like colonies, but not HSC colonies in culture (43).

Evidence Against a Bone Marrow-Derived Endothelial Cell

The bone marrow origins of EPCs were established in mice through a series of bone marrow transplantation experiments in which genetically labeled bone marrow was transplanted into wild type recipients. In the resulting BM chimeras, cells of donor origin were found to incorporate directly into the endothelium. However, a number of reports have since surfaced that contradict some of the initial findings regarding the bone marrow origins of endothelial cells. Rajantie, et al. (44) observed that, following transplantation of transgenic-GFP expressing BM in a sub-lethally irradiated WT recipient, GFP+ cells were detectable in a setting of VEGF-induced angiogenesis and B16 melanoma. However, no GFP+ *endothelial* cells were detected. The majority of the GFP+ donor cells expressed the leukocyte and monocyte markers CD45 and CD11b, respectively, with a subset of GFP+ cells expressing NG2-proteoglycan (44). Expression of NG2-proteoglycan.indicates a pericyte-like, but not endothelial-like, phenotype. This report also demonstrated the importance of using scanning laser confocal microscopy for

colocalization studies. Many of the BM-derived cells identified in ischemic tissue were so close to the blood vessel intima that they could only be identified as pericytes following z-stack analysis through the tissue section. The discrepancy between this report and the results of earlier studies could be attributed to the use of confocal imaging, which prevented the false identification of bone marrow-derived endothelial cells.

Ziegelhoeffer et al. (3) used another BMT approach in which GFP-labeled donor cells were transplanted into lethally irradiated wild type recipients. In both hind limb ischemia and BSF-1 tumor models, GFP+ cells were detected around growing vessels, but none of the GFP+ cells could be definitively identified as endothelial cells (3). The GFP+ cells did stain positively for FGF-2, VEGF, and MCP-1, suggesting a paracrine role in augmenting neovascularization (3).

Case, et al. (43) utilized the GFP-BMT approach in a novel model of hypoxia-induced angiogenesis by housing animals in a hypoxic environment. Following exposure to hypoxia, an increase in blood vessel number was observed in the spinotrapezius muscle, and GFP+ cells were detected around nascent blood vessels (43). However, as observed by Ziegelhoeffer et al, (3), no GFP+ cells incorporated into the endothelium (43). Despite the absence of true BM-derived endothelial cells, a paracrine support role for these cells was suggested given that they expressed VEGF and MMP-9 (43). Case, et al. (43) utilized an additional BMT strategy in which donor marrow from mice containing the GFP gene transcriptionally regulated by the Tie-2 promoter was used to determine the contributions of BM-derived cells to blood vessels. In this case no GFP+ cells (and therefore no bone marrow-derived endothelial cells) were found in a setting of hypoxia-induced neovascularization (4).

Purhonen, et al. (45) performed BMT experiments utilizing GFP-labeled donor cells transplanted into lethally irradiated WT recipients, and found no BM-derived ECs in VEGF-induced angiogenesis, a B16 melanoma, or an *in vivo* matrigel plug. Transplants with donor marrow from VEGFR2-LacZ or Tie1-LacZ reporter mice (in which the VEGFR2 or Tie1 promoters drive expression of LacZ) indicated the presence of rare populations of cells expressing VEGFR-2 or Tie-1 in the bone marrow. However, these cells did not incorporate into the endothelium (45). In order to examine the role of EPCs in a non-myeloablative setting, a parabiosis model in which a GFP reporter and an APCmin mouse shared a circulatory system was also utilized. Again, no GFP+ ECs were detected within APCmin adenomas (45).

Pro-angiogenic Monocytes

Increasing evidence suggests that monocytes may have the ability to acquire an endothelial-like phenotype under specific culture conditions. Several studies have examined the role of monocytes in the formation of early EPCs in culture. Schmeisser, et al. (46) plated the monocytic CD14+/CD34- fraction of PB-MNCs in endothelial culture conditions and observed an adherent cell population with an endothelial-like morphology develop within 4 days. Expression of the endothelial markers von Willibrand Factor (vWF), eNOS, and VE Cadherin was retained up to 4 weeks in culture (46). Since the adherent cells grew from cells enriched for CD14, the authors concluded that the colonies arose from monocytes. Over the 4 weeks in culture, however, CD14 expression became diminished with a concomitant *increase* in CD68 expression, perhaps indicating that the cells had undergone a phenotypic switch to macrophages (46). Others have observed a

similar increase in endothelial-specific markers with a concurrent decrease in monocytic markers from CD14-enriched cells (47).

In order to assess the origins of the adherent population of cells from EPC culture assays, Rehman, et al. (48) performed surface marker analysis on PB-MNCs cultured for 4 days. Nearly all of the cells expressed the leukocyte antigen CD45, and >90% of the cells expressed the monocyte marker CD14 and myeloid marker CD11b. Conversely, endothelial and hematopoietic stem cell (HSC) markers (VE Cadherin, E-selectin, CD31, CD133 and ckit) were all expressed in less than 5% of total adherent cells. The authors concluded that the endothelial cells observed later in culture were derived from a monocytic population since the majority of the starting population was positive for CD14 and CD11b (48). These results raise the possibility that EPCs or, more specifically, early EPCs, are either monocytes or a subset of monocytes capable of undergoing an endothelial-like transformation.

The role of monocytes in the formation of CFU-ECs (EC culture of PB-MNCs following adherence depletion) has also been examined. Rohde, et al. (49) observed that cultured CD14+ (monocytes) or CD14- (non-monocytes) cells alone did not lead to CFU formation. However, adding CD14+ cells to a CD14- population restored the colony forming ability of the cells (49). These results indicate that monocytes may serve as a source of paracrine signaling in CFU-EC colonies.

Implantation of monocyte-derived EPCs was used to demonstrate a functional role for monocytes in neovascularization. Urbich, et al. (50) injected 4 day cultured EPCs from either CD14+ or CD14- cell populations into the ischemic hind limb of Nude mice, and saw equivalent improvement in blood flow for both groups. When freshly isolated

CD14+ cells were implanted, however, no improvement in blood flow was observed (50). Bailey, et al. (51) determined that a myeloid population within the bone marrow was capable of giving rise to endothelial cells in the hepatic portal vein. An isolated myeloid subpopulation defined as Lin-/sca1-/ckit+/CD34+/FcγR_{low} and FcγR_{high} cells from genetically tagged mice were used in BMT experiments, and found to incorporate in the endothelium of the hepatic portal vein. A similar result was also seen in a parabiosis model, confirming the incorporation of BM cells into the endothelium in a non-radioablative setting (51). Grunewald, et al. (52) examined the role of myeloid cells in a setting of VEGF-induced angiogenesis using a liver or myocardial-specific tet-activated VEGF over-expresser in a bone marrow transplant model. Donor GFP+ cells, obtained from the bone marrow of myeloid-specific CX3CR1-GFP mice, were recruited to both liver and myocardium following induction of VEGF expression (52). Despite the presence of GFP+ BM-derived cells in a setting of angiogenesis, there was no observable incorporation of BM-derived cells into the endothelium (52). These data suggest that myeloid cells play a significant role in angiogenesis, but don't necessarily differentiate into endothelial cells.

A growing number of reports have implicated a circulating monocyte/myeloid cell population in tumor angiogenesis. Tie-2 expressing monocytes (TEMs) were first observed by De Palma, et al. (53) following transduction of bone marrow with a lentivirus expressing GFP under control of Tie-2 transcriptional regulatory elements (53). In a BMT model where the donor cells were labeled with the Tie-2-GFP lentivirus, TEMs were found abundantly localized adjacent to nascent tumor vessels. However, the majority of TEMs expressed CD45, indicating that they were of hematopoietic origin and

not true EPCs. Using a similar lentiviral strategy, De Palma, et al. (53) used the Tie-2 promoter to drive expression of the HSV-TK suicide gene in bone marrow cells. Following administration of ganciclovir, a reduction in circulating TEMs and concurrent decrease in tumor volume was noted (53). These experiments established a functional role for TEMs in tumor angiogenesis. An additional subset of Tie2+ cells, characterized as Tie2+/CD13+/Sca1+/CD45-/CD31- , was also observed in tumors. Based on surface marker expression, this cell type was characterized as a mesenchymal stem cell-derived pericyte *not* of endothelial or hematopoietic origin (54).

Another monocyte-like cell type potentially relevant to angiogenesis was isolated from ovarian carcinomas, and found to express both the monocytic marker CD14 and the endothelial marker VE Cadherin. These cells, identified as Vascular Leukocytes (VLs), demonstrated the ability to form vessel-like structures in matrigel (55) and have subsequently been found in a variety of tumors (56). Like TEMs, VLs were determined to be of hematopoietic origin. Furthermore, VLs were highly responsive to VEGF, and underwent an endothelial-like differentiation following exposure to VEGF in tumors (57). Pulaski, et al. (56) were able to selectively deplete VLs using saporin toxin conjugated to an anti-CD52 antibody. In an ovarian tumor model, mice that received treatment of the CD52-saporin toxin showed a reduction in VL number, concurrent with a reduction in tumor volume and an increase in lifespan compared to controls (56).

The function of VLs in tumor angiogenesis appears to be mediated, at least in part, by TNFα. Li, (58) showed that TNFα induced an endothelial-like phenotype in VLs *in vitro* (58). The implantation of tumor cells expressing low levels of TNFα led to robust tumor growth and angiogenesis. However, cells expressing either high levels of TNFα or

no TNFα showed abrogated tumor formation with impaired angiogenesis (58). This result was in contrast to that found by De Palma, et al. (59), who showed that targeted TNFα over expression in TEMs led to a reduction in tumor formation (59). The discrepancy in between these studies could be due to either the relative levels of TNFα expressed, or the fact that two different cell types were examined. The latter seems less likely, however, because a comparative analysis of TEMs and VLs showed that nearly all VLs were TEMs, while half of TEMS were VLs (56).

Ahn and Brown (60) observed that bone marrow-derived cells localized in tumors following BMT with GFP-labeled donor cells did not differentiate into endothelial cells, but were instead a subset of CD11b+ myeloid cells. The authors noted that Matrix Metalloproteinase-9 (MMP-9) colocalized to the CD11b+ cells within the tumors, suggesting that the bone marrow-derived CD11b+ cells expressed MMP-9 (60). A role for MMP-9 in angiogenesis was further established by studies with MMP-9 knockout animals, which showed impaired tumor formation. Transplantation of WT marrow into MMP-9 KO animals restored tumorigenic ability (60). The functional role of CD11b cells was also explored in a tumor model using a transgenic mouse that expressed the diphtheria toxin receptor (DTR) under control of the CD11b promoter. Treatment of these mice with diphtheria toxin led to ablation of CD11b cells, and resulted in significant inhibition of tumor formation (60).

In addition to TEMs, VLs and CD11b+ cells, a number of other monocyte/myeloid derived cells have been implicated in tumor angiogenesis (61). Unfortunately, since the markers used to identify each of these subpopulations are expressed on multiple cell types, it is extremely difficult to distinguish between the

different groups of monocytes/myeloid-derived cells. It is likely that there is considerable overlap between the different monocytes/myeloid-derived cell types involved in tumor formation. A direct comparison of several tumor related bone marrow derived-myeloid cells showed striking similarity between some cell types (62), suggesting the potential for a shared lineage.

Not only is there a potential phenotypic overlap of these cell types, but functional redundancy is also likely. Pahler, et al. (63) noticed a decrease in macrophage number in cervical tumors from CCR2-null mice, but only minor differences in tumor size and progression were observed compared to WT controls. The authors concluded that this result was due to a compensatory effect from an increase in neutrophil infiltration (63). In addition to the difficulties encountered in characterizing the subsets of myeloid-derived cells involved in tumor formation, determining the relative functional role and contribution of each cell type adds an additional layer of complexity to the field.

Clinical EPC Studies

The therapeutic potential of EPCs was explored at the onset of their discovery when Asahara et al. (1) implanted *ex vivo* expanded EPCs in the ischemic hind limb of mice. From a theoretical perspective, a highly proliferative pro-angiogenic cell within the peripheral blood is an ideal source for cell therapy treatment of acute myocardial infarction (AMI), angina, or peripheral limb ischemia (PLI). However, the successful use of EPCs in a clinical setting has been complicated by a number of factors.

The lack of a concise definition for EPCs has plagued clinicians attempting to utilize PB or BM-derived cells for therapeutic neovascularization. The rarity of cells

defined as circulating EPCs has also been problematic, leading researchers to employ more straightforward approaches: using non- selected, whole PB (64; 65) or BM-MNCs (11, 45, 46, 48, 49, 50, 51, 52). Others have attempted to enrich PB cells for populations of pro-angiogenic cells by selecting for CD34 (74; 75) or CD133 positive cells (76; 77; 78) isolated from either BM or PB. An advantage to using a sorted or unsorted cell population directly from the BM or PB is that no *ex vivo* culture or expansion is required. This is of particular importance for treatment of AMI when faster isolation and preparation of the cells potentially allows for intervention prior to the onset of irreversible tissue damage. An additional benefit of using whole or sorted cells is that Good Manufacturing Practice (GMP) facilities are not required for preparation. For clinics and hospitals that lack GMP facilities, this provides a treatment option without a significant increase in cost to the institution. Despite these caveats, *ex vivo* expanded cells have been used therapeutically, albeit in a 3-day EPC culture system (78; 79; (81).

Although some clinical trials have shown modest improvement in cardiac function following cell therapy for treatment of AMI (66; 71; 76; 77), others have shown no improvement over patients receiving standard therapies (17; 69; 70). One study found an improvement in left ventricular ejection fraction (LVEF) at 6 months (67), but no differences were observed at an 18 month follow-up (68). These initial studies demonstrated feasibility for using PB or BM cells for treatment of AMI, but improvements in cardiac function following cell therapy have been minimal thus far.

There are a number of limitations with progenitor cell therapy that could be curtailing the potential of EPC treatment. Once such constraint is that the number of cells which can be isolated from a single donor is finite, limiting the total number of cells that

can be transplanted back into the patient. To achieve comparable delivery of cells in a human to that seen in successful animal studies, an unrealistically large number of cells are needed. The importance of cell number in humans was addressed by Meluzin, et al. (73), who observed a dose dependent improvement in LVEF following intracoronary infusion of BM-MNCs for treatment of AMI. In this study, patients who received a higher cell dose (10^8 cells) showed improvement over standard treatment groups while those that received a lower cell dose (10^7 cells) saw no improvement (73).

Although the use of EPCs as an autologous cell source for treatment of CVD is an appealing therapy, the approach is not without its drawbacks. A number of CVD risk factors have been shown to correlate with reduced EPC number and/or function, including total cholesterol (2; 41), LDL cholesterol (2; 19), Type I and II diabetes (82; 83; 84), and smoking (40). Patients suffering from AMI are likely to have several of these risk factors. As a result, the EPC pool in patient populations with AMI (and therefore requiring cell therapy) is likely impaired. It stands to reason that the depleted EPC pool would have lower regenerative capacity relative to EPCs isolated from healthy individuals. In fact, several studies have found the number of circulating EPCs to be lower in patients with vascular disease such as coronary artery disease (CAD) (85), erectile dysfunction (86), and stroke (87). Surprisingly, an increase in EPCs was observed in patients who had suffered an AMI (39; 88). It is possible that traumatic vascular event such as AMI may illicit an acute reparative response in the form of an increased number of circulating EPCs. However, the long-term effects of AMI likely lead to a reduced number and impaired function of circulating progenitors. Indeed, although EPC number was initially increased at the onset of heart failure, a reduction in EPC number was

observed in the late stages of heart failure compared to controls (89). Although EPCs may be a convenient autologous cell source easily isolated from PB, the impairment in function resulting from vascular disease presents a challenge that must be overcome for successful use of EPCs for therapeutic augmentation of angiogenesis.

Apoptosis and Bax

Apoptosis, or programmed cell death, can be initiated by a number of internal or external stimuli, leading to activation of either the extrinsic or intrinsic apoptotic cascades (Figure 2.2). The extrinsic pathway is triggered by the binding of ligands (FasL, TRAIL) to the extracellular domain of their respective membrane-bound death receptors (Fas, TRAIL-R1,2). The cytoplasmic domain of the death receptors (DR) are maintained in a death inducing signaling complex (DISC) with FADD, Pro-Caspase-8, Pro-Caspase-10, and $FLIP_{L/S}$. Binding of ligand to the DR results in proteolytic activation of Caspase-8 and Caspase-10 which activate additional effector caspases to continue the apoptotic program (90). Additionally, activated caspase-8 can cleave the cytosolic proapoptotic Bid protein. The cleaved product, tBid, is then translocated to the mitochondria where it further propagates the apoptosis pathway (91).

The intrinsic pathway is activated by environmental stresses such as hypoxia, UV-damage, and growth factor starvation, but does not require extracellular ligand binding for initiation of apoptosis. The initial phase of the intrinsic pathway is regulated by the Bcl-2 family of proteins (Figure 2.3). In the absence of an apoptotic stimulus, the pro-survival members of the Bcl-2 family (Bcl-2, Bcl-X_L, Mcl-1, Bcl-w and A1) dimerize

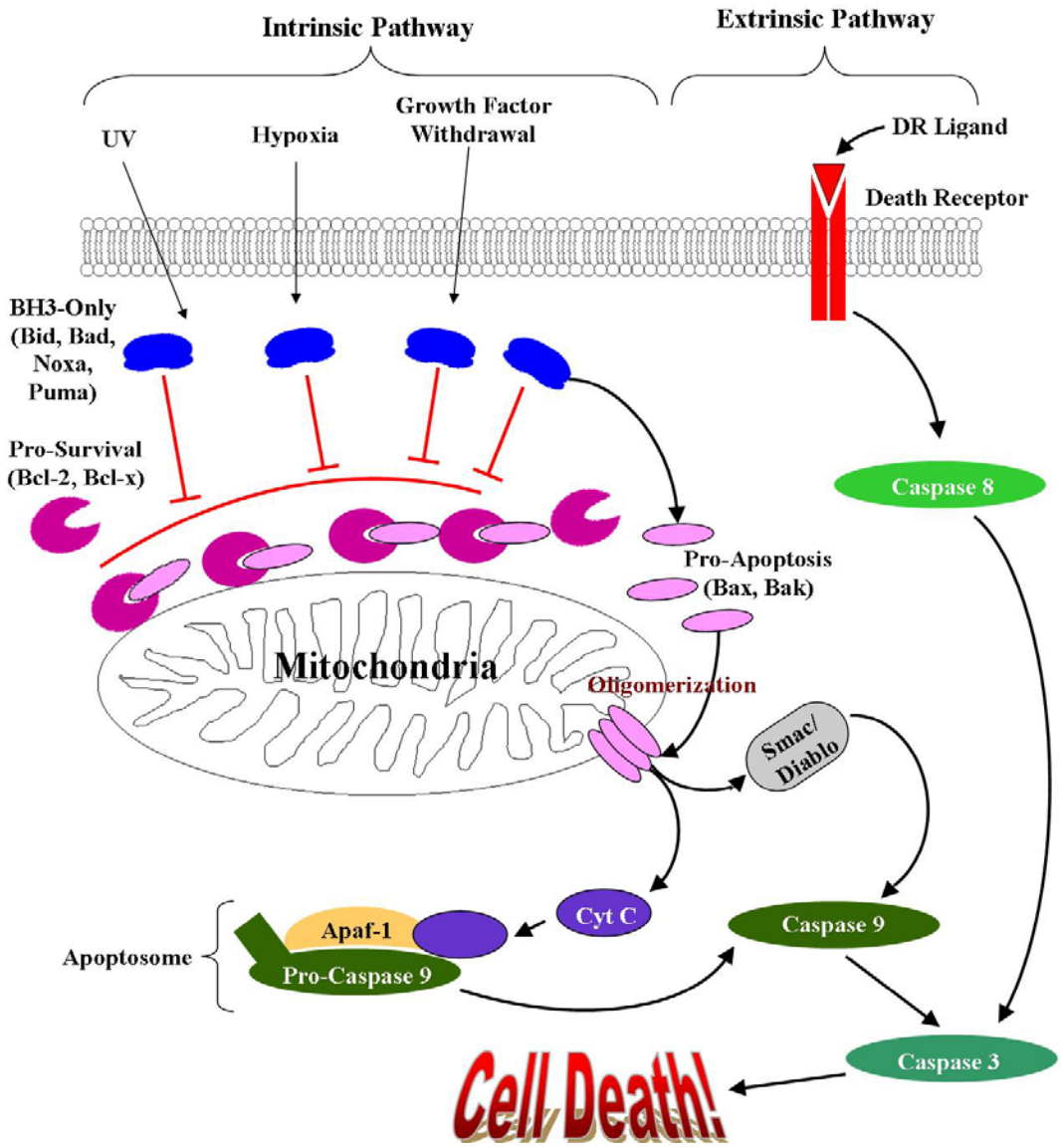

Figure 2.2: The intrinsic and extrinsic apoptosis pathways. The Extrinsic pathway is activated by binding ligand to the death receptors (DR), such as Fas or TNF-R. Caspases 8 and 10 are proteolitically activated at the cytoplasmic tail of the DRs, which then activate Caspase 3 and the rest of the apoptosis cascade. The intrinsic pathway, on the other hand, is initiated in response to environmental stresses. The BH3-only proteins (blue) either directly activate the pro-apoptotic Bcl-2 family members (Bax and Bak, in pink) or sequester the pro-survival proteins (purple) so that Bax and Bak aggregate and form pore complexes in the mitochondria outer membrane (MOM). Cytochrome c is then released from the MOM, which binds Apaf-1 and Pro-Caspase 9 to form the apoptosome. Caspase 9 is then activated by proteolytic cleavage. Smac/Diablo released from the mitochondria can also activate Caspase 9, which continues to propagate the Caspase cascade, resulting in apoptotic cell death.

with the multi-domain pro-apoptotic Bcl-2 family members (Bax, Bak and Bok), sequestering the pro-apoptotic members to prevent induction of cell death. The third Bcl-2 family member, the BH3-only proteins (Nox, Puma, Bim, Bid, Bad, Bik), are involved in activation of the pro-apoptotic members. The mechanism by which this activation occurs is currently under debate. Once activated, the pro-apoptotic family members oligomerize and form pore complexes within the mitochondrial outer membrane (MOM), permitting membrane depolarization and causing the release of cytochrome c and Smac/Diablo from the intermembrane space. The proteins released from the MOM then bind apoptosis protease-activating factor 1 (Apaf-1) and Pro-Caspase-9 in a complex called the apoptosome. When bound in the apoptosome, Pro-Caspase-9 is cleaved into the active form Caspase-9, which in turn activates Caspase-3 and the rest of the Caspase cascade.

The Bcl-2 proteins are categorized into family members based on Bcl-2 homology (BH) domains 1-4. The pro-survival members contain all four of the BH domains and a transmembrane (TM) domain, while the pro-apoptotic members contain the TM domain and BH1-3. The BH3-only members contain only the BH3 domain and the TM domain. The interplay between the three groups of family members, and particularly the role of the BH3-only proteins, has recently been a source of controversy.

Two models are currently hypothesized to explain the interactions of the Bcl-2 family of proteins: the direct and indirect activation models. In the direct activation model (93), the BH3-only proteins are divided into two groups: the activators and the sensitizers. The activators directly bind the pro-apoptotic family members, leading to activation of Bax/Bak and subsequent pore formation in the MOM. The sensitizers, on

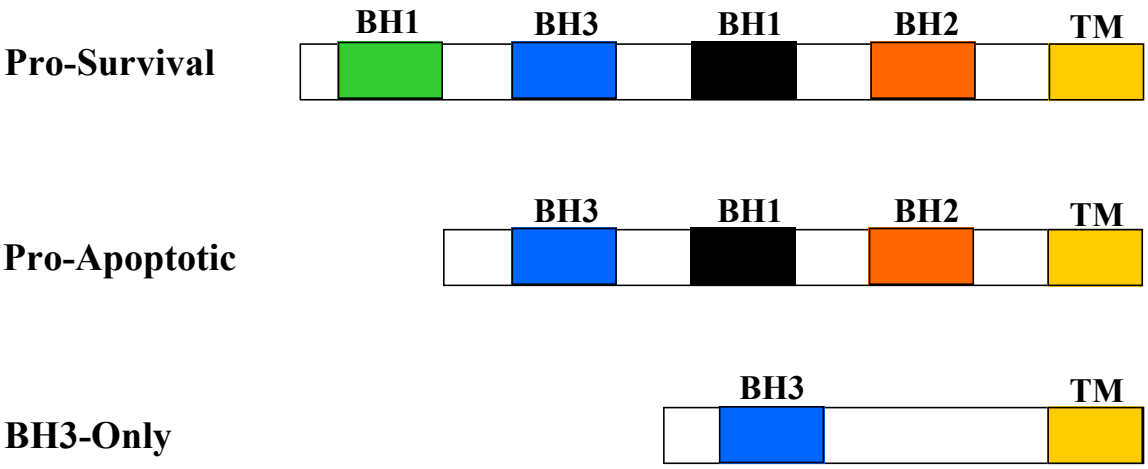

Figure 2.3: The Bcl-2 Family Members. The B-cell Lymphoma-2 (Bcl-2) family contains three members (pro-survival, pro-apoptotic, and BH3-only proteins), all of which share Bcl-2 Homology (BH) domains. The pro-survival members contain all four of the BH domains, as well as a transmembrane domain, and exert their effect by binding and sequestering the pro-apoptotic family members. The pro-apoptotic family members lack the BH4 domain, but contain BH domains 1-3, as well as a transmembrane domain. When activated, the pro-apoptotic family members form pores in the mitochondrial outer membrane (MOM), causing the release of Cytochrome c. Finally, the BH3-only family members contain only the BH3 domain. At present, the mechanism of BH3-only initiated apoptosis is unclear. In the "direct activation" hypothesis, the BH3-only proteins bind the pro-apoptotic family members, which results in pore formation and Cytochrome c release. In the "indirect activation" hypothesis, the pro-apoptotic members aggregate and form pore complexes in the MOM due to sequestration of the pro-survival members by the BH3-only proteins.

the other hand, bind the pro-survival proteins, which prevents apoptosis inhibition by sequestering the pro-survival proteins and preventing them from binding Bax/Bak. Several groups have reported an interaction between the BH3-only proteins Bid (or the cleaved form tBid), Puma, and Bim, with the pro-apoptotic Bcl-2 family member Bax (93; 94; 95), supporting the direct activation hypothesis. Gavathiotis, et al. (96) identified a unique interaction site for Bim (BH-3 only) on Bax (pro-apoptotic) and found that point mutations in this site prevented Bim-induced apoptosis (96). The authors concluded that the binding of Bim to the novel interaction site on Bax resulted in Bax activation (i.e.

direct activation). The BH3-only protein Bad, on the other hand, can only further propagate apoptosis by sequestering the pool of pro-survival Bcl-x_L (93; 95), suggesting that Bad acts as a sensitizer.

In the indirect activation model, BH3-only proteins do not interact with the pro-survival proteins directly. MOM depolarization is achieved simply by sequestering the pro-survival proteins so that pro-apoptotic proteins can homo-oligomerize and form pore complexes. Willis, et al. (98) proposed this model after showing that Bid, Bim and Puma could induce apoptosis without interacting directly with the pro-apoptotic proteins Bax or Bak (98).

The pro-apoptotic protein Bax is a key mediator in the formation of pores within the MOM. Structurally, Bax contains 8 amphipathic α-helices surrounding a single hydrophobic α-helix groove, and bears a striking similarity to the bacterial diphtheria toxin (99; 100). Like diphtheria toxin, it has been presumed that activated Bax is capable of forming a pore complex that, when inserted in the MOM, facilitates the release of cytochrome C. Specifically, the α5/α6 region of Bax is responsible for formation of these pores (101). As a result of its ability to induce apoptotic cell death, Bax has been a popular therapeutic target for gene therapy in treatment of cancer (102; 103; 104; 105; 106; 107).

Genetic Ablation Strategies

A number of strategies utilizing a "suicide gene" have been employed to selectively eliminate certain cell types. Over expression of both the diphtheria toxin (DT) and diphtheria toxin receptor (DTR) are techniques that have been extensively

characterized in cell depletion studies. The DT consists of two subunits: subunits A and B. In most eukaryotic cells, internalization of DT via endocytosis is mediated by the DTB subunit. Once internalized, the A subunit then catalyzes the ADP-ribosylation of elongation factor-2, leading to inhibition of protein translation and, ultimately, cell death (108). Over expression of the DTA gene under control of a tissue-specific promoter has been widely used in a transgenic mouse setting to prevent the development of specific cell types (109; 110; 111; 112). A transgenic mouse has also been generated using a tetracycline-responsive promoter to drive DTA expression, permitting temporal control of cell ablation (113). Both spatial and temporal control of cell ablation was achieved with a Cre-inducible DTA mouse (111; 112; 113; 114; 115). In this system, the DTA transgenic can be crossed with any Cre or inducible Cre mouse currently available to generate mice lacking the cell types in which Cre is expressed.

The DTR transgenic system was developed to capitalize on the resistance of murine cells to DT toxicity. The full length DT is internalized by the binding of the DTB subunit with the heparin-binding EGF-like growth factor receptor (HB-EGF, or the DTR). However, the DTB subunit only weakly binds the murine HB-EGF, so that mouse cells are highly resistant to DT toxicity (119). Over-expression of the human DTR gene in transgenic mice allows inducible cell ablation following administration of DT. The DTR system has been used for tight spatio-temporal control of cell ablation in a number of transgenic animals (117; 120; 121).

Another popular gene therapy strategy for the elimination of specific cell types has been the use of the herpes simplex virus-thymidine kinase (HSV-TK) system. The HSV-TK protein converts ganciclovir to toxic nucleotide analogues, disrupting DNA

synthesis and eventually causing cell death (122). In a transgenic mouse setting, administration of ganciclovir to a transgenic animal will only ablate cells expressing the HSV-TK gene. When gene expression is driven with tissue-specific regulatory elements in a transgenic setting, the HSV-TK system can be used for spatio-temporal deletion of specific cell types (123; 124).

Background Summary

Despite the explosion of research over the past decade in the area of EPCs, the fundamental mechanism by which bone marrow-derived cells contribute to neovascularization remains unknown. Although initial studies demonstrated that EPCs participate in nascent blood vessel formation by direct incorporation into the endothelium (1; 12; 125; 126)14; 15; 127), a number of reports refute this hypothesis (3; 4; 43; 44; 45). Instead, it has been proposed that bone marrow-cells home to incipient vessels and reside in a perivascular location within the vessel wall, augmenting angiogenesis through paracrine pathways. This hypothesis has been supported by the characterization of colonies generated from circulating EPCs, many of which appear to be derived from monocytes. Several bone marrow-derived monocyte-like cells have recently been shown to play a functional role in tumor angiogenesis, albeit without incorporation into the endothelium. The varying progenitor cell definitions, disparate reports over the contributions of bone marrow cells toward neovascularization, and controversy over whether bone marrow cells differentiate into endothelium obviates the need for a strict definition and rigid characterization of circulating pro-angiogenic cells. To this end, we have developed a novel method for fluorescent labeling of bone marrow subpopulations,

with broad applicability towards lineage tracking and BM-subpopulation depletion studies.

CHAPTER 3

TWO MOUSE MODELS FOR ENDOTHELIAL PROGENITOR CELL DEPLETION

Introduction

The initial characterization of an Endothelial Progenitor Cell (EPC) in 1997(1) challenged the prevailing paradigm of post-natal blood vessel growth. Previously it had been assumed that new vessels formed through expansion and remodeling of pre-existing vascular networks (5; 6). However, the work by Asahara et al. (1) for the first time suggested that a circulating cell in the peripheral blood could also contribute to neovascularization. Subsequent studies confirmed that EPCs originate in the bone marrow (12; 13; 20; 12; 30; 127; 128; 129), supporting the existence of a circulating adult hemangioblast.

The absence of a surface marker to uniquely identify EPCs *in vivo* has led to considerable confusion within the field, and no consensus has been reached as to the role that circulating peripheral blood-derived cells play in various settings of post-natal neovascularization. Endothelial Progenitor Cells from blood samples are typically identified and characterized by one of two methods: surface antigen presentation or expansion and differentiation *ex vivo*. In the former strategy, positive selection for a combination of the surface markers CD34, Vascular Endothelial Growth Factor Receptor-2 (VEGFR-2), CD133, and CD31, or the exclusion of markers such as CD45 and CD14, have been used to isolate or enrich for EPCs from PB-MNCs. The combination of antigens CD34, VEGFR-2, and CD133 were originally used for EPC identification due to their presence on either hematopoietic stem cells (HSCs; CD34,

CD133) or endothelial cells (VEGFR-2 and CD31). Although PB-MNCs expressing these markers may contain a progenitor population, it is also possible that sorting strategies based on these markers isolates an enriched HSC population that aberrantly express some endothelial markers.

The second method of EPC identification involves the generation of endothelial-like colonies from peripheral blood samples. EPCs obtained from PB samples expanded *ex vivo* contain multiple cell types from different origins (21; 22; 25; 29) although it is unclear which (if any) of these cells are directly involved in blood vessel growth. The use of several different culture methods for *ex vivo* expansion/differentiation of PB-MNCs has also generated conflicting data (28), and made comparative analysis between studies extremely difficult. The lack of consistency in defining and characterizing EPCs has also led to a number of reports that refute the ability of bone marrow cells to incorporate into blood vessels *in vivo* (3; 44; 45).

The objective of this study was to definitively resolve the functional contribution of bone marrow-derived EPCs in post-natal neovascularization. The first step in reaching this objective was to rigidly define the target cell population. For the purpose of this study, we define "EPCs" as all bone marrow-derived cells that differentiate into mature endothelial cells *in vivo*. Mature endothelial cells are further defined as cells that express VE Cadherin. It follows that, for this study, EPCs are all bone marrow-derived cells that express VE Cadherin.

Our overall approach was to generate a mouse model in which the ability to produce viable EPCs was drastically reduced or eliminated. The general strategy, outlined in Figure 3.1, was to genetically engineer bone marrow cells so that as they

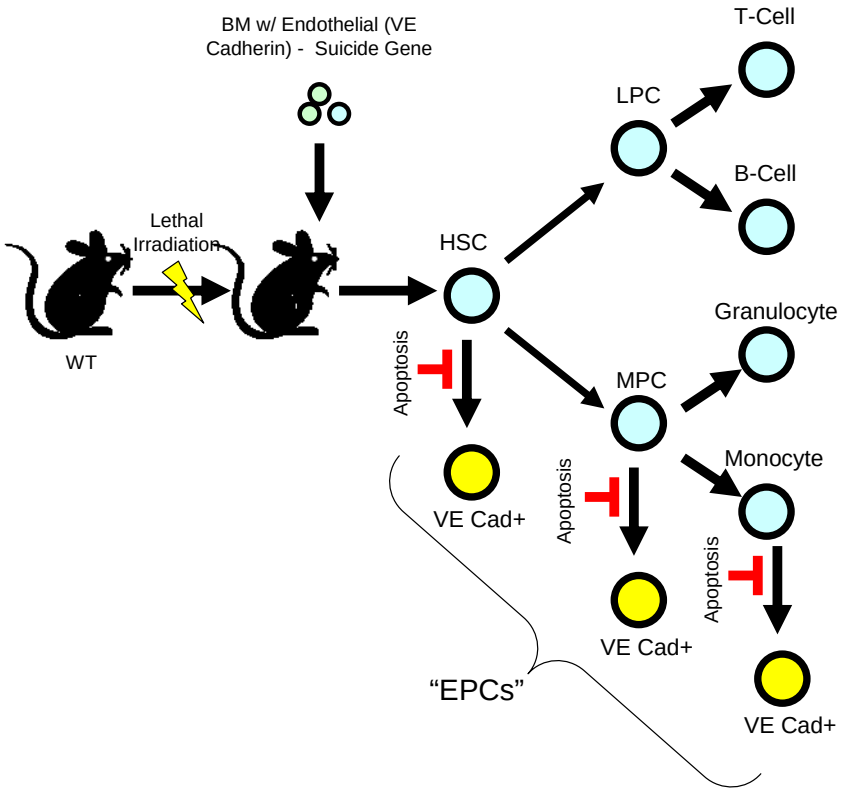

Figure 3.1: General Strategy for EPC Depletion. The general strategy for EPC depletion involves the genetic manipulation of bone marrow so that the cells contain a suicide gene regulated by VE Cadherin transcription. The manipulated bone marrow is then transplanted into a WT, lethally irradiated host. All bone marrow cells then contain the VE Cadherin regulated suicide gene. The majority of bone marrow cells do not express VE Cadherin, so they are unaffected by the genetic manipulation. However, all bone marrow-derived cells that begin to express VE Cadherin (and only those that begin to express VE Cadherin) undergo apoptosis regardless of lineage. WT=Wild Type, BM=Bone Marrow, HSC=Hematopoietic Stem Cell, LPC=Lymphoid Progenitor Cell, MPC=Myeloid Progenitor Cell.

differentiate toward an endothelial lineage, they undergo apoptosis. To this end, we first devised a retroviral (RV) bone marrow-transduction strategy in which an expression construct could be delivered to the bone marrow. The construct was designed so that as bone marrow cells express VE Cadherin (an endothelial cell marker), they will undergo apoptosis. However, our vector, the Retrovirus for Endothelial cell Death (RED), was unable to effectively initiate apoptosis in target cells, rendering this strategy unusable for BMT experiments. Therefore, we employed a second strategy in which the RED

construct was included in a transgenic mouse line (referred to as the Cre-Induced Endothelial cell Death [CrIED] mouse) that we planned to use in bone marrow transplantation experiments. Due to unanticipated complications in our strategy, the CrIED transgenic did not function as predicted, and we were unable to perform BMT experiments.

Methods

Animals

Male ROSA26-βgeo mice(130), CAG-cre/Esr1 mice(131), and wild type C57BL/6 mice were purchased from the Jackson Laboratory. Tie2Cre-ER^{T2} (132) mice were generously donated by Dr. Hanjoong Jo (Emory University, Wallace H. Department of Biomedical Engineering). All animals were fed a standard chow diet ad libitum and had free access to water. All protocols were approved by the Institutional Animal Care and Use Committee and carried out in accordance with the federal guidelines on the principles for the care and use of animals in research.

Generation of Retroviral Plasmids

All plasmids were propagated in Top10 E.Coli (Invitrogen). Transformed E.Coli were grown on LB-Agar plates containing 50 μg/mL of ampicillin. For large scale plasmid preparation, inoculated cultures were grown overnight in 2 L Erlenmeyer flasks containing 200 mL of LB-broth supplemented with 50 μg/mL of ampicillin. Plasmid DNA was isolated using Qiagen HiSpeed Plasmid Maxi-prep.

Construct pFloxLuc: 5' and 3' loxP sites were added sequentially to the pGL3-basic vector (Promega) encoding modified firefly luciferase. Forward and reverse single strand oligonucleotides (Table A1) were synthesized (IDT DNA Technologies) and annealed so that the double stranded sequence contained a HindIII overhang with complete HindIII recognition site at the 5'end, a loxP sequence, and a HindIII overhang lacking the complete recognition site at the 3' end. The annealed, double-stranded oligo was then ligated into the HindIII site located in the MCS of the pGL3-basic vector. A second pair of forward and reverse single strand oligonucleotides (See Appendix B) were synthesized and annealed so that the double stranded sequence contained SalI overhang lacking the complete recognition site at the 5'end, a loxP sequence, and a SalI overhang with complete SalI recognition site at the 3' end. The annealed, double-stranded oligo was then ligated into the SalI site at the 3' end of the luciferase gene. The resulting construct, termed pFloxLuc, contained a modified firefly luciferase gene and polyadenylation signal flanked by LoxP sequences.

Construct pRED/REF: The pRED and pREF retroviral plasmids were constructed from the pTJ124 vector backbone (Donated by Dr. TJ Murphy, Emory University). A polylinker sequence containing ApaI, DraIII, HindIII, and SalI restriction sites was ligated into pTJ124 following removal of the Zeo-eGFP sequence by digestion with StuI and NotI. The resulting plasmid, termed pSRO2, was essentially an empty MMLV-based SIN vector with a multiple cloning site between the retroviral LTR's. Either the ΔN-Bax sequence from pBax-N1 (for pRED) or the EGFP coding sequence from pEGFP-N1 (for pREF) was cloned into the ApaI and DraIII sites of pSR02. The floxed luciferase sequence from pFlox-luc was then cloned into the HindIII and SalI sites of pSR02.

Finally, the 2.5 kb fragment of the murine VE Cadherin promoter (from pVECad, donated by Dr. Roy Sutcliffe, Emory University, Department of Medicine) was ligated into the remaining SalI site. The sequence of the resulting plasmids, termed pRED and pREF, was verified by restriction digests and direct sequencing.

Construct pREF3: The EGFP coding sequence from pEGFP-N1 was cloned into the ApaI and DraIII sites of pSR02. The 2.5 kb fragment of the murine VE Cadherin promoter was then ligated into the SalI site of pSR02. The resulting sequence construct, pREF3, was identical to pREF2 except it lacked the floxed luciferase reporter.

Generation of Transgenic IED mice

The VE-Cadherin promoter-floxed luciferase- ΔN-Bax fragment from pRED and VE-Cadherin promoter – EGFP fragment from pREF3 were isolated by digestion with SalI and DraIII and gel purified. Pronuclear micro-injections were performed by the Emory Transgenic Mouse and Gene Targeting Core in C57BL/6 embryos, which were transferred to pseudo pregnant females for the generation of founders. PCR from tail biopsies of offspring identified two founders.

Retroviral Production

The 293-derived Phoenix Amphotropic (Phx-Ampho) and Ecotropic (Phx-Eco) packaging cell lines (ATCC) were grown to 80% confluence in 100ml plates with growth media consisting of DMEM (Gibco) supplemented with 10% Fetal Bovine Serum, L-glutamine, and Pen/Strep (Invitrogen). Before transfection, 10 ml of fresh media was

added to each plate. Transfections were performed following the JetPRIME™ manufacturers recommended protocol (Polyplus). Briefly, 10 μg of plasmid DNA was added to 500 μL of JetPRIME™ buffer and briefly vortexed and centrifuged. Twenty μL of JetPRIME™ were then added to the DNA mixture, which was again briefly vortexed and centrifuged. The DNA/JetPRIME™ mixture was incubated for 10 minutes at room temperature, then the solution was added to the cells in a drop-wise manner and transported to a 37 C^o/5% CO_2 incubator. After 6-8 hours, transfection media was aspirated and replaced with 25ml of fresh media. Twenty-four hours after the start of transfection, the media was again aspirated, 9 ml of fresh media was added, and the cells were transferred to a 32 C^o/5% CO_2 incubator. Fourty-eight hours after transfection, the conditioned media was collected in a 10 mL syringe and passed through a 45μm low protein binding filter and either frozen and stored at -80˚Cor used immediately for transduction. Conditioned media was collected afterward at 12 hour intervals for up to 7 days following transfection.

Bone Marrow Isolation and Transduction

A detailed protocol for bone marrow transduction is included in the Appendix. The transduction protocol was modified from Ide, et al (133). Briefly, mice were euthanized by CO_2 inhalation and the long bones were flushed with cold PBS. Bone marrow cells were labeled with anti-Sca1-PE antibodies (Miltenyi), then separated with anti-PE micro-beads (Miltenyi) using an AutoMACS sorter (Miltenyi). Sorted cells were cultured in Stempro-34 media (Invitrogen) supplemented with mSCF (100 ng/ml, Sigma), Flt-3 (100 ng/ml, R and D), Il-3 (20 ng/ml, Sigma), and Il-11 (100 ng/ml, Sigma) for 24

hours. Retroviral supernatant was centrifuged overnight at 4˚C and 9000g, then the resulting pellet was resuspended at 1/20 the original volume in complete Stempro-34 with cytokines. Retrovirus was bound to retronectin coated plates by centrifugation for 1 hr at 4˚C and 2500 rpm. Bone marrow cells were plated on RV/retronectin plates, and cultured for 24 hrs at 32 C^o.

Cell Lines and Culture

The NIH/3T3 cells (ATCC) were grown at 37 C^o, 5% CO_2 in DMEM supplemented with 10% calf serum, L-glutamine, and Pen/Strep, respectively. The 3T3 cells were grown in 10 cm tissue culture-treated dishes to 80% confluence, then passaged at a ratio of 1:5. SVEC4-10, HMEC-1, and MS1 cells (all obtained from ATCC) were grown at 37 C^o, 5% CO_2 in DMEM supplemented with 10% fetal bovine serum, L-glutamine, and Pen/Strep in 10 cm tissue culture-treated dishes coated with gelatin until 80% confluent, then passage at a ratio of 1:5.

For transduction, cells were plated in 6-well dishes at 40% confluence. Two mL of retrovirus and media was added per well, and supplemented with 8 μg/mL polybrene (Sigma). Plates were spun in a spinning bucket rotary centrifuge pre-warmed to 32˚Cfor 1 hr, then returned to the inital culture conditions.

Retroviral Titration

A qPCR-based titration kit (Clontech) was used to determine viral copy number in each viral supernatant. Viral RNA from 150 μL of retroviral supernatant was isolated and DNase purified. Reverse transcription and qPCR was performed in a 96-well light

cycler (Applied Biosystems). Threshold cycle values were calculated for serial dilutions of RNA from each virus, and copy number was calculated from an exponential standard curve generated from serial dilutions of premade MMLV-RNA standards.

qRT-PCR

Genomic DNA or mRNA was purified using a commercial kit (Qiagen). RNA was reverse transcribed into cDNA using the SuperScript™ III First Strand Synthesis System (Invitrogen), which was subsequently purified using a commercially available kit (Qiagen). Primers were designed using PrimerQuest software (IDT DNA technologies) for mouse VE Cadherin, EGFP, and mouse 18s. SYBR Green intercalating dye (Applied Biosystems) was used to perform real time PCR with the ABI Prism 7700 Sequence Detection System (Applied Biosystems). Standards for each gene were amplified from cDNA and purified. Standard concentrations were determined using spectrophotometric measurement at 260 nm, and standards were serially diluted to an appropriate range of concentrations. Transcript concentration in template cDNA solutions was quantified from the linear standard curve, normalized to 18s copy number, and expressed as copies per 10^6 18s.

TUNEL Stain

Mice were euthanized by CO_2 inhalation, and pressure fixed in 10% formalin. Liver, heart, lung, spleen, kidney and aorta were dissected, embedded in OCT medium, and snap frozen at -80 ^oC. Tissues were sectioned in 7 μm slices, then stained using an ApopTag Red apoptosis detection kit (Millipore) according to the manufacturers'

instructions. The ApopTag is based on the TUNEL assay, and labels the 3'-OH termini generated in apoptotic cells. Images were recorded with a Zeiss upright fluorescence microscope.

Luciferase Assay

Cell and tissue lysates were isolated using the Promega luciferase assay system. For tissue isolation, samples were homogenized for 30 seconds in a rotary tissue homogenizer, centrifuged for 1 minute at 10,000g, and then the supernatants were removed for analysis. Total protein content was determined using a modified BCA assay (Biorad), and luminescence was quantified using a Zylux luminometer.

Chemiluminescence Imaging

Mice were anesthetized by i.p. injection of a mixture of xylazine (10 mg/kg) and ketamine (80 mg/kg) and, prior to imaging, all hair was removed from the legs and lower abdomen using depilatory cream (Nair, manufacturer). Sterile filtered luciferin substrate dissolved in PBS was administered via i.p. injection (150 mg/kg). Mice were placed on a heated stage in an IVIS Lumina system (Caliper Life Sciences) and chemiluminescent images were recorded 3 minutes following luciferase injections. After imaging was completed, mice were allowed to recover from anesthesia on a heating pad before being returned to their normal housing facilities.

Results

A Retroviral Bone Marrow Transduction Approach for Eliminating EPCs

Our initial approach was to implement a retroviral bone marrow-transduction and transplantation procedure that would allow us to selectively ablate EPCs. As stated previously, we defined EPCs as all bone marrow-derived cells that express VE Cadherin. The proposed Bone Marrow Transduction and Transplantation (BMTT) strategy is outlined in Figure 3.2. In the BMTT approach, bone marrow cells are transduced *ex vivo* with a retrovirus containing a suicide gene driven by the VE Cadherin promoter. The genetically modified cells are then transplanted into a lethally irradiated WT host, so that only the bone marrow contains the desired transgene. Following hematopoietic reconstitution, the entire marrow compartment (including all cells *derived* from bone marrow) of the recipient animal carries the retroviral construct. Since VE Cadherin is only expressed in mature endothelial cells, the majority of the cells from the BM are unaffected by the suicide gene. In any BM cells that differentiate toward an endothelial lineage (i.e., BM-derived endothelial cells), the transgene is activated, causing cell death. As a result, the transplant recipient, containing RV-transduced marrow, is unable to produce viable BM-derived endothelial cells.

Implementation of the BMTT strategy required careful design of the Retrovirus for Endothelial cell Death (RED) construct. To circumvent a potential reduction in titer due to expression of a toxic gene product in the retroviral packaging cell line, we incorporated the cre/LoxP system in our construct design. The RED vector was derived from TJ124 (Figure 3.2): a self-inactivating Moloney murine leukemia virus (SIN-MMLV) with a mutation in the 3' long terminal repeat (LTR) TATA-box that inactivates

the endogenous retroviral promoter. To generate RED, the murine VE Cadherin promoter driving expression of a floxed luciferase reporter gene (including a poly-adenylation [poly-A] signal) upstream of a sequence corresponding to amino acids 112-192 of the human Bax gene (ΔN-Bax) and a second poly-A signal was inserted in place of the cytomegalovirus promoter/enhanced green fluorescent protein (CMV-EGFP) sequence between the retroviral LTRs of TJ124 (Figure 3.2). The RED expression construct was incorporated into the retroviral backbone in reverse orientation (i.e. in the 3' to 5' direction) as additional security to prevent expression of the toxic ΔN-Bax protein in the packaging cell line and to avoid truncation of the viral RNA due to the presence of an internal poly-A signal between the retroviral LTRs.

A Retrovirus for Endothelial cell Fluorescence (REF, Figure 3.2) was generated identically to RED, except that EGFP was inserted in place of the ΔN-Bax gene. Both the RED and REF constructs were designed so that when a homogeneous cell population was transduced (i.e. bone marrow), only the cells that differentiate into endothelial cells undergo apoptosis (with RED) or become fluorescently labeled (with REF), respectively. A simplified Retrovirus for Endothelial cell Fluorescence version 3 (REF3, Figure 3.2) was also generated which contains the VE Cadherin promoter directly driving expression of EGFP.

Feasibility of a Bone Marrow Transduction Strategy

Due to the large number of RV constructs and packaging systems available, as well as the innumerable reports for the optimization of RV-mediated bone marrow transduction, we sought to establish a consistent methodology utilizing RV vectors for

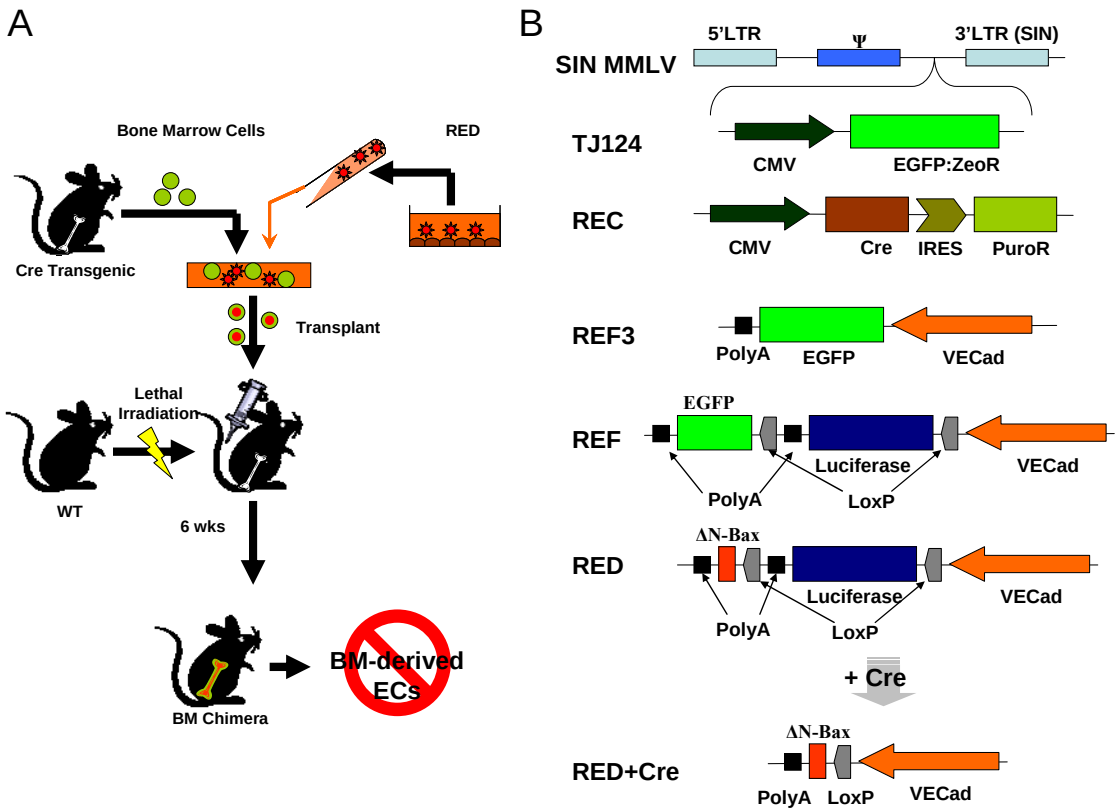

Figure 3.2: Strategy for Retrovirus-Induced Bone Marrow-derived Endothelial Cell Ablation. The Bone Marrow Transduction and Transplantation (BMTT) strategy requires the isolation of bone marrow cells from a mouse ubiquitously expressing Cre recombinase. Bone marrow cells are transduced with the RED vector; a construct that induces cell death in an endothelial-specific manner. Cells containing the RED construct are transplanted into a lethally irradiated WT host. After engraftment, bone marrow cells from the resulting chimera will undergo apoptosis if they differentiate into endothelial cells. B) All constructs were derived from a self-inactivating (SIN) MMLV vector. TJ124 contains a CMV promoter driving expression of the EGFP/Zeocin resistance gene. The REC vector consists of a CMV promoter driving expression of Cre recombinase, with an Internal Ribosome Entry Site (IRES) regulating expression of Puromycin resistance. REF3 contains an internal VE Cadherin promoter driving expression of EGFP, followed by a poly-A sequence. The Insert is in reverse orientation to the retroviral LTRs to allow transcription through the poly-A sequence during virus production. The REF construct contains the VE Cadherin promoter driving expression of a floxed luciferase reporter, upstream of EGFP. This construct generates endothelial specific expression of luciferase until activated by Cre, at which point the floxed reporter is excised and EGFP is expressed. The RED construct contains the VE Cadherin promoter driving expression of a floxed luciferase reporter, upstream of ΔN-Bax, thus generating endothelial specific expression of luciferase until activated by Cre, at which point the floxed reporter is excised and Δ-Bax is expressed, resulting in apoptotic cell death.

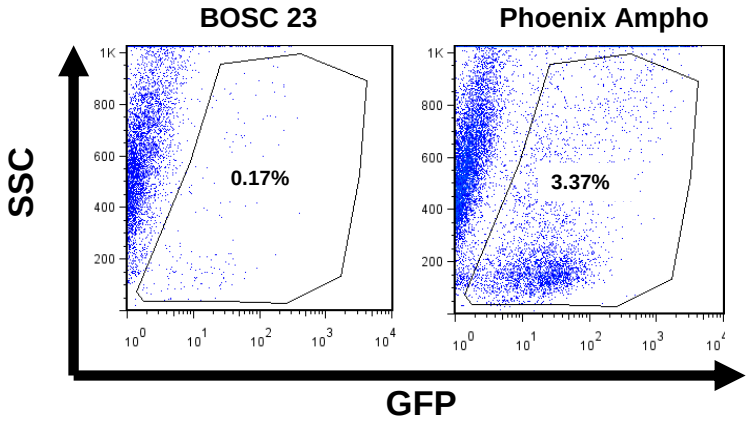

Figure 3.3: Comparison of BOSC23 and Phoenix Ampho Packaging Cell Lines Flow cytometry was performed on unsorted bone marrow transduced with TJ124 (containing an internal CMV promoter driving GFP expression) retroviral supernatant obtained from BOSC23 or Phoenix Ampho packaging cell lines. The number of GFP positive cells was higher when transduced with virus generated from the Phoenix Ampho packaging cell line.

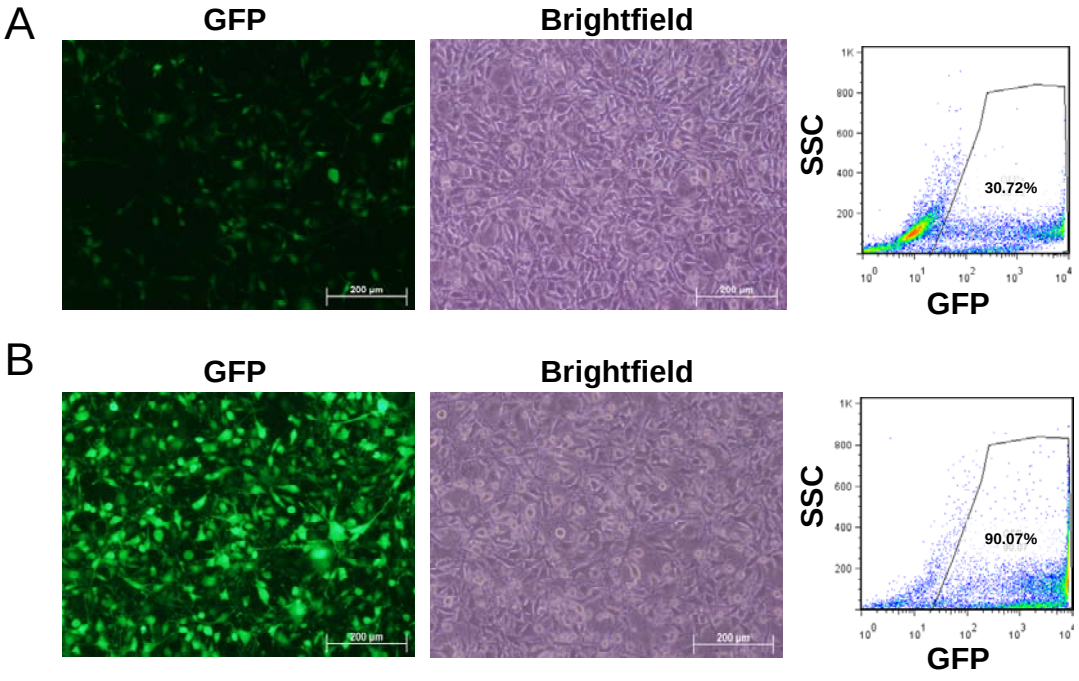

Figure 3.4: Effect of LSC on transduction efficiency. 3T3 cells were transduced with non-concentrated (A) or 10X concentrated with LSC (B) TJ124 retrovirus, then imaged for fluorescence and examined with flow cytometry. Concentration by LSC increased the amount of GFP positive cells more than 3-fold.

transduction of bone marrow prior to testing our custom-designed constructs. Following a simplified protocol established by Gough and Raines (134), we transduced murine bone marrow cells with RV supernatant containing TJ124 (an MMLV-based SIN vector with CMV driven EGFP) generated from either BOSC 23 (135) or Phoenix Ampho (136) packaging cell lines. GFP expression in TJ124-transduced cells was near baseline following infection with supernatant from the BOSC 23 cell line, and only observed in ~3% of TJ124-transduced cells infected with supernatant collected from the Phoenix Ampho cell line (Figure 3.3). Due to the observed inefficiency of gene delivery to bone marrow cells, we explored additional techniques to improve transduction rates.

Significant improvements in titer have been obtained by concentration of RV supernatant with overnight, low speed centrifugation (LSC) (133). In our hands, transduction of 3T3 cells improved 3-fold following 10x concentration of TJ124 (generated with the Phoenix Ampho packaging line) using LSC (Figure 3.4).

Improvements in bone marrow transduction have also been reported following enrichment for cells expressing Stem Cell Antigen 1 (Sca1). Magnetic bead sorting resulted in an increase in Sca1 purity to ~85%, compared to ~5% in whole bone marrow (Figure 3.5). Sorting for Sca1 prior to the addition of 20x concentrated TJ124 RV supernatant enabled transduction efficiencies of 20% in bone marrow cells when GFP expression was analyzed by flow cytometry 48 hours after transduction (Figure 3.5). Transduction efficiencies could be further enhanced through the use of retronectin-mediated transduction with a concentrated MSCV vector expressing GFP. Lethally irradiated mice receiving transplants of cells transduced with concentrated RV through retronectin enhanced transduction led to over 85% of PB-MNCs expressing GFP

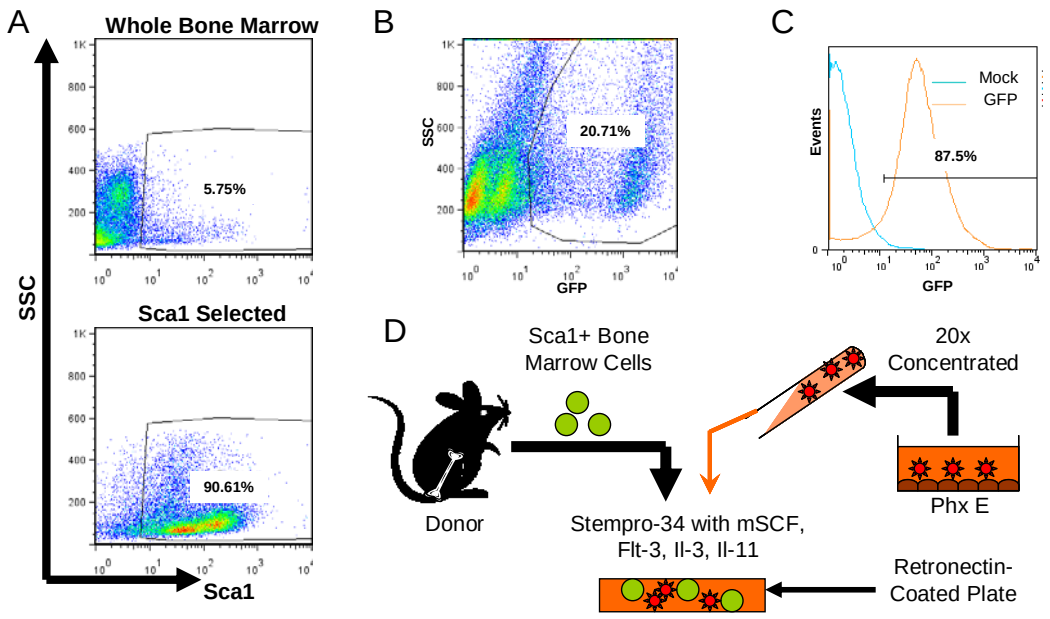

Figure 3.5: Optimized Bone Marrow Transduction Protocol. (A) Flow cytometry for Sca1+ in whole bone marrow before (top) and after (bottom) enrichment with magnetic bead sorting. (B) Flow cytometry for GFP expression in Sca1+ cells 48 hours after transduction with 20X LSC concentrated TJ124. (C) Flow cytometry on peripheral blood sample of a BMT mouse receiving cells transduced with an MSCV vector expressing GFP and Retronectin-enhanced transduction protocols following Sca1 selection. The schematic in (D) shows the final BM transduction protocol. Donor cells are sorted for Sca1+ and cultured with concentrated RV in Stempro-34 media with a cytokine cocktail on Retronectin coated plates. (C courtesy of Dr. Natalia Landazuri; Orange is MSCV-GFP transduced, blue is untreated).

(Figure 3.5, see *Methods* for a detailed protocol). Our final bone marrow transduction protocol consisted of a Sca1 sort, culture in mitogenic media, followed by a retronectin-facilitated transduction using virus concentrated with LSC (Figure 3.5). The ability to consistently achieve transduction efficiencies of at least 85% demonstrated the feasibility of using an MMLV-based vector for gene delivery to bone marrow cells in mice.

An *in vitro* System for Assessment of Retroviral Function

To establish a system for evaluating the efficacy of the RV constructs *in vitro*, we examined the susceptibility of various cell lines to retroviral-mediated gene transfer. An

immortalized mouse lymphoid endothelial line [SVEC4-10 (137)], a human dermal microvascular endothelial cell line [HMEC-1 (138)], and a mouse embryonic fibroblast cell line [NIH/3T3 (139)] were transduced with concentrated TJ124. Robust fluorescence was seen in all cell types, with >90% of SVEC4-10 and 3T3 cells expressing GFP. The HMEC-1 line showed more modest transduction efficiency, with ~35% of the cells expressing GFP (Figure 3.6).

Activity of the mouse VE Cadherin promoter was then examined by transducing different cell types with 10x concentrated REF3 (in which the VE Cadherin promoter drives GFP expression directly). As shown in Figure 3.6, the percentage of GFP+ cells in both SVEC4-10 and HMEC-1 cells was markedly lower following REF3 transduction (3.3% and 1.4%, respectively) than TJ124 transduction (84.9% and 35.3%, respectively). Interestingly, transduction of 3T3 cells with REF3 yielded the highest number of GFP+ cells out of the 3 cell lines. The low fluorescence intensity of cells transduced with REF3 indicates that the VE Cadherin promoter provides weak transcriptional activity. The weak fluorescence and low transduction efficiencies in the SVEC4-10 and HMEC-1 lines was suprising, since we anticipated robust activity of the VE Cadherin promoter in endothelial cells.

Attempted *In vitro* Validation of RED/REF

Although the VE Cadherin promoter showed limited activity when delivered to endothelial cells with a retrovirus, it was still necessary to assess the functionality of

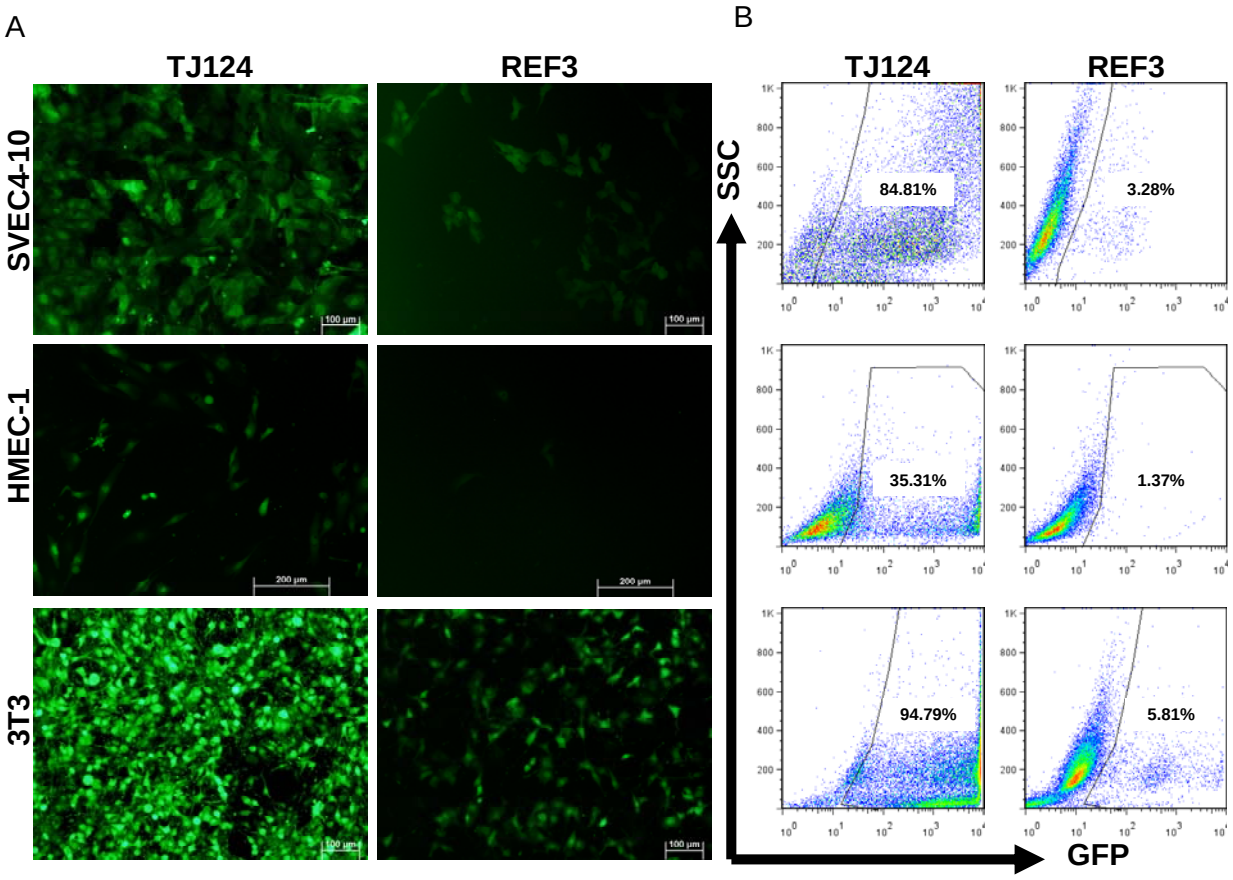

Figure 3.6: Evaluation of Cell Lines For Use In Assessment of Construct Function. SVEC4-10, HMEC-1, and 3T3 cells were transduced with either 10x concentrated TJ124 or REF3. GFP was detected either microscopically (A) or with flow cytometry (B). All cell lines showed robust GFP expression following transduction with TJ124. GFP was detected in all cell lines following transduction with REF3, but expression was reduced compared to that seen following TJ124 transduction.

RED and REF *in vitro*. HMEC-1 cells were first transduced with a retrovirus containing a bicistronic expression cassette to overexpress Cre recombinase and confer puromycin resistance (REC). Following antibiotic selection, the cells (HMEC-1/Cre) were transduced with REF and assessed for GFP expression with flow cytometry. Even after 3 rounds of transduction with REF, we were unable to detect any GFP (Figure 3.7).

However, HMEC-1/Cre cells transduced with TJ124 in parallel expressed GFP in nearly 75% of the cells.

The absence of GFP in REF transduced HMEC-1/Cre cells indicated that the REF construct was not efficiently transducing the target cells, or that Cre-mediated recombination was inhibited. To address this issue, luciferase activity was examined following RED/REF transduction. Measurement of luciferase activity allowed us direct assessment of the retroviral VE Cadherin promoter activity within the RED and REF constructs. Two cell lines, SVEC4-10 and 3T3 cells, were transduced with REF and RED, and then cell lysates were assayed for chemiluminescence using a luciferase assay. Both RED and REF transduced SVEC4-10 cells exhibited luciferase activity above baseline (Figure 3.7). 3T3 cells transduced with RED and REF showed higher luciferase activity than SVEC4-10 cells (Figure 3.7), but the values were still extremely low. The results from the luciferase assay indicate the presence of luciferase in lysate from RED and REF transduced SVEC4-10 and 3T3 cells, albeit at very low levels. These data verify that the luciferase gene was functional in both constructs. However, we could not determine whether the low level of luciferase activity was due to low transduction rates of RED and REF, inactivation of the vectors following transduction, or low transcriptional activity of the VE Cadherin promoter.

Retroviral Integration

The use of a tissue-specific promoter confounded our ability to determine the overall transduction efficiency with RED, REF and REF3 vectors. Since GFP fluorescence was used as an endpoint, it was impossible to determine if the absence of

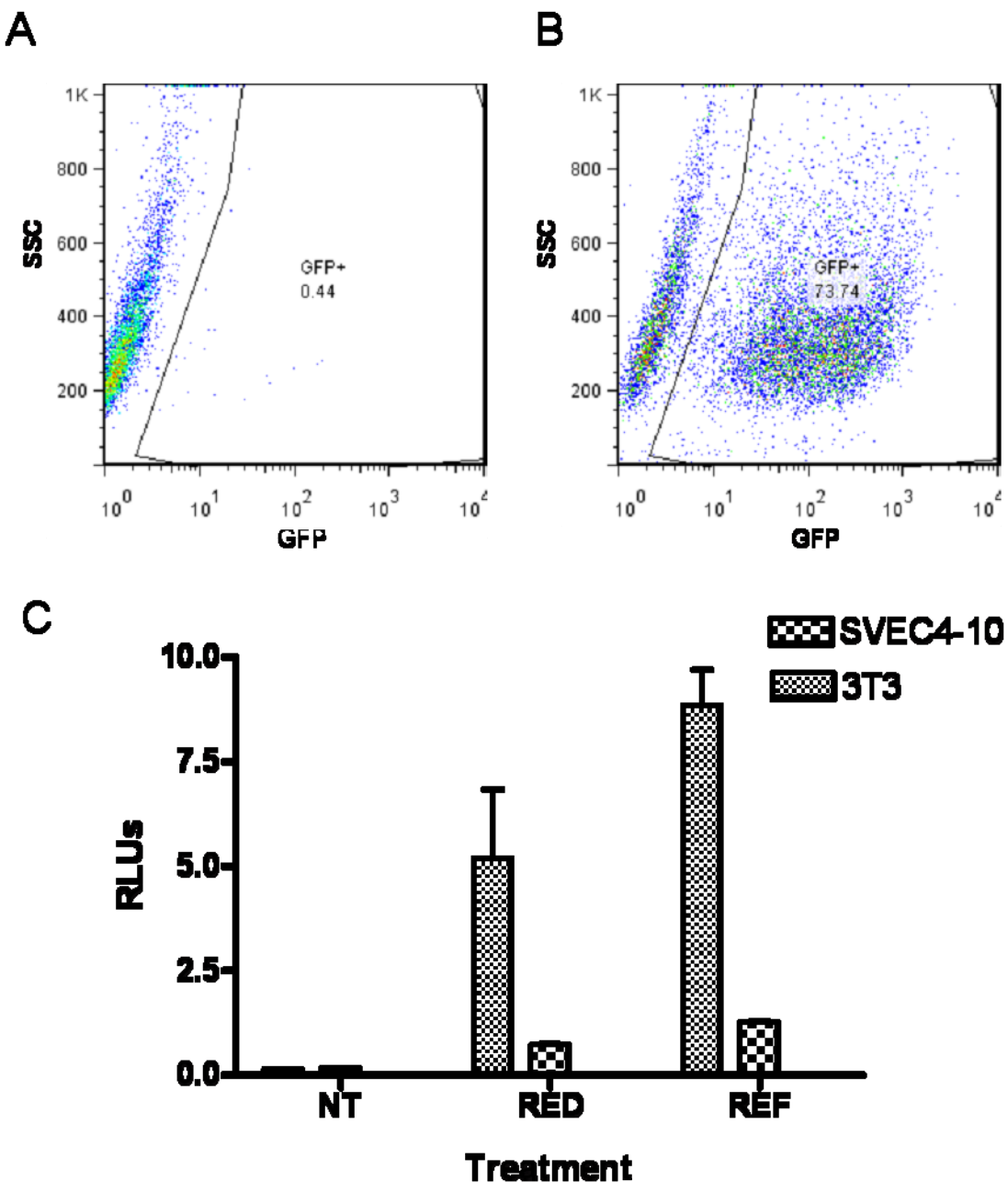

Figure 3.7: REF and RED Function *in vitro*. SVEC4-10 were transduced with REC and selected for puromycin resistance. Flow cytometry was performed on the SVEC4-10/Cre cells following transduction with REF (A) or TJ124 (B). TJ124 transduction generated an increase in the percentage of cells expressing GFP, while transduction with REF3 led to no appreciable GFP fluorescence. C) Lysates from SVEC4-10 and 3T3 cells transduced with either RED or REF showed low luciferase activity, but chemiluminescence was elevated over baseline.

signal was due to ineffective transduction or inactivity of the VE Cadherin promoter following transduction cells. Fifty-one percent of 3T3 and 24% of MS1 cells (an immortalized mouse endothelial cell line) transduced with TJ124 expressed GFP. However less than 2% of either cell type expressed GFP when transduced with REF3 (Figure 3.8). We anticipated a low percentage of GFP+ events in 3T3 cells containing the REF3 construct, since the VE Cadherin promoter should not be active in fibroblasts. However, if both viruses were produced at equivalent titers, we expected the frequency of GFP-positive MS1 cells after transduction with REF3 to have been equivalent to that seen following transduction with TJ124. In light of this evidence, we hypothesized that our tissue specific vectors were not generated at comparable titers.

A retroviral titering kit that determines the number of viral RNA copies in an aliquot of viral supernatant via qRT-PCR by amplification of the RV packaging sequence, was then used to estimate titer for the different vectors. This approach allowed us to circumvent the complications associated with titering tissue-specific vectors. As shown in Table 3.1, PhxE packaging cells produced virions at an equivalent rate for TJ124, REF, and REF3; a surprising result given the low number of GFP+ cells following REF and REF3 transduction. To explore the possibility that REF and REF3 were incorporating into target cells with less efficiency than TJ124, qRT-PCR for GFP was performed on genomic DNA from transduced 3T3 and MS1 cells. Remarkably, relative GFP copy number in genomic DNA from TJ124 transduced cells was ~10 times higher then in genomic DNA from REF or REF3 transduced cells (Figure 3.8). This suggests that, although REF and REF3 virus were packaged as competently as TJ124, the

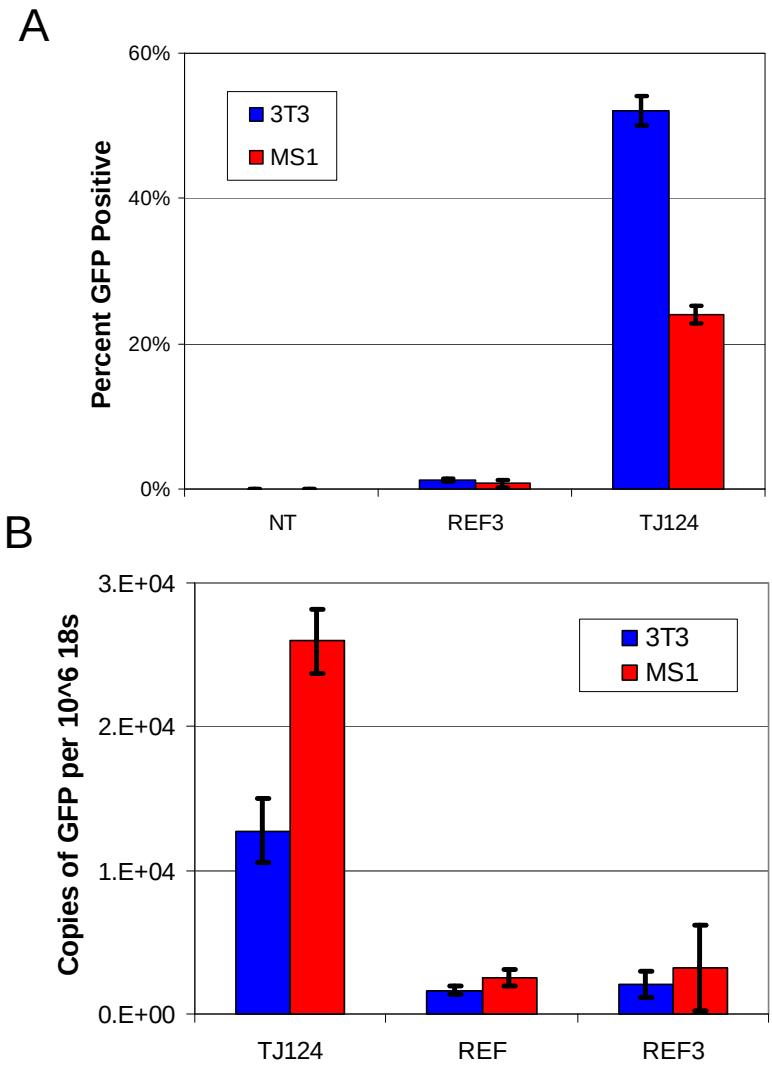

Figure 3.8: Genomic Integration of Vector DNA following REF and REF3 Transduction. A) Flow cytometry on MS1 and 3T3 cells following transduction with TJ124 showed. B) Quantitative Real Time-PCR for EGFP indicated a 10 to 20-fold higher frequency of genomic integration following transduction with TJ124 compared to REF or REF3.

ability of the vectors to incorporate into the host cells genomic DNA was greatly diminished.

A Transgenic Bone Marrow Transplantation Approach to Eliminating EPCs

The difficulties encountered using the BMTT approach led us to pursue an alternative transgenic mouse strategy for EPC depletion studies. Two female founders

Table 3.1: Estimated viral load of vectors. The number of viral RNA copies per mL of viral supernatant was determined using quantitative real-time PCR.

Vector	vRNA copies/mL
TJ124	9.83 E+09
REF	5.85 E+10
REF3	5.10 E+10

were established that carried the RED and REF3 transgenes (founders 15 and 19), which were then crossed with male CAGGCre^{TM} mice. Protein lysates isolated from tail clippings were taken from both founders and their F1 progeny, and a luciferase assay was performed to assess transgene function. Some of the offspring from the #19 founder contained the transgene, as confirmed by PCR analysis, but tail lysates showed no luciferase activity. However, all offspring from the #15 founder that contained the transgene (as confirmed by PCR analysis) also showed robust luciferase activity (data not shown). These results indicate that there were multiple integration sites in the #19 founder, at least one of which contained an inactive copy of the transgene. Therefore, all subsequent studies were performed on mice from the #15 founder.

The proposed transgenic mouse approach to eliminate bone marrow-derived endothelial cells is outlined in Figure 3.9. In this strategy, bone marrow from the CrIED mouse is transplanted into a lethally irradiated recipient. The resulting BM-chimera contains the CrIED transgene only in the bone marrow. When given tamoxifen (TM), the luciferase gene from the RED construct is then excised. Due to the inherent specificity of the VE Cadherin promoter, the toxic ΔN-Bax is only expressed as the bone marrow cells differentiate into endothelial cells (i.e. EPCs).

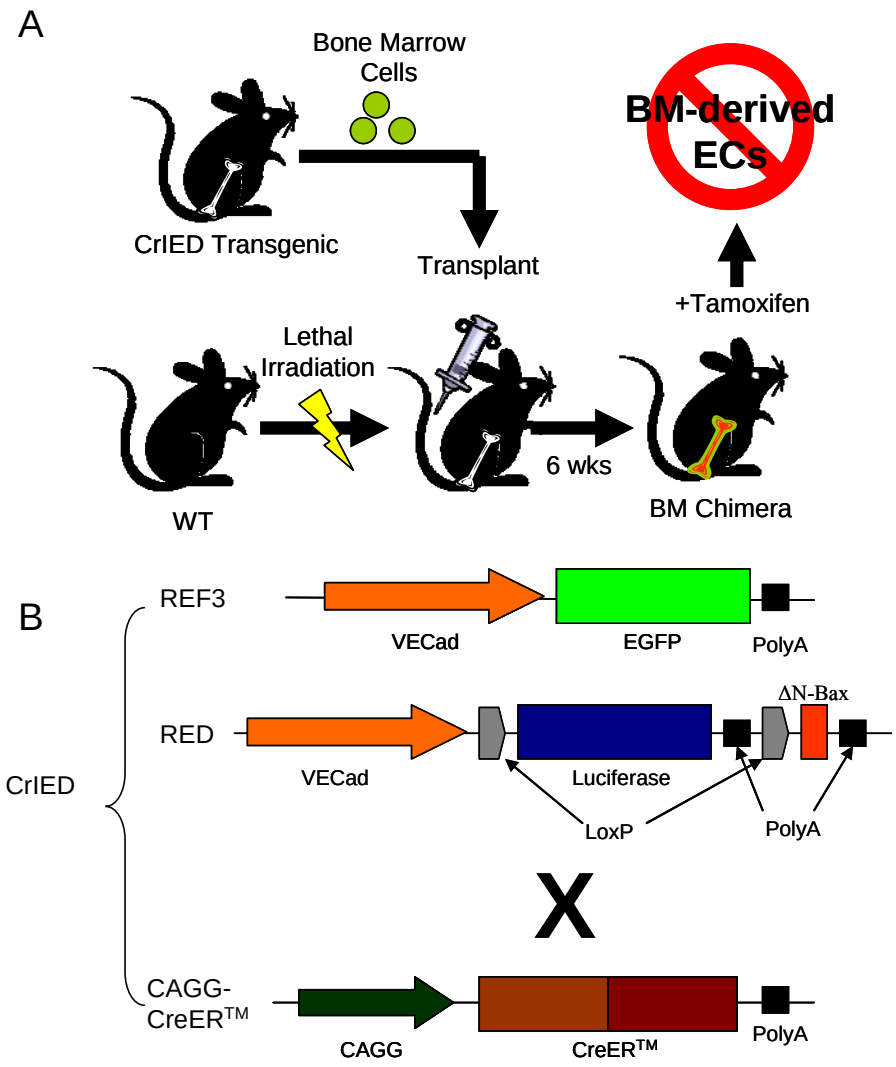

Figure 3.9: General CrIED transgenic strategy. (A) In the CrIED BMT strategy, bone marrow from mice containing the Cre Inducible Endothelial cell Death (CrIED) transgenes is transplanted into a lethally irradiated WT recipient. Following engraftment, the chimeras are treated with Tamoxifen to activate cre-mediated recombination. Any bone marrow-derived cells that begin differentiation into endothelial cells will undergo apoptosis. (B) The CrIED transgenic contains 3 expression constructs: RED, REF3, and CAGCreER^{TM}.

Functional Assessment of CrIED Transgene *ex vivo*

In order to examine the function of our transgenic construct, an *ex vivo* approach was utilized that permitted avoidance of the complexity frequently encountered in an

intact animal. Aortic endothelial cells from the CrIED transgenic mouse were isolated and immortalized with the SV-40 Large T antigen and expanded in culture (cells were generated by Chi When Ni, Emory University). Flow cytometry was performed to detect GFP expression in immortalized mouse aortic endothelial cells (iMAECs) derived from CrIED or C57BL/6J. There was no detectable GFP fluorescence in CrIED/iMAECs, and no discernable shift in the fluorescence intensity compared to C57B/6J/iMAECs (Figure 3.10). The absence of any GFP signal in CrIED/iMAECs indicates that the VE Cadherin-EGFP expression construct is not functional in the CrIED mouse.

We next examined luciferase activity in cell lysates from CrIED/iMAECs. Although VE Cadherin expression by qRT-PCR in iMAECs was low (data not shown), we were able to detect a slight but significant increase in luminescence in lysates from CrIED/iMAECs compared to lysates from C57BL/6/iMAECs (Figure 3.10). The magnitude of the signal was not as high as we had anticipated, but the data indicated that luciferase was indeed expressed by the RED transgene in cultured CrIED/iMAECs.

The ΔN-Bax gene was activated in culture by the addition of 4-hydroxytamoxifen (4-OHT) to the culture media of CrIED/iMAECs. Cell viability was assessed from 0 to 48 hours following addition of 4-OHT. No cytotoxicity was observed in either CrIED/iMAECs or C57B/6J/iMAECs (Figure 3.11). The failure to detect dead cells in culture was unexpected, but was at first attributed to the low activity of the VE Cadherin promoter.

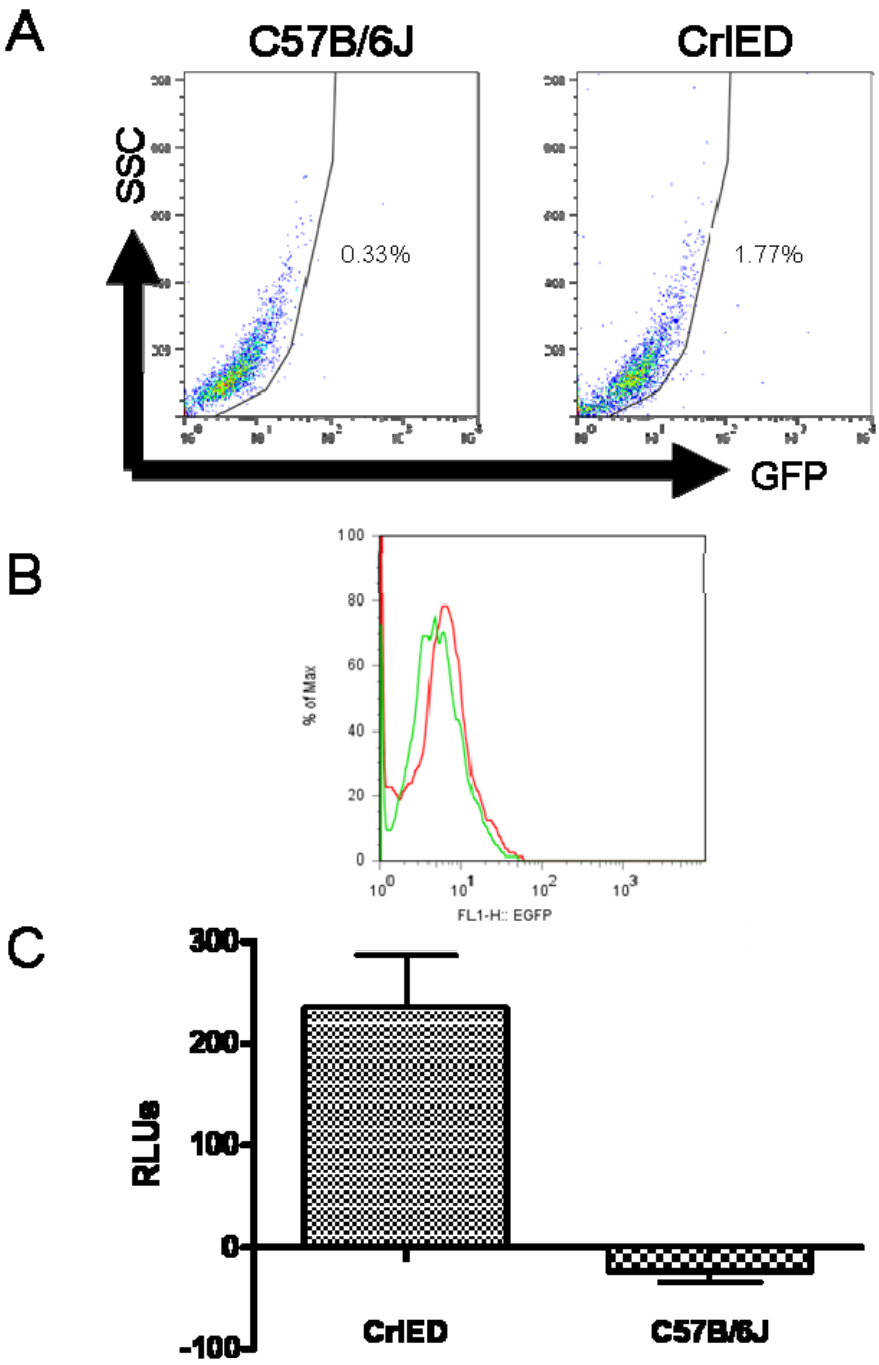

Figure 3.10: Characterization of iMAECs from CrIED mice. Aortic endothelial cells were isolated from C57B/6J and CrIED mice, and immortalized with the SV-40 Large T antigen to generate iMAECs. CrIED iMAEC showed no detectible GFP positive cells (A) or shift in GFP fluorescence (B) when analyzed with flow cytometry. (C) Chemiluminescence of lysates isolated from iMAECs assessed to determine luciferase activity in iMAECs. Luciferase activity in lysates from CrIED-derived iMAECs was extremely faint, but above WT values.

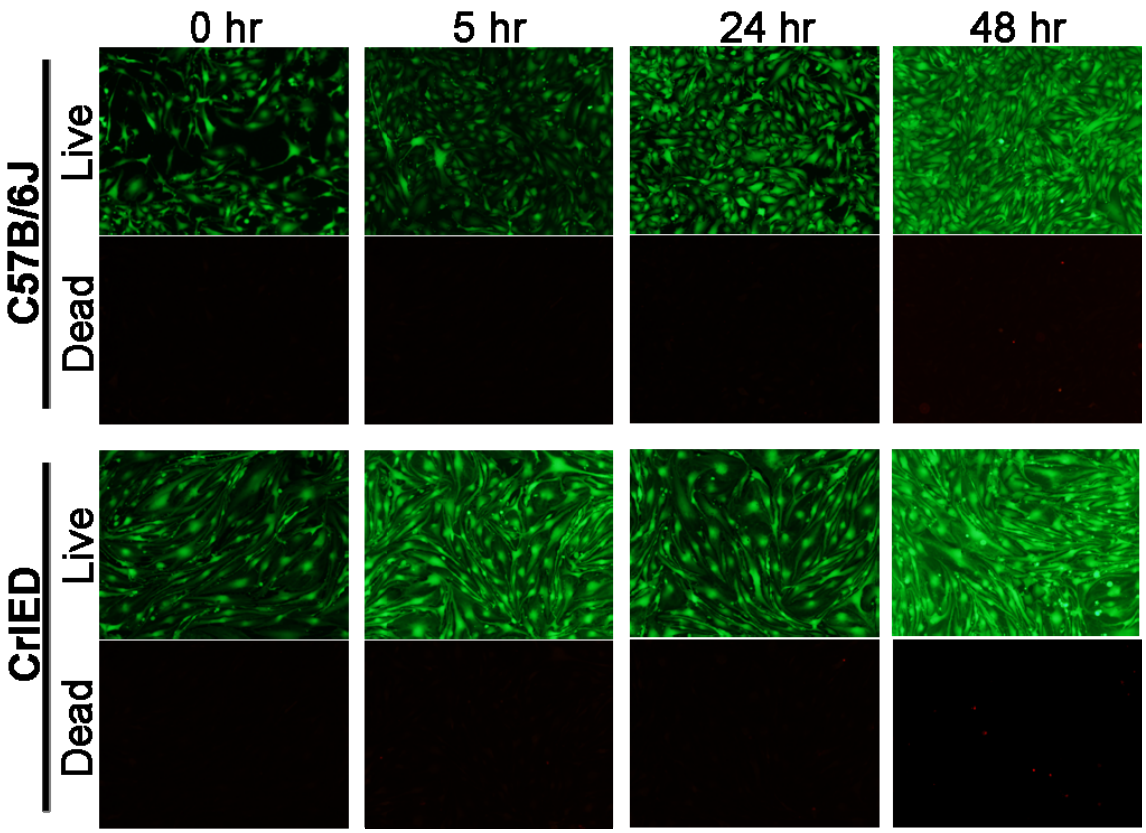

Figure 3.11: Sensitivity of CrIED-Derived iMAECs to 4-Hydroxytamoxifen. iMAECs from CrIED and C57B/6J were cultured in normal media supplemented with 4-hydroxytamoxifen to induce Cre recombination, then stained with a Live/Dead kit from 0-48 hours. No changed in cell viability was observed between groups. Green = Live, Red = Dead.

Luciferase activity *In Vivo*

The transcriptional activity of the VE Cadherin promoter was much lower than anticipated in all cell culture experiments. We hypothesized that the low promoter activity was a result of the *in vitro* environment, and that *in vivo* gene regulation by the VE Cadherin promoter would be stronger. Therefore, we sought to examine the activity of the VE Cadherin promoter *in vivo*. Transgenic CrIED mice were injected with D-luciferin substrate in PBS and imaged simultaneously using an IVIS chemiluminescence imaging system. No luminescence was observed in the WT animals, but luminescence

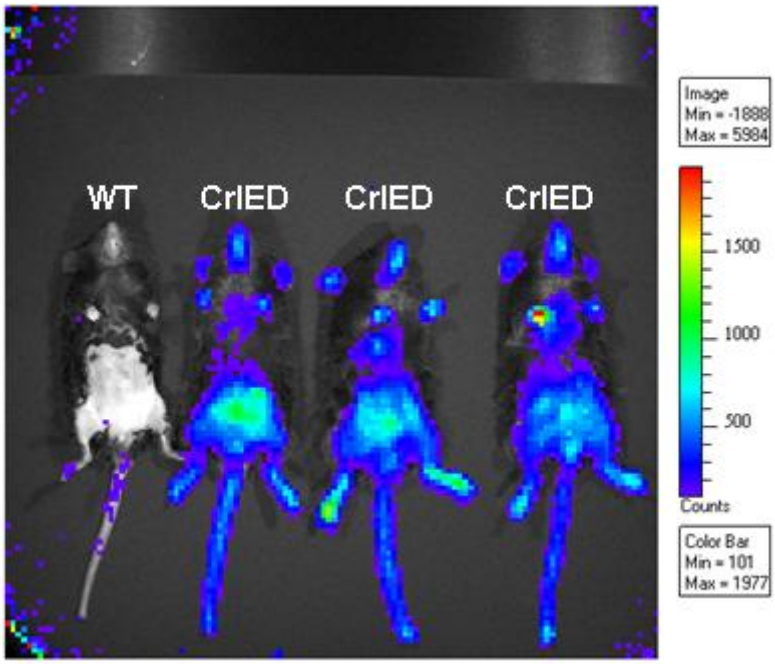

Figure 3.12: Chemiluminescence of CrIED mice. WT and CrIED mice were injected with D-luciferin substrate and imaged with an IVIS chemiluminescence imaging system. Chemiluminescence was easily detected in the CrIED transgenic animals, but none was observed in the WT.

signal was detected at all of the exposed skin in the CrIED animals (Figure 3.12). This data verified that the luciferase gene was indeed expressed, but the luminescence imaging system did not have the spatial resolution to determine if luciferase was expressed in a tissue-specific manner.

Results from earlier *in vitro* experiments, specifically the comparison of GFP expression between REF3 transduced 3T3 and MS1 cells (Figure 3.8), suggested that VE Cadherin expression was *not* restricted to endothelial cells. To address the issue of promoter specificity *in vivo,* we attempted to stain tissues sections from CrIED mice using an antibody for luciferase. Unfortunately, no anti-luciferase antibody was found that performed well in histological applications. As an alternative approach to address

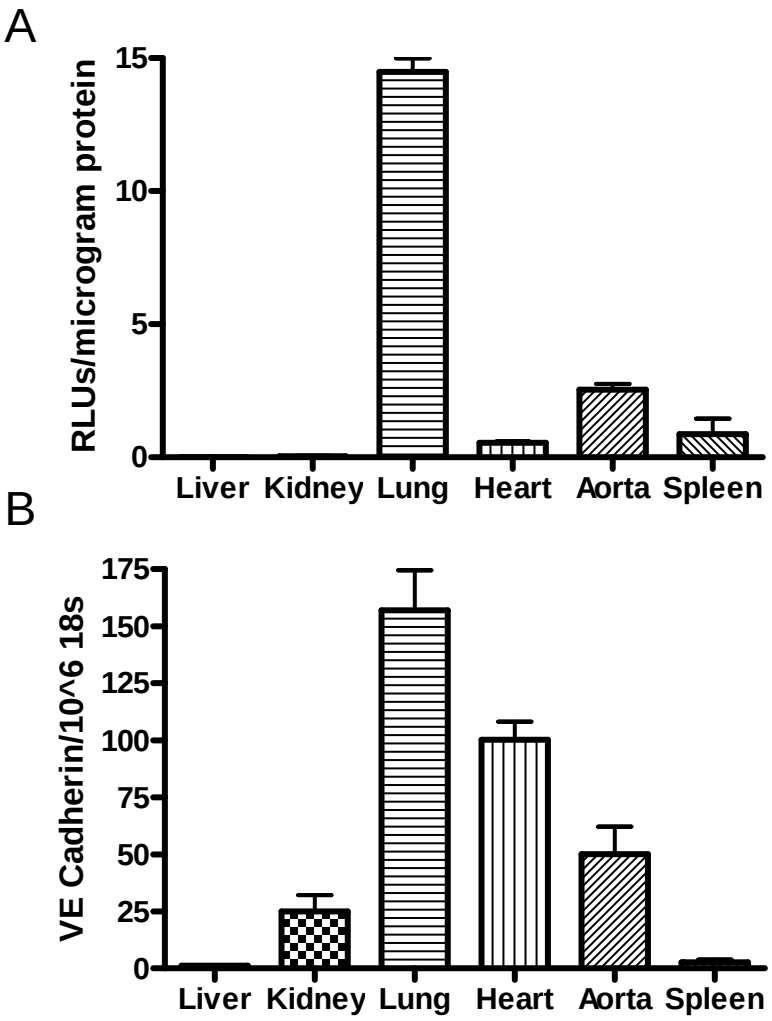

Figure 3.13: Luciferase Activity In CrIED Tissue Lysates. Both protein lysates and mRNA were isolated from tissue samples of liver, kidney, lung, heart, aorta and spleen in CrIED mice. A) Luciferase activity in protein lysates isolated showed abundant levels of luciferase in the lung and Aorta. B) qPCR on mRNA isolated from the same tissues was performed to assess VE Cadherin expression . A similar trend was noted between A and B, with the exception that VE Cadherin and luciferase levels within heart tissue.

promoter specificity, luciferase activity was examined in protein lysates from multiple dissected tissues. Using this method, differential expression of luciferase was observed throughout liver, kidney, lung, aorta, heart and spleen. Luciferase activity was highest in the lung and aorta (both endothelial-rich tissues), moderately expressed in the heart and

spleen, and barely detectable in the liver and kidney (Figure 3.13). VE Cadherin gene expression was then measured in the same tissues by qRT-PCR (Figure 3.13). Lung and aorta showed high VE Cadherin expression similar to that observed in the luciferase assay. Minor discrepancies were noted between luciferase activity and qRT-PCR data in the heart and kidney, which showed high VE Cadherin expression but relatively low luciferase activity. In general, however, these data suggest that the VE Cadherin promoter in the CrIED transgene confers endothelial specific expression of the luciferase reporter.

Induction of Cre Activity and Absence of Apoptotic Cell Death

For EPC depletion, it was only necessary to use bone marrow from the CrIED mouse. However, to ensure that the transgene was functioning properly, TM was administered to the intact CrIED mouse. Not surprisingly, the TM treated CrIED mice quickly showed signs of distress and soon had to be euthanized. TUNEL stain on lung sections revealed considerable apoptosis, while no apoptosis could be detected in the liver (Figure 3.14). These data indicate that apoptosis was localized to the same tissues in which high luciferase activity was detected. Unfortunately, several of the WT animals treated with TM also showed signs of distress. Those animals were also euthanized, and TUNEL stain on WT lung tissue showed a similar staining pattern to that seen in the CrIED lung (Figure 3.14).

Since the initial dose of tamoxifen (10 mg/day) was lethal in all mice, a dose response curve was generated by treating mice with daily injections of 0 to 10 mg of tamoxifen for up to 5 days. Significant mortality was observed above the 3 mg/day dose

(Figure 3.14). Lungs from animals receiving each dose were isolated and luciferase activity was measured from the extracted protein. A dose-dependent decrease in luminescence was observed following TM delivery, with all treatment groups showing a loss of luciferase activity relative to the TM-treated IED only mice (i.e. mice lacking the inducible Cre so that luciferase activity was maintained following TM treatment). These results indicate a functional Cre/LoxP system in the CrIED transgene (i.e. a loss in luciferase activity due to excision of the gene) but the apoptosis seen by TUNEL stain was due to the toxicity of excessive tamoxifen levels and not ΔN-Bax expression.

To further verify that the Cre/LoxP system was functional, CAG-cre/Esr1 mice were crossed with ROSA26-βgeo mice and treated with 3 mg TM/day in parallel with CrIED mice. Upon TM-mediated activation of Cre, CAG-cre/Esr1x ROSA26-βgeo mice express the βgeo gene and stain positively for β-gal activity. As shown in Figure 3.15, multiple tissues stained positively for β-gal activity following TM administration, indicating successful recombination. However, none of the CrIED mice showed signs of physical distress, and TUNEL stain of the multiple tissues failed to detect significant apoptosis (data not shown). Taken together, these data demonstrate that the CrIED transgene functions only as a VE Cadherin luciferase reporter, but the inducible expression of ΔN-Bax does NOT cause cell death.

Discussion

The data presented here are the results of two attempts to generate a mouse model of EPC depletion. Unfortunately, neither approach attained the desired objective. Broadly speaking, the failure of both strategies was the "top-down" implementation of

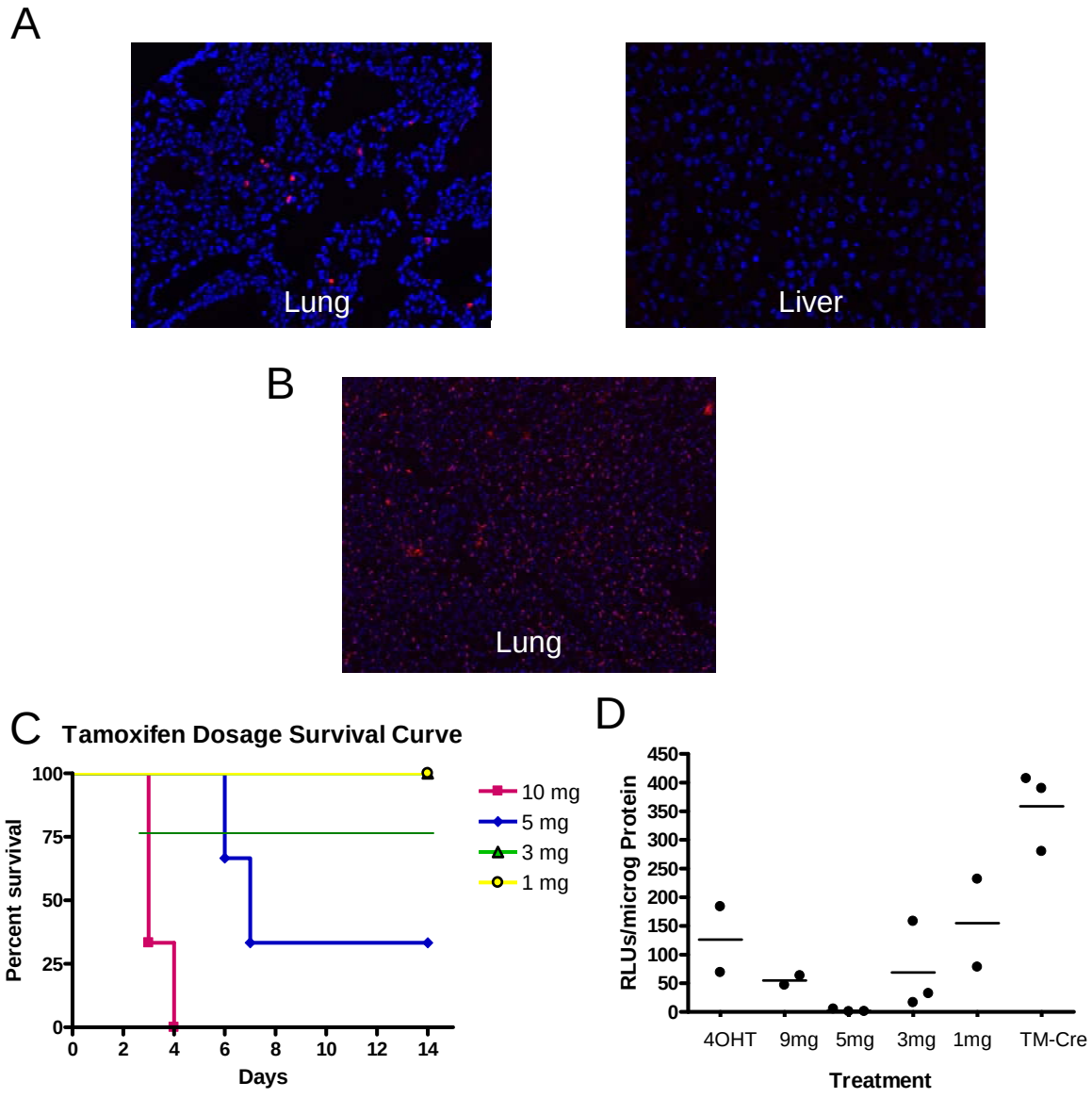

Figure 3.14: Apoptosis In CrIED Tissue Following Tamoxifen Treatment. CrIED mice treated with 10 mg/mouse/day of tamoxifen showed signs of distress and were sacrificed within 4 days. A) TUNEL staining on lung showed evidence of apoptosis restricted to the lung, while no apoptosis was detected in the liver. WT animals treated with TM doses >3 mg also showed signs of distress, so were sacrificed tissues were isolated. B) TUNEL staining on lung from WT mice showed a similar pattern of apoptotic staining was seen in the lung of CrIED animals (B). C) A Kaplan-Meier survival curve in WT mice showed TM-induced toxicity in doses greater than 3 mg/mouse indicating that deaths seen were not due to the CrIED construct. D) A dose response to tamoxifen treatment was performed, and luciferase activity was examined in lysates from lungs of TM-treated CrIED mice isolated immediately following sacrifice. A dose-dependent decrease in luciferase activity indicates gene excision due to cre-mediated recombination.

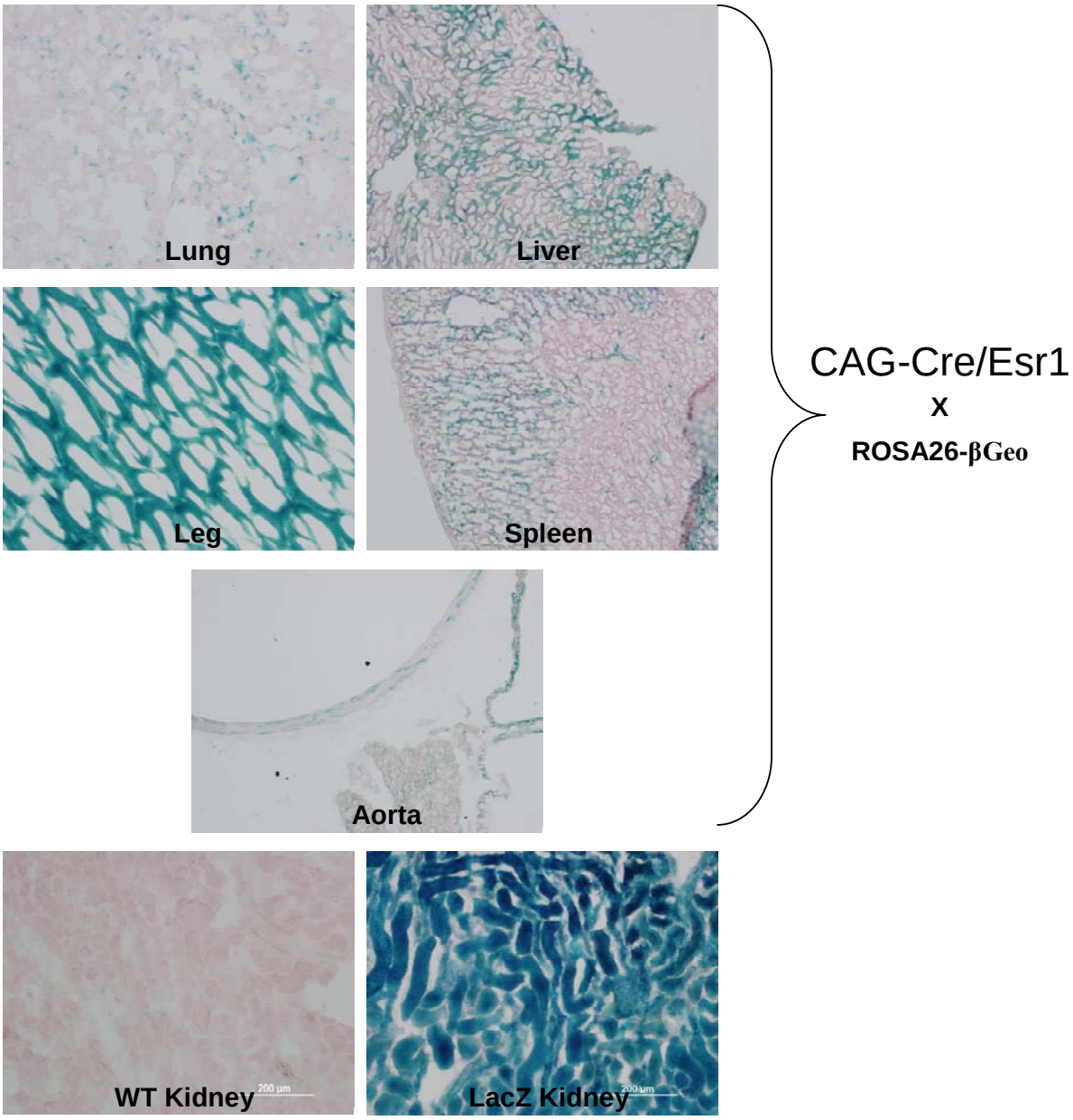

Figure 3.15: Tamoxife-induced Cre Activity In CAGCre^{TM} Mice. CAGCre^{TM} mice were crossed with R26R mice. Following 3 days of treatment with 1 mg/mouse TM, tissues were stained for β-gal activity. Evidence of recombination was seen in multiple tissues of the transgenic but not in WT controls. Kidney from a LacZ reporter mouse was used as a positive control.

each system. Rather than individually testing each component of the retroviral constructs (i.e. the promoter, luciferase reporter, cre/loxP system and ΔN-Bax activity), we first generated the complete RED vector. When the vector did not work, it was then necessary

to backtrack to isolate the problem. A factor further confounding our results was the apparent disconnect observed between VE Cadherin expression *in vitro* and *in vivo*. We assumed that the VE Cadherin promoter, while nearly inactive in cultured endothelial cells, would confer endothelial specific gene expression in the intact animal. However, our inability to use the VE Cadherin promoter to robustly activate our construct *in vitro* prevented us from validating functionality of all aspects of the vector prior to its utilization in a transgenic setting.

The use of retroviral constructs for expression of exogenous genes in the bone marrow is a challenging task that has been limited by the inability to efficiently transduce a majority of the bone marrow compartment. Despite the ability of other groups to achieve maximum transduction efficiencies of <50%, experience with our protocol indicates that nearly the entire bone marrow population can be transduced (Figure 3.5). Several caveats to our strategy exist, however. First, we must be able to generate extremely high titers of retrovirus. Second, our promoter cannot be silenced; a problem frequently observed following bone marrow transduction. We assumed that the limiting factor in our procedure was the aforementioned titer problem. However, the RED and REF constructs appeared to generate a sufficient number of infectious particles. The problem, rather, was a reduction in the frequency of viral-to-host genomic integration. Although virus particles were generated, they were not infectious. The inefficient integration of our construct was entirely unanticipated, and we can only speculate as to why this occurred.

During virus production, the retroviral plasmid is transfected into a packaging cell line where viral genes are previously introduced *in trans.* The viral RNA is the

transcribed from the 5'LTR to the 3'LTR of the transfected plasmid, where a poly adenylation (poly-A) sequence in the 3' U3 region halts transcription. Once integrated into the host genome, the same poly-A signal in the U3 region of the 3'LTR regulates mRNA capping of the viral transcript in the host cell (140; 141). In the RED, REF and REF3 constructs, however, the use of an internal poly-A signal required us to insert the expression construct in reverse orientation relative to the direction of the retroviral LTRs. Therefore, full viral RNA would theoretically be transcribed from the 5'LTR to 3'LTR without premature transcriptional terminate. We predicted that this orientation would generate high titer retrovirus, as the inclusion of an internal poly-A signal has been reported to improve virus performance(142; 143). Sequence analysis of our constructs, however, showed that the SV40 poly-A sequence downstream of EGFP, ΔN-Bax, and luciferase in RED, REF and REF3 also contained the AAUAAA poly-A motif in *reverse* orientation. This cryptic poly-A signal could lead to premature transcriptional termination of the viral RNA in packaging cells, resulting in deletion of the 3'LTR and the inability of infectious particles to integrate in the genome of the host cell. The 5'LTR and viral packaging sequence would remain unaffected, so that the shortened transcript would still be packaged and delivered to the target cells. This hypothesis could easily be tested by generating a series of deletion mutants removing portions of the cryptic poly-A sequence, or replacing the existing bi-directional poly A sequence with a unidirectional poly-A.

During the course of this thesis work, a study was published in which a strategy similar to our own was employed to eliminate bone marrow cells. DePalma, et al. (53) generated a lentiviral vector that expressed the HSV-TK gene driven by Tie-2

transcriptional regulatory elements. The construct was used to transduce bone marrow cells, which were then transplanted into recipient mice. Administration of ganciclovir was used to transiently reduce the number of circulating Tie-2 positive cells, which in turn reduced the extent of tumor formation in a mouse model (53). The same constructs were then used to generate a transgenic mouse, which resulted in the identity of Tie2 expressing monocytes (TEMs) (54). Elimination of circulating TEMS severely abrogated tumor formation, demonstrating the functional significance of this cell type. Another study used a similar HSV-TK-based lentiviral vector that targeted ALL bone marrow-derived cells (not just those of an endothelial phenotype) in several models of neovascularization, and found that the continued presence of bone marrow cells in the regenerative milieu was a requisite for blood vessel growth (144). Although there are some weaknesses in the approaches described in these reports, these two groups successfully implemented strategies remarkably similar to our BMTT approach.

While still in the process of validating RED function *in vitro*, we generated the transgenic CrIED mouse. Surprisingly, activity of the VE Cadherin promoter (as assessed by luciferase activity) was easily detectible in the intact animal. Luciferase activity was highly variable in lysates obtained from different tissues, suggesting regulation in an endothelial-specific manner. Sequence analysis of a PCR amplicon generated from CrIED genomic DNA confirmed that sequence of the CrIED transgene *in vivo* matched the predicted sequence of our expression construct (data not shown). Unfortunately, the entire RED construct did not function as we anticipated, since TM treatment did not induce apoptosis in the endothelium. The potential impact of the CrIED mouse has also been mitigated somewhat, as De Palma, et al. expanded on the

development of a Tie2-HSV-TK lentivirus by using the lentiviral construct in a transgenic setting (54). These studies established a functional role for Tie-2 expressing PB-MNCs in tumor angiogenesis.

In retrospect, the RED construct we generated included several design flaws that may have led to our inability to induce endothelial apoptosis in the CrIED mouse. Due to the orientation of the loxP sites, cryptic start codons were present upstream of the luciferase gene (and hence upstream of the ΔN-Bax gene following recombination). Translation from one of the cryptic ATG sequences would retain the peptide sequence of the luciferase gene but not ΔN-Bax following Cre-mediated recombination. If translation was initiated from the cryptic ATG, luciferase expression would be maintained, but no ΔN-Bax protein would be generated. To circumvent this problem, we should have inserted the loxP sites in reverse orientation.

The pronuclear microinjection technique that we utilized to generate the CrIED mouse was also not the ideal strategy for generating transgenic mice containing loxP sites. Pronuclear microinjections typically lead to a single integration site, with multiple copies inserted in tandem (145). The presence of multiple pairs of loxP sites would generate many different possible recombination events, only a few of which would result in ΔN-Bax expression. The net effect is a considerable reduction in recombination efficiency in the presence of Cre.

The most likely cause of construct failure is not the minutia of the construct design described above, but rather the failure of ΔN-Bax to successfully induce apoptosis. This hypothesis is the basis of Chapter 4, and as such will not be discussed further here.

CHAPTER 4

DELETION OF THE BH3 DOMAIN INHIBITS THE APOPTOSIS-INDUCING ABILITY OF BAX

Introduction

In Chapter 3, we devised a strategy in which overexpression of a pro-apoptotic gene (ΔN-Bax) was expected to induce cell death in endothelial cells of a transgenic mouse. However, following ΔN-Bax expression, no apoptosis was observed in the endothelium of these animals. This surprising result led us to question the mechanism of ΔN-Bax activity. In this chapter, we sought to explore the role of ΔN-Bax in apoptosis more fully.

The process of programmed cell death, or apoptosis, is a complex, highly regulated pathway mediated by a plethora of signaling molecules. The extrinsic apoptotic pathway is initiated by the extracellular binding of ligands such as FasL and TRAIL to the death receptors, which leads to further activation of the caspase cascade. The intrinsic pathway, on the other hand, is initiated by cellular stresses such as hypoxia, DNA damage, and growth factor starvation. Activation of the intrinsic pathway leads to the release of cytochrome c from the mitochondria outer membrane (MOM). Cytochrome c then binds with Apaf-1 to form the apoptosome complex. The apoptosome complex then initiates the caspase cascade, eventually leading to cell death.

One of the key mediators of the intrinsic pathway is the pro-apoptotic protein, Bax. A member of the Bcl-2 family of proteins, Bax is activated by specific apoptotic stimuli which causes its translocation from the cytosol to the MOM. Once targeted to the MOM, Bax forms aggregates that lead to MOM depolarization (146; 147). Bax contains

8 amphipathic α-helices surrounding a single hydrophobic α-helix groove, and bears a striking structural similarity to the bacterial diphtheria toxin (99; 100). Diphtheria toxin gains entry into eukaryotic cells by insertion of the B subunit into the cell membrane, which is followed by aggregation and pore formation. Presumably Bax facilitates the release of cytochrome C by a similar mechanism; i.e. by insertion within the MOM and formation of a pore complex. The α5/α6 region of Bax, in particular, has been implicated in the formation of MOM pores(101). As a result of its ability to induce apoptosis, Bax has been a popular choice as a potential therapeutic target for cancer gene therapy (102; 103; 104; 105; 106; 107).

In the absence of an apoptotic stimulus Bax is sequestered by survival proteins, such as Bcl-2, so that the apoptotic activity of Bax is blocked (148; 149) 147). As a result, overexpression of recombinant Bax for gene therapy can be inhibited by endogenous anti-apoptotic regulators. To ensure total cell death in tumorigenic cells, Usui et al. (151) generated a construct containing a truncated form of the human Bax gene lacking the N-terminus of the full-length peptide sequence (152). The truncated protein, ΔN-Bax, lacks the BH3 domain required for dimerization with Bcl-2 (150). Therefore, the cytotoxic effect of ΔN-Bax continues unabated by the cells endogenous anti-apoptotic mechanism. The ΔN-Bax fragment (consisting of the sequence pertaining to amino acids 112-196 of the full length Bax) was used in an adenoviral vector for treatment of a mouse model of non-small cell lung carcinoma (151). Injection of tumors with the ΔN-Bax adenovirus halted progression of tumor formation, and in some cases led to complete tumor remission. However, the mechanism of ΔN-Bax-induced cell death was never fully established.

To determine the specific role of ΔN-Bax in apoptosis, we developed expression plasmids for ΔN-Bax and an EGFP:ΔN-Bax fusion protein. These constructs were transfected in multiple cell lines *in vitro* to assess the efficacy of ΔN-Bax as a potential target for induction of apoptosis.

Methods

Plasmid Construction and Propagation

All plasmids were propagated in Top10 E.Coli (Invitrogen). Transformed E.Coli were grown on LB-Agar plates containing 100 μg/mL of Kanamycin. For large scale plasmid preparation, inoculated cultures were grown in 2L Erlenmeyer flasks containing 200 mL of LB-broth supplemented with of 100 μg/mL Kanamycin. Cultures were propagated overnight in a rotary shaker at 250 rpm and 37 ^{o}C. Plasmid DNA was isolated using Qiagen HiSpeed Plasmid Maxi-prep.

pEGFP:ΔN-Bax: Polymerase Chain Reaction (PCR) primers were designed to amplify the 3' region of the human Bax-α gene corresponding to amino acids 112-192 (see appendix for primer sequences). For cloning purposes, a BsrGI restriction site was incorporated into the forward primer immediately upstream of the alanine codon. A NotI restriction site was incorporated into the reverse primer immediately downstream of the final cysteine codon of Bax-α. PCR was performed using Platinum Taq Hi-fidelity Polymerase (Invitrogen) under the manufacturers specified conditions with the following thermocycler settings: 5 cycles X [95 ^{o}C, 30s denaturing, 50 ^{o}C, 1 minute annealing, 68 ^{o}C, 1 minute extension] followed by 27 cycles X [95 ^{o}C, 30s denaturing, 58 ^{o}C, 1 minute annealing, 68 ^{o}C, 1 minute extension]. The amplified PCR product was then ligated into

the corresponding restriction sites of the pEGFP-N1 plasmid (Clontech). The resulting plasmid contained the first alanine codon of the ΔN-Bax sequence immediately downstream of the final 3' Lysine codon of the EGFP gene. A stop codon was not included at the 3' end of the ΔN-Bax sequence, resulting in a C-terminal tail containing the 7 amino acid sequence CGRDSRS following the terminal glycine residue corresponding to amino acid 192 in the full length Bax-α gene.

pBax-N1: PCR primers were designed to amplify the 3' region of the human Bax-α gene containing the sequence corresponding to amino acids 112-192. The forward primer was designed to include a Kozak sequence (containing a methionine [ATG] codon) upstream of the first Alanine codon of the ΔN-Bax sequence and immediately downstream of an AgeI restriction site. The reverse primer was modified to so that the resultant product contained a stop codon (TGA) between the final Glycine codon at the 3' end of ΔN-Bax, and the NotI restriction site. PCR was performed using Platinum Taq Hi-fidelity Polymerase (Invitrogen) under the manufacturer's conditions with the following thermocycler settings: 5 cycles X [95 ^{o}C, 30s denaturing, 50 ^{o}C, 1 minute annealing, 68 ^{o}C, 1 minute extension] followed by 27 cycles X [95 ^{o}C, 30s denaturing, 58 ^{o}C, 1 minute annealing, 68 ^{o}C, 1 minute extension]. The amplified PCR product was then ligated into the corresponding AgeI and NotI restriction sites of the pEGFP-N1 plasmid.

Cell lines and culture

HEK-293 cells and NIH/3T3 cells (ATCC) were grown at 37 C^{o}, 5% CO_2 in DMEM supplemented with 10% fetal bovine serum, L-glutamine, and Pen/Strep or DMEM supplemented with 10% calf serum, L-glutamine, and Pen/Strep, respectively.

Both 293 and 3T3 cells were grown in 10 cm tissue culture-treated dishes until 80% confluent, and passaged at a ratio of 1:5. Human Umbilical Vein Endothelial Cells (HUVECs) were purchased from Lonza. Cells were grown at 37 C^o, 5% CO_2 in EGM-2 endothelial growth medium. HUVECs were grown in 10 cm tissue culture-treated dishes until a monolayer formed, then passaged at a ratio of 1:5. HCT-15 cells (generously donated by REMEDI, National University of Ireland, Galway) were grown at 37 C^o, 5% CO_2 in DMEM supplemented with 10% fetal bovine serum, L-glutamine, and Pen/Strep.

Transfection

HEK-293 cells were transfected using Lipofectamine 2000 (Invitrogen) according to the supplier's recommendations. Briefly, cells were grown to 50% confluence in 6-well tissue culture treated dishes. Twenty-four hours prior to transfection, full media was replaced with antibiotic-free media. DNA complexes were formed in 500 μL of DMEM (without serum or antibiotics) with 8 micrograms of DNA and 10 μL of Lipofectamine 2000. After removing the old media from the cells, the DNA complexes were added drop wise then slowly swirled for even distribution. After 6 hours of incubation, the complexes were removed and replaced with full media. For all time points, 0 hrs corresponds to point at which the DNA complexes were replaced with fresh media.

HUVECs, 3T3, and HCT-15 cells were transfected using the AMAXA electroporation system with the HUVEC Nucleofector Kit, Nucleofector Kit R, and Nucleofector Kit V, respectively. Transfections were performed according to the manufacturer's recommendations. Briefly, cells were grown until ready for passage, then dissociated from the culture dish using gentle trypsinization. Trypsin was neutralized

using full media, and the total cell number was calculated with a hemocytometer. Following gentle centrifugation, the supernatant was aspirated and the pellet resuspended in 100 μL of Nucleofector solution. Unless otherwise stated, for each transfection 4 μg of plasmid DNA was added to the cell mixture, and then transferred to a Nucleofector cuvette for electroporation. Immediately following electroporation, cells were resuspended in the appropriate volume of full media and plated in a 6-well dish.

Imaging

GFP expression in transfected cells was imaged using an Olympus inverted fluorescent microscope or a Zeiss confocal laser scanning microscope.

Western Blot

A rabbit polyclonal anti-Bax antibody generated from a synthetic peptide corresponding to amino acids 150-165 of human Bax, and a rabbit polyclonal anti-GFP antibody were obtained from Abcam (catalogue numbers ab16837 and ab290, respectively). Protein was extracted from transfected cells using RIPA lysis buffer with protease inhibitors, and total protein was quantified using a modified Bradford assay (Biorad). Twenty micrograms of protein per sample was separated in a 10% polyacrylamide gel, and then transferred overnight to a nitrocellulose membrane. Membranes were blocked for 1 hr at room temperature in 1% TBS-tween and 5% skim milk, and then incubated with the primary antibody overnight at 4 ^{o}C in 1% TBS-tween and 1% skim milk. Secondary antibody incubation was performed in 1% TBS-tween and

1% skim milk with goat anti-rabbit horseradish peroxidase conjugates, then imaged using an ECL imaging kit (Amersham).

qRT-PCR

RNA was purified using a commercial kit (Qiagen) and reverse transcribed into cDNA using the SuperScript™ III First Strand Synthesis System (Invitrogen), which was subsequently purified using a commercially available kit (Qiagen). Primers were designed using PrimerQuest software (IDT DNA technologies) for the 3' end of human Bax, EGFP, and mouse 18s. SYBR Green intercalating dye (Applied Biosystems) was used to perform real time PCR with the ABI Prism 7700 Sequence Detection System (Applied Biosystems). Standards for each gene were amplified from cDNA and purified. Standard concentrations were determined using spectrophotometric measurement at 260 nm, and standards were serially diluted to an appropriate range of concentrations. Transcript concentration in template cDNA solutions was quantified from the linear standard curve, normalized to 18s copy number, and expressed as copies per 10^6 18s.

Nuclear Fragmentation

Cells were isolated via tryspsinization, washed with cold PBS, and then fixed for 10 minutes in 1% paraformaldehyde/PBS at 4 ^{o}C. Following fixation, cells were again washed in cold PBS then pelleted via centrifugation. After resuspension in 100 microliters of PBS, the cell solution was cytospun transferred to glass slides. Slides were subsequently mounted with fluorescence mounting medium with DAPI (Vectashield) and imaged.

Flow Cytometry

Transfected adherent cells were isolated via trypsinization, washed with full media to neutralize the trypsin, and then resuspended in cold PBS prior to analysis. Expression of EGFP was quantitatively assessed using a BD FACSort flow cytometer. 5,000-50,000 events were recorded, and flourescence was measured using a 488 nm laser with 530nm +/- 15nm detectors

Annexin V stain

293 cells were transfected with pGL3-basic or pΔN-Bax-N1using Lipofectamine 2000 (Invitrogen) in 6-well dishes. Camptothecin was added to the media of untransfected cells as a positive control. Twenty-four hours after transfection, cells were trypsinized to generate a single cell suspension, then stained with Annexin V-PE staining kit (Invitrogen). Results were analyzed using a BD FACSort flow cytometer. Annexin V positive/Propidium Iodide (PI) negative cells were considered apoptotic, and Annexin V/PI double positive cells were quantified as dead. Post acquisition analysis was performed using FlowJo software (Treestar, Inc.).

YO-PRO-I Stain

3T3 cells were transfected with pGL3-basic or pΔN-Bax-N1 using nucleofection and cultured in 6-well plates. Camptothecin was added to the media of untransfected cells as a positive control. Camptothecin hours after transfection, the Vybrant Apoptosis Assay Kit 4 (Invitrogen) was used to stain cells. Results were analyzed using a BD FACSort

flow cytometer. YO-PRO-1 positive/Propidium Iodide (PI) negative cells were considered apoptotic, and YO-PRO-1/PI double positive cells were quantified as dead. Post acquisition analysis was performed using FlowJo software.

MTT Assay

293 cells were transfected with pEGFP-N1 or pΔN-Bax-N1 in a flat-bottomed 96-well plate using Lipofectamine 2000. Four days after transfection, a Cell-Titer 96 MTT assay was performed (Promega). Cells were incubated overnight under standard culture conditions with the manufacturer's dye solution, then absorbance was measured at 570 nm using a 96-well plate reader.

Results

Generation of ΔN-Bax Constructs

We generated two expression constructs containing the C-terminal region of the human pro-apoptotic Bax gene (ΔN-Bax) for transfection experiments in cultured cells. In order to aid in the visualization of ΔN-Bax over-expression, one construct was generated containing ΔN-Bax fused to the C-terminus of enhanced green fluorescent protein (EGFP) under transcriptional control of the cytomegalovirus (CMV) promoter. The ΔN-Bax sequence was generated from a cDNA library derived from the HL60 cell line and cloned into the pEGFP-N1 vector. The resulting construct, identified as pEGFP:ΔN-Bax (Figure 4.1), contains the ΔN-Bax fragment immediately following the final Lysine codon of EGFP, allowing for in-frame translation of the ΔN-Bax protein. To eliminate the possibility that EGFP fusion would interfere with the native activity of ΔN-

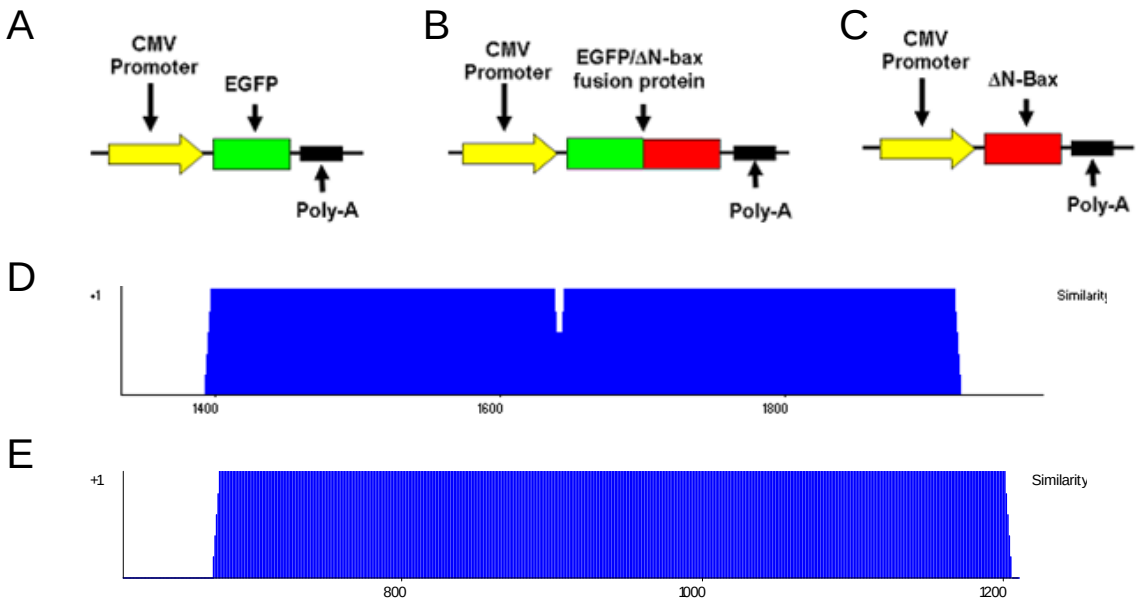

Figure 4.1: Plasmids Containing ΔN-Bax Sequence. To generate ΔN-Bax expression constructs, the sequence pertaining to amino acids 112-192 of the human Bax gene was cloned in frame to the EGFP sequence of pEGFP-N1. A) pEGFP-N1. B) pEGFP:ΔN-Bax (B), containing a EGFP:ΔN-Bax fusion protein. C) pΔN-Bax-N1, in which the EGFP gene in pEGFP-N1 was replaced entirely with ΔN-Bax . D) Direct sequencing of pEGFP:ΔN-Bax indicated a deletion in the stop codon of the ΔN-Bax fragment, leading to translation of a 7 amino acid C-terminal tail. E) Sequencing of pΔN-Bax-N1 confirmed the predicted sequence.

Bax, a construct lacking EGFP was also generated. The pΔN -Bax-N1 construct (Figure 4.1) contains ΔN-Bax driven directly by the CMV promoter. Sequences of both pEGFP-N1 and pΔN -Bax-N1 were confirmed by restriction digest and direct sequencing (Figure 4.1).

Expression of ΔN-Bax induces changes in HEK-293 cell morphology

Our preliminary transfection experiments were carried out in the HEK-293 cells. The HEK-293 line, derived from human embryonic kidney cells, is widely noted for the ease in which it is transfected by calcium-phosphate and poly-cation mediated gene

delivery methods. In our hands, 293 cells transfected with pEGFP-N1 using Lipofectamine-2000 showed robust EGFP expression 24 hrs after addition of the plasmid (Figure 4.2). Visual inspection of the cells at low magnification indicated strong EGFP fluorescence and a high transfection efficiency. Closer examination of the EGFP-expressing cells revealed diffuse fluorescence signal throughout the cells, and morphology consistent with that of non-transfected cells.

After transfection of HEK-293 cells with pEGFP:ΔN-Bax, the percentage of GFP-positive cells after 24 hours was dramatically lower than that seen following transfection with pEGFP-N1. The intensity of GFP fluorescence was also noticeably weaker in pEGFP:ΔN-Bax transfected cells compared to pEGFP-N1 transfected cells. When viewed under higher magnification, the cells expressing EGFP:ΔN-Bax had a rounded morphology indicative of the "blebbing" often observed in adherent cells undergoing apoptosis. Additionally, individual EGFP:ΔN-Bax positive cells exhibited an uneven, heterogeneous EGFP signal. This distinctive punctate patterning is similar to that seen in previously published reports, in which expression of GFP-Bax fusion proteins was detected in apoptotic cells (147; 149).

Frequency and Intensity of EGFP Fluorescence In Cells Expressing EGFP:ΔN-Bax

Expression of EGFP was quantitatively assessed in 3T3 cells using flow cytometry within 6 hours of transfection with either pEGFP-N1 or pEGFP:ΔN-Bax. The total number of EGFP-positive cells was noticeably lower in the pEGFP:ΔN-Bax transfected group than in the pEGFP-N1 transfected group (Figure 4.3). Mean percentage of EGFP-positive cells was 2.5-fold higher in cells transfected with pEGFP-N1 than in

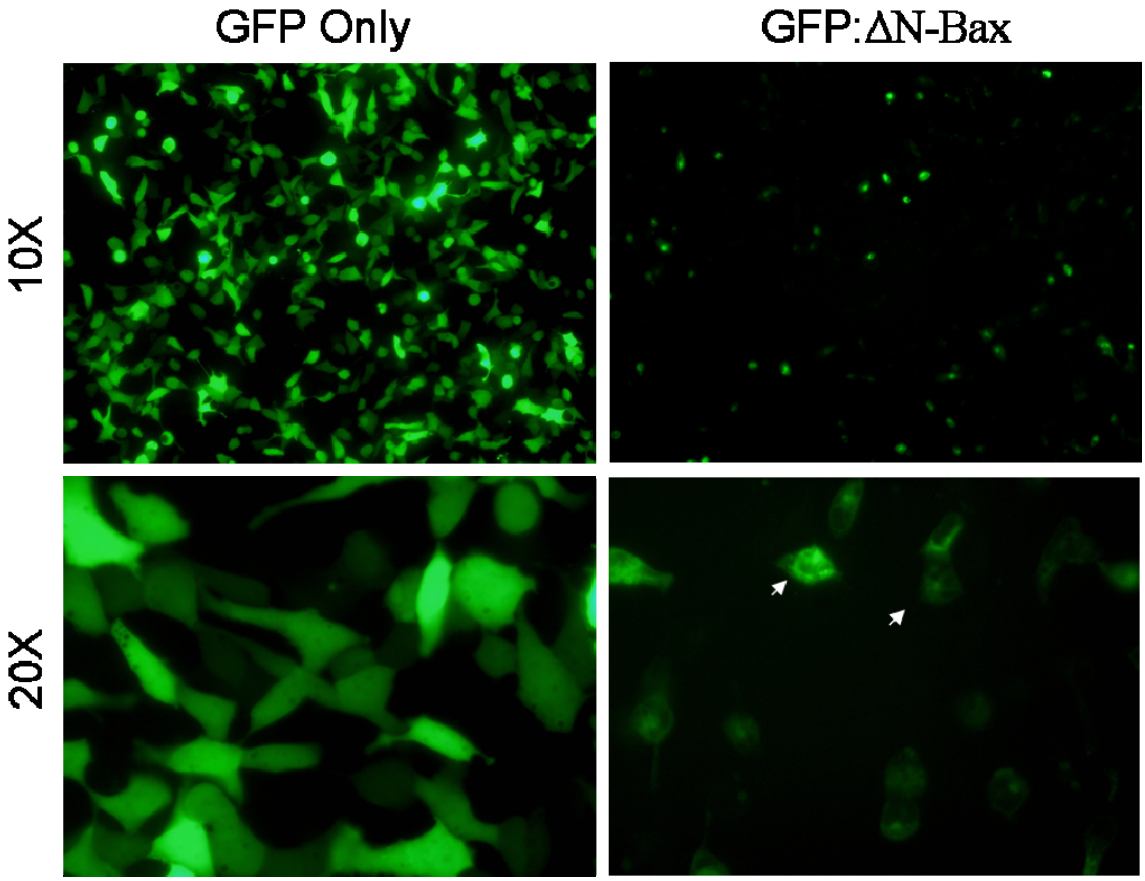

Figure 4.2: Cell Morphology Following EGFP:ΔN-Bax Expression. HEK293 cells were transfected with pEGFP-N1 or pEGFP:ΔN-Bax and imaged with an inverted fluorescent microscope at 48 hours. Membrane blebbing (arrows) seen in cells expressing pEGFP:ΔN-Bax is indicative of apoptotic cell death.

cells transfected with pEGFP:ΔN-Bax. Furthermore, intensity of the EGFP signal was considerably lower in cells expressing EGFP:ΔN-Bax.

Transfection Efficiency Is Unaffected by DNA Concentration

Transfection protocols can be highly erratic, with optimal transfection conditions varying widely between different cell types. Furthermore, different plasmids transfected

into the *same* cell type may result in markedly different transfection efficiencies. In order to ensure that the differences in GFP expression observed between pEGFP-N1 and pEGFP:ΔN-Bax were due to the effect of the fusion protein and not sub-optimal transfection conditions, we independently optimized transfection conditions for both the pEGFP-N1 and pEGFP:ΔN-Bax plasmids in NIH-3T3 cells. Transfections were performed using the AMAXA electroporation system and the concentration of plasmid DNA for both plasmids was varied from 2-8 μg per transfection. No significant change in transfection efficiency was observed for either pEGFP-N1 or pEGFP:ΔN-Bax over the range of DNA concentrations tested. (Figure 4.3). Under all conditions, pEGFP-N1 transfection efficiencies were 3-fold higher than pEGFP:ΔN-Bax.

EGFP:ΔN-Bax Protein Forms Extra-Nuclear Aggregates

To further examine the morphological effects of EGFP:ΔN-Bax expression and sub-cellular localization of the fusion protein, we imaged transfected 3T3 cells using scanning laser confocal microscopy. We observed that, when transfected with the pEGFP:ΔN-Bax plasmid, the number of fluorescent 3T3 cells would gradually decrease. To visualize the cells when GFP flourescence was highest, confocal images were captured 4 hours after transfection with the Amaxa Nucleofection system.

Cells transfected with pEGFP-N1 (Figure 4.4) exhibited a homogeneous, diffuse EGFP signal throughout the cytoplasm and nucleus. Morphologically, cells expressing EGFP were indistinguishable from non-transfected cells. Cells expressing the EGFP:ΔN-Bax fusion protein, on the other hand, contained distinct aggregates of the fusion protein. The majority of the aggregates were largely extra-nuclear, indicating episomal regulation

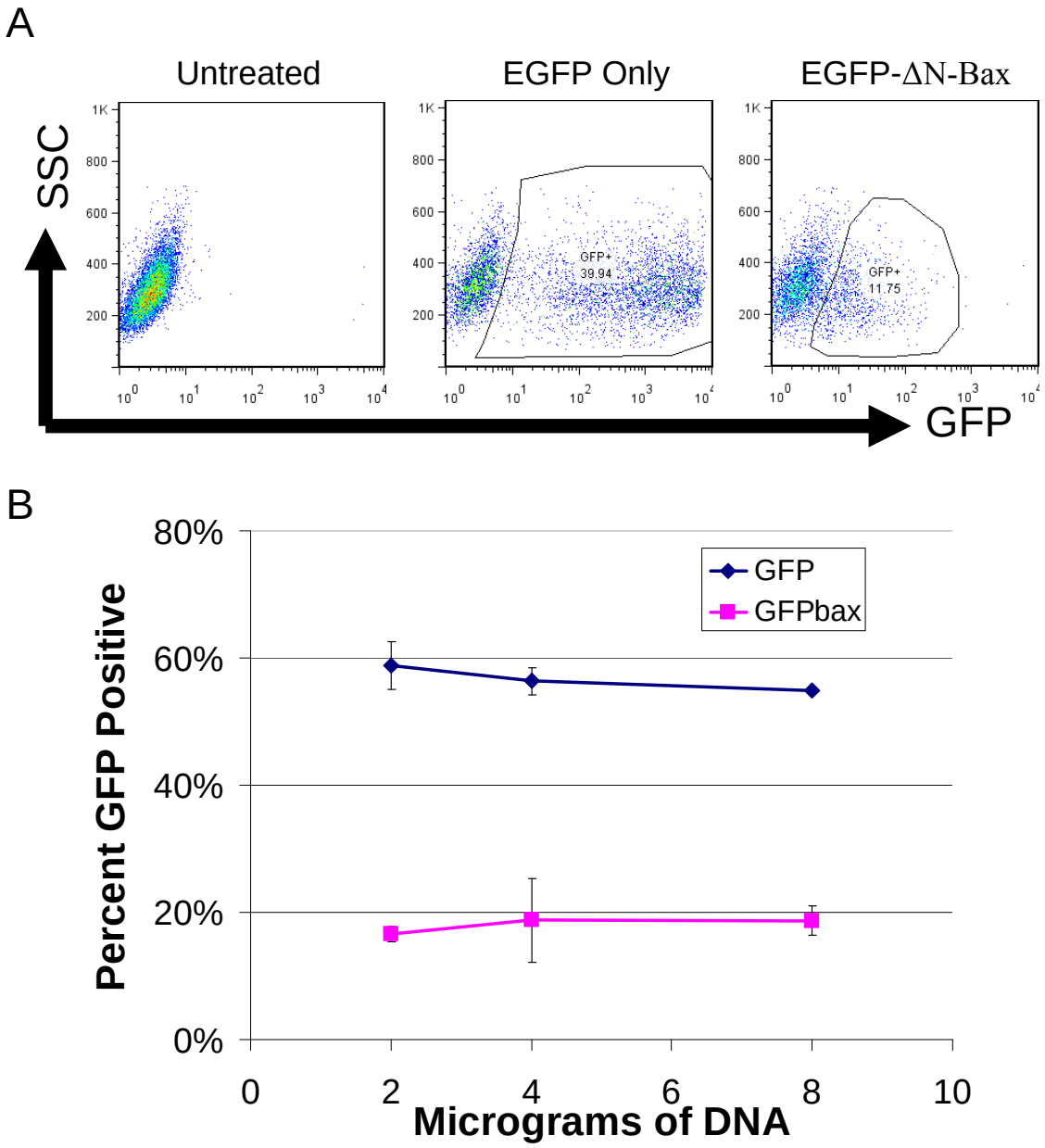

Figure 4.3: Flourescence of Cells Expressing EGFP:ΔN-Bax or EGFP. Flow cytometry was performed on 293 cells transfected with pEGFP-N1 or pEGFP:ΔN-Bax. A) A dot plot of transduced cells shows both the number of GFP positive cells and the fluorescence intensity was lower in cells expressing EGFP:ΔN-Bax compared to EGFP alone. B) The quantity of DNA used for transfection of each plasmid was varied from 2-8 µg. Flow cytometry was performed to quantify the number of GFP-expressing cells. No change in GFP positive cells was observed when the quantity of DNA used for transfection was varied.

and compartmentalization. In a non-apoptotic state, full length Bax forms a heterodimer with Bcl-2 in the cytoplasm. However, upon apoptotic activation, Bax is translocated to the mitochondria forming pore complexes which lead to depolarization of the mitochondrial membranes. Therefore, we attributed the aggregation seen in cells expressing the EGFP:ΔN-Bax fusion protein to mitochondrial translocation during a pro-apoptotic state.

Temporal expression of EGFP:ΔN-Bax

Visual observation of 3T3 cells transfected with pEGFP:ΔN-Bax confirmed that GFP flourescence decreased within 24 hours of transfection to nearly undetectable levels within 48 hours. Using flow cytometry, the percentage of EGFP positive 3T3 cells was quantified from 4-48 hours following transfection with pEGFP:ΔN-Bax or pEGFP-N1 (Figure 4.5). Transfection with pEGFP-N1 resulted in sustained fluorescence in 38-55% of the cell population throughout the time course. Cells transfected in parallel with the pEGFP:ΔN-Bax fusion construct, however, reached a maximum transfection efficiency of 20% after just 4 hours. By 48 hours, GFP fluorescence was undetectable by flow cytometry. The loss of fluorescence could potentially be caused by accelerated degradation of the plasmid DNA, RNA or protein. However, this scenario is unlikely since cells transfected with the plasmid encoding EGFP alone exhibited constant fluorescence over the same time course. Therefore, we suspected that the loss of fluorescence was due to apoptosis of the transfected cells.

Our interest in ΔN-Bax protein (as described in Chapter 3) was for the induction of apoptosis in endothelial cells *in vivo*. To assess ΔN-Bax in endothelial cells *in vitro*,

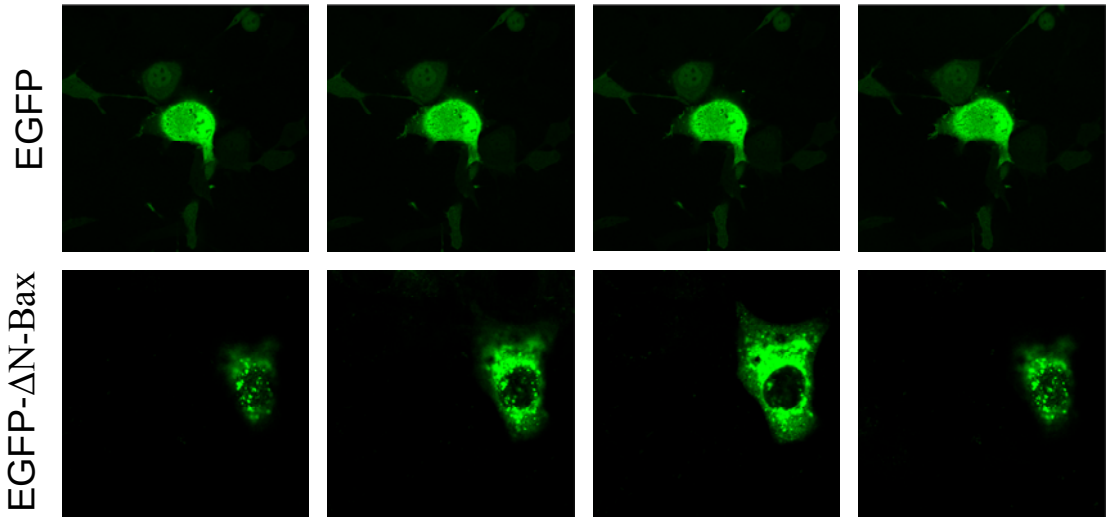

Figure 4.4: EGFP:ΔN-Bax Expression Results In Punctate Extra-nuclear Aggregation. 3T3 cells were transfected with pEGFP-N1 or pEGFP:ΔN-Bax and imaged with confocal microscopy after 6 hours. Confocal slices through cells transfected with pEGFP-N1 show homogeneous, diffuse fluorescence. Cells expressing the EGFP:ΔN-Bax fusion protein exhibit punctate fluorescence that is largely extranuclear.

we performed transfection experiments in Human Umbilical Vein Endothelial Cells (HUVECs). As we observed in 3T3 cells, HUVECs transfected with pEGFP:ΔN-Bax showed a steady decrease in GFP expression from 35% at 4 hours post-transfection to nearly undetectable levels after 48 hours. HUVECs transfected with pEGFP-N1, however, maintained consistent transfection efficiencies of ~55% during the time course. We attributed the reduction, and eventual loss, of EGFP signal to cell death as a result of eGFP-Bax induced apoptosis.

Since the initial transfection experiments with pEGFP:ΔN-Bax were performed in HEK-293 cells, we also examined the temporal effects of EGFP expression quantitatively in this cell line. The percentage of EGFP-positive HEK-293 following transfection with pEGFP:ΔN-Bax remained relatively constant at ~35% until 96 hours

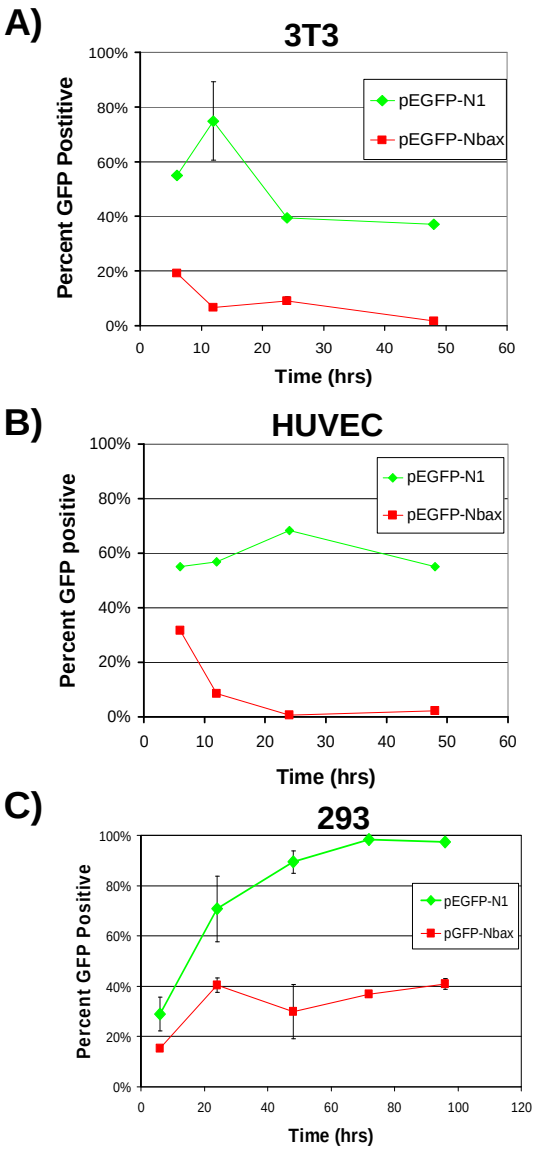

Figure 4.5: Timecourse of Flourescence Following Transfection. Flow cytometry was performed on (A) 3T3 cells, (B) HUVECs, and (C) 293 cells at multiple time points following transfection with either pEGFP-N1 or pEGFP:ΔN-Bax. Both 3T3 and HUVECs transfected with pEGFP:ΔN-Bax showed an immediate loss of GFP expression within 24 hours which was undetectable after 48 hours. EGFP expression remained constant in these cells over the time course following pEGFP-N1 transfection. GFP expression in 293 cells transfected with pEGFP:ΔN-Bax was maintained over the time course, but was considerably less than that seen following pEGFP-N1 transfection.

after treatment. Comparatively, transfection of HEK293 cells with pEGFP-N1 resulted in transfection efficiencies of 95% over the same time course. Peak levels of fluorescence in

pEGFP-N1 transfected cells were not reached until 72 hours post-transfection, while peak EGFP levels were reached 24 hours following transfection with pEGFP:ΔN-Bax. The sustained fluorescence in HEK-293 cells transfected with pEGFP:ΔN-Bax contradicts the findings from 3T3 and HUVECs, where fluorescence was extinguished within 48 hours. These disparate results could indicate either cell-type specific toxicity of ΔN-Bax, or differences in EGFP:ΔN-Bax degradation rates.

EGFP:ΔN-Bax Expression Leads To Changes In Nuclear Morphology

Loss of EGFP signal, though a potential consequence of cell death, does not necessarily indicate that apoptosis has occurred. In order to directly address whether EGFP:ΔN-Bax expression correlates to apoptotic cell death, the nuclear microstructure of HCT-15 cells following transfection with pEGFP:ΔN-Bax was examined . Fluorescence was considerably less intense and transfection efficiencies were lower in HCT-15 cells transfected with pEGFP:ΔN-Bax compared to cells transfected with pEGFP-N1. Fluorescence in cells transfected with pEGFP:ΔN-Bax was nearly undetectable after 24 hours, so cells were stained with DAPI and nuclear morphology was examined at 12 and 15 hours post-transfection.

Despite visual inspection after 12 hours, the frequency of EGFP positive cells was dramatically lower in cells transfected with pEGFP:ΔN-Bax than with pEGFP-N1 alone (Figure 4.6). At both time points, fluorescent cells transfected with pEGFP:ΔN-Bax exhibited a fractured, condensed, and highly textured nuclear staining pattern (Figure 4.6). This type of nuclear fragmentation, due to the cleavage of DNA during the apoptotic

program, is a hallmark of apoptosis and was only seen in cells expressing EGFP:ΔN-Bax, but not in those expressing EGFP alone.

Detection of ΔN-Bax in transfected cells

Although the EGFP:ΔN-Bax fusion protein allowed visualization of cells expressing the truncated Bax fusion protein, the EGFP tag has the potential to interfere with the apoptosis inducing-activity of the Bax fragment. The inclusion of a 7 amino acid extension at the C-terminal end of EGFP:ΔN-Bax could further inhibit the endogenous activity of the truncated protein. Therefore, we sought to determine the apoptotic effect of expression of the *non*-fusion protein, or ΔN-Bax alone.

The absence of a fluorescent tag in the pΔN-Bax-N1 construct prevented us from assessing transfection efficiencies using the pΔN-Bax-N1 plasmid. Therefore, it was extremely difficult to determine the net apoptotic effect of ΔN-Bax expression in transfected cells. Quantification of gene product using qRT-PCR showed that relative mRNA levels of ΔN-Bax in cells transfected with pΔN-Bax-N1 were comparable to relative levels of EGFP mRNA in cells transfected with pEGFP-N1 (Figure 4.7). However, using an antibody raised against a peptide fragment containing amino acids 150-165 of the full length Bax, we were unable to detect a band representative of the ΔN-Bax protein via western blot of lysates from transfected 293 cells. The native full length Bax was observed at 22kDa, but no band could be seen at the size 6 kDa size predicted for ΔN-Bax (Figure 4.7). The inability to detect ΔN-Bax in lysate from cells transfected with pΔN-Bax-N1 could be indicative of the hypertoxic effect of the ΔN-Bax protein. Even a trace amount of the protein, though undetectable by standard biochemical

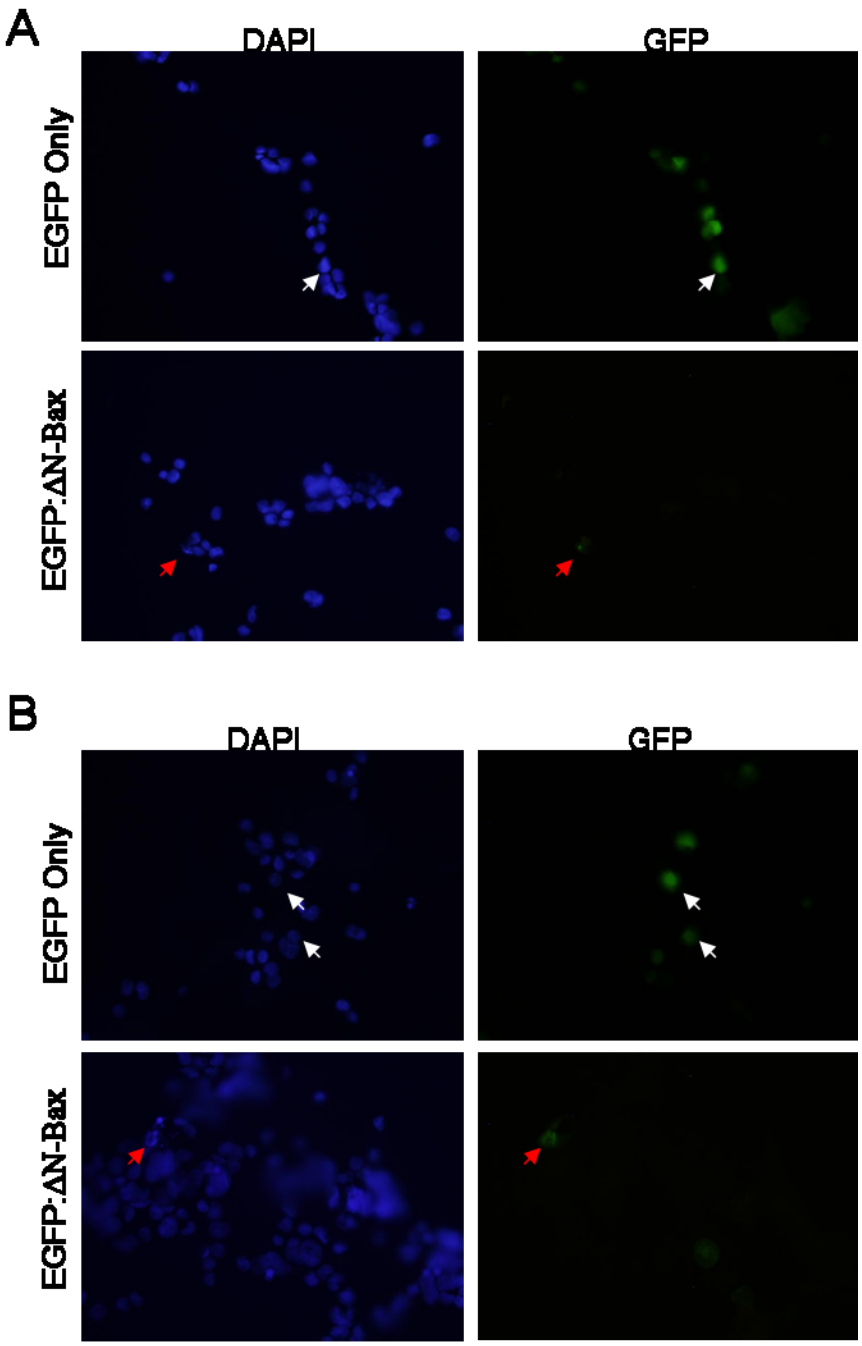

Figure 4.6: Nuclear Fragmentation of Transfected Cells. HCT-15 cells were transfected with pEGFP-N1 or pEGFP:ΔN-Bax. Transfected cells were then cytospun and mounted with DAPI, then imaged at (A) 12 and (B) 15 hours after transfection. The majority of cells expressing EGFP showed intact, non-apoptotic nuclear staining (white arrows). Cells expressing EGFP:ΔN-Bax frequently had small, fragmented nuclei (red arrows) indicative of apoptosis.

techniques, could cause the cells to undergo apoptosis before they are capable of producing a detectable quantity of ΔN-Bax. It is also possible, however, that the pΔN-Bax-N1 plasmid translates an out of frame protein, which could result in a peptide sequence different from the predicted ΔN-Bax sequence. Interestingly, when a western blot was performed on lysate from 293 cells transfected with pEGFP:ΔN-Bax using an anti-GFP antibody, a light band was detected at 33 kDa (Figure 4.7). The intensity of this band was extremely faint compared to the GFP band seen in lysate from cells transfected with pEGFP-N1, but it corresponds to the predicted size of the EGFP:ΔN-Bax fusion protein. This indicates that either the anti-Bax antibody is not sensitive enough to detect the trace amount of EGFP:ΔN-Bax fusion protein, ΔN-Bax generates a peptide sequence unrecognizable by the Bax antibody, or ΔN-Bax is degraded so quickly it cannot be detected by western blot.

ΔN-Bax Does Not Induce Apoptosis

Loss of plasma membrane asymmetry is one of the earliest features of apoptosis, causing cytoplasmic phosphatidylserine to be exposed to the extracellular environment. Cells in the early stages of apoptosis stain positively for Annexin V, which preferentially binds the exposed, extracellular phosphatidylserine, but the intact membrane prevents staining with Propidium Iodide (PI). Late-stage apoptotic cells, whose membranes have been compromised, stain positive for both Annexin V and PI. As a means of quantifying the overall apoptotic effect of ΔN-Bax expression, 3T3 cells were transfected with either pEGFP-N1 or pΔN-Bax-N1 and 24 hours later stained with an Annexin V-PE conjugate and PI. Surprisingly, there was no change in Annexin V or PI staining between pEGFP-

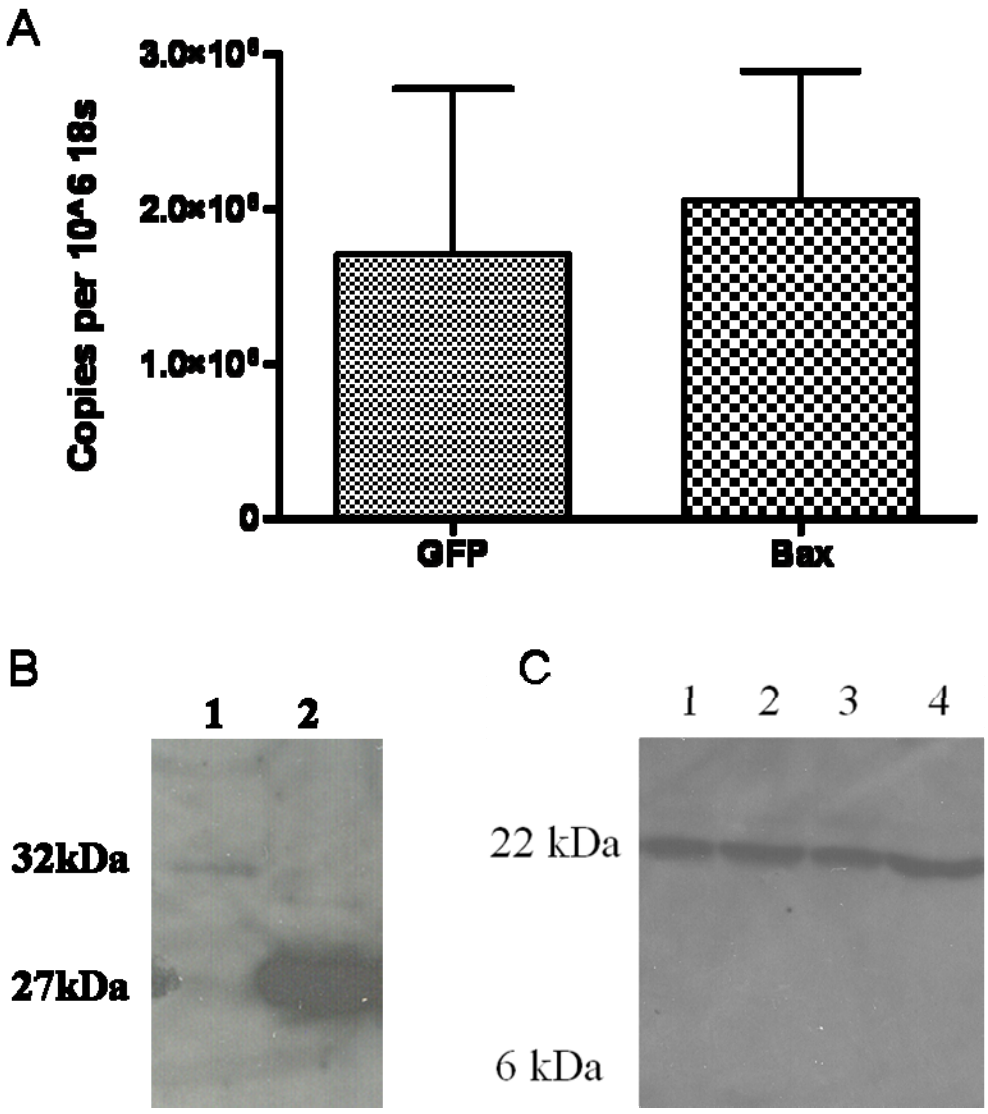

Figure 4.7: Detection of ΔN-Bax mRNA and Protein In Transfected Cells. A) qRT-PCR was performed on RNA isolated from 3T3 cells 24 hours following transfection with pEGFP-N1 or pc. Copy number was determined for GFP and Bax in cells transfected with pEGFP-N1 or pΔN-Bax-N1, respectively. B) Western blot with an anti-GFP antibody was able to detect a faint 32 kDa band in lysate from 3T3 cells transfected with the EGFP:ΔN-Bax fusion construct (lane 1). The WT GFP band was observed at 27 kDa in lysates from cells expressing transfected with pEGFP-N1 (lane 2). C) Lysate from cells transfected with pΔN-Bax was probed with an anti-Bax antibody. Only the native form (22kDa) of Bax could be detected in 4 separate trasnfections (lanes 1-4). No band was observed at 6kDa; the predicted size of or ΔN-Bax. All lanes contain lysate from 3T3 cells 24 hrs after transfection with pΔN-Bax.

N1 and pΔN-Bax-N1 transfected cells (Figure 4.8). Camptothecin treatment, which was used as a positive control, induced a robust increase in both early apoptotic and dead cells. This result is in contrast to our earlier findings, and suggests that ΔN-Bax may *not* induce apoptosis.

Changes in membrane permeability resulting from apoptosis can also be detected with nucleic acid dyes, which have variable access to the nucleus depending on the stage of apoptosis. The YO-PRO-1 dye is cell permeable during early apoptosis, while PI can only access the nuclear components during late stage apoptosis. 3T3 cells were transfected with either pBax-N1 or the pGL3-basic vector, stained with YO-PRO-1 and PI, then analyzed with flow cytometry. Fourty-eight hours after transfection, ΔN-Bax generated no noticeable change in apoptosis compared to the pGL3-basic control (Figure 4.8). 3T3 cells treated with camptothecin, on the other hand, showed a significant increase in YO-PRO-1 staining over the same time course. Due to the fact that YO-PRO-1 is an early indicator of apoptotic cell death, it is possible that at 48 hours the apoptotic program has progressed past the point of selective cell permeability. However, there was also no detectable change in PI staining, which signifies that there was no increase in cell death (i.e. late apoptosis) following ΔN-Bax expression .

The net effect of ΔN-Bax-induced cell death on metabolic activity was assessed using a modified MTT assay. The colorimetric MTT assay quantifies the conversion of a soluble tetrazolium dye to a non-soluble formazan byproduct by live cells. Cells which have undergone apoptosis (and are therefore metabolically inactive) are unable to generate the soluble formazan product. Five days following transfection of 293 cells with pEGFP-N1 or pΔN-Bax-N1, there was no observable difference between the transfection

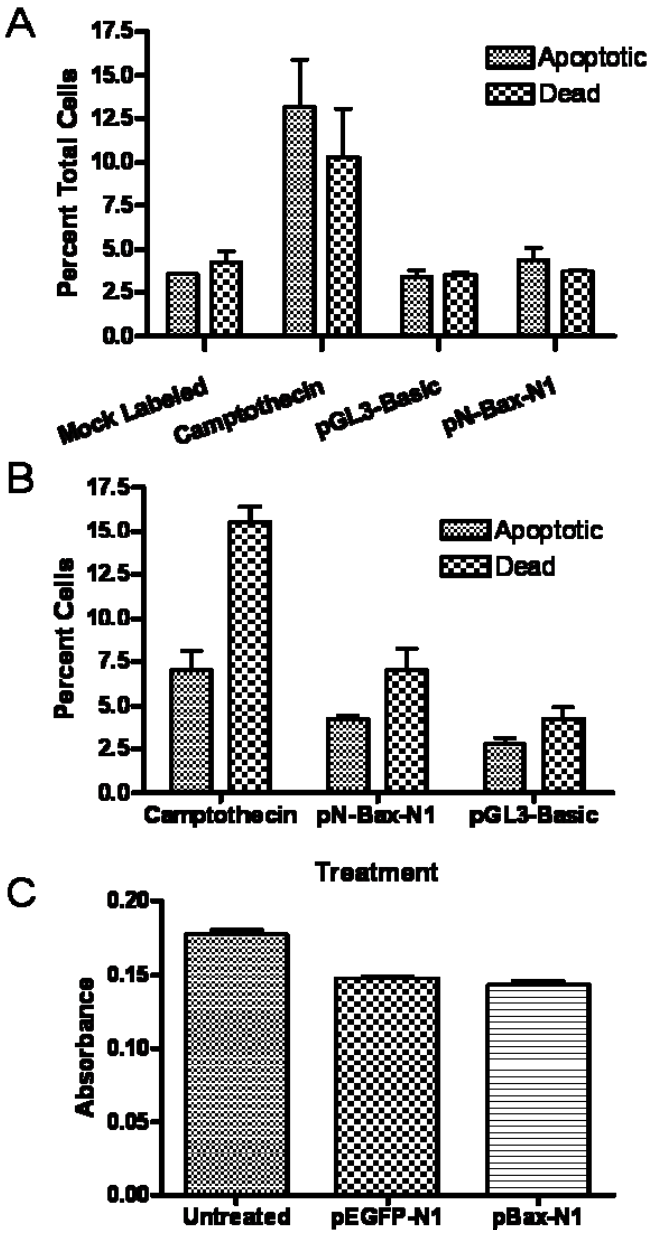

Figure 4.8: Apoptosis Following Transfection With pΔN-Bax-N1. A) Flow cytometry was performed 24 hours after transfection of 3T3 cells with pGL3-basic or pΔN-Bax-N1, and apoptosis was assessed by Annexin V staining. Apoptotic cells stained positively for Annexin V, while dead cells stained positively for both Annexin V and Propidium Iodide. B) YO-PRO-1 staining was performed 24 hours after transfection of 3T3 cells with pGL3-basic or pΔN-Bax-N1, and apoptosis was quantified using flow cytometry. Apoptotic cells stained positively for YO-PRO-1, while dead cells stained positively for both YO-PRO-1 and Propidium Iodide. C) Metabolic activity was analyzed in 293 cells following transduction with pΔN-Bax-N1 or pEGFP-N1 using an MTT assay.

groups. However, both groups of transfected cells showed a modest reduction in metabolic activity compared to the untreated control group.

We assessed three different indicators of apoptosis to determine the effect of ΔN-Bax expression on cell death, and in each case we were unable to detect ΔN-Bax-induced cell death. Taken together, these data suggest that the temporal loss of florescence observed following pEGFP:ΔN-Bax transfection, may be attributable to accelerated protein degradation rates rather loss of cell viability.

Discussion

Although the role of Bax in the apoptotic pathway has been studied extensively, the mechanism by which Bax leads to mitochondrial dysfunction, as well as its interaction with other Bcl-2 family members, is not fully understood. Despite the enigmatic nature of the protein, over-expression of Bax has been widely exploited as a means to induce apoptosis. Our goal in the previous chapter was to develop a potent vector for the induction of apoptosis. Therefore, in this chapter, we explored the use of a truncated form of the human Bax gene in an expression construct as a means for augmenting cell death. The truncated Bax, which consisted of amino acids 112-192 of the full-length protein, was selected because it had previously been used for treatment of a mouse model of non-small cell lung cancer in an adenoviral vector (151). The enhanced potency seen with ΔN-Bax compared to full-length Bax made it a particularly appealing candidate for our bone marrow transplantation strategy.

Using an adenoviral strategy to overexpress ΔN-Bax, Usui et al. (151) were able to initiate cell death in 80% of A549 cells 48 hours after infection. The disparity between

results noted by Usui et al. (151) and the results observed here could potentially be attributed to differences in the cell type used. It is also important to note the role vector type could potentially play in the gene transfer process. Adenoviral vectors, as used by Usui et al. (151), permit high infection efficiency and sustained gene expression over reasonable time courses. More standard plasmid transfection techniques, such as the Lipofectamine 2000 and Amaxa electroporation techniques that we employed, may convey considerably lower transfection efficiencies. Furthermore, the transfection procedure itself can lead to substantial cellular toxicity.

Prior to the publication by Usui et al. (151), the same group reported that transient transfection of FDC-P1 cells using electroporation with an ΔN-Bax expression vector led to apoptosis in just 2% of cells (152). The percentage of apoptotic cells increased to 4% when ΔN-Bax was co-transfected with Bcl-2 or Bcl-X_L. Transfection of full length Bax was only able to induced apoptosis in <1% of cells when co-transfected with Bcl-2 or Bcl-X_L, compared to ~4% when co-transfected with a neomycin resistance cassette. These two reports, which were generated by the same group, show remarkable differences in potency of ΔN-Bax expression. The disparate results noted between these two reports, as well as the absence of a noticeable effect of ΔN-Bax expression in our own study, raise questions about the interpretation of the results reported by Usui et al (151).

In our hands, transfection with a plasmid containing ΔN-Bax showed no pro-apoptotic effect that could be directly attributed to ΔN-Bax expression. Interpretation of our results is somewhat confusing, however, due to our inability to directly observe the expression of ΔN-Bax without the GFP tag. The sequencing data from pΔN-Bax -N1

aligned correctly with the predicted sequence, and no cryptic start codons were detectable that could potentially lead to an out-of-frame polypeptide. Furthermore, robust ΔN-Bax message was detected using qRT-PCR. Although the PCR primers were unable to distinguish the truncated transcript from the native form, the inability to detect message in cells not transfected with pΔN-Bax -N1 suggest that that endogenous levels of full length Bax were insignificant compared to that seen in transfected cells. The presence of ΔN-Bax mRNA suggests that the ΔN-Bax gene *was* expressed. Ideally we would have liked to detect the expressed protein directly; however the majority of the antibodies for Bax are raised against a peptide fragment derived from the N-terminal region of the full length protein. The antibody used in Figure 4.7 should have been capable of detecting both the native and recombinant forms of Bax; however we were only able to detect a band corresponding to the full length protein.

In an effort to circumvent the issue of ΔN-Bax detection, we generated a EGFP:ΔN-Bax fusion construct which allowed us to visually observe transfected cells. Although we were still unable to quantify the apoptotic effect of EGFP:ΔN-Bax expression, distinct phenotypic changes in transfected cells were observed that could be attributed to apoptosis. Endogenous Bax is largely cytosolic in the absence of apoptotic stimuli. Following activation of the intrinsic pathway, a change in Bax conformation leads to translocation of Bax from the cytoplasm to the MOM (147). Imaging of cells expressing a Bax-GFP fusion (containing the full length Bax) results in a diffuse, homogeneous fluorescence pattern throughout the cell. Following apoptosis, a punctate signal is observed which colocalizes to the mitochondria (147); (153); 154). The resultant fluorescent patterning is markedly similar to that which we observed following

transfection with pEGFP:ΔN-Bax (Figure 4.4). The same punctate GFP patterning was also seen when cells expressed a GFP-Bax fusion protein containing a single serine deletion (amino acid 184) in the C-terminal transmembrane domain of full length Bax. The deletion led to changes in protein confirmation so that it resided permanently in MOM-bound form. Expression of the Bax deletion mutant also lead to a modest increase in toxicity relative to the native form (153).

Given the results described here characterizing expression of the EGFP:ΔN-Bax fusion construct, in addition to the absence of any net effect of ΔN-Bax expression alone, it is the opinion of this author that expression of ΔN-Bax does NOT result in apoptotic cell death. The rationale for this conclusion is largely based on speculation, although there is a plethora of literature which supports this hypothesis.

Despite the extensive research exploring the functional role of Bax in apoptosis, the mechanism by which it contributes to MOM instability is not well understood. It is widely accepted that the intrinsic apoptotic pathway is highly dependent on Bax and the rest of the Bcl-2 family members. The interplay between the three established Bcl-2 family member groups and their relative concentrations is a requisite event for the initiation of the apoptotic pathway, and could offer some insight into why ΔN-Bax is not capable of inducing cellular toxicity as expected.

The first group of the Bcl-2 family contain the survival proteins (Bcl-2, Bcl-X_L), each of which contain 4 of the Bcl-2 homology domains (BH1-4). The second group of the Bcl-2 family, the pro-apoptotic proteins (Bax, Bak and Bok), contain only the domains BH1-3. The third family, the BH3-only proteins (Bim, Bid) contain only the BH3 domain .

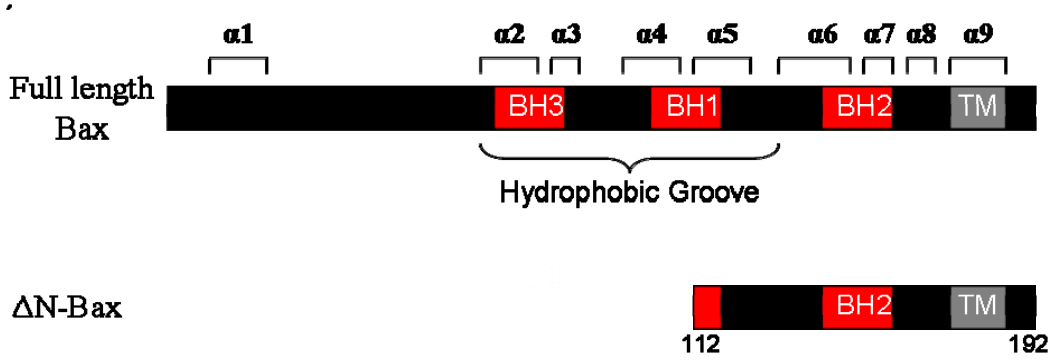

Figure 4.9: Structure of Bax. The full length Bax protein consists of 9 amphipathic α helices. In the 3-dimensional conformation, a hydrophobic groove is formed between α2-α5. The BH3 domain is essential for BH3-only activation of apoptosis as well as well as the homo-oligimerization required for pore formation in the MOM. The TM domain of ΔN-Bax keeps it restricted to the MOM.

The structure of full length Bax consists of 8 amphipathic α-helices surrounding a single hydrophobic groove. Figure 4.9 shows the distribution of the 8 α-helices along the Bax gene, as well as the positioning of each of the BH-domains. Bak, another pro-apoptotic Bcl-2 family member, may be associated with the mitochondria even in the absence of apoptotic stimuli (147), but inactive Bax exists in a cytosolic state. The three-dimensional structure of Bax undergoes a multistep transition starting from the inactive cytosolic state and end in the formation of a pore complex in the MOM. In a non-apoptotic setting, the BH1, BH2 and BH3 domains of the survival protein Bcl-2 form a hydrophobic groove on the protein surface (155) that accommodates the corresponding BH3 domain of Bax. The result is that Bax is sequestered and unable to homodimerize, leading to inhibition of its innate death-inducing abilities (149; 148). Bax is only translated to the MOM once the cell death program has been initiated (147). In it's inactive state, the hydrophobic transmembrane (TM) C-terminal tail of Bax is folded into the hydrophobic pocket created by the BH1, BH2 and BH3 domains (154), thereby preventing insertion of the protein in the MOM. Bax undergoes a conformational change

following apoptotic activation that exposes the C-terminal tail and allows for insertion in the MOM (153; 156). Targeted mutations and deletions in Bax have been generated that leave the TM tail exposed and result in MOM localization even in the absence of apoptotic stimuli. Permanent translocation of Bax to the mitochondria using the deletion mutants generates a more cytotoxic effect than the WT protein (101; 153; 156; 157). The ΔN-Bax construct utilized in our study lacks the BH3 and BH1 domains necessary for maintaining the "inactive" cytosolic conformation (Figure 4.9). Therefore, ΔN-Bax may exist in an uninhibitable MOM-targeted state. The result of the ΔN-Bax conformation, observed in cells expressing the EGFP:ΔN-Bax fusion construct, is that ΔN-Bax has a continually exposed TM domain which keeps the protein bound within the MOM.

Usui, et al.(151) hypothesized that because ΔN-Bax lacks the BH3 domain required for binding Bcl-2, it was a more potent inducer of apoptosis than the full length protein (151). More recently, however, the importance of the BH3 domain in Bax activation has been demonstrated, suggesting that perhaps the α2-α5 helices are required for pore formation and cytochrome *c* release from the MOM (96; 158; 159; 160). Direct activation of Bax by BH3-only proteins is also mediated by interaction with the BH3 domain of Bax (93; 95; 96). Given these reports, it seems likely that ΔN-Bax (lacking helices α1-α4 and the entire BH3 domain) is unable to be activated by BH3-only proteins and unable to oligomerize and form pores in the MOM. As a result, the ΔN-Bax fragment is essentially a MOM-targeting sequence without apoptosis-inducing ability.

From our results, the only evidence that would suggest a pro-apoptotic effect of EGFP:ΔN-Bax was the temporal loss of fluorescence noted in 3T3 and HUVECs transfected with EGFP:ΔN-Bax. However, the lack of sustained GFP expression could

also be explained by an increased rate of protein degradation. In fact, the α5 region of Bax is highly susceptible to ubiquitin degradation (161). In the case of full length Bax, the α5 helix is shielded within the hydrophobic pocket of the folded protein. However the ΔN-Bax peptide leaves the α5 helix fully exposed. This altered conformation could lead to accelerated degradation rates which would explain the loss of fluorescence observed in our results.

Expression of ΔN-Bax alone may not be enough to induce apoptosis. However, it may cause cells to be more susceptible to Bax-mediated apoptosis. In essence, the membrane-bound ΔN-Bax may be "poised to strike", so that if the endogenous apoptotic program is activated the cells undergo death faster and more effectively. There are several future experiments that may help to determine what role, if any, ΔN-Bax has in apoptosis. We suspect that ΔN-Bax and the EGFP:ΔN-Bax fusion protein are automatically targeted to the MOM. This hypothesis could be confirmed with co-localization of mitochondrial staining and EGFP fluorescence.

Regardless of the mechanism with which ΔN-Bax interacts with the endogenous apoptosis pathway, expression of ΔN-Bax alone is ineffective at inducing apoptosis. These results also explain why no apoptosis was seen following tamoxifen administration in the transgenic CrIED mice described in Chapter 3; ΔN-Bax expression does not kill cells. Based on these results, we abandoned the strategy of using ΔN-Bax for induction of apoptosis altogether.

CHAPTER 5

A RETROVIRAL-MEDIATED STRATEGY FOR FLOURESCENT LABELING OF BONE MARROW SUBPOPULATIONS

Introduction

In Chapter 3, two different strategies for the elimination of Endothelial Progenitor Cells (EPCs) were described. We were unable to implement either the retroviral or transgenic strategies for the elimination of bone marrow-derived EPCs. Realizing that the failure of these approaches was ultimately due to the complexity of our experimental design, we sought to employ a more straightforward methodology to identify subpopulations of bone marrow cells and determine the role of these cells in neovascularization

Increasing evidence suggests that bone marrow-derived cells play a key role in the formation of new blood vessels, redefining the prevailing paradigm of post-natal neovascularization. A number of reports have identified bone marrow (BM)-derived precursor cells that incorporated into the endothelial layer and contributed directly to the growth of new blood vessels (12; 13; 126; 14; 127; 128; 162). Recently, these findings have been challenged by reports (3; 44; 45) which refute claims of the direct involvement of bone marrow cells in endothelial regeneration. Instead of transdifferentiating into endothelial cells, it has been argued that BM-derived cells aggregate around nascent vessels in a perivascular location within the vessel wall, potentially augmenting angiogenesis through a paracrine role rather than the formation of *de novo* blood vessels

A growing body of work in the cancer literature indicates that cells of myeloid origin may be relevant to tumor angiogenesis (163; 164). Several important

subpopulations have been implicated in the formation of tumors, such as tumor associated macrophages (TAMs), Tie-2 expressing monocytes (TEMs) (54), vascular leukocytes (55), and myeloid derived suppressor cells (MDSCs) (165). The majority of these myeloid-derived cells do not incorporate directly into the endothelium, but they have been shown to express some endothelial-type markers and their depletion from the angiogenic milieu of tumorigenic tissue has been shown to suppress tumor vessel formation (53; 54; 60). Although each of the myeloid-derived cell types were identified by independent methods, phenotypic overlap between the cell types is likely, given their functional and genetic similarities (62). The apparent heterogeneity of pro-angiogenic cell populations in peripheral blood, and a lack of consensus regarding characterization of these different cell populations, obviates the need for systematic assessment of BM-derived cell types involved in neovascularization.

Colony forming assays are frequently used to identify endothelial progenitor cell (EPC) populations from peripheral blood. However, several different assays exist that generate endothelial colonies from PB-MNCs, with each assay likely identifying a different population of cells (28). Endothelial progenitor cells derived from an adherent cell population that forms within 7 days in endothelial-rich culture are frequently referred to as "early EPCs". A second, highly proliferative population referred to as outgrowth endothelial cells (OECs) can be identified after 21 days under the same culture conditions (24). Colony forming unit endothelial cells (CFU-ECs) are derived from an adherence *depleted* population of PB-MNCs, and give rise to small endothelial-like cell clusters after 5 days(2).

In addition to the colony forming assays, another common method often employed to identify circulating progenitor cells is through surface marker identification via flow cytometry. In this technique, categorization is based on a combination of surface markers such as CD34, CD133, and VEGFR-2 (32; 84; 88; 89; 166). Flow cytometry is an extremely fast and highly quantitative method of characterizing cells, but it suffers from several limitations. Most importantly, the markers used to define a progenitor cell population are not unique. Although the combination of CD34, CD133, and VEGFR-2 are frequently used to quantify the number of endothelial progenitor cells, it has been demonstrated that cells that co-express all of these markers are unable to fully differentiate into endothelial cells in culture (43). Low levels of circulating CD34+/CD133+/VEGFR-2+ cells may serve as an indicator of impaired vascular function (40; 42; 82; 86; 87), however this cell population does not directly incorporate into the endothelium. Furthermore, there is a marked absence of data linking circulating EPCs (as defined by these surface markers) to the EPC colonies formed in culture assays.

An additional limitation to the use of surface markers for EPC identification is that surface antigens cannot be used to predict a functional role in neovascularization. Expression of CD34, for example, can only be used as an indicator of hematopoietic pluripotency; and even this characteristic has recently been challenged (167; 168). The marker CD34 cannot be used to conjecture the functional fate of cells, as its expression does not confer a functional outcome. Characterization of intracellular protein expression could potentially offer more insight into progenitor cell function. For example, if a population of circulating cells that express VEGF could be identified, then it would reason that those cells would augment angiogenesis through VEGF secretion if recruited

to ischemic tissue. Similarly, if circulating cells that express eNOS could be prospectively identified, it follows that those cells would augment angiogenesis in ischemic tissues through generation of nitric oxide. Staining for intracellular proteins such as VEGF and eNOS requires membrane permeabilization, resulting in a loss of cell viability (169). Consequently, in order to monitor the expression of intracellular proteins in live circulating cells *in vivo*, transgenic reporter mice are necessary. The use of transgenic mice for cell labeling is an approach that is both extremely time consuming and costly due to generation and maintenance of the animal colonies.

To circumvent the problems associated with intracellular labeling techniques, we have developed a novel method for the fluorescent labeling of bone marrow cells using self-inactivating retroviral vectors with tissue specific promoters. Using the VEGF, VE Cadherin and eNOS transcriptional regulatory sequences, we were able to transduce mouse bone marrow with a unique set of retroviral constructs. Following transplantation into lethally irradiate recipients, we were able to identify novel populations of bone marrow-derived cells based on promoter-specific activation of a fluorescent reporter gene.

Methods

Animals

Wild type C57BL/6J mice were purchased from the Jackson Laboratory. All animals were fed standard chow ad libitum and had free access to water. All protocols were approved by the Institutional Animal Care and Use Committee and done in

accordance with the federal guidelines on the principles for the care and use of animals in research.

Generation of Retroviral Plasmids

All plasmids were propagated in Top10 E.Coli (Invitrogen). Transformed E.Coli were grown on LB-Agar plates containing 100 μg/mL of Kanamycin. For large scale plasmid preparation, inoculated cultures were grown in 2L Erlenmeyer flasks containing 200 mL of LB-broth supplemented with 100 μg/mL Kanamycin. Cultures were propagated overnight in a rotary shaker at 250 rpm and 37 ^{o}C. Plasmid DNA was isolated using Qiagen HiSpeed Plasmid Maxi-prep.

All constructs were derived from the pQCXIX (Clontech) vector. To generate the constructs, pQCXIX was first digested with Not I and Mlu I. The fragment containing an Internal Ribosome Entry Site (IRES) was separated by electrophoresis in a 1% gel. The remaining sequence was extracted and religated with T4 DNA Polymerase (New England Biolabs). For pSINrv:CMV-tdT, the tdTomato sequence from ptdTomato (Clontech) was cloned into the EcoRI and XhoI sites remaining in the QCXIX backbone.

A promoterless vector, pSINrv:X-tdT, was generated by digesting pSINrv:CMV-tdT with Stu I and Not I (New England Biolabs). The fragment containing the CMV promoter was separated by electrophoresis in a 1% gel. The remaining sequence was extracted and religated with T4 DNA Polymerase.

To generate pSINrv:eNOS-tdT, the 1.8 kb fragment of the eNOS promoter was amplified from genomic mouse DNA by PCR (See appendix for primers) using Hi-Fidelity Platinum Taq DNA Polymerase (Invitrogen). The PCR product was incorporated

into pCR4 using a TOPO-TA cloning kit (Invitrogen), and the sequence was verified with direct sequencing. Pac I and BsI WI restriction sites were added to the 5' and 3' ends, respectively, of the promoter sequence through a second round of PCR using the pCR4-eNOS plasmid as a template. The resulting PCR product was cloned into the corresponding Pac I and BsI WI restriction sites of pSINrv:X-tdT.

To generate pSINrv:VEGF-tdT, the 1.8 kb fragment of the VEGF promoter was generated by PCR from genomic mouse DNA (See appendix for primers) using Hi-Fidelity Platinum Taq DNA Polymerase (Invitrogen). The PCR product was incorporated into pCR4 using a TOPO-TA cloning kit (Invitrogen), and the sequence was verified with direct sequencing. Pac I and BsI WI restriction sites were added to the 5' and 3' ends, respectively, of the promoter sequence through a second round of PCR using the pCR4-VEGF plasmid as a template. The resulting PCR product was cloned into the corresponding Pac I and BsI WI restriction sites of pSINrv:X-tdT.

To generate pSINrv:CD68-tdT, PCR was used to add Pac I and BsI WI to the CD68 promoter from pDRIVE-mCD68 (Invivogen). The resulting 0.6 kb PCR product was cloned into the corresponding Pac I and BsI WI restriction sites of pSINrv:X-tdT.

To generate pSINrv:VE Cad-tdT, Pac I and BsI WI restriction sites were added to the 5' and 3' ends, respectively, of the VE Cadherin promoter sequence through PCR using the murine VE Cadherin promoter sequence from pVEcad (generously donated by Dr. Roy Sutliff, Emory University) as a template. The resulting PCR product was cloned into the corresponding Pac I and BsI WI restriction sites of pSINrv:X-tdT.

Retroviral Production

293-derived Phoenix Ecotropic (Phx-Eco) packaging cell lines [3] (ATCC) were grown to 80% confluence in 100ml plates with growth media consisting of DMEM (Gibco) supplemented with 10% Fetal Bovine Serum, L-glutamine, and Pen/Strep. Before transfection, 10 ml of fresh media was added to each plate. Transfections were performed following the JetPRIME^{TM} manufacturers recommended protocol (Polyplus). Briefly, 10 μg of plasmid DNA was added to 500 μL of JetPRIME^{TM} buffer then briefly vortexed and centrifuged. 20 μL of JetPRIME^{TM} was then added to the DNA mixture, which was again briefly vortexed and centrifuged. Following a 10 minute incubation at room temperature, the DNA/ JetPRIME^{TM} solution was added to the cells in a drop-wise manner and transported to a 37 C^{o}/5% CO_2 incubator. After 6-8 hours, transfection media was aspirated and replaced with 25ml of fresh media. 24 hours after the start of transfection, the media was again aspirated, 9 ml of fresh media was added, and the cells were transferred to a 32 C^{o}/5% CO_2 incubator. 48 hours after transfection, the conditioned media was collected in a 10 mL syringe and passed through a 45μm low protein binding filter (Nunc) and either frozen and stored at -80 ˚C or used immediately for transduction. Conditioned media was collected afterward at 12 hour intervals for up to 7 days following transfection.

Bone Marrow Isolation and Transduction

A detailed protocol for bone marrow transduction, modified from Ide et al. (133), is included in the Appendix. Briefly, mice were euthanized by CO_2 inhalation and long bones were flushed with cold PBS. Bone marrow cells were labeled with anti-Sca1-PE

antibodies, then separated with anti-PE micro-beads using an AutoMACS sorter (Miltenyi). Sorted cells were cultured in Stempro-34 media supplemented with mSCF (100 ng/ml, Sigma), Flt-3 (100 ng/ml, R and D), Il-3 (20 ng/ml, Sigma), and Il-11 (100 ng/ml, Sigma) for 24 hrs. RV supernatant was centrifuged overnight at 4˚C and 9000g, and resuspended in 1/20 the original volume of complete Stempro-34 with cytokines. Retrovirus was bound to retronectin coated plates by centrifugation for 1 hr at 4 ˚C and 2500rpm. Bone marrow cells were plated on RV/retronectin plates, and cultured for 24 hrs at 32 C^o.

Bone Marrow Transplants

One day prior to transplantation, recipient mice were irradiated with 11Gy in order to eliminate the regenerative capacity of the endogenous bone marrow. On the day of transplantation, bone marrow cells modified by retroviral transduction were washed in sterile phosphate buffered saline (PBS) containing 2% fetal calf serum. Recipient mice were anethsetized with Avertin, 375-mg/kg, and given $5x10^5$ cells by retro-orbital injection. For 3 weeks following transplantation, mice were mainatainied on broad spectrum antiobiotics delivered through the drinking water. Mice were allowed an additional 3 weeks of recovery prior to experimentation.

Cell Lines and Culture

NIH/3T3 cells were grown at 37 C^o, 5% CO_2 in DMEM supplemented with 10% calf serum, L-glutamine, and Pen/Strep. 3T3 cells were grown in 10 cm tissue culture-treated dishes until 80% confluent, then passaged at a ratio of 1:5. MS1 cells (ATCC)

were grown at 37 C^o, 5% CO_2 in DMEM supplemented with 10% fetal bovine serum, L-glutamine, and Pen/Strep in 10 cm tissue culture-treated dishes coated with gelatin until 80% confluent, then passaged at a ratio of 1:5.

Flow Cytometry

Mice were sacrificed and 0.5-1.0 mL of peripheral blood was collected in a 1.5 mL micro-centrifuge tube from the right ventricle in 100 μL of heparin sodium solution. RBC lysis was performed with Pharym-Lyse (BD Bioscience) to obtain PB-MNCs. For CD14 staining, 1e6 cells were suspended in FACS staining buffer (BD Biosciences) and incubated with anti-CD14-PerCP cy5.5 antibody (eBioscience). For VEGFR-2, CD34, and CD45 staining, 1e6 cells were preincubated with 1 μg mouse seroblock (R and D systems), then stained with anti-CD34-eflour450, anti-CD45-eflour APC-750 , and anti-Flk1-APC antibodies (eBioscience) in FACS staining buffer. For eNOS and VEGF staining, cells were treated with fixation and permeabilization solution (BD Bioscience) following RBC lysis, and labeled with either anti-eNOS-Alexa647 (BD Bioscience) or anti-VEGF-APC (R and D Systems) antibodies. Flow cytometry was performed with a BD LSRII analyzer (BD Biosciences), and a minimum of 50,000 events were recorded. Dot plots were generated in BD FACSDiva, and analysis was performed using FlowJo software.

***In vivo* Matrigel Assay**

Matrigel (BD Biosciences) was mixed with 0.5 μg/mL bFGF (BD Biosciences) and 64 U/mL heparin sodium (BD Biosciences), and $1x10^6$ MS1 cells transduced with

SINrv:CMV-tdT. The matrigel mixture (500 μL) was implanted subcutaneously in the dorsal region of athymic Nude mice (Charles River). After 7 days, animals were euthanized by CO_2 inhalation, and matrigel plugs were removed and fixed in 10% formalin for 4 hours. Following fixation, matrigel was snap-frozen in OCT medium and stored at -80 ^{o}C.

Histology

Matrigel was sectioned into 7 μm thick sections and mounted with Vectashield fluorescence mounting media with DAPI (Vector Labs). Images were recorded using a Ziess upright fluorescence microscope.

Results

Design of SINrv:X-tdT constructs

A series of retroviral plasmids were generated out of a SIN-MMLV vector so that expression of the fluorescent protein tdTomato could be regulated by an internal promoter. These constructs are referred to as SIN Retrovirus:X-tdTomato, or SINrv:X-tdT, where X represents the promoter sequence contained in the construct. To generate the promoterless vector, the tdTomato CDS was inserted into an empty SIN-MMLV vector between the retroviral LTRs, downstream of an MMLV packaging sequence and the promoter cloning sites (Figure 5.1). Five different promoters were identified based on their potential relevance to the process of neovascularization (Table 5.1), which were then cloned into the empty promoter cloning site in pSINrv:X-tdT. A 2.5 kb fragment of the murine Vascular Endothelial (VE) Cadherin promoter (170) was used to confer

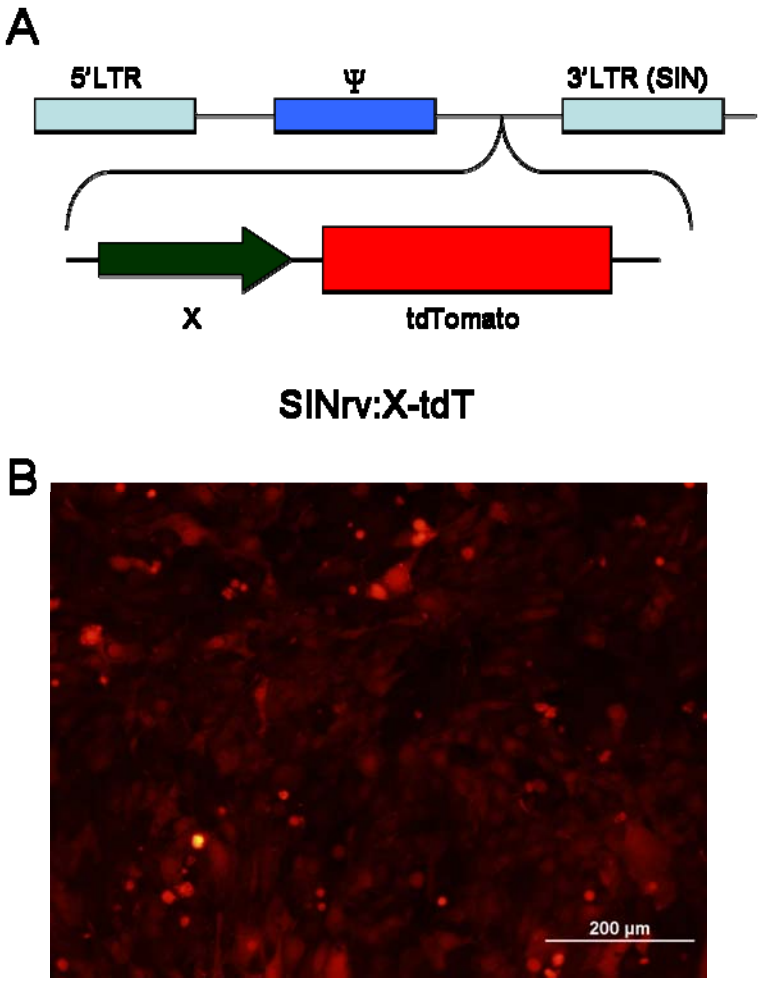

Figure 5.1: SINrv Construct Design. A) The SINrv:X-tdT vector consists of a SIN-MMLV-based backbone with cloning space for an internal promoter (X) driving the fluorescent protein tdTomato, inserted between the packaging sequence (Ψ) and the 3'LTR. B)Visual detection of tdTomato expression using fluorescence microscopy in 3T3 cells transduced with SINrv:CMV-tdT (which contains an internal CMV promoter to drive expression of tdTomato).

endothelial specific expression of tdTomato in target cells and a 0.8 kb fragment of the CD68 promoter/enhancer (171) was used to confer macrophage specific expression following transduction. Additionally, a 1.8 kb fragment containing both the genomic sequence upstream of the murine VEGFa exon 1 (and including the 5'UTR) (172) and a 1.8 kb of the 5'flanking region of murine eNOS (173) were used for the VEGF and eNOS

promoters, respectively. For a constitutively active control retrovirus, the 0.5 kb fragment of the human cytomegalovirus immediate-early promoter (CMV) was used to direct tdTomato expression. All promoter sequences were confirmed via restriction digestion and direct sequencing. 3T3 cells transduced with SINrv:CMV-tdT (which utilizes the CMV promoter to drive expression of the tdTomato gene) exhibited dramatic red fluorescence, verifying function of the reporter gene (Figure 5.1).

Retroviral Promoter Activity in MS1 cells

An immortalized mouse endothelial cell line (MS1) was transduced with SINrv:eNOS-tdT, SINrv:VEcad-tdT, SINrv:VEGF-tdT and SINrv:CMV-tdT, and then imaged for fluorescence. Activity of the CD68 promoter was not assessed *in vitro*. Transduction with SINrv:CMV-tdT resulted in high levels of tdTomato expression. Intensity of the fluorescence was clearly lower when tdTomato was regulated by the eNOS, VEGF or VE Cadherin promoters compared to CMV, but was detectable nonetheless (Figure 5.2). All of the promoters also generated visible fluorescence in 3T3 cells. Since eNOS and VE Cadherin promoters are tightly regulated and should confer strict endothelial specificity, it was surprising that tdTomato was detected in 3T3 cells transduced with either SINrv:eNOS-tdT or SINrv:VEcad-tdT . These findings could indicate promiscuity of the promoters, although it is also possible that 3T3 cells aberrantly express eNOS and VE Cadherin.

Transduced MS1 cells were analyzed by flow cytometry for quantitative comparison of promoter activity. While nearly 30% of MS1 cells expressed tdTomato following transduction with SINrv:CMV-tdT, constructs containing the vascular promoters (VEGF,

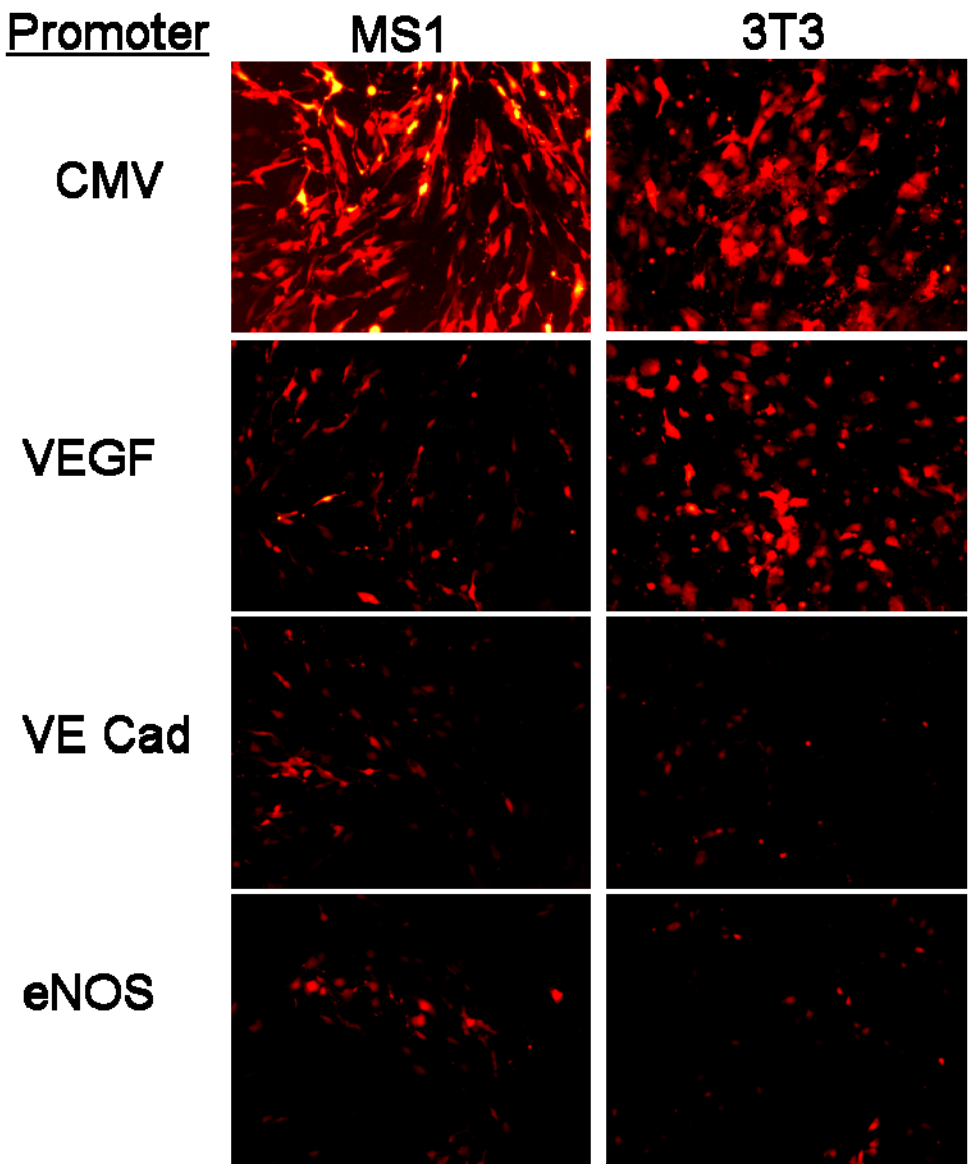

Figure 5.2: Validation of retroviral constructs *in vitro*. MS1 and 3T3 cells were transduced with SINrv:CMV-tdT, SINrv:VEGF-tdT, SINrv:VEcad-tdT, and SINrv:eNOS-tdT. Fluorescent images were recorded after 72 hours. Red indicates tdTomato fluorescence.

VE Cadherin, eNOS) generated transduction efficiencies of 11% or less. The lower frequency of tdTomato positive cells could be attributed to a 3-fold reduction in titer observed when the CMV promoter was replaced with eNOS, VEGF, or VE Cadherin (data not shown). Mean Fluorescence Intensity (MFI), calculated for tdtomato-positive

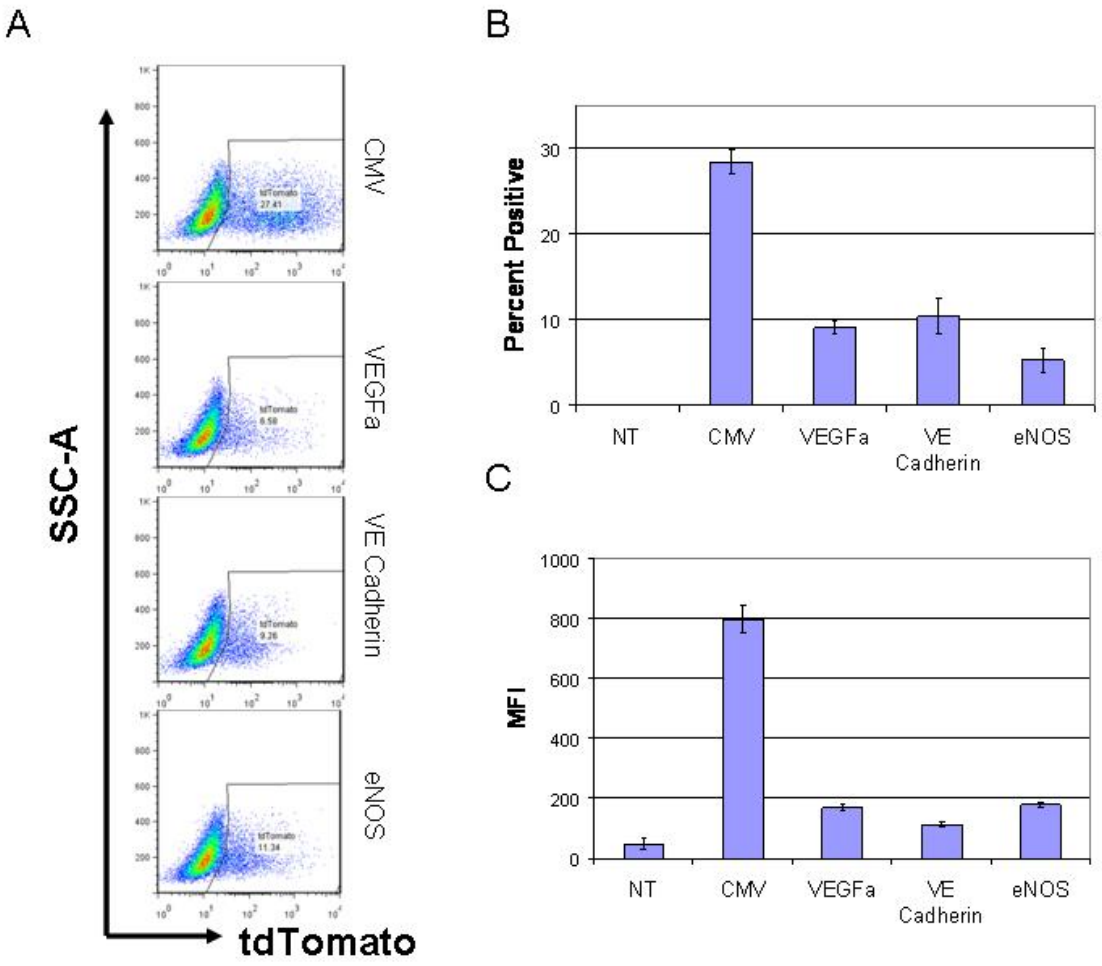

Figure 5.3: Promoter Characterization In MS1 Cells. Flow cytometry was performed on MS1 cells transduced with the SINrv series of retroviral constructs. A) Dot plots of MS1 cells transduced with different SINrv constructs compare the different promoters used. B) The percentage of positive cells was quantified for each promoter. C) Mean Fluorescence Intensity was determined using the positive gated events in the tdTomato channel. For all groups N=4. Error bars indicate standard deviation.

cells in each treatment group, was also significantly lower when tdTomato was regulated by the vascular promoters compared to CMV (Figure 5.3). VE Cadherin generated the weakest signal (Figure 5.3), followed by VEGF and then eNOS.

Enrichment of tdTomato-positive cells with FACS

An inherent advantage of using a fluorescent protein to genetically label cells, is that live cells can then be sorted using Flourescence Assisted Cell Sorting (FACS). To determine if a heterogeneous cell population could be enriched for tdTomato positivity, FACS was performed on a mixed population of MS1 cells transduced with SINrv:VEGF-tdT. Prior to sorting, less than 4% of the total cell population expressed tdTomato. Analysis of the cells post-sort indicated that greater than 99% of the cells expressed tdTomato (Figure 5.4). These data demonstrate that sorting for tdTomato can generate highly pure samples from rare populations of cells. Therefore, our tdTomato labeling approach could be extremely valuable in isolating specific cell populations for cell therapy applications.

Detection of Fluorescently Labeled Cells *in vivo*

The eventual goal of this project was to utilize the SINrv:X-tdT vectors for live cell tracking in a setting of neovascularization *in vivo.* To validate this strategy, MS1 cells transduced with SINrv:CMV-tdT were seeded in matrigel which was then implanted subcutaneously in athymic Nude mice. At 7 days, the matrigel plugs were removed and sectioned for histological analysis. Cells within the matrigel plug expressing tdTomato were clearly visualized with fluorescence microscopy (Figure 5.5), supporting the feasibility of this strategy.

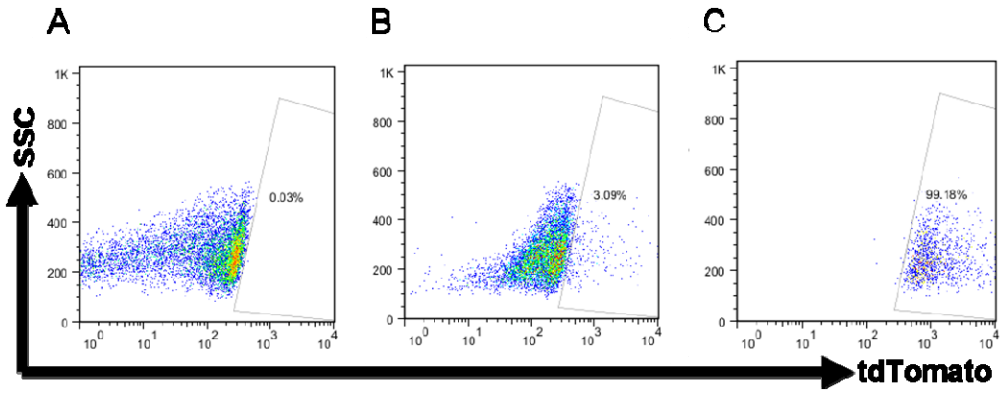

Figure 5.4: tdTomato Enrichment With FACS. A mixed population of MS1 cells labeled with SINrv:VEGF-tdT and unlabeled MS1 cells was enriched using FACS. A) Negative control. B) Starting population of fluorescent and non fluorescent cells. Only 3% of the starting population expressed tdTomato. C) Post sort analysis demonstrating >99% of the total cell population was tdTomato-positive.

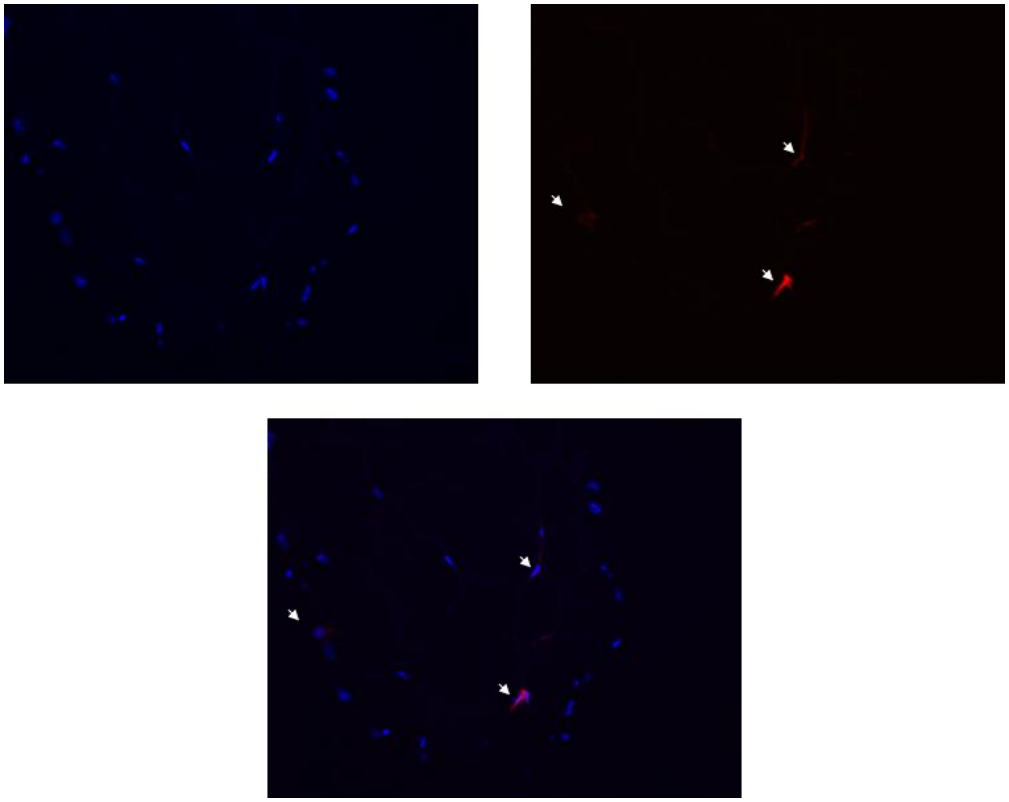

Figure 5.5: *In vivo* Monitoring of tdTomato Expression. MS1 cells transduced with SINrv:CMV-tdT were mixed with Matrigel and bFGF, then injected subcutaneously in Nude mice. Plugs were removed at 7 days then imaged for fluorescence. Arrows represent tdTomato positive cells within the Matrigel Plug. Top Left: DAPI. Top Right: tdTomato. Bottom: Merged Image. All images taken at 20x magnification.

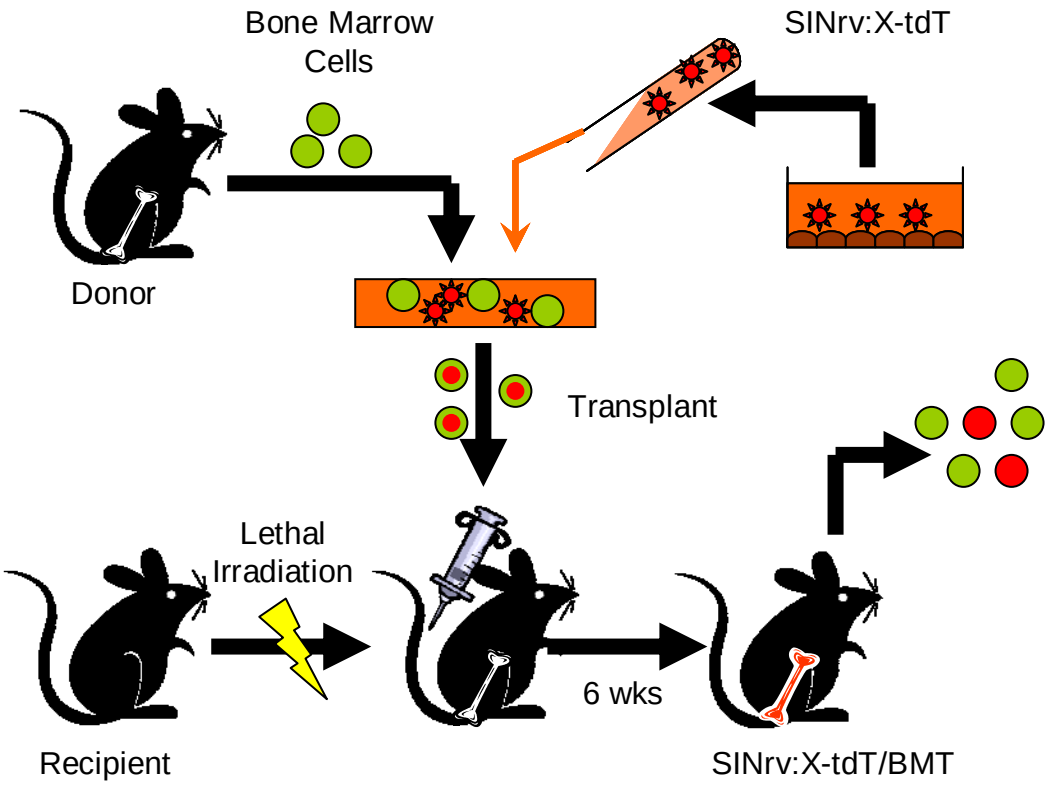

Figure 5.6: Bone Marrow Labeling Strategy. In the retroviral transduction strategy, bone marrow cells are isolated from C57B6/J mice, and cultured with viral supernatant containing one of the SINrv:X-tdT viruses. Transduced cells are transplanted into a lethally irradiated host, and allowed to engraft for 6 weeks. The resulting BM chimera is referred to as a SINrv:X-tdT/BMT mouse. Following engraftment, bone marrow-derived cells in which the retroviral promoter is active can be detected by flow cytometry or fluorescence microscopy.

Retroviral Bone Marrow Transduction Strategy

For live cell tracking of bone marrow subpopulations, we employed a retroviral mediated-bone marrow transduction and transplantation approach. Our general strategy, outlined in Figure 5.6, was to isolate bone marrow cells from donor mice, transduce the cells with one of the SINrv:X-tdT vectors, then transplant the genetically modified cells into a lethally irradiated WT host. Following engraftment, only the bone marrow component of the SINrv:X-tdT BMT chimera (SINrv:X-tdT/BMT) contains the retroviral transgene. Therefore, only the BM-derived cells in which the retroviral promoter is active

express tdTomato. Using this technique we were able to specifically label certain subpopulations within the bone marrow based on promoter specificity.

In order to validate the transduction/transplant approach, we transduced isolated bone marrow cells with the SINrv:CD68-tdT vector. Transduced BM cells propagated in Methocult media were assayed for colony formation and visualized for fluorescence. The majority of colonies did not express tdTomato, but several fluorescent colony forming unit-macrophage (CFU-M) colonies were observed (Figure 5.7). Flow cytometry on both PB and BM isolated from SINrv:CD68-tdT/BMT mice at 6 weeks post-transplant identified a small population of low side scatter (SSC^{Low}) cells that expressed tdTomato (Figure 5.7), potentially identifying a bone marrow-derived macrophage or macrophage precursor.

tdTomato Expression Following Bone Marrow Transduction

Bone marrow cells were isolated from C57B6/J mice, sorted for Sca1+, and then transduced with either SINrv:CMV-tdT, SINrv:VEGF-tdT, SINrv:VEcad-tdT, or SINrv:eNOS-tdT. A sample of transduced BM was then cultured in Methocult and assayed for colony formation, while the remaining cells were transplanted into lethally irradiated WT recipients and allowed to engraft for 6 weeks. The transplant recipients receiving transduced marrow were referred to as SINrv:X-tdT/BMT mice.

Transduced BM grown in Methocult formed multiple colony forming unit-granulocyte (CFU-G) colonies. A large proportion of the CFU-G colonies in cells transduced with SINrv:CMV-tdT expressed tdTomato. Fluorescent colonies in the remaining groups were extremely rare, though clearly detectable (Figure5.8). After 6

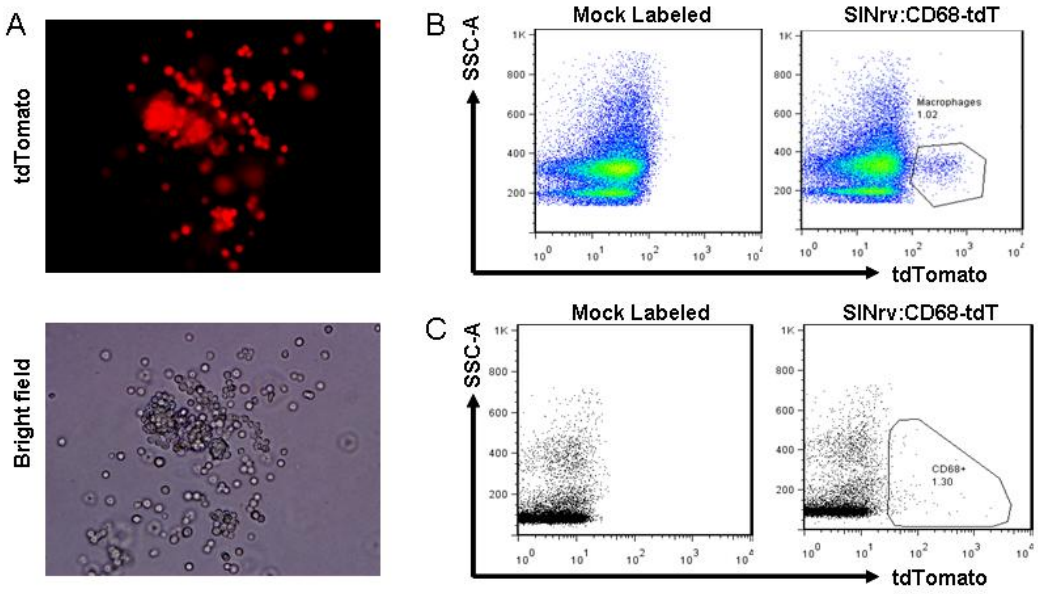

Figure 5.7: Validation of Bone Marrow Transplant Strategy. Bone marrow cells were transduced with SINrv:CD68-tdT and grown in Methocult media for 7 days to allow colony formation. (A) Fluorescent CFU-M colonies were detected, indicating successful transduction. Transduced cells transplanted into lethally irradiated hosts were allowed to engraft for 6 weeks. (B) BM and (C) PB were harvested and analyzed by flow cytometry to detect cells expressing tdTomato.

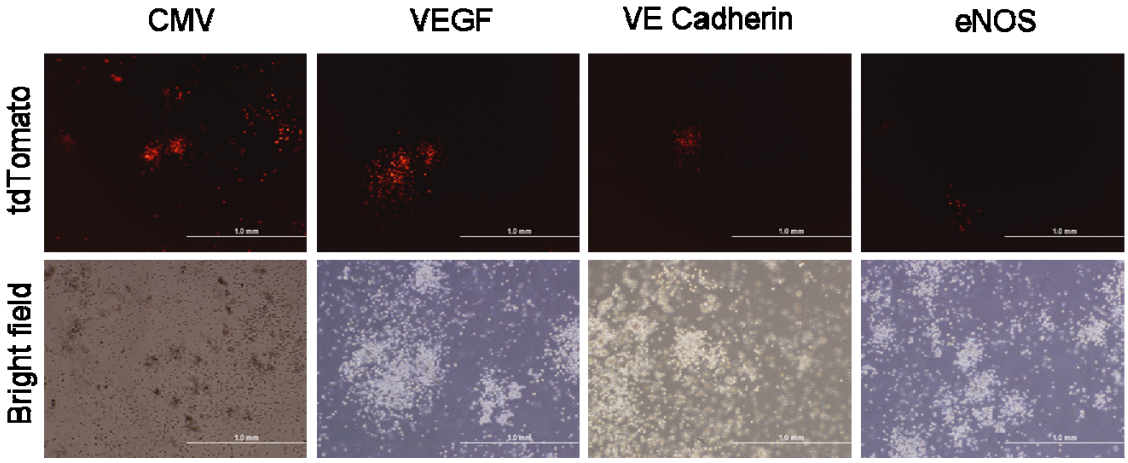

Figure 5.8: Expression of tdTomato In Transduced Bone Marrow Colonies. Following transduction with SINrv:CMV-tdT, SINrv:VEGF-tdT, SINrv:VEcad-tdT, SINrv:eNOS-tdT, BM cells were grown in methocult and imaged for fluorescence after 7 days. tdTomato-positive CFU-Gs were detected in all groups, however frequency of positive colonies was much higher in SINrv:CMV-tdT cells.

weeks of engraftment, PB-MNCs from SINrv:X-tdT/BMT mice were analyzed using flow cytometry. Only 7.23 % (+/-2.79 SD) of PB-MNCs obtained from SINrv:CMV-tdT/BMT mice expressed tdTomato. Such a low percentage of transduced cells was surprising given the ubiquitous nature of the CMV promoter and the robust expression seen from the SINrv:CMV-tdT construct *in vitro*. This result indicated either low transduction efficiency or silencing of the CMV promoter. Given the number of fluorescent colonies seen in the Methocult assay following SINrv:CMV-tdT transduction**,** we suspected the latter to be the case. The percentage of tdTomato positive PB-MNCs were less than 1.5% in all other transplant groups (Table 5.1). Although these percentages were relatively low, this result was expected given the rarity of the target cell populations. The tdTomato positive population was clearly discernable in all groups, despite the low percentages of fluorescent cells. The low numbers of circulating tdTomato cells in the SINrv:VEGF-tdT, SINrv:VEcad-tdT, or SINrv:eNOS-tdT/BMT groups were likely due to the rarity of the cell populations in which the vector promoters were active, and not because of low transduction rates.

Specificity of Retroviral Promoters *in vivo*

The successful labeling of bone marrow cells using a retroviral BMT strategy is dependent upon two factors: 1) the ability to transduce all of the bone marrow cells and 2) the specificity of the retroviral promoter *in vivo*. The use of a tissue-specific promoter makes it difficult to address the former, because transduction efficiency does not correlate to the percentage of fluorescent cells. Cells in which the retroviral construct is present but the promoter is inactive cannot be detected by flow cytometry. Therefore, we

Table 5.1: Total tdTomato Expression in PB of SINrv:X-tdT/BMT mice. The predicted specificity for each promoter in the SINrv:X-tdT/BMT mice, as well the percentage of tdTomato positive cells in total PB-MNCs for each group. Average percentage given +/- standard deviation. N=2-3 for each group.

Construct	Promoter	Specificity	%tdT+ in PB
SINrv:CMV-tdT	CMV	All	7.23 +/- 2.79
SINrv:VEGF-tdT	VEGFa	Vascular	1.43 +/- 0.28
SINrv:VEcad-tdT	VE Cadherin	Vascular/Endothelial	0.175 +/- 0.12
SINrv:eNOS-tdT	eNOS	Vascular	0.71 +/- 0.10
SINrv:CD68-tdT	CD68	Macrophage	ND

sought to determine the efficiency with which each subpopulation was labeled.

In order to determine the labeling efficiency, transduced PB cells from each group were stained with antibodies for the proteins corresponding to each retroviral promoter. When PB-MNCs were stained with an antibody for VE Cadherin, a large amount of non-specific background stain was observed (data not shown). As a result, we were unable to determine whether the tdTomato-positive cells derived from SINrv:VEcad-tdT/BMT marrow were also positive for VE Cadherin via antibody labeling. Permeabilization of PB-MNCs permitted staining for VEGF and eNOS, which was then quantified using flow cytometry. (Figure 5.9 and 5.10, respectively). Unfortunately, the permeabilization and fixation steps required for intracellular staining completely abolished tdTomato fluorescence. The loss of flourescence prevented us from co-labeling tdTomato-positive cells from SINrv:VEGF-tdT/BMT and SINrv:eNOS-tdT/BMT with VEGF and eNOS antibodies, respectively. Although colocalization of signal could not be assessed, a striking similarity between the number of tdTomato positive cells in unstained PB from SINrv:VEGF-tdT/BMT mice, and the number of VEGF+ cells as determined by antibody

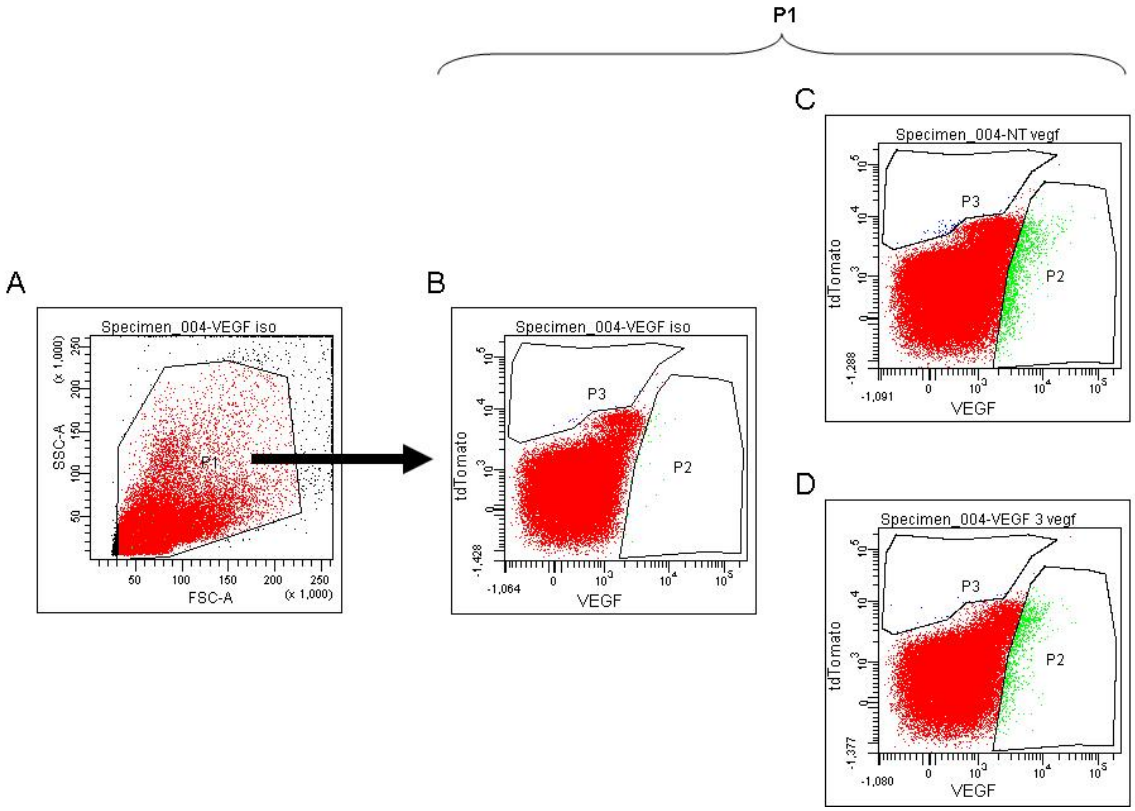

Figure 5.9: Intracellular VEGF staining of PB from SINrv:VEGF-tdT/BMT mice. PB-cells from untreated and SINrv:VEGF-tdT/BMT mice were permeabilized and stained for VEGF. (A) Events for analysis were gated based on SSC and FSC properties. Included events are from gate P1. (B) Untreated isotype controls were used to determine positive events in VEGF (P2) and tdTomato (P3) channels. VEGF expression was assessed in (C) untreated and (D) SINrv:VEGF-tdT/BMT samples. Note that permeabilization/fixation completely abolished tdTomato fluorescence.

Table 5.2: Comparison of Antibody Staining and tdTomato Expression. Quantification of the average number of positive events as determined by anti-VEGF or anti-eNOS antibody staining compared to tdTomato expression. Values are percentage of total cells +/- standard deviation.

Construct	% Stain Positive	% tdT Positive
SINrv:VEGF-tdT	1.72 +/- 0.81	1.43 +/- 0.28
SINrv:eNOS-tdT	0.70 +/- 0.10	0.71 +/- 0.10

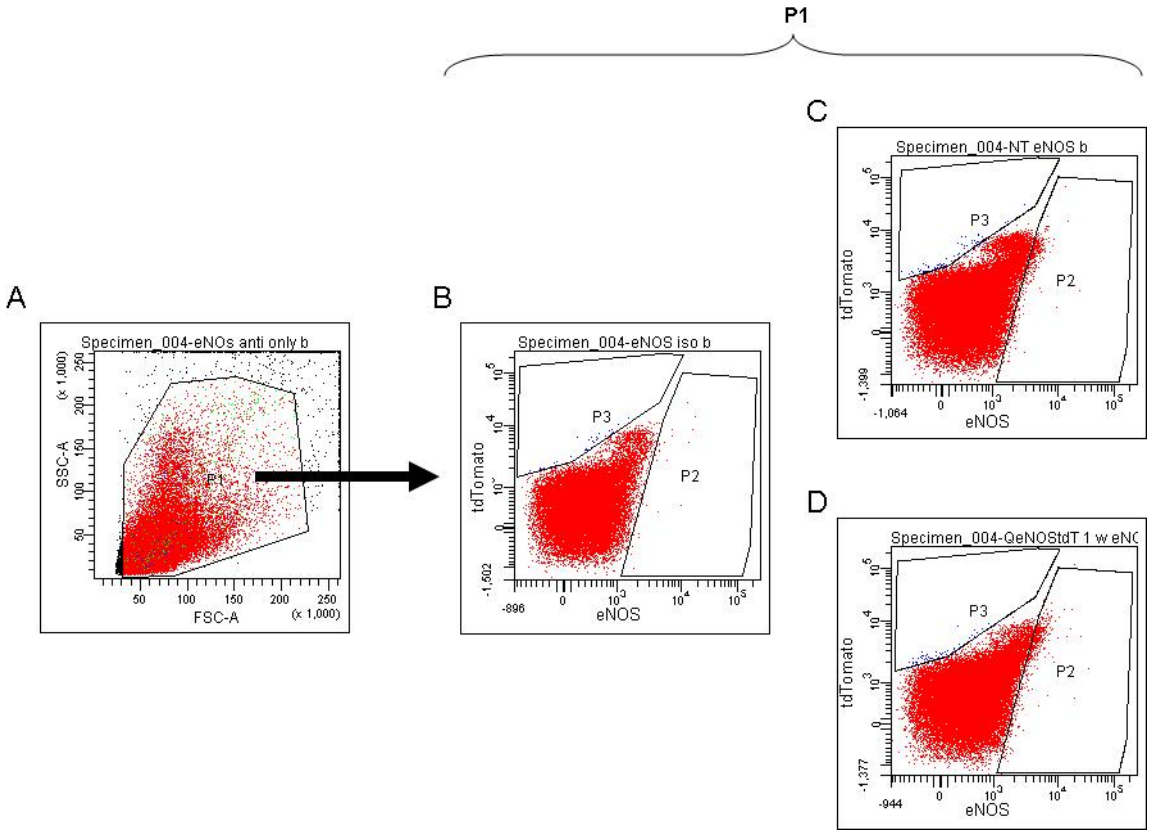

Figure 5.10: Intracellular eNOS Staining of PB From SINrv:VEGF-tdT/BMT Mice. PB-cells from untreated and SINrv:eNOS-tdT/BMT mice were permeabilized and stained for eNOS. (A) Events for analysis were gated based on SSC and FSC properties. Included events are from gate P1. (B) Untreated isotype controls were used to determine positive events in eNOS (P2) and tdTomato (P3) channels. eNOS expression was assessed in (C) untreated and (D) SINrv:eNOS-tdT/BMT samples. Note that permeabilization/fixation completely abolished tdTomato fluorescence.

staining was observed (Table 5.2). This similarity was also observed between the number of tdTomato-positive cells in unstained PB from SINrv:eNOS-tdT/BMT mice, and the number of eNOS+ cells as determined by antibody staining (Table 5.2). These results suggest that expression of tdTomato from the retroviral promoters mimicked expression of the endogenous genes *in vivo*.

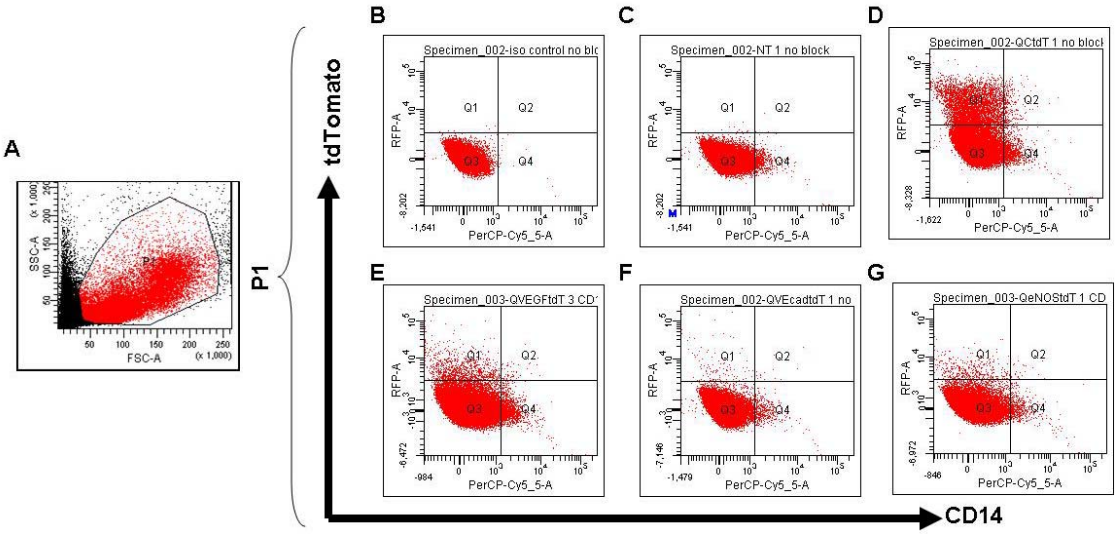

Figure 5.11: Flow Cytometric Analysis of CD14 Expression In Peripheral Blood From SINrv:X-tdT/BMT Mice. PB-MNCs were isolated from SINrv:X-tdT/BMT mice and stained for CD14 expression. A) Gating strategy was based on SSC and FSC properties to eliminate background autofluorescence and exclude debris. B) Untreated isotype controls were used to set gates for tdTomato fluorescence and CD14 expression. C, D, E, F and G are representative plots from Untreated, SINrv:CMV-tdT/BMT, SINrv:VEGF-tdT/BMT, SINrv:VEcad-tdT/BMT, and SINrv:eNOS-tdT/BMT mice, respectively. Bi-exponential plots were used to visualize all events.

CD14 Expression In Peripheral Blood Following Bone Marrow Transplantation

Assessment of CD14 expression in PB was used to evaluate the number of monocytes in the tdTomato+ population for each BMT group. Peripheral blood MNCs were stained with a CD-14 antibody and analyzed by flow cytometry (Figure 5.11). The percentage of CD14+ cells out of the total PB-MNC population remained constant across all treatment groups, demonstrating that the retroviral BMT procedure did not lead to changes in the monocyte population (Figure 5.12). Furthermore, no differences across groups were observed when the percentage of tdTomato positive cells that co-expressed

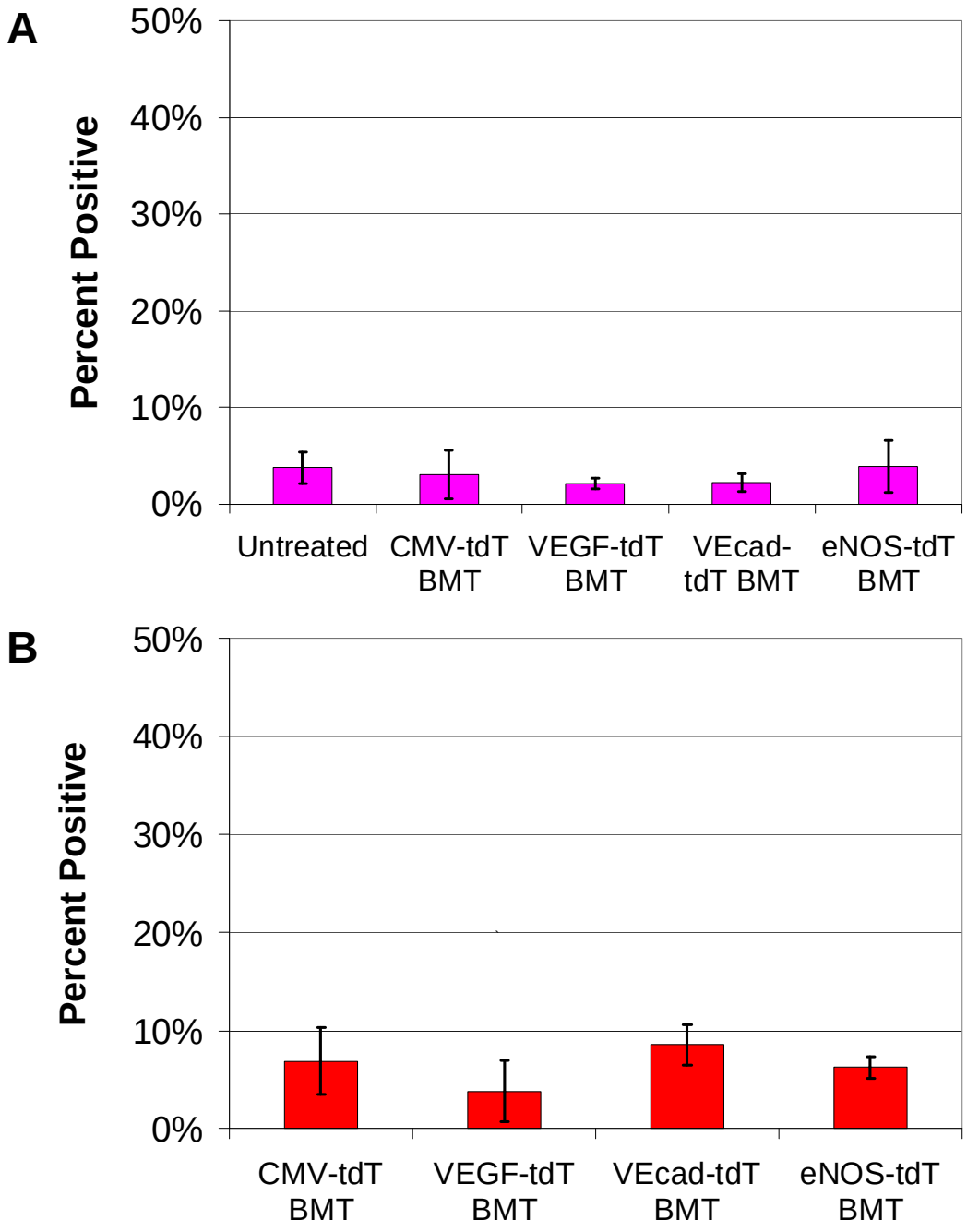

Figure 5.12: Quantification of CD14 expression in BMT-PB. Quantification of flow cytometric data was used to determine CD14 expression in PB of different treatment groups. A) Comparison of the total percentage of CD14 positive cells in PB of all treatment groups. B) Percentage of CD14 positive events within the tdTomato fluorescent cells was compared between treatment groups. N=2-3/group. Error bars indicate standard deviation.

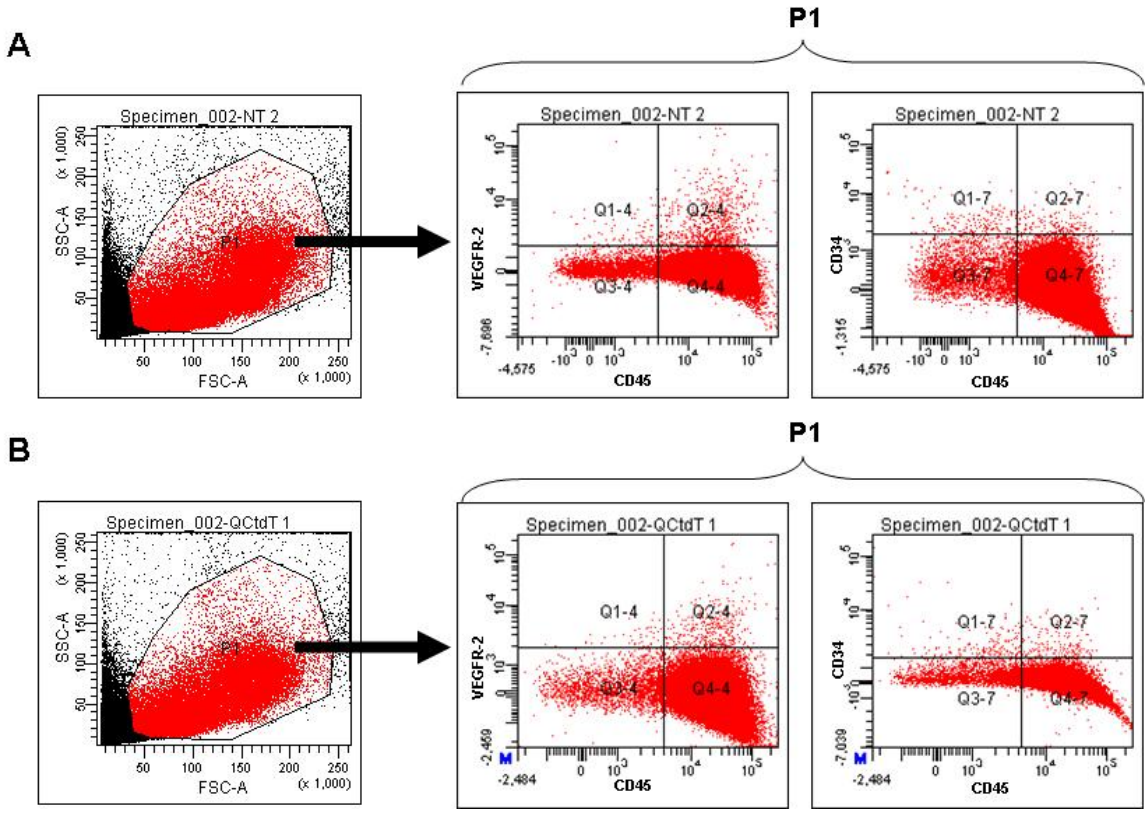

Figure 5.13: PB-MNCs Are Fully Reconstituted Following Retroviral Transduction. Peripheral blood from BMTT mice was stained for CD45, CD34 and VEGFR2. Flow cytometry on (A) untreated vs. (B) SINrv:CMV-tdT/BMT PB showed similar FSC vs. SSC, CD45, CD34, and VEGFR2 expression. Events utilized for analysis were gated based on SSC and FSC properties to eliminate background autofluorescence and exclude debris (P1). Positive events were determined based on isotype controls (not shown).

CD14 was determined (Figure 5.12). The low percentage of tdTomato positive cells expressing CD14 suggests that the majority of circulating VEGF+, VE Cadherin+, and eNOS+ cells are not monocytes.

Characterization of Progenitor Cell Markers on Genetically Labeled Cells

Our interest in labeling subpopulations of bone marrow cells was to determine the role of the different BM cell types in blood vessel growth and maintenance. To compare tdTomato BM populations with previously described progenitor cell populations,

Table 5.3: Summary of Flow Cytometry On PB From SINrv:X-tdT/BMT Mice. Flow cytometry was used to quantify different subpopulations as either a percentage of the total number of cells, or a percentage of the total number of tdTomato positive cells +/- standard deviation. N=2-3 for each group.

	CD34+/VEGFR-2+		CD45+/CD34-/VEGFR-2-		CD45-/CD34+	
Group	% of total	% of tdTomato	% of total	% of tdTomato	% of total CD45-	% of tdTomato CD45-
Untreated	0.08 +/- 0.03	NA	98.79 +/- 0.67	NA	0.14 +/- 0.06	NA
SINrv:CMV-tdT	0.19 +/- 0.01	0.36 +/- 0.13	98.34 +/- 0.16	98.41 +/- 0.17	0.20 +/- 0.05	18.52 +/- 7.77
SINrv:VEGFa-tdT	0.10 +/- 0.05	0.80 +/- 1.03	98.98 +/- 0.42	98.42 +/- 1.52	0.11 +/- 0.09	58.81 +/- 48.74
SINrv:VEcad-tdT	0.10 +/-0.04	6.20 +/- 3.79	98.74 +/- 0.36	85.87 +/-12.91	0.08 +/- 0.01	75.00 +/- 35.35
SINrv:eNOS-tdT	0.08 +/- 0.01	1.83 +/- 1.11	98.94 +/- 0.29	97.70 +/- 0.65	0.25 +/-0.07	85.16 +/- 0.77

expression of CD45, CD34 and VEGFR-2 in PB from SINrv:X-tdT/BMT mice was analyzed with multicolor flow cytometry. Expression of CD45, CD34 and VEGFR-2 was maintained across groups following bone marrow transduction (Figure 5.13), indicating that the retroviral transduction/BMT procedure did not alter leukocyte or progenitor cell populations in PB-MNCs.

The majority of PB-MNCs in all groups were CD45-positive (>85%). A small percentage of cells (<0.2%) were double positive for the progenitor cell markers CD34 and VEGFR-2 (Figure 5.13 and Table 5.3). The percentage of tdTomato+-positive cells that expressed both CD34 and VEGFR2 was somewhat higher in the SINrv:VEcad-tdT/BMT and SINrv:eNOS-tdT/BMT groups, however the low frequency of total tdTomato-positive cells led to considerable variability in this result. The majority of the tdTomato positive cells in each group were CD45+/CD34-/VEGFR2- (Figure 5.14 and Table 5.3), which was comparable to that seen in the ungated population of cells. The expression of CD45 suggests that these cells are of hematopoietic origin, but the absence of CD34 indicates that they were not an HSC. Although less than 1% of the tdTomato-positive populations for all groups were CD45-negative, the majority of the tdTomato+/CD45- cells from the SINrv:VEcad-tdT/BMT and SINrv:eNOS-tdT/BMT

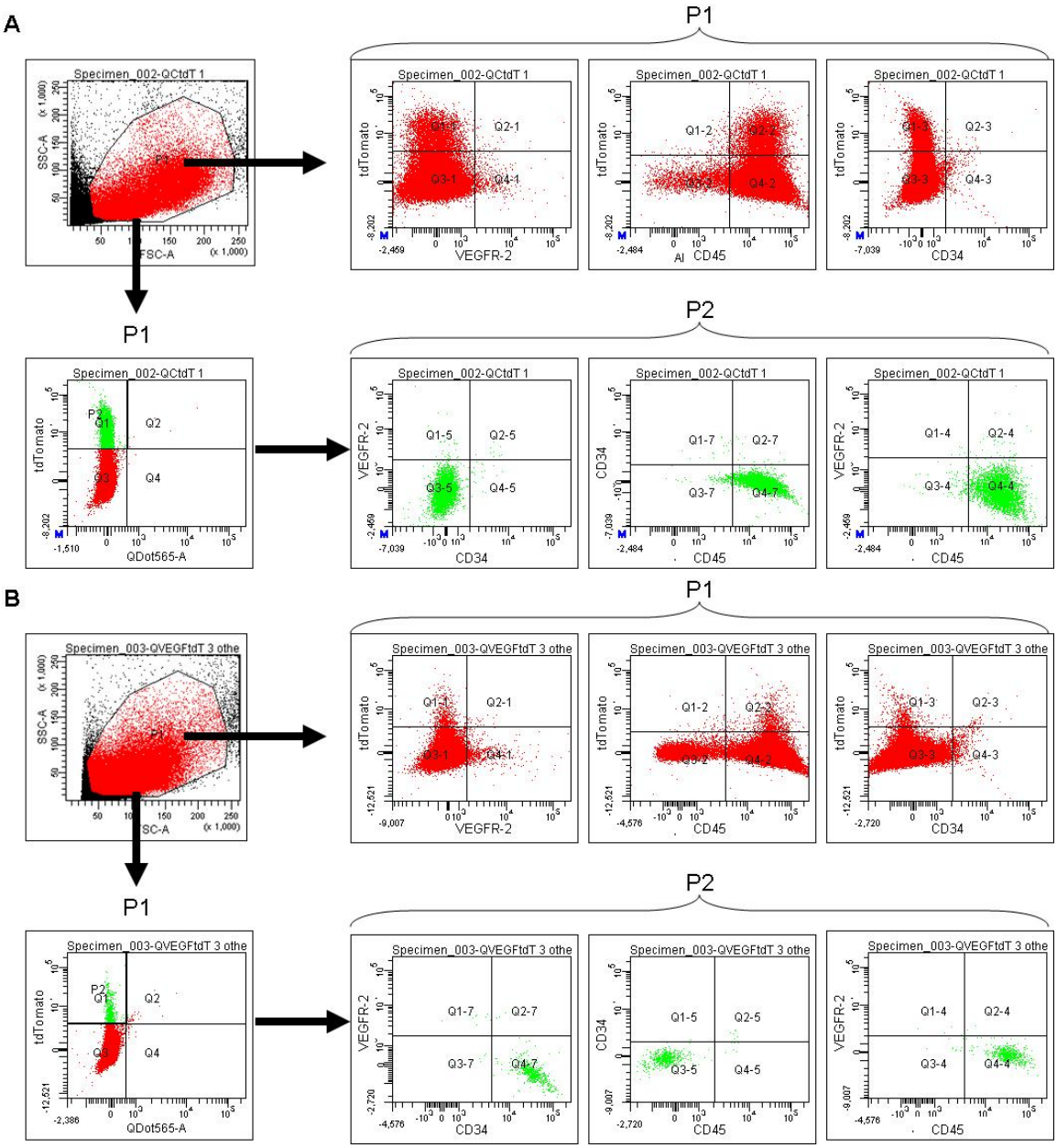

Figure 5.14 (continued on next page)

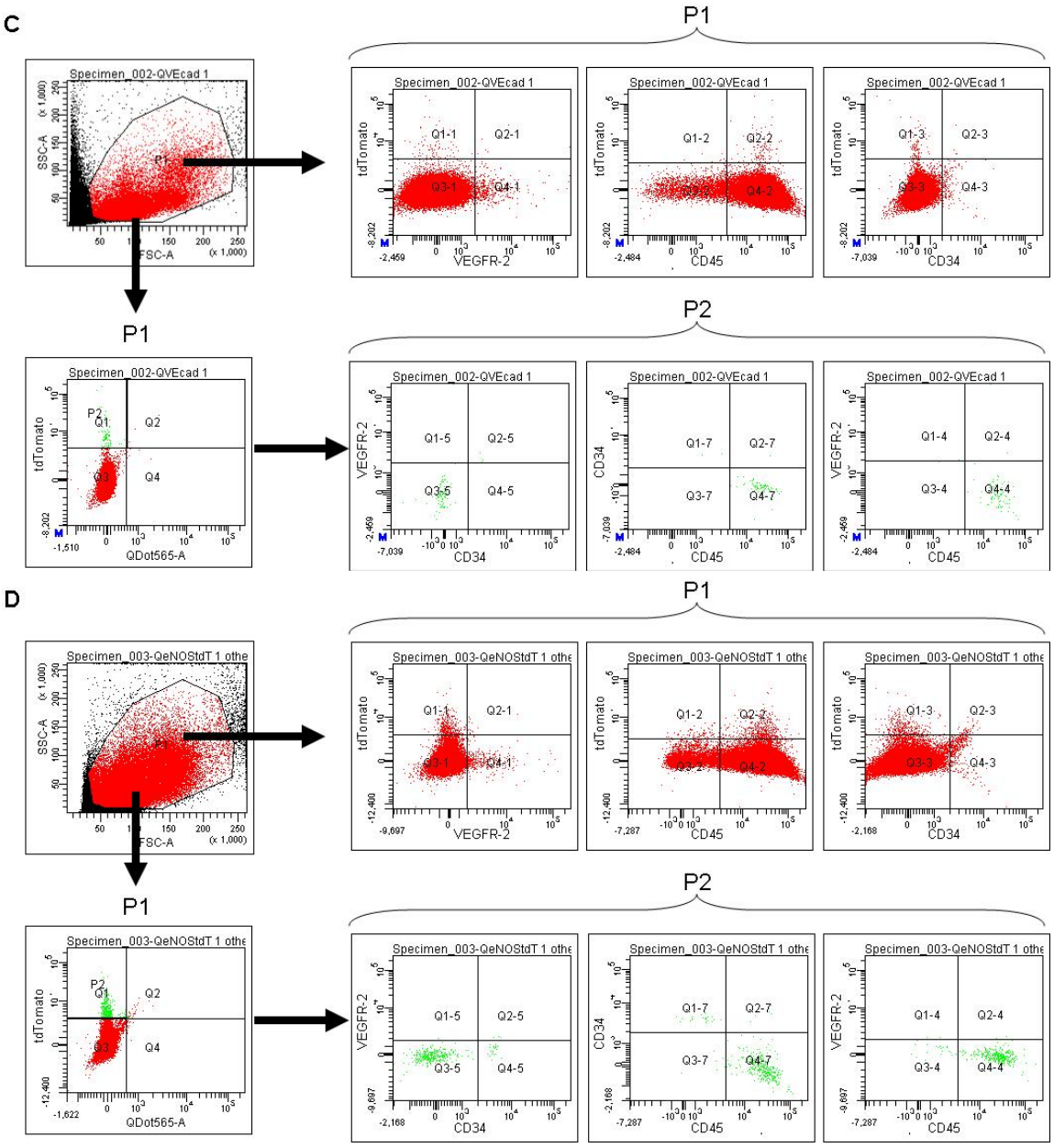

Figure 5.14: Characterization of tdTomato Positive Cells In PB From SINrv:X-tdT/BMT Mice. PB from different treatment groups were stained for VEGFR-2, CD45, and CD34 and analyzed with multicolor flow cytometry. Cells were first gated based on SSC and FSC properties (P1), and then gates for positive events were determined using isotype controls. Total cells were analyzed for antigen expression, and then tdTomato positive cells only were gated and assessed for expression of each surface marker. A, B, C and D are representative PB samples from SINrv:CMV-tdT/BMT mice, SINrv:VEGF-tdT/BMT mice, SINrv:VEcad-tdT/BMT mice, and SINrv:eNOS-tdT/BMT mice, respectively.

groups were CD34-positive. This suggests that the VE Cad+ and eNOS+ populations may be enriched for hematopoietic progenitor cells. However, due to the small sample size in these experiments, these results should be interpreted with caution.

Discussion

Here we have demonstrated a novel method for the fluorescent labeling and live cell tracking of bone marrow cells *in vivo.* The use of self-inactivating retroviral vectors containing the VEGF, and eNOS promoters allowed us to identify rare populations of circulating BM-derived cells in the peripheral blood, which may play a role in neovascularization. Due to the intracellular localization of VEGF and eNOS, antibody labeling techniques for these proteins are not permitted in live cells. Our approach, however, allows for the identification of VEGF and ENOS expression in *viable* cells. Circulating cells that express VEGF, if recruited to areas of ischemic tissue, would promote vascularization do to secretion of VEGF. Therefore, the tdTomato+ cells from SINrv:VEGF-tdT/BMT mice could be potent regulators of angiogenesis. The eNOS protein localizes at caveoli on the cytoplasmic side of the plasma membrane (174) and leads to the generation of nitric oxide. Therefore, eNOS expressing cells could be recruited to the blood vessel wall during angiogenesis and secrete nitric oxide, thereby representing a population of cells with pro-angiogenic potential.

Unlike VEGF and eNOS, it is possible to identify VE Cadherin by staining of surface markers with antibodies. However, the paucity of VE Cadherin-positive cells in PB of mice makes it extremely difficult to distinguish true VE Cadherin-positive cells from background using flow cytometry. The SINrv:VEcad-tdT/BMT mice contain a

small but distinct population of circulating tdTomato+ cells. Since VE Cadherin is a marker of mature endothelial cells, this population may represent a true endothelial precursor.

To summarize these data, the use of self-inactivating retroviral vectors for labeling of BM-cells represents a convenient method for live-cell tracking of VEGF, eNOS and VE Cadherin expressing cells *in vivo*. Furthermore, we have demonstrated that it is possible to isolate tdTomato+ cells using this retroviral-mediated approach, so that in the future purified cell populations can be isolate for use in therapeutic neovascularization.

An alternative approach for tracking specific subsets of BM-derived cells involves the use of transgenic mice. In this strategy, bone marrow from fluorescently labeled transgenic mice is transplanted into wild type recipients, permitting the tracking of BM-derived cell types. In fact, several GFP reporter mice have been generated using VEGF (175; 176) and eNOS (177; 178) promoter elements. Transgenic mice have also been developed which employ the VE Cadherin promoter to drive expression of Cre recombinase (179) or a tamoxifen-inducible Cre-fusion protein (180). Our approach offers several advantages over a transgenic strategy. With the retroviral-mediated methodology described here, it is not necessary to establish and maintain a colony of transgenic animals, saving a considerable amount of time and money. Our vectors also provide considerable plasticity in experimental approach, since they can be used with any available knockout or transgenic mouse without the need for additional breeding with GFP or LacZ reporter mice. Our retroviral based system is also extremely versatile. A new promoter can quickly be cloned into the empty SINrv:X-tdT vector, virus can be

generated, and transplants can be performed within several weeks. Generation of a new tissue specific transgenic-reporter mouse, on the other hand, requires considerably more time at a substantially higher cost.

The circulating VEGF+ cells identified in PB-MNCs could potentially be a pro-angiogenic cell source involved in neovascularization. Culturing of adherent cells from human PB-MNCs in endothelial-favorable growth conditions leads to the formation of early-EPC colonies in 7 days, followed by highly proliferative outgrowth endothelial cells (OECs) at 21 days(24). The early EPC population has been shown to express high levels of VEGF compared to OECs (22; 23), and transplantation of a mixed population of early EPCs and OECs into nude mice showed greater angiogenic response than either cell type alone(23). Therefore, it may be possible to prospectively identify early EPCs based on VEGF expression. In future work, we will explore the link between circulating VEGF+ cells and early EPC formation, as well as their potential role in a setting of neovascularization.

In contrast to VEGF, eNOS expression is higher in OECs derived from cultured PB-MNCs than in early EPCs(21). Furthermore, only GFP+ positive BM cells isolated from eNOS-GFP transgenic mice were capable of forming CFU-ECs; depletion of the GFP+ cells from PB-MNCs prevented CFU-EC formation (181). The angiogenic potential of bone marrow cells in eNOS -/- mice is also severely impaired (182; 183), suggesting a functional role for eNOS in neovascularization. The SINrv:eNOS-tdT/BMT mice may be a useful tool in determining which cell populations are capable of forming OECs and CFU-ECs. Furthermore, the tdTomato+ cells from these mice may represent a

population of cells that are functionally relevant toward blood vessel growth and repair. This hypothesis will be explored in future work.

Expression of VE Cadherin is frequently used to identify cells from EPC culture assays as "endothelial cells". VE Cadherin expression has been documented in Early EPCs, OECs and CFU-ECs (29). However, it is unclear whether VE Cadherin expression is a result of the culture conditions, or if the cells that give rise to the colonies already expressing VE Cadherin. Existing data seems to support the former, since VE Cadherin expression can be induced in a purified monocyte population (49). The use of our SINrv:VEcad-tdT/BMT mice clearly identified a subset of VE Cadherin+ cells. Future studies will determine if the VE Cadherin+ circulating cells are capable of forming EPCs in culture, and potentially prospectively identifying cultured EPCs.

A recent study, in which a lineage tracking system was used to examine the role of VE Cadherin in embryonic vasculogenesis and hematopoiesis, found that at least a fraction of hematopoietic cells in the adult are derived from VE Cadherin expressing cells in the aortic-gonado-mesenephros (AGM) region during embryonic development. Using lineage tracing techniques, it was concluded that the hematopoietic cells arise from VE Cadherin-positive endothelium within the AGM. These results suggest that during a brief period of embryonic development, the hemangioblast is identifiable by VE Cadherin expression. An intriguing possibility is that this observation may be recapitulated in the adult mouse in a setting of hematopoietic reconstitution. The tdTomato+ population identified in SINrv:VEcad-tdT/BMT mice may identify the elusive adult hemangioblast. We have developed a second set of retroviral vectors in which tdTomato is replaced with Cre recombinase gene to explore this hypothesis. Transduction of donor cells from a

floxed reporter mouse with a VE Cadherin-Cre retrovirus will allow us to determine if any of the hematopoietic cells reconstituted in a lethally irradiated transplant currently express or have expressed VE Cadherin at some point during their differentiation.

In summary, we have developed a novel method of fluorescently labeling bone marrow subpopulations using retroviral-mediated bone marrow transplantation approach. This highly versatile methodology has broad applications in elucidating the role of bone marrow-derived progenitor cells in post-natal neovascularization.

CHAPTER 6

SUMMARY AND FUTURE CONSIDERATIONS

Specific Aims I and II

The retroviral strategy outlined in Chapter 3, which utilized the RED vector to overexpress ΔN-Bax, was unsuccessful at inducing cell death in targeted endothelial cells. As we established in Chapter 4, expression of the ΔN-Bax fragment does not lead to apoptosis. However, successful implementation of this approach was hindered by our failure to systematically build the complexity of our construct design.

Before we had tested any individual features included in the RED vector, we generated the full RED and REF plasmids. Therefore, when evaluation of the construct yielded negative results, we had to back-track significantly to isolate potential problems. A continued source of trouble in this approach was the use of the VE Cadherin promoter. While it is generally accepted that the VE Cadherin promoter confers the greatest specificity for endothelial-specific gene expression (179; 180; 170), we found that the promoter fragment we used led to weak gene expression *in vitro*. Multiple endothelial cell lines were transduced with the REF3 construct (containing the VE Cadherin promoter driving expression of GFP directly), however in each case the promoter was too weak to allow for effective characterization of the RED construct. We suspected that the weak transcriptional activity of the promoter was due to culture conditions *in vitro*. When used *in vivo*, we reasoned that the VE Cadherin promoter would robustly express our transgene. In fact, this hypothesis was confirmed following generation of the transgenic CrIED mouse. The CrIED mouse contained the same transgene as that contained in the RED vector. However, in contrast to the VE Cadherin promoter activity detected in

cultured endothelial cells, VE Cadherin activity in the CrIED mouse was robust in highly vascularized issues such as lung and aorta.

We initially hypothesized that our inability to utilize the RED and REF constructs was due to low titer. Surprisingly, retroviral titer (as determined by qPCR on retroviral supernatant) from these constructs was comparable to that of the control virus, TJ124. However, qRT-PCR on genomic DNA from transduced target cells indicated that integration of TJ124 in target cells was significantly higher than that seen with RED and REF. The inability of RED and REF to integrate into the genomic DNA of target cells may have been due to a cryptic poly-A signal contained in the vector insert. The poly-A sequence could have prematurely terminated transcription of the viral mRNA so that the 3'LTR was not included in the virion. The absence of the 3'LTR would not effect virion production, but would severely impair integration following transduction. Cloning cDNA generated from the viral mRNA could confirm this hypothesis, however we felt it unnecessary to pursue this approach, and eventually abandoned the retroviral strategy altogether to focus on the transgenic CrIED mouse.

The generation of the transgenic CrIED mouse confirmed the functionality of the VE Cadherin-luciferase reporter portion of our construct. Unfortunately, following tamoxifen induced Cre activation and recombination, we did not observe endothelial cell death as anticipated. Although some design flaws in our construct may have contributed to our inability to induce endothelial cell apoptosis, it is more likely that expression of ΔN-Bax fragment did not induce apoptosis. The results from Chapter 4 supported this hypothesis, so we abandoned the CrIED approach as well.

ΔN-Bax in Apoptosis

The ΔN-Bax constructs generated in Chapter 3 (containing the sequence corresponding to the C-terminal region of Bax) were unable to reliably induce apoptosis in endothelial cells (or, for that matter, any other cells). Although changes in cell morphology were observed following ΔN-Bax-EGFP fusion protein expression, expression of ΔN-Bax did not cause cellular toxicity as we anticipated. Our data strongly suggest that the ΔN-Bax fragment is permanently bound to the mitochondrial outer membrane (MOM), however we lack direct evidence to support this conclusion.

Determining the cellular localization of ΔN-Bax is an imperative step in elucidating the functional contribution of the C-terminal fragment of Bax in apoptosis. We hypothesize that α-helices 6-9 are responsible for MOM-translocation and aggregation prior to pore formation, but it is α-helices 2-5 that are responsible for the physical formation of the pore itself. We anticipate studies utilizing the EGFP-ΔN-Bax construct used in concert with Mitotracker red (184) will allow us to visually confirm the direct involvement of EGFP-ΔN-Bax with the mitochondria. If indeed the truncated ΔN-Bax is localized to the MOM, the functional role of the α-helices 6-9 can be more closely studied.

Although it was surprising that ΔN-Bax expression did not lead to robust cell death, we neglected to determine whether expression of EGFP-ΔN-Bax *sensitizes* cells to apoptotic signals. Ongoing studies will explore whether the localization of ΔN-Bax in the MOM results in sensitization of cells to specific apoptotic stimuli. The aggregation of ΔN-Bax at the MOM may leave the cell "locked and loaded" for apoptosis. Various stimuli that activate the intrinsic apoptotic pathway (UV exposure, hypoxia, serum

starvation) may be necessary for the toxicity of ΔN-Bax overexpression to be apparent. Cells that might be otherwise resistant to certain apoptotic stimuli may gain sensitivity to these stimuli following ΔN-Bax overexpression. Hypersensitivity to apoptosis would be extremely relevant in a setting of cancer and, were this result true, ΔN-Bax might provide a novel therapeutic target for sensitizing cancer cells to apoptotic stimuli.

The specific function of α-helices 6-9 can also be examined in an artificial lipid membrane. For these studies, lipid vesicles containing recombinant ΔN-Bax would be generated and used to encapsulate FITC-labeled dextran molecules of varying size (146; 148). Florescence of the artificial membrane bound vesicles could be used to determine if α-helices 6-9 can indeed form pore structures in lipid membranes. Addition of t-Bid, Bim or Puma to the artificial membrane system would allow us to determine whether binding of BH3-only proteins is a prerequisite to pore formation by ΔN-Bax. Involvement of the BH3-only proteins might aid in resolving the direct versus indirect activation debate surrounding BH3-only induced apoptosis.

Specific Aim III

The results from Chapter 5, although still somewhat preliminary, clearly demonstrate the feasibility of a retroviral bone marrow transduction and transplantation approach to labeling subpopulations of cells within the bone marrow. Using the VEGF, eNOS and VE Cadherin promoters, we were able to clearly identify fluorescently labeled cells circulating in the peripheral blood. This SINrv:X-tdT/BMT strategy is particularly valuable because it does not require cell permeabilization to detect protein expression, hence preserving cell viability. Furthermore, the strength of tdTomato fluorescence

allows for accurate detection of rare events, as was observed when using the VE Cadherin promoter. We also demonstrated that genetically labeling cells with a fluorescent protein permits enrichment for rare events through FACS, allowing isolation of cells that are identifiable based on the expression of intracellular proteins

Current bone marrow labeling strategies include antibody staining and the use of transgenic reporter mice. Antibody labeling is fast, convenient, cost effective, and allows for the identification of multiple antigens simultaneously. A major weakness of the antibody-based approach is that recognition of intracellular proteins, which could potentially reveal functional characteristics of the cells, requires permeabilization of the cell membrane resulting in a loss of cell viability. Therefore bone marrow cells sorted based on staining of intracellular antigens cannot be used for cell therapy strategies and the augmentation of neovascularization in animal models.

Transgenic reporter mice can be used to circumvent the viability problems associated with antibody staining. Indeed, several VEGF-GFP reporter mice (176; 185), eNOS-GFP (177), and eNOS-LacZ (186) reporter mice have been produced. Generation of bone marrow chimeras by transplantation of marrow from these transgenic animals into wild type recipients permits tracking of eGFP-positive or LacZ-positive bone marrow cells. However, experiments on these mice are restricted to the strains on which the transgenic animals are bred. Cell tracing is not possible in knockout animals or other transgenic mice without crossing them with the reporter strains. The inconvenience of a transgenic mice strategy for BM cell labeling purposes is particularly evident in the case of the VE Cadherin promoter. Both VE Cadherin-Cre (179) and VE Cadherin-tamoxifen inducible-Cre transgenic mice (180) have been generated. To track VE Cadherin

expressing BM cells, the VE Cadherin Cre mouse must first be crossed with a Flox-reporter mouse, and only the bone marrow from the offspring can be used for cell tracking experiments. This scenario clearly demonstrates that the use of transgenic animals is extremely restrictive in terms of time and associated costs. The SINrv:X-tdT/BMT strategy, on the other hand, can easily be utilized with any knockout, transgenic, or background strain.

The potential versatility that the SINrv:X-tdT/BMT methodology affords significant advantage. Any transcriptional regulatory sequence can be cloned into the empty SINrv:X-tdT vector, and therefore a plethora of subpopulations within the bone marrow can easily be targeted. This approach is ideally suited for the isolation of regulatory T-cells, (T_{reg}). Currently, identification of T_{reg} cells in mice requires intracellular staining of the FoxP3 transcription factor(187). Isolation of T_{reg} cells requires use of transgenic mice containing a FoxP3-GFP fusion protein. However, fusion of the GFP gene inactivates the FoxP3 protein, so that only heterozygous mice carry both the GFP reporter and a functional FoxP3 protein (188). Generation of a SINrv:FoxP3-tdT construct would not only provide a simple method for quantification of T_{reg} cells, but would also allow for the identification and isolation of T_{reg} cells from any knockout or transgenic mouse line without the need for additional breeding.

Limitations

Despite the many advantages described above, the SINrv:X-tdT/BMT strategy is not without its limitations. One issue that has not been resolved is the overall transduction efficiency following reconstitution *in vivo*. Since our constructs are self-inactivating

vectors with tissue-specific promoters, we are unable to determine the transduction efficiency by examination of tdTomato expression alone. Even if the majority of the bone marrow cells carry our transgene, only those in which the promoter is active will be fluorescent. We attempted to address the issue by co labeling cells transduced with SINrv:VEGF-tdT and SINrv:ENOS-tdT with antibodies for VEGF and eNOS, respectively. Our rationale was that determining the percentage of tdTomato-positive cells that co stained with antibodies for VEGF and eNOS would allow us to estimate our labeling efficiency. While we observed that the percentage of labeled cells was comparable to the percentage of tdTomato positive cells in both groups, the permeabilization of the cells required for intracellular staining completely abolished tdTomato fluorescence. As a result, we were unable to observe co localization of signal.

A quantitative PCR-based technique could also be used to estimate transduction efficiency with the SINrv:X-tdT vectors. Individual colonies could be picked from BM cells derived from the SINrv:X-tdT/BMT mice and grown in Methocult media. PCR performed on isolated genomic DNA from each of these colonies could identify the number of colonies which contain the retroviral transgene, and therefore estimate transduction efficiency. Although extremely laborious and time consuming, this approach would provide an estimate of our overall transduction efficiency.

The problem of transduction efficiency was evident in the SINrv:CMV-tdT/BMT mice. The CMV promoter should be efficiently expressed constitutively across all cell types. However, we found only ~7% of PB-MNCs were fluorescent following bone marrow engraftment. Although this result could be indicative of low transduction efficiency, we suspect that instead this is due to silencing of the CMV promoter. The

phenomenon of retroviral promoter silencing is frequently observed a number of situations, notably in the generation of induced pluripotent stem cells (iPSCs) (189). Silencing of the CMV promoter has been specifically observed after transduction of bone marrow cells (190), and viral transgene expression following long-term engraftment of transduced cells is considerably lower in constructs containing the CMV promoter compared to other constitutively active promoters, such as PGK (53).To ascertain whether the CMV promoter was silenced, we replaced the tdTomato CDS in SINrv:CMV-tdT with the CDS for Cre recombinase. The resulting construct, renamed SINrv:CMV-Cre (Figure 6.1), was used to transduce bone marrow from a floxed GFP reporter mouse (191). In this mouse, cells express GFP at the ROSA26 locus following Cre-mediated recombination of a floxed stop sequence upstream of the GFP reporter. Therefore, cells that express Cre will also express GFP. Even if Cre expression is lost, the cells and all of their progeny will continue to express GFP, since expression of the reporter gene is regulated by the ROSA26 locus. In the event of promoter silencing, we expect a low percentage of tdTomato positive cells in SINrv:CMV-tdT/BMT mice, and a high percentage of GFP+ cells in SINrv:CMV-Cre/floxed GFP/BMT mice. In fact, this is precisely what we observed (Figure 6.2). Roughly 7% of PB-MNCs from SINrv:CMV-tdT/BMT expressed tdTomato, but ~30% of PB-MNCs and bone marrow cells from the SINrv:CMV-Cre/floxed GFP/BMT mice expressed GFP.

Although we have expounded on the versatility of our SINrv:X-tdT vectors and the ability to use any promoter to drive tdTomato expression, careful consideration is warranted in selection of transcriptional regulatory sequences. In order for the viral

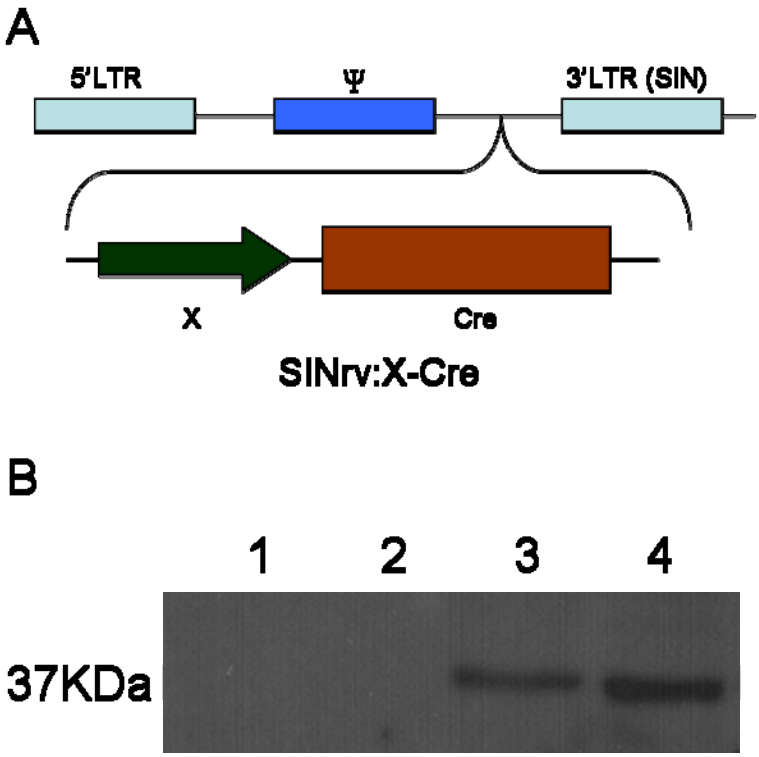

Figure 6.1: Design and Validation of SINrv:X-Cre Vectors. The SINrv:X-Cre vectors (A) were created by replacing the tdTomato sequence in SINrv:X-tdT with the bacteriophage P1 Cre recombinase (192). B) Western blot for Cre on lysates from cells transduced with SINrv:CMV-Cre. The band at 37 kDa represents Cre.

mRNA to be efficiently packaged, the transcript length (from 5'LTR to 3'LTR) should be kept under 8 kb (193). Therefore, promoter size in the SINrv:X-tdT must be less than 5 kb to prevent a reduction in titer. The use of MMLV-based retroviral vectors may also result in insertional mutagenesis(194; 195), so this approach may have limitations in certain tumor models.

Future Directions

There are a number of animal models in which the SINrv:X-tdT/BMT approach will be implemented immediately. Bone marrow-derived cells are recruited to sites of nascent vessel formation in both the hind limb ischemia and matrigel plug assays (12; (14); 3). Given this data, we first plan to address whether the number of circulating

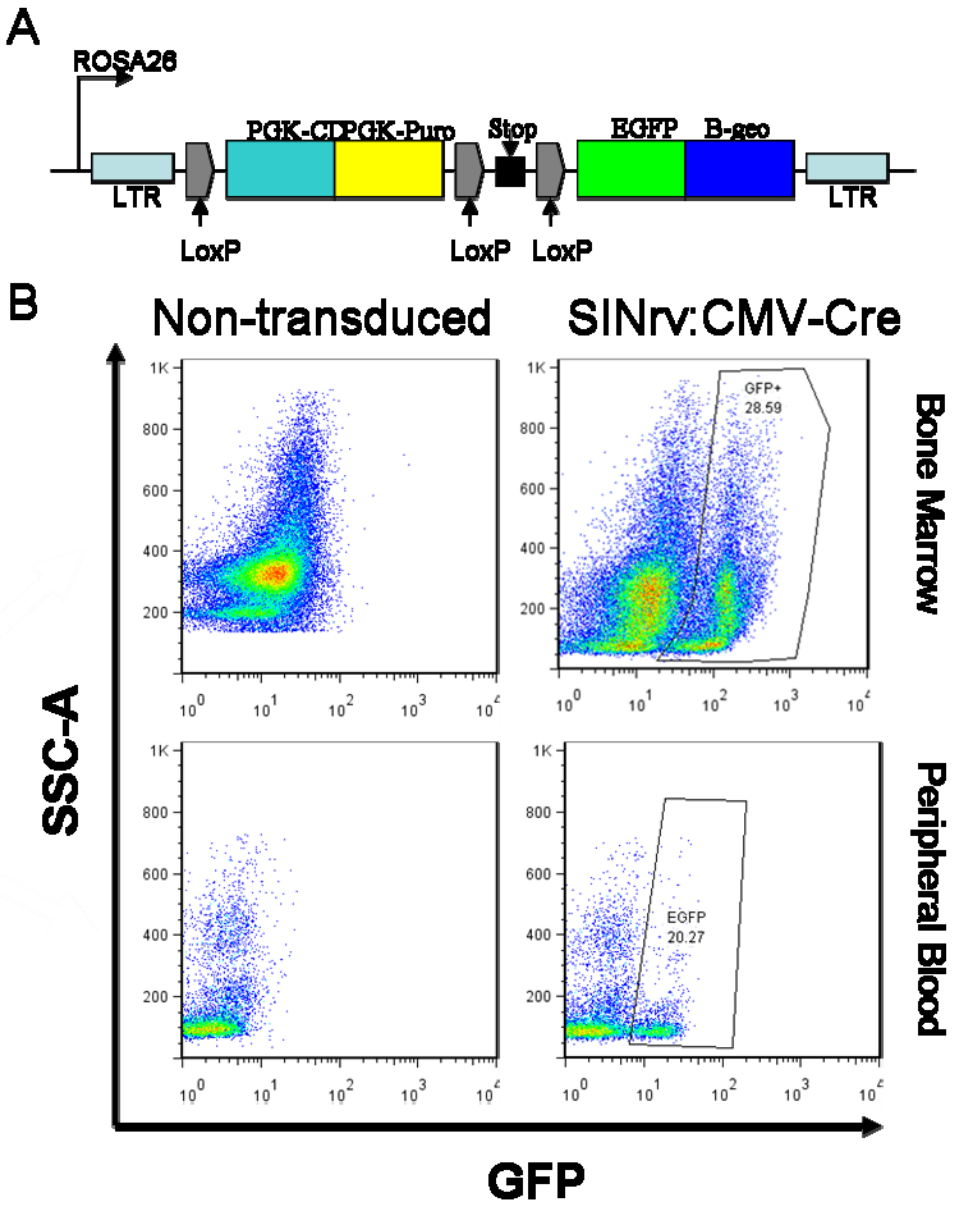

Figure 6.2: GFP Expression Following Retrovirus-Induced Cre Expression In ROSA26-GFP^{Flox} BM and PB. Bone marrow was isolated from ROSA26-GFP^{Flox} mice, transduced with the SINrv:CMV-Cre vector, and transplanted into lethally irradiated WT recipients. A) The ROSA26-GFP^{Flox} construct contains a PGK driven cytosine deaminase gene (PGK-CD) and PGK driven puromycin resistance gene (PGK-Puro) flanked by loxP sites. Downstream of PGK-Puro is a floxed triple poly-adenylation sequence (STOP). An enhanced green fluorescent protein-βgeo fusion protein (EGFP-βgeo) completes the construct. The entire construct was targeted to the Rosa26 locus and is inserted between 2 long terminal repeats (LTRs). B) Bone marrow and peripheral blood isolated from mice receiving ROSA26-GFP^{Flox} marrow transduced with SINrv:CMV-Cre expressed EGFP, while no fluorescence was detected in untreated controls.

tdTomato-positive cells in SINrv:X-tdT/BMT mice increases in response to HLI or matrigel injections. Second, we will perform histological analysis of sections of the surgical leg or matrigel to determine if tdTomato-positive cells are recruited to sights of neovascularization. This data could potentially identify VEGF, eNOS, or VE Cadherin-positive cells in the PB as significant contributors to post-natal blood vessel growth, and permit the characterization of new progenitor cell populations.

As demonstrated in Chapter 5, it is possible to isolate tdTomato-positive cells using FACS. Enriched cell populations isolated from the bone marrow or peripheral blood of SINrv:X-tdT/BMT mice for re-implantation in the ischemic hind limb of wild type mice could be used for therapeutic augmentation of blood vessel growth. A comparison between mice receiving sorted or unsorted BM cell populations will allow us to determine if the progenitor populations isolated from SINrv:X-tdT/BMT mice have enhanced pro-angiogenic capacity. These experiments could potentially identify a novel target for therapeutic neovascularization.

We have also begun to pursue a strategy for the lineage tracing of bone marrow cells. By replacing the tdTomato CDS in the SINrv:X-tdT constructs with the CDS for bacterial Cre recombinase, we were able to generate the SINrv:X-Cre series of vectors (Figure 6.1). The constructs were verified by restriction digest, and western blot on lysates from 3T3 cells transduced with SINrv:CMV-Cre showed a distinct band corresponding to the correct size of the Cre protein (Figure 6.1). For lineage tracing experiments, donor BM will be obtained from ROSA26-EGFP^{Flox} transgenic mice (191). These mice contain a floxed puromycin resistance gene and stop signal upstream of the GFP coding region targeted to the ROSA26 locus (Figure 6.2). The stop sequence blocks

transcription of the GFP gene, so that the reporter construct is silent in all cells. In the presence of Cre, however, the stop sequence and puromycin resistance cassette are excised, leading to robust GFP expression. The expression of GFP is then driven directly by the ROSA26 locus. The site specific recombination is irreversible, so even if Cre expression is stopped, the cell will continue to express GFP. Furthermore, the Cre-mediated recombination results in permanent genomic modification, so that all progeny will also express GFP (Figure 6.3).

The SINrv:X-Cre vectors will be used in BM transduction/transplantation experiments in which donor marrow is obtained from ROSA26-EGFP^{Flox} mice, transduced with SINrv:X-Cre vectors, and transplanted into lethally irradiated hosts. Preliminary experiments using ROSA26-EGFP^{Flox} bone marrow transduced with SINrv:CMV-Cre and transplanted into lethally irradiated wild type mice have confirmed the feasibility of this approach (Figure 6.2). Recombination mediated by retroviral expressed Cre led to GFP expression in nearly 30% of the bone marrow and peripheral blood cells. Further implementation of this strategy will allow us to determine if the progenitor cells identified in chapter 5 are terminally differentiated, or if the expression of VEGF, eNOS, and VE Cadherin in PB-MNCs identify a more primitive cell population that give rise to a larger progenitor pool.

In Chapter 5, we speculated that VE Cadherin positive PB-MNCs could be the elusive adult hemangioblast that is often alluded to in the literature, but has never been found. It was shown in the mouse embryo that VE Cadherin positive endothelial cells in the aortic-gonado-mesenephros (AGM) region ultimately gave rise to a significant portion of the hematopoietic population (196). Using an inducible reporter system

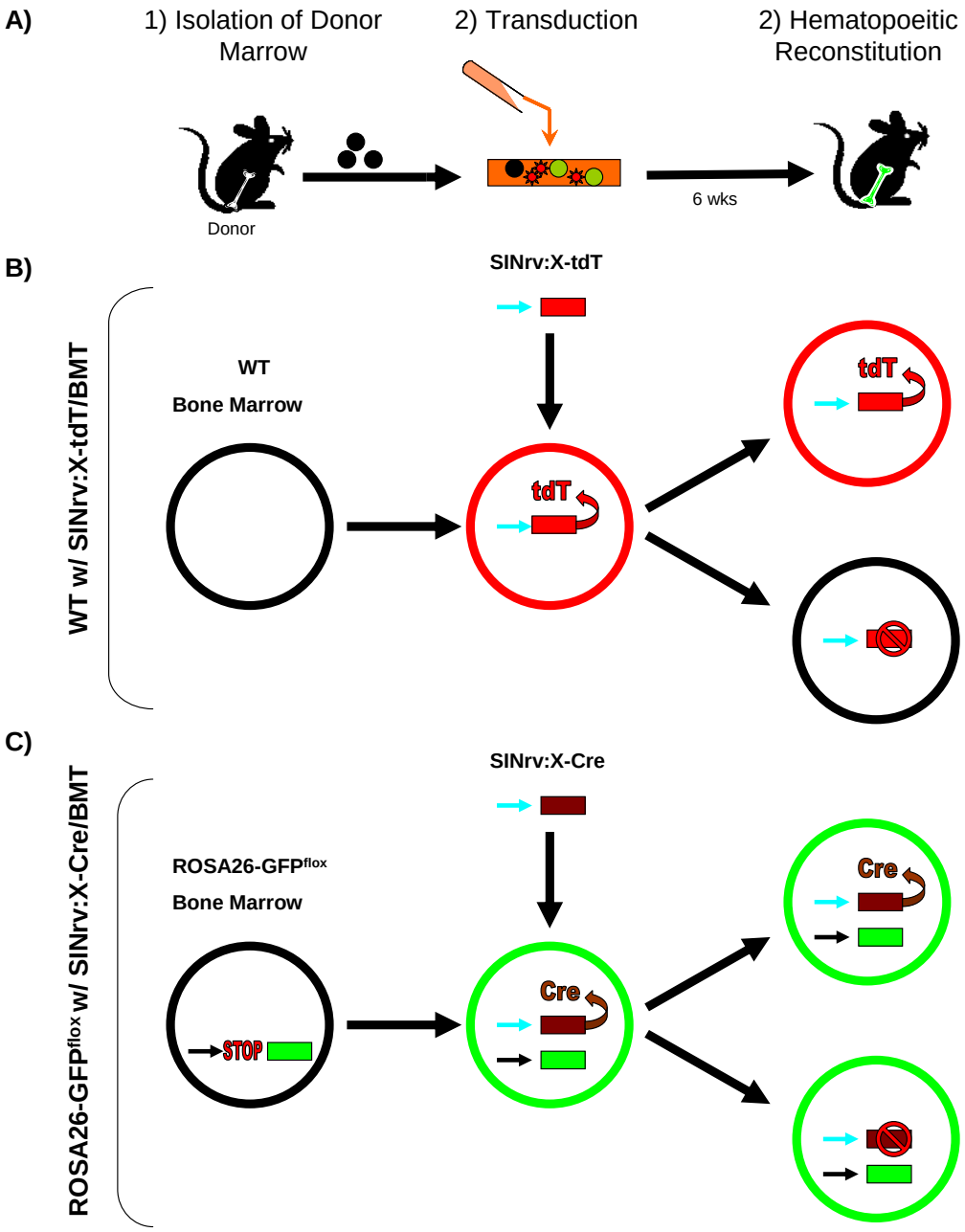

Figure 6.3: SINrv:X-Cre Lineage Tracing Strategy. A) Our overall approach will be to transduce cells from a donor mouse with a retrovirus, then transplant the cells into a lethally irradiated WT animal. B) In the SINrv:X-tdT/BMT strategy, WT BM cells are isolated and transduced with a SINrv:X-tdT vector. Following differentiation, cells in which the retroviral promoter is active will express tdTomato. All remaining cells will not. C) In the ROSA26-GFP^{Flox} with SINrv:X-Cre/BMT strategy, bone marrow will be isolated from ROSA26-GFP^{Flox} mice and transplanted into lethally irradiated WT recipients. Cre expression will result in excision of the STOP sequence, leading to GFP fluorescence. Once Cre-mediated recombination has occurred, both the parent cell and all progeny will continue to express GFP.

Zovein, et al. (196) found that endothelial cells in the embryonic AGM, as defined by VE Cadherin expression, were capable of long term hematopoietic reconstitution. The endothelium of the AGM exclusively gave rise to HSCs; in fact, lineage tracing revealed that the mesenchymal cells of the AGM (defined by the expression of myocardin) were incapable of hematopoiesis (196). Given these data, it is possible that a portion of VE Cadherin positive cells in the bone marrow are capable of generating hematopoietic progeny. During reconstitution of the HSC population following myeloablative therapy, the primitive HSCs may express VE Cadherin. Using the lineage tracking system with a Cre retrovirus and floxed-GFP reporter mouse described above, any hematopoietic populations that arise from a VE Cadherin positive precursor can be identified.

The SINrv:X-Cre vectors could be used generate a model in which bone marrow subpopulations are eliminated; similar to the approach that was unsuccessfully attempted in Chapter 4. We have obtained a transgenic ROSA26-GFP-DTA mouse which contains a floxed GFP reporter gene upstream of the sequence encoding diphtheria toxin subunit A (DTA) targeted to the ROSA26 locus. ROSA26-GFP-DTA mice (114) ubiquitously express GFP, but transcription of the DTA gene is prevented by a triple poly-adenylation sequence downstream of the GFP coding region (Figure 6.4). In the presence of Cre recombinase, the GFP and poly-A signal are excised, resulting in DTA expression and eventual cell death. When crossed with $Na_v1.7$-cre mice, the ROSA26-GFP-DTA mice generated progeny that lacked a subset of $Na_v1.7$ neurons. The double transgenic mice showed normal neurologic function, but elicited a severely blunted pain response (197).

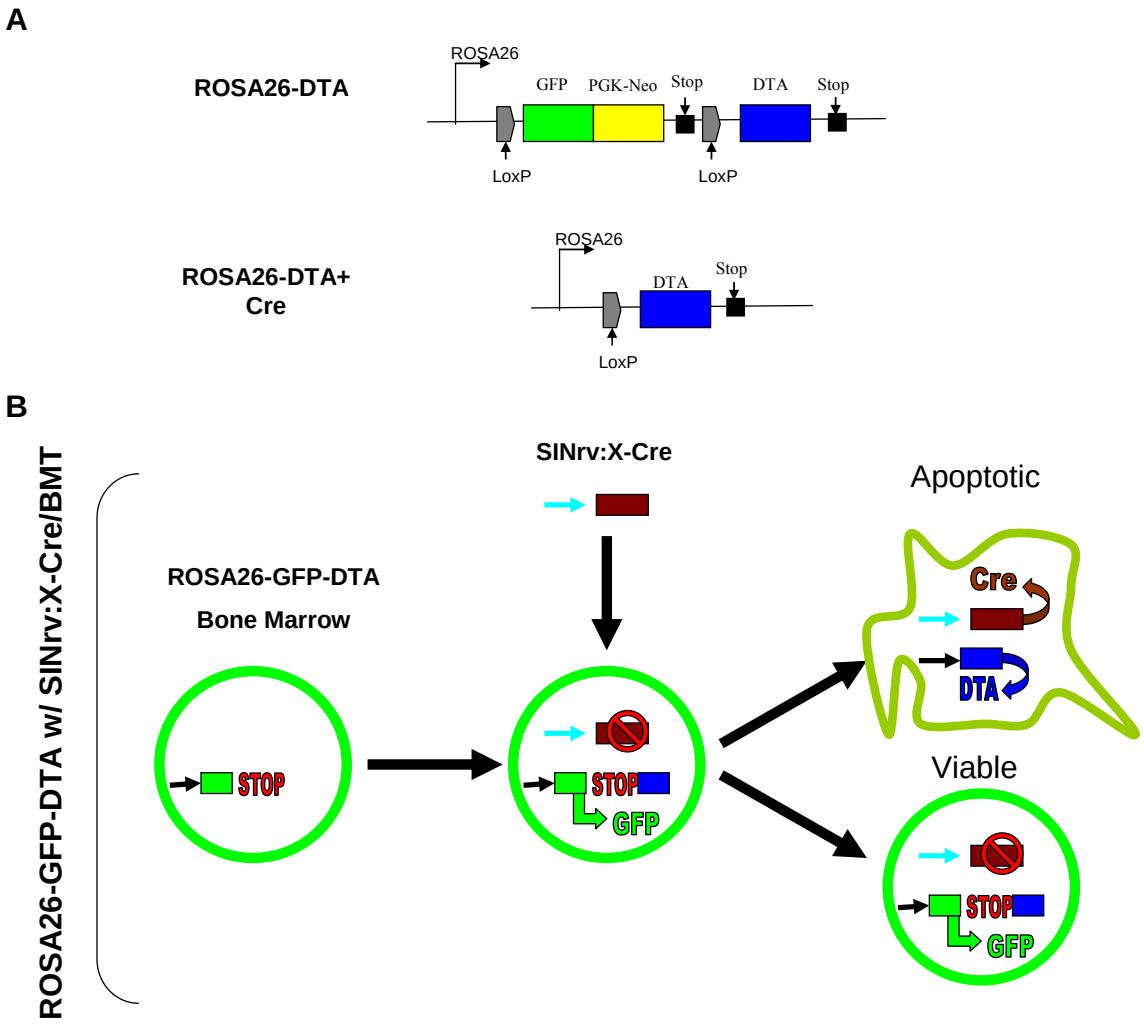

Figure 6.4: Future Strategy For Depletion of Bone Marrow Subpopulations. Transduction of bone marrow from ROSA26-GFP-DTA mice with the SINrv:X-Cre vectors will allow us to eliminate subpopulations of cells from the bone marrow. A) The construct contains a floxed GFP reporter/PGK-neomycin resistance cassette with triple poly-adenylation sequence targeted to the ROSA26 locus. In the presence of Cre recombinase, the floxed sequence is excised, resulting in diphtheria toxin A (DTA) expression (Modified from (114)). B) Bone marrow isolated from ROSA26-GFP-DTA mice will be isolated and transduced with one of the SINrv:X-Cre vectors. When Cre is expressed, the GFP reporter will be excised, and the cells will undergo apoptosis. However, if Cre is not expressed, cells will remain viable and GFP-positive.

We plan to use the SINrv:X-Cre vectors to transduce bone marrow obtained from ROSA26-GFP-DTA mice, and transplant it into lethally irradiated WT recipients. The resulting SINrv:X-Cre/BMT should undergo complete hematopoietic reconstitution, but

all cells in which the retroviral promoter is active will undergo apoptosis. Therefore, it is possible to generate mice in which BM and PB populations are depleted of all VEGF+, eNOS+, or VE Cadherin+ cells and their progeny. Using techniques such as microCT (198) and LDPI (199), the extent of blood vessel growth in the ischemic hind limb or subcutaneous matrigel plug can be quantified. Combining the use of these assays with ROSA26-GFP-DTA SINrv:X-Cre/BMT mice, we can elucidate the functional contributions of each individual cell type in a setting of post-natal neovascularization.

In this thesis we have demonstrated a novel strategy for fluorescently labeling subpopulations within the bone marrow. Using this technique, we have identified three populations of circulating cells which may be comprised of pro-angiogenic progenitors. Future work will reveal the therapeutic potential of these cells, and establish the lineage of these cells and their progeny. Finally, we will explore the functional role of these cells in models of post-natal neovascularization, allowing us to uniquely define EPCs.

APPENDIX A

BONE MARROW TRANSDUCTION PROTOCOL

(Courtesy of Dr. Natalia Landazuri)

Separation of Sca+ cells

1. Get bone marrow from femur and tibia (flush with DMEM/FBS/PS)
2. Count nucleated cells (mix cells with 2% acetic acid to exclude RBC). Set aside at least 500 000 cells for FACS.
3. Spin down (300g, 10min).
4. Resuspend in 90ul buffer per 10^7 cells (buffer: MACS rinsing buffer with MACS BSA diluted 1:20) + 10ul of blocking reagent (Miltenyi 130-092-575).
5. Add 10ul PE-anti-Sca antibody per 10^7 cells (Miltenyi 130-093-224)
6. Incubate in the fridge for 10 min (dark)
7. Wash cells by adding 2ml of buffer per 10^7 cells. Centrifuge 10 min, 300g.
8. Resuspend in 80ul of buffer per 10^7 cells. Add 20ul of Anti-PE micro beads (Miltenyi 130-048-801) per 10^7 cells.
9. Incubate for 15min in the fridge.
10. Wash cells by adding 2ml of buffer per 10^7 cells. Centrifuge 10 min, 300g.
11. Resuspend up to 10^8 cells in 500ul of buffer.
12. Magnetic separations using autoMACS. Possel-S.
13. Collect positive and negative fractions. Count cells. Set aside at least 200000 cells per fraction for FACS.

Culture of Sca1+ cells

Resuspend Sca1+ cells from 1-2 mice in 1ml of StemPro media containing Pen/Strep (1%), L-Glutamine (1%), nutrient supplement (40X), mSCF (100 ng/ml), mIL-3 (20 ng/ml), hIL-11 (100ng/ml), mFlt-3 (100 ng/ml). Plate in 1 well of a 6-well plate.

Coat wells with retronectin

1. Make a 1 mg/ml stock of retronectin (in water). Filter 0.22 um. Store at -20C.
2. Dilute the stock to 40 ug/ml (25X) in PBS. Add 2 ml/well of a 6-well dish (non-tissue culture treated). Incubate for 2hrs at RT or O/N at 4C.
3. To block, add PBS/2%BSA fraction V. Incubate for 30 min at RT.
4. Wash with PBS.

Transduction of Sca1+ cells

1. Add 1-2 ml of concentrated virus per well. Spin down 2500 rpm for 1hr at 4C.
2. Centrifuge cells. Resuspend in virus SN from step 1. Add supplements (see table above). Incubate at 32C for 4 hrs, then at 37C.

Measure transduction efficiency

1. Methylcellulose
    a. Plate ~1000 cells in 1.2ml/well of methylcellulose (in a 6-well plate, non-tissue culture treated). Thaw methylcellulose at room temperature. Add cells to methylcellulose and vortex. Allow for bubbles to rise. Transfer cells to a well using a syringe with thick needle.

b. Incubate at 37C for 1 week.

c. Count %transduced colonies (GFP+)

2. RT-PCR

a. Spin down ~100000 cells

b. Isolate genomic DNA using DNeasy kit (Qiagen)

c. RT-PCR for GFP or transgene.

APPENDIX B

PCR AND CLONING OLIGONUCLEOTIDES

Primer Name	Sequence
m18s for	gaacgtctgccctatcaact
m18s rev	ccaagatccaactacgagct
VE cad/BsiWI for	ggttttcgtacgctagtagcagaaacaag
VE cad/Pac1rev	ggttttttaattaagtcgagagtctgtcca
VEGFa for	tttagaagatgaaccgtaagcctag
VEGFa rev	gatacctctttcgtctgctga
VEGFa for/Age1	ggaccggttttagaagatgaaccgtaa
VEGFa for/BsiWI	ggcgtacgtttagaagatgaaccgtaa
meNOS for	aaaagcaaggatgagggataatataa
meNOS rev	gccagctgacctcaactctgccgcac
meNOS (BsiWI) for	gcccgtacgaaaagcaaggatgagggataa
meNOS (PacI) rev	gccttaattaagccagctgacctcaactctg
CD68 prom (BsiWI) for	gcccgtacgactagttgattactgaat
CD68 prom (Pac1) rev	gccttaattaaggcagagatgctcagacca

REFERENCES

1. Asahara T, Murohara T, Sullivan A, Silver M, Van Der Zee R, Li T, et al. Isolation of Putative Progenitor Endothelial Cells for Angiogenesis [Internet]. Science. 1997 ;275(5302):964-966.Available from: http://www.sciencemag.org/cgi/doi/10.1126/science.275.5302.964

2. Hill JM, Zalos G, Halcox JP, Schenke WH, Waclawiw Ma, Quyyumi Aa, et al. Circulating endothelial progenitor cells, vascular function, and cardiovascular risk. [Internet]. The New England journal of medicine. 2003 ;348(7):593-600.Available from: http://www.ncbi.nlm.nih.gov/pubmed/12584367

3. Ziegelhoeffer T, Fernandez B, Kostin S, Heil M, Voswinckel R, Helisch A, et al. Bone marrow-derived cells do not incorporate into the adult growing vasculature. [Internet]. Circulation research. 2004 ;94(2):230-8.Available from: http://www.ncbi.nlm.nih.gov/pubmed/14656934

4. O'Neill TJ, Wamhoff BR, Owens GK, Skalak TC. Mobilization of bone marrow-derived cells enhances the angiogenic response to hypoxia without transdifferentiation into endothelial cells. [Internet]. Circulation research. 2005 ;97(10):1027-35.Available from: http://www.ncbi.nlm.nih.gov/pubmed/16210550

5. Risau W. Mechanisms of angiogenesis [Internet]. Nature. 1997 ;38671-4.Available from: http://www.nature.com/nature/journal/v386/n6626/abs/386671a0.html

6. Folkman J. Angiogenesis in cancer, vascular, rheumatoid and other disease [Internet]. Nature medicine. 1995 ;1(1):27–30.Available from: http://www.nature.com/nm/journal/v1/n1/abs/nm0195-27.html

7. Heil M, Eitenmüller I, Schmitz-Rixen T, Schaper W. Arteriogenesis versus angiogenesis: similarities and differences. [Internet]. Journal of cellular and molecular medicine. 2006 ;10(1):45-55.Available from: http://www.ncbi.nlm.nih.gov/pubmed/16563221

8. Duvall CL. THE ROLE OF OSTEOPONTIN IN POSTNATAL VASCULAR GROWTH : FUNCTIONAL EFFECTS IN ISCHEMIC LIMB COLLATERAL VESSEL FORMATION AND LONG BONE FRACTURE HEALING THE ROLE OF OSTEOPONTIN IN POSTNATAL VASCULAR GROWTH : FUNCTIONAL EFFECTS IN ISCHEMIC LIMB COLLATERAL VES. Biomedical Engineering PhD Thesis. 2007 ;(May):

9. Hirschi KK, Ingram Da, Yoder MC. Assessing Identity, Phenotype, and Fate of Endothelial Progenitor Cells [Internet]. Arteriosclerosis, Thrombosis, and

Vascular Biology. 2008 ;28(9):1584-1595.Available from: http://atvb.ahajournals.org/cgi/doi/10.1161/ATVBAHA.107.155960

10. Solovey a, Lin Y, Browne P, Choong S, Wayner E, Hebbel RP. Circulating activated endothelial cells in sickle cell anemia. [Internet]. The New England journal of medicine. 1997 ;337(22):1584-90.Available from: http://www.ncbi.nlm.nih.gov/pubmed/9371854

11. Woywodt A, Blann AD, Kirsch T, Erdbruegger U, Banzet N, Haubitz M, et al. Isolation and enumeration of circulating endothelial cells by immunomagnetic isolation: proposal of a definition and a consensus protocol. [Internet]. Journal of thrombosis and haemostasis : JTH. 2006 ;4(3):671-7.Available from: http://www.ncbi.nlm.nih.gov/pubmed/16460450

12. Asahara T, Masuda H, Takahashi T, Kalka C, Pastore C, Silver M, et al. Bone marrow origin of endothelial progenitor cells responsible for postnatal vasculogenesis in physiological and pathological neovascularization [Internet]. Circulation research. 1999 ;85(3):221.Available from: http://circres.ahajournals.org/cgi/content/abstract/circresaha;85/3/221

13. Shi Q, Rafii S, Wu M, Wijelath E, Yu C, Ishida A, et al. Evidence for circulating bone marrow-derived endothelial cells [Internet]. Blood. 1998 ;92(2):362.Available from: http://bloodjournal.hematologylibrary.org/cgi/content/abstract/92/2/362

14. Takahashi T, Kalka C, Masuda H, Chen D, Silver M, Kearney M, et al. Ischemia- and cytokine-induced mobilization of bone marrow-derived endothelial progenitor cells for neovascularization. [Internet]. Nature medicine. 1999 ;5(4):434-8.Available from: http://www.ncbi.nlm.nih.gov/pubmed/17711709

15. Asahara T, Takahashi T, Masuda H, Kalka C, Chen D, Iwaguro H, et al. VEGF contributes to postnatal neovascularization by mobilizing bone marrow-derived endothelial progenitor cells. [Internet]. The EMBO journal. 1999 ;18(14):3964-72.Available from: http://www.ncbi.nlm.nih.gov/pubmed/10406801

16. Tateishi-Yuyama E. Therapeutic angiogenesis for patients with limb ischemia by autologous transplantation of bone-marrow cells: a pilot study and a randomized controlled trial [Internet]. ACC Current Journal Review. 2002 ;11(6):86.Available from: http://linkinghub.elsevier.com/retrieve/pii/S1062145802009741

17. Strauer BE. Repair of Infarcted Myocardium by Autologous Intracoronary Mononuclear Bone Marrow Cell Transplantation in Humans [Internet]. Circulation. 2002 ;106(15):1913-1918.Available from: http://circ.ahajournals.org/cgi/doi/10.1161/01.CIR.0000034046.87607.1C

18. Vasa M, Fichtlscherer S, Adler K, Aicher A, Martin H, Zeiher AM, et al. Increase in Circulating Endothelial Progenitor Cells by Statin Therapy in Patients With Stable Coronary Artery Disease [Internet]. Circulation. 2001 ;103(24):2885-2890.Available from: http://circ.ahajournals.org/cgi/doi/10.1161/hc2401.092816

19. Vasa M, Fichtlscherer S, Aicher a, Adler K, Urbich C, Martin H, et al. Number and Migratory Activity of Circulating Endothelial Progenitor Cells Inversely Correlate With Risk Factors for Coronary Artery Disease [Internet]. Circulation Research. 2001 ;89(1):e1-e7.Available from: http://circres.ahajournals.org/cgi/doi/10.1161/hh1301.093953

20. Lin Y, Weisdorf D, Solovey A, Hebbel R. Origins of circulating endothelial cells and endothelial outgrowth from blood [Internet]. Journal of clinical Investigation. 2000 ;105(1):71–77.Available from: http://www.jci.org/cgi/content/abstract/105/1/71

21. Gulati R, Jevremovic D, Peterson TE, Chatterjee S, Shah V, Vile RG, et al. Diverse origin and function of cells with endothelial phenotype obtained from adult human blood. [Internet]. Circulation research. 2003 ;93(11):1023-5.Available from: http://www.ncbi.nlm.nih.gov/pubmed/14605020

22. Hur J, Yoon C, Kim H, Choi J, Kang H, Hwang K, et al. Characterization of two types of endothelial progenitor cells and their different contributions to neovasculogenesis. [Internet]. Arteriosclerosis, thrombosis, and vascular biology. 2004 ;24(2):288-93.Available from: http://www.ncbi.nlm.nih.gov/pubmed/14699017

23. Yoon C, Hur J, Park K, Kim J, Lee C, Oh I, et al. Synergistic neovascularization by mixed transplantation of early endothelial progenitor cells and late outgrowth endothelial cells: the role of angiogenic cytokines and matrix metalloproteinases. [Internet]. Circulation. 2005 ;112(11):1618-27.Available from: http://www.ncbi.nlm.nih.gov/pubmed/16145003

24. Sieveking DP, Celermajer DS, Ng MK. Strikingly Different Angiogenic Properties of Endothelial Progenitor Cell Subpopulations. Journal of the American College of Cardiology. 2008 ;51(6):

25. Ingram D, Mead L, Tanaka H, Meade V, Fenoglio A, Mortell K, et al. Identification of a novel hierarchy of endothelial progenitor cells using human peripheral and umbilical cord blood [Internet]. Blood. 2004 ;104(9):2752.Available from: http://bloodjournal.hematologylibrary.org/cgi/content/full/bloodjournal;104/9/2752

26. Ingram D, Mead L, Moore D, Woodard W, Fenoglio A, Yoder M. Vessel wall-derived endothelial cells rapidly proliferate because they contain a complete

hierarchy of endothelial progenitor cells [Internet]. Blood. 2005 ;105(7):2783.Available from: http://bloodjournal.hematologylibrary.org/cgi/content/abstract/105/7/2783

27. Zengin E, Chalajour F, Gehling U, Ito W, Treede H, Lauke H, et al. Vascular wall resident progenitor cells: a source for postnatal vasculogenesis [Internet]. Development. 2006 ;133(8):1543.Available from: http://dev.biologists.org/cgi/content/full/133/8/1543

28. Chao H, Hirschi KK. Hemato-vascular origins of endothelial progenitor cells? [Internet]. Microvascular research. 2010 ;1933Available from: http://www.ncbi.nlm.nih.gov/pubmed/20149806

29. Yoder M, Mead L, Prater D, Krier T, Mroueh K, Li F, et al. Redefining endothelial progenitor cells via clonal analysis and hematopoietic stem/progenitor cell principals [Internet]. Blood. 2007 ;109(5):1801.Available from: http://bloodjournal.hematologylibrary.org/cgi/content/abstract/109/5/1801

30. Pelosi E, Valtieri M, Coppola S, Botta R, Gabbianelli M, Lulli V, et al. Identification of the hemangioblast in postnatal life [Internet]. Blood. 2002 ;100(9):3203.Available from: http://bloodjournal.hematologylibrary.org/cgi/content/abstract/100/9/3203

31. Gehling UM, Ergün S, Schumacher U, Wagener C, Pantel K, Otte M, et al. In vitro differentiation of endothelial cells from AC133-positive progenitor cells. [Internet]. Blood. 2000 ;95(10):3106-12.Available from: http://www.ncbi.nlm.nih.gov/pubmed/10807776

32. Peichev M, Naiyer aJ, Pereira D, Zhu Z, Lane WJ, Williams M, et al. Expression of VEGFR-2 and AC133 by circulating human CD34(+) cells identifies a population of functional endothelial precursors. [Internet]. Blood. 2000 ;95(3):952-8.Available from: http://www.ncbi.nlm.nih.gov/pubmed/10648408

33. Friedrich EB, Walenta K, Scharlau J, Nickenig G, Werner N. CD34-/CD133+/VEGFR-2+ endothelial progenitor cell subpopulation with potent vasoregenerative capacities. [Internet]. Circulation research. 2006 ;98(3):e20-5.Available from: http://www.ncbi.nlm.nih.gov/pubmed/16439688

34. Shaffer RG, Greene S, Arshi a, Supple G, Bantly a, Moores JS, et al. Effect of acute exercise on endothelial progenitor cells in patients with peripheral arterial disease [Internet]. Vascular Medicine. 2006 ;11(4):219-226.Available from: http://vmj.sagepub.com/cgi/doi/10.1177/1358863x06072213

35. Sandri M, Adams V, Gielen S, Linke A, Lenk K, Kränkel N, et al. Effects of exercise and ischemia on mobilization and functional activation of blood-derived progenitor cells in patients with ischemic syndromes: results of 3 randomized

studies. [Internet]. Circulation. 2005 ;111(25):3391-9.Available from: http://www.ncbi.nlm.nih.gov/pubmed/15956121

36. Laufs U, Werner N, Link A, Endres M, Wassmann S, Jürgens K, et al. Physical training increases endothelial progenitor cells, inhibits neointima formation, and enhances angiogenesis. [Internet]. Circulation. 2004 ;109(2):220-6.Available from: http://www.ncbi.nlm.nih.gov/pubmed/14691039

37. Powell TM, Paul JD, Hill JM, Thompson M, Benjamin M, Rodrigo M, et al. Granulocyte colony-stimulating factor mobilizes functional endothelial progenitor cells in patients with coronary artery disease. [Internet]. Arteriosclerosis, thrombosis, and vascular biology. 2005 ;25(2):296-301.Available from: http://www.ncbi.nlm.nih.gov/pubmed/15569821

38. Dome B, Timar J, Dobos J, Meszaros L, Raso E, Paku S, et al. Identification and clinical significance of circulating endothelial progenitor cells in human non-small cell lung cancer. [Internet]. Cancer research. 2006 ;66(14):7341-7.Available from: http://www.ncbi.nlm.nih.gov/pubmed/16849585

39. Massa M, Rosti V, Ferrario M, Campanelli R, Ramajoli I, Rosso R, et al. Increased circulating hematopoietic and endothelial progenitor cells in the early phase of acute myocardial infarction [Internet]. Blood. 2005 ;105(1):199.Available from: http://bloodjournal.hematologylibrary.org/cgi/content/abstract/105/1/199

40. Kondo T, Hayashi M, Takeshita K, Numaguchi Y, Kobayashi K, Iino S, et al. Smoking cessation rapidly increases circulating progenitor cells in peripheral blood in chronic smokers. [Internet]. Arteriosclerosis, thrombosis, and vascular biology. 2004 ;24(8):1442-7.Available from: http://www.ncbi.nlm.nih.gov/pubmed/15191940

41. Chen JZ, Zhang FR, Tao QM, Wang XX, Zhu JH, Zhu JH. Number and activity of endothelial progenitor cells from peripheral blood in patients with hypercholesterolaemia. [Internet]. Clinical science (London, England : 1979). 2004 ;107(3):273-80.Available from: http://www.ncbi.nlm.nih.gov/pubmed/15099190

42. MacEneaney OJ, Kushner EJ, Van Guilder GP, Greiner JJ, Stauffer BL, DeSouza Ca. Endothelial progenitor cell number and colony-forming capacity in overweight and obese adults. [Internet]. International journal of obesity (2005). 2009 ;33(2):219-25.Available from: http://www.ncbi.nlm.nih.gov/pubmed/19079361

43. Case J, Mead LE, Bessler WK, Prater D, White Ha, Saadatzadeh MR, et al. Human CD34+AC133+VEGFR-2+ cells are not endothelial progenitor cells but distinct, primitive hematopoietic progenitors. [Internet]. Experimental

hematology. 2007 ;35(7):1109-18.Available from: http://www.ncbi.nlm.nih.gov/pubmed/17588480

44. Rajantie I, Ilmonen M, Alminaite A, Ozerdem U, Alitalo K, Salven P. Adult bone marrow-derived cells recruited during angiogenesis comprise precursors for periendothelial vascular mural cells [Internet]. Blood. 2004 ;104(7):2084.Available from: http://bloodjournal.hematologylibrary.org/cgi/content/abstract/104/7/2084

45. Purhonen S, Palm J, Rossi D, Kaskenp\\"a\\"a N, Rajantie I, Yl\\"a-Herttuala S, et al. Bone marrow-derived circulating endothelial precursors do not contribute to vascular endothelium and are not needed for tumor growth [Internet]. Proceedings of the National Academy of Sciences. 2008 ;105(18):6620.Available from: http://www.pnas.org/content/105/18/6620.full

46. Schmeisser A, Garlichs C, Zhang H, Eskafi S, Graffy C, Ludwig J, et al. Monocytes coexpress endothelial and macrophagocytic lineage markers and form cord-like structures in Matrigel® under angiogenic conditions [Internet]. Cardiovascular research. 2001 ;49(3):671.Available from: http://cardiovascres.oxfordjournals.org/content/49/3/671.full

47. Pujol B, Lucibello F, Gehling U, K. Endothelial-like cells derived from human CD14 positive monocytes [Internet]. Cell Proliferation. 2002 ;287-300.Available from: http://www3.interscience.wiley.com/journal/119010175/abstract

48. Rehman J. Peripheral Blood "Endothelial Progenitor Cells" Are Derived From Monocyte/Macrophages and Secrete Angiogenic Growth Factors [Internet]. Circulation. 2003 ;107(8):1164-1169.Available from: http://circ.ahajournals.org/cgi/doi/10.1161/01.CIR.0000058702.69484.A0

49. Rohde E, Malischnik C, Thaler D, Maierhofer T, Linkesch W, Lanzer G, et al. Blood monocytes mimic endothelial progenitor cells. [Internet]. Stem cells (Dayton, Ohio). 2006 ;24(2):357-67.Available from: http://www.ncbi.nlm.nih.gov/pubmed/16141361

50. Urbich C, Heeschen C, Aicher A, Dernbach E, Zeiher A, Dimmeler S. Relevance of monocytic features for neovascularization capacity of circulating endothelial progenitor cells [Internet]. Circulation. 2003 ;108(20):2511.Available from: http://circ.ahajournals.org/cgi/content/abstract/108/20/2511

51. Bailey AS, Willenbring H, Jiang S, Anderson Da, Schroeder Da, Wong MH, et al. Myeloid lineage progenitors give rise to vascular endothelium. [Internet]. Proceedings of the National Academy of Sciences of the United States of America. 2006 ;103(35):13156-61.Available from: http://www.ncbi.nlm.nih.gov/pubmed/16920790

52. Grunewald M, Avraham I, Dor Y, Bachar-Lustig E, Itin A, Jung S, et al. VEGF-induced adult neovascularization: recruitment, retention, and role of accessory cells. [Internet]. Cell. 2006 ;124(1):175-89.Available from: http://www.ncbi.nlm.nih.gov/pubmed/16413490

53. De Palma M, Venneri MA, Roca C, Naldini L. Targeting exogenous genes to tumor angiogenesis by transplantation of genetically modified hematopoietic stem cells. [Internet]. Nature medicine. 2003 ;9(6):789-95.Available from: http://www.ncbi.nlm.nih.gov/pubmed/12740570

54. De Palma M, Venneri MA, Galli R, Sergi Sergi L, Politi LS, Sampaolesi M, et al. Tie2 identifies a hematopoietic lineage of proangiogenic monocytes required for tumor vessel formation and a mesenchymal population of pericyte progenitors. [Internet]. Cancer cell. 2005 ;8(3):211-26.Available from: http://www.ncbi.nlm.nih.gov/pubmed/16169466

55. Conejo-Garcia J, Buckanovich R, Benencia F, Courreges M, Rubin S, Carroll R, et al. Vascular leukocytes contribute to tumor vascularization [Internet]. Blood. 2005 ;105(2):679-681.Available from: http://bloodjournal.hematologylibrary.org/cgi/content/abstract/105/2/679

56. Pulaski HL, Spahlinger G, Silva Ia, McLean K, Kueck AS, Reynolds RK, et al. Identifying alemtuzumab as an anti-myeloid cell antiangiogenic therapy for the treatment of ovarian cancer. [Internet]. Journal of translational medicine. 2009 ;749.Available from: http://www.ncbi.nlm.nih.gov/pubmed/19545375

57. Conejo-Garcia JR, Benencia F, Courreges M, Kang E, Mohamed-Hadley A, Buckanovich RJ, et al. Tumor-infiltrating dendritic cell precursors recruited by a beta-defensin contribute to vasculogenesis under the influence of Vegf-A. [Internet]. Nature medicine. 2004 ;10(9):950-8.Available from: http://www.ncbi.nlm.nih.gov/pubmed/15334073

58. Li B, Vincent A, Cates J, Brantley-Sieders DM, Polk DB, Young PP. Low levels of tumor necrosis factor alpha increase tumor growth by inducing an endothelial phenotype of monocytes recruited to the tumor site. [Internet]. Cancer research. 2009 ;69(1):338-48.Available from: http://www.ncbi.nlm.nih.gov/pubmed/19118019

59. De Palma M, Mazzieri R, Politi LS, Pucci F, Zonari E, Sitia G, et al. Tumor-targeted interferon-alpha delivery by Tie2-expressing monocytes inhibits tumor growth and metastasis. [Internet]. Cancer cell. 2008 ;14(4):299-311.Available from: http://www.ncbi.nlm.nih.gov/pubmed/18835032

60. Ahn G, Brown JM. Matrix metalloproteinase-9 is required for tumor vasculogenesis but not for angiogenesis: role of bone marrow-derived

myelomonocytic cells. [Internet]. Cancer cell. 2008 ;13(3):193-205.Available from: http://www.ncbi.nlm.nih.gov/pubmed/18328424

61. Coffelt SB, Lewis CE, Naldini L, Brown JM, Ferrara N, De Palma M. Elusive identities and overlapping phenotypes of proangiogenic myeloid cells in tumors. [Internet]. The American journal of pathology. 2010 ;176(4):1564-76.Available from: http://www.ncbi.nlm.nih.gov/pubmed/20167863

62. Pucci F, Venneri M, Biziato D, Nonis A, Moi D, Sica A, et al. A distinguishing gene signature shared by tumor-infiltrating Tie2-expressing monocytes, blood" resident" monocytes, and embryonic macrophages suggests common functions and developmental relationships [Internet]. Blood. 2009 ;114(4):901.Available from: http://bloodjournal.hematologylibrary.org/cgi/content/abstract/114/4/901

63. Pahler J, Tazzyman S, Erez N, Chen Y, Murdoch C, Nozawa H, et al. Plasticity in tumor-promoting inflammation: impairment of macrophage recruitment evokes a compensatory neutrophil response [Internet]. Neoplasia (New York, NY). 2008 ;10(4):329.Available from: http://www.ncbi.nlm.nih.gov/pmc/articles/PMC2288539/

64. Li Z, Zhang M, Jing Y, Zhang W, Liu Y, Cui L, et al. The clinical study of autologous peripheral blood stem cell transplantation by intracoronary infusion in patients with acute myocardial infarction (AMI). [Internet]. International journal of cardiology. 2007 ;115(1):52-6.Available from: http://www.ncbi.nlm.nih.gov/pubmed/16822566

65. Tatsumi T, Ashihara E, Yasui T, Matsunaga S, Kido A, Sasada Y, et al. Intracoronary transplantation of non-expanded peripheral blood-derived mononuclear cells promotes improvement of cardiac function in patients with acute myocardial infarction. [Internet]. Circulation journal : official journal of the Japanese Circulation Society. 2007 ;71(8):1199-207.Available from: http://www.ncbi.nlm.nih.gov/pubmed/17652881

66. Fernández-Avilés F, San Román JA, García-Frade J, Fernández ME, Peñarrubia MJ, de la Fuente L, et al. Experimental and clinical regenerative capability of human bone marrow cells after myocardial infarction. [Internet]. Circulation research. 2004 ;95(7):742-8.Available from: http://www.ncbi.nlm.nih.gov/pubmed/15358665

67. Wollert KC, Meyer GP, Lotz J, Ringes-Lichtenberg S, Lippolt P, Breidenbach C, et al. Intracoronary autologous bone-marrow cell transfer after myocardial infarction: the BOOST randomised controlled clinical trial. [Internet]. Lancet. 2004 ;364(9429):141-8.Available from: http://www.ncbi.nlm.nih.gov/pubmed/15246726

68. Meyer GP, Wollert KC, Lotz J, Steffens J, Lippolt P, Fichtner S, et al. Intracoronary bone marrow cell transfer after myocardial infarction: eighteen months' follow-up data from the randomized, controlled BOOST (BOne marrOw transfer to enhance ST-elevation infarct regeneration) trial. [Internet]. Circulation. 2006 ;113(10):1287-94.Available from: http://www.ncbi.nlm.nih.gov/pubmed/16520413

69. Kuethe F, Richartz BM, Sayer HG, Kasper C, Werner GS, Höffken K, et al. Lack of regeneration of myocardium by autologous intracoronary mononuclear bone marrow cell transplantation in humans with large anterior myocardial infarctions. [Internet]. International journal of cardiology. 2004 ;97(1):123-7.Available from: http://www.ncbi.nlm.nih.gov/pubmed/15336818

70. Lunde K, Solheim S, Forfang K, Arnesen H, Brinch L, Bjørnerheim R, et al. Anterior myocardial infarction with acute percutaneous coronary intervention and intracoronary injection of autologous mononuclear bone marrow cells: safety, clinical outcome, and serial changes in left ventricular function during 12-months' follow-up. [Internet]. Journal of the American College of Cardiology. 2008 ;51(6):674-6.Available from: http://www.ncbi.nlm.nih.gov/pubmed/18261689

71. Schächinger V, Erbs S, Elsässer A, Haberbosch W, Hambrecht R, Hölschermann H, et al. Intracoronary bone marrow-derived progenitor cells in acute myocardial infarction. [Internet]. The New England journal of medicine. 2006 ;355(12):1210-21.Available from: http://www.ncbi.nlm.nih.gov/pubmed/19996415

72. Gyöngyösi M, Lang I, Dettke M, Beran G, Graf S, Sochor H, et al. Combined delivery approach of bone marrow mononuclear stem cells early and late after myocardial infarction: the MYSTAR prospective, randomized study. [Internet]. Nature clinical practice. Cardiovascular medicine. 2009 ;6(1):70-81.Available from: http://www.ncbi.nlm.nih.gov/pubmed/19002124

73. Meluzín J, Janousek S, Mayer J, Groch L, Hornácek I, Hlinomaz O, et al. Three-, 6-, and 12-month results of autologous transplantation of mononuclear bone marrow cells in patients with acute myocardial infarction. [Internet]. International journal of cardiology. 2008 ;128(2):185-92.Available from: http://www.ncbi.nlm.nih.gov/pubmed/17764767

74. Boyle AJ, Whitbourn R, Schlicht S, Krum H, Kocher A, Nandurkar H, et al. Intra-coronary high-dose CD34+ stem cells in patients with chronic ischemic heart disease: a 12-month follow-up. [Internet]. International journal of cardiology. 2006 ;109(1):21-7.Available from: http://www.ncbi.nlm.nih.gov/pubmed/15970342

75. Losordo DW, Schatz Ra, White CJ, Udelson JE, Veereshwarayya V, Durgin M, et al. Intramyocardial transplantation of autologous CD34+ stem cells for intractable angina: a phase I/IIa double-blind, randomized controlled trial. [Internet].

Circulation. 2007 ;115(25):3165-72.Available from: http://www.ncbi.nlm.nih.gov/pubmed/17562958

76. Bartunek J, Vanderheyden M, Vandekerckhove B, Mansour S, De Bruyne B, De Bondt P, et al. Intracoronary injection of CD133-positive enriched bone marrow progenitor cells promotes cardiac recovery after recent myocardial infarction: feasibility and safety. [Internet]. Circulation. 2005 ;112(9 Suppl):I178-83.Available from: http://www.ncbi.nlm.nih.gov/pubmed/16159812

77. Stamm C, Kleine H, Choi Y, Dunkelmann S, Lauffs J, Lorenzen B, et al. Intramyocardial delivery of CD133+ bone marrow cells and coronary artery bypass grafting for chronic ischemic heart disease: safety and efficacy studies. [Internet]. The Journal of thoracic and cardiovascular surgery. 2007 ;133(3):717-25.Available from: http://www.ncbi.nlm.nih.gov/pubmed/17320570

78. Stamm C, Westphal B, Kleine H, Petzsch M, Kittner C, Klinge H, et al. Autologous bone-marrow stem-cell transplantation for myocardial regeneration. [Internet]. Lancet. 2003 ;361(9351):45-6.Available from: http://www.ncbi.nlm.nih.gov/pubmed/12517467

79. Schächinger V, Assmus B, Britten MB, Honold J, Lehmann R, Teupe C, et al. Transplantation of progenitor cells and regeneration enhancement in acute myocardial infarction: final one-year results of the TOPCARE-AMI Trial. [Internet]. Journal of the American College of Cardiology. 2004 ;44(8):1690-9.Available from: http://www.ncbi.nlm.nih.gov/pubmed/15489105

80. Assmus B. Transplantation of Progenitor Cells and Regeneration Enhancement in Acute Myocardial Infarction (TOPCARE-AMI) [Internet]. Circulation. 2002 ;106(24):3009-3017.Available from: http://circ.ahajournals.org/cgi/doi/10.1161/01.CIR.0000043246.74879.CD

81. Assmus B, Honold J, Schächinger V, Britten MB, Fischer-Rasokat U, Lehmann R, et al. Transcoronary transplantation of progenitor cells after myocardial infarction. [Internet]. The New England journal of medicine. 2006 ;355(12):1222-32.Available from: http://www.ncbi.nlm.nih.gov/pubmed/16990385

82. Loomans CJ, de Koning EJ, Staal FJ, Rookmaaker MB, Verseyden C, de Boer HC, et al. Endothelial progenitor cell dysfunction: a novel concept in the pathogenesis of vascular complications of type 1 diabetes. [Internet]. Diabetes. 2004 ;53(1):195-9.Available from: http://www.ncbi.nlm.nih.gov/pubmed/14693715

83. Pistrosch F, Herbrig K, Oelschlaegel U, Richter S, Passauer J, Fischer S, et al. PPARgamma-agonist rosiglitazone increases number and migratory activity of cultured endothelial progenitor cells. [Internet]. Atherosclerosis. 2005 ;183(1):163-7.Available from: http://www.ncbi.nlm.nih.gov/pubmed/15907852

84. Tepper OM. Human Endothelial Progenitor Cells From Type II Diabetics Exhibit Impaired Proliferation, Adhesion, and Incorporation Into Vascular Structures [Internet]. Circulation. 2002 ;106(22):2781-2786.Available from: http://circ.ahajournals.org/cgi/doi/10.1161/01.CIR.0000039526.42991.93

85. Heeschen C, Lehmann R, Honold J, Assmus B, Aicher A, Walter DH, et al. Profoundly reduced neovascularization capacity of bone marrow mononuclear cells derived from patients with chronic ischemic heart disease. [Internet]. Circulation. 2004 ;109(13):1615-22.Available from: http://www.ncbi.nlm.nih.gov/pubmed/15037527

86. Foresta C, Caretta N, Lana a, Cabrelle a, Palù G, Ferlin a. Circulating endothelial progenitor cells in subjects with erectile dysfunction. [Internet]. International journal of impotence research. 2005 ;17(3):288-90.Available from: http://www.ncbi.nlm.nih.gov/pubmed/15729373

87. Ghani U, Shuaib A, Salam A, Nasir A, Shuaib U, Jeerakathil T, et al. Endothelial progenitor cells during cerebrovascular disease. [Internet]. Stroke; a journal of cerebral circulation. 2005 ;36(1):151-3.Available from: http://www.ncbi.nlm.nih.gov/pubmed/15576657

88. Shintani S, Murohara T, Ikeda H, Ueno T, Honma T, Katoh a, et al. Mobilization of Endothelial Progenitor Cells in Patients With Acute Myocardial Infarction [Internet]. Circulation. 2001 ;103(23):2776-2779.Available from: http://circ.ahajournals.org/cgi/doi/10.1161/hc2301.092122

89. Valgimigli M, Rigolin GM, Fucili A, Porta MD, Soukhomovskaia O, Malagutti P, et al. CD34+ and endothelial progenitor cells in patients with various degrees of congestive heart failure. [Internet]. Circulation. 2004 ;110(10):1209-12.Available from: http://www.ncbi.nlm.nih.gov/pubmed/15249502

90. Mahmood Z, Shukla Y. Death receptors: targets for cancer therapy. [Internet]. Experimental cell research. 2010 ;316(6):887-99.Available from: http://www.ncbi.nlm.nih.gov/pubmed/20026107

91. Li J, Yuan J. Caspases in apoptosis and beyond. [Internet]. Oncogene. 2008 ;27(48):6194-206.Available from: http://www.ncbi.nlm.nih.gov/pubmed/18931687

92. Kang MH, Reynolds CP. Bcl-2 inhibitors: targeting mitochondrial apoptotic pathways in cancer therapy. [Internet]. Clinical cancer research : an official journal of the American Association for Cancer Research. 2009 ;15(4):1126-32.Available from: http://www.ncbi.nlm.nih.gov/pubmed/19228717

93. Letai A, Bassik MC, Walensky LD, Sorcinelli MD, Weiler S, Korsmeyer SJ. Distinct BH3 domains either sensitize or activate mitochondrial apoptosis, serving

as prototype cancer therapeutics [Internet]. Cancer Cell. 2002 ;2(3):183-192.Available from: http://dx.doi.org/10.1016/S1535-6108(02)00127-7

94. Kuwana T, Bouchier-Hayes L, Chipuk J, Bonzon C, Sullivan B, Green D, et al. BH3 domains of BH3-only proteins differentially regulate Bax-mediated mitochondrial membrane permeabilization both directly and indirectly [Internet]. Molecular cell. 2005 ;17(4):525–535.Available from: http://linkinghub.elsevier.com/retrieve/pii/S1097276505010774

95. Cartron P, Gallenne T, Bougras G, Gautier F, Manero F, Vusio P, et al. The first alpha helix of Bax plays a necessary role in its ligand-induced activation by the BH3-only proteins Bid and PUMA. [Internet]. Molecular cell. 2004 ;16(5):807-18.Available from: http://www.ncbi.nlm.nih.gov/pubmed/15574335

96. Gavathiotis E, Suzuki M, Davis ML, Pitter K, Bird GH, Katz SG, et al. BAX activation is initiated at a novel interaction site. [Internet]. Nature. 2008 ;455(7216):1076-81.Available from: http://www.ncbi.nlm.nih.gov/pubmed/18948948

97. Giam M, Huang D, Bouillet P. BH3-only proteins and their roles in programmed cell death [Internet]. Oncogene. 2009 ;27S128–S136.Available from: http://www.nature.com/onc/journal/v27/n1s/abs/onc200950a.html

98. Willis SN, Fletcher JI, Kaufmann T, van Delft MF, Chen L, Czabotar PE, et al. Apoptosis initiated when BH3 ligands engage multiple Bcl-2 homologs, not Bax or Bak. [Internet]. Science (New York, N.Y.). 2007 ;315(5813):856-9.Available from: http://www.ncbi.nlm.nih.gov/pubmed/17289999

99. Schendel SL, Montal M, Reed JC. Bcl-2 family proteins as ion-channels. [Internet]. Cell death and differentiation. 1998 ;5(5):372-80.Available from: http://www.ncbi.nlm.nih.gov/pubmed/10200486

100. Qian S, Wang W, Yang L, Huang H. Structure of transmembrane pore induced by Bax-derived peptide: Evidence for lipidic pores [Internet]. Proceedings of the National Academy of Sciences. 2008 ;105(45):17379.Available from: http://www.pnas.org/cgi/content/abstract/105/45/17379

101. Nouraini S, Six E, Matsuyama S, Krajewski S, Reed JC. The putative pore-forming domain of Bax regulates mitochondrial localization and interaction with Bcl-X(L). [Internet]. Molecular and cellular biology. 2000 ;20(5):1604-15.Available from: http://www.ncbi.nlm.nih.gov/pubmed/10669738

102. Kagawa S, Gu J, Swisher S, Ji L, Roth J, Lai D, et al. Antitumor effect of adenovirus-mediated Bax gene transfer on p53-sensitive and p53-resistant cancer lines [Internet]. Cancer Research. 2000 ;60(5):1157.Available from: http://cancerres.aacrjournals.org/cgi/content/abstract/60/5/1157

103. Pirocanac E. Bax-Induction Gene Therapy of Pancreatic Cancer [Internet]. Journal of Surgical Research. 2002 ;106(2):346-351.Available from: http://linkinghub.elsevier.com/retrieve/pii/S0022480402964735

104. Huang X, Lin T, Gu J, Zhang L, Roth Ja, Stephens LC, et al. Combined TRAIL and Bax gene therapy prolonged survival in mice with ovarian cancer xenograft. [Internet]. Gene therapy. 2002 ;9(20):1379-86.Available from: http://www.ncbi.nlm.nih.gov/pubmed/12365003

105. J G, M A, Ja R, B F. hTERT promoter induces tumor-specific Bax gene expression and cell killing in syngenic mouse tumor model and prevents systemic toxicity. Gene Therapy. 2002 ;930-37.

106. Huang J, Gao J, Lv X, Li G, Hao D, Yao X, et al. Target gene therapy of glioma: overexpression of BAX gene under the control of both tissue-specific promoter and hypoxia-inducible element. Acta Biochimica et Biophysica Sinica. 2010 ;1 - 7.

107. Hioki M, Kagawa S, Fujiwara T, Sakai R, Kojima T, Watanabe Y, et al. Combination of oncolytic adenovirotherapy and Bax gene therapy in human cancer xenografted models. Potential merits and hurdles for combination therapy. [Internet]. International journal of cancer. Journal international du cancer. 2008 ;122(11):2628-33.Available from: http://www.ncbi.nlm.nih.gov/pubmed/18338751

108. Jr AP. Diphtheria toxin [Internet]. Annual Review of Biochemistry. 1977 ;87(1):89-95.Available from: http://arjournals.annualreviews.org/doi/abs/10.1146%2Fannurev.bi.46.070177.000441

109. Bartell J, Fantz D, Davis T, Dewey M, Kistler M, Kistler W. Elimination of male germ cells in transgenic mice by the diphtheria toxin A chain gene directed by the histone H1t promoter [Internet]. Biology of reproduction. 2000 ;63(2):409.Available from: http://www.biolreprod.org/content/63/2/409.full

110. Palmiter RD, Behringer RR, Quaife CJ, Maxwell F, Maxwell IH, Brinster RL. Cell lineage ablation in transgenic mice by cell-specific expression of a toxin gene. [Internet]. Cell. 1987 ;50(3):435-43.Available from: http://www.ncbi.nlm.nih.gov/pubmed/3649277

111. Aguila HL, Hershberger RJ, Weissman IL. Transgenic mice carrying the diphtheria toxin A chain gene under the control of the granzyme A promoter: expected depletion of cytotoxic cells and unexpected depletion of CD8 T cells. [Internet]. Proceedings of the National Academy of Sciences of the United States of America. 1995 ;92(22):10192-6.Available from: http://www.ncbi.nlm.nih.gov/pubmed/7479752

112. Klaus S, Münzberg H, Trüloff C, Heldmaier G. Physiology of transgenic mice with brown fat ablation: obesity is due to lowered body temperature. [Internet]. The American journal of physiology. 1998 ;274(2 Pt 2):R287-93.Available from: http://www.ncbi.nlm.nih.gov/pubmed/9486283

113. Lee P, Morley G, Huang Q, Fischer a, Seiler S, Horner JW, et al. Conditional lineage ablation to model human diseases. [Internet]. Proceedings of the National Academy of Sciences of the United States of America. 1998 ;95(19):11371-6.Available from: http://www.ncbi.nlm.nih.gov/pubmed/9736743

114. Ivanova A, Signore M, Caro N, Greene N, Copp A, Martinez-Barbera J. In vivo genetic ablation by Cre-mediated expression of diphtheria toxin fragment A [Internet]. Genesis (New York, NY: 2000). 2005 ;43(3):129.Available from: http://www.ncbi.nlm.nih.gov/pmc/articles/PMC2233880/

115. Brockschnieder D, Pechmann Y, Sonnenberg-Riethmacher E, Riethmacher D. An improved mouse line for Cre-induced cell ablation due to diphtheria toxin A, expressed from the Rosa26 locus [Internet]. genesis. 2006 ;44(7):322–327.Available from: http://www3.interscience.wiley.com/journal/112658897/abstract

116. Brockschnieder D, Lappe-Siefke C, Goebbels S, Boesl M, Nave K, Riethmacher D. Cell depletion due to diphtheria toxin fragment A after Cre-mediated recombination [Internet]. Molecular and cellular biology. 2004 ;24(17):7636.Available from: http://mcb.asm.org/cgi/content/abstract/24/17/7636

117. Buch T, Heppner F, Tertilt C, Heinen T, Kremer M, Wunderlich F, et al. A Cre-inducible diphtheria toxin receptor mediates cell lineage ablation after toxin administration [Internet]. Nature Methods. 2005 ;2(6):419–426.Available from: http://www.nature.com/nmeth/journal/v2/n6/abs/nmeth762.html

118. Sato M, Tanigawa M. Production of CETD transgenic mouse line allowing ablation of any type of specific cell population [Internet]. Molecular reproduction and development. 2005 ;72(1):54–67.Available from: http://www3.interscience.wiley.com/journal/110496977/abstract

119. Mitamura T, Higashiyama S, Taniguchi N, Klagsbrun M, Mekada E. Diphtheria toxin binds to the epidermal growth factor (EGF)-like domain of human heparin-binding EGF-like growth factor/diphtheria toxin receptor and inhibits specifically its mitogenic activity [Internet]. Journal of Biological Chemistry. 1995 ;270(3):1015.Available from: http://www.jbc.org/content/270/3/1015.short

120. Jung S, Unutmaz D, Wong P, Sano G, De los Santos K, Sparwasser T, et al. In vivo depletion of CD11c(+) dendritic cells abrogates priming of CD8(+) T cells by exogenous cell-associated antigens. [Internet]. Immunity. 2002 ;17(2):211-20.Available from: http://www.ncbi.nlm.nih.gov/pubmed/12196292

121. Saito M, Iwawaki T, Taya C, Yonekawa H, Noda M, Inui Y, et al. Diphtheria toxin receptor–mediated conditional and targeted cell ablation in transgenic mice [Internet]. nature biotechnology. 2001 ;19(8):746–750.Available from: http://www.nature.com/nbt/journal/v19/n8/abs/nbt0801_746.html

122. Borrelli E, Heyman R, Hsi M, Evans RM. Targeting of an inducible toxic phenotype in animal cells. [Internet]. Proceedings of the National Academy of Sciences of the United States of America. 1988 ;85(20):7572-6.Available from: http://www.ncbi.nlm.nih.gov/pubmed/2845412

123. Friedrich G, Soriano P. Promoter traps in embryonic stem cells: a genetic screen to identify and mutate developmental genes in mice. [Internet]. Genes & development. 1991 ;5(9):1513-23.Available from: http://www.ncbi.nlm.nih.gov/pubmed/1653172

124. Tian B, Han L, Kleidon J, Henke C. An HSV-TK transgenic mouse model to evaluate elimination of fibroblasts for fibrosis therapy. [Internet]. The American journal of pathology. 2003 ;163(2):789-801.Available from: http://www.ncbi.nlm.nih.gov/pubmed/12875998

125. Grant MB, May WS, Caballero S, Brown Ga, Guthrie SM, Mames RN, et al. Adult hematopoietic stem cells provide functional hemangioblast activity during retinal neovascularization. [Internet]. Nature medicine. 2002 ;8(6):607-12.Available from: http://www.ncbi.nlm.nih.gov/pubmed/12042812

126. Jackson Ka, Majka SM, Wang H, Pocius J, Hartley CJ, Majesky MW, et al. Regeneration of ischemic cardiac muscle and vascular endothelium by adult stem cells. [Internet]. The Journal of clinical investigation. 2001 ;107(11):1395-402.Available from: http://www.ncbi.nlm.nih.gov/pubmed/11390421

127. Murayama T, Tepper O, Silver M, Ma H, Losordo D, Isner J, et al. Determination of bone marrow-derived endothelial progenitor cell significance in angiogenic growth factor-induced neovascularization in vivo [Internet]. Experimental hematology. 2002 ;30(8):967–972.Available from: http://linkinghub.elsevier.com/retrieve/pii/S0301472X02008676

128. Bailey A, Jiang S, Afentoulis M, Baumann C, Schroeder D, Olson S, et al. Transplanted adult hematopoietic stems cells differentiate into functional endothelial cells [Internet]. Blood. 2004 ;103(1):13.Available from: http://bloodjournal.hematologylibrary.org/cgi/content/full/bloodjournal;103/1/13

129. Loges S, Fehse B, Brockmann M, Lamszus K, Butzal M, Guckenbiehl M, et al. Identification of the adult human hemangioblast [Internet]. Stem Cells and Development. 2004 ;13(3):229–242.Available from: http://www.liebertonline.com/doi/abs/10.1089/154732804323099163

130. Mao X, Fujiwara Y, Orkin SH. Improved reporter strain for monitoring Cre recombinase-mediated DNA excisions in mice. [Internet]. Proceedings of the National Academy of Sciences of the United States of America. 1999 ;96(9):5037-42.Available from: http://www.ncbi.nlm.nih.gov/pubmed/10220414

131. Hayashi S, McMahon AP. Efficient recombination in diverse tissues by a tamoxifen-inducible form of Cre: a tool for temporally regulated gene activation/inactivation in the mouse. [Internet]. Developmental biology. 2002 ;244(2):305-18.Available from: http://www.ncbi.nlm.nih.gov/pubmed/11944939

132. Forde A, Constien R, Gr&#65533;ne H, H&#65533;mmerling G, Arnold B. Temporal Cre-mediated recombination exclusively in endothelial cells using Tie2 regulatory elements [Internet]. Genesis. 2002 ;33(4):191-197.Available from: http://doi.wiley.com/10.1002/gene.10117

133. Ide LM, Javazon E, Spencer HT. Transduction of murine hematopoietic stem cells and in vivo selection of gene-modified cells. [Internet]. Methods in molecular biology (Clifton, N.J.). 2008 ;433213-28.Available from: http://www.ncbi.nlm.nih.gov/pubmed/18679626

134. Gough P, Raines E. Gene therapy of apolipoprotein E-deficient mice using a novel macrophage-specific retroviral vector [Internet]. Blood. 2002 ;101(2):200207213.Available from: http://bloodjournal.hematologylibrary.org/cgi/content/abstract/2002-07-2158v1

135. Pear WS, Nolan GP, Scott ML, Baltimore D. Production of high-titer helper-free retroviruses by transient transfection. [Internet]. Proceedings of the National Academy of Sciences of the United States of America. 1993 ;90(18):8392-6.Available from: http://www.ncbi.nlm.nih.gov/pubmed/7690960

136. Grignani F, Kinsella T, Mencarelli A, Valtieri M, Riganelli D, Lanfrancone L, et al. High-efficiency gene transfer and selection of human hematopoietic progenitor cells with a hybrid EBV/retroviral vector expressing the green fluorescence protein [Internet]. Cancer research. 1998 ;58(1):14.Available from: http://cancerres.aacrjournals.org/cgi/content/abstract/58/1/14

137. O'connell K, Edidin M. A mouse lymphoid endothelial cell line immortalized by simian virus 40 binds lymphocytes and retains functional characteristics of normal endothelial cells [Internet]. The Journal of Immunology. 1990 ;144(2):521.Available from: http://www.jimmunol.org/cgi/content/abstract/144/2/521

138. Ades E, Candal F, Swerlick R, George V, Summers S, Bosse D, et al. HMEC-1: establishment of an immortalized human microvascular endothelial cell line [Internet]. Journal of Investigative Dermatology. 1992 ;99(6):683–690.Available from:

http://www.nature.com/jid/journal/v99/n6/abs/5611816a.html?referer=www.clickfind.com.au

139. Jainchill J, Aaronson S, Todaro G. Murine sarcoma and leukemia viruses: assay using clonal lines of contact-inhibited mouse cells [Internet]. Journal of Virology. 1969 ;4(5):549.Available from: http://jvi.asm.org/cgi/content/abstract/4/5/549

140. Guntaka RV. Transcription termination and polyadenylation in retroviruses. [Internet]. Microbiological reviews. 1993 ;57(3):511-21.Available from: http://www.ncbi.nlm.nih.gov/pubmed/7902524

141. Goff S. Genetics of retroviral integration [Internet]. Annual review of genetics. 1992 ;26(1):527–544.Available from: http://arjournals.annualreviews.org/doi/abs/10.1146/annurev.ge.26.120192.002523

142. Hettle S, Darnbrough C, Watts P, MacDonald C. Effects of an internal transcription unit and its orientation on retrovirus titre and expression [Internet]. Cytotechnology. 1997 ;24(1):31–38.Available from: http://www.springerlink.com/index/T12L603247237172.pdf

143. Maxwell IH, Brown JL, Maxwell F. Inefficiency of expression of luciferase reporter from transfected murine leukaemia proviral DNA may be partially overcome by providing a strong polyadenylation signal. [Internet]. The Journal of general virology. 1991 ;72 (Pt 7)1721-4.Available from: http://www.ncbi.nlm.nih.gov/pubmed/1649905

144. Ziebart T, Yoon C, Trepels T, Wietelmann A, Braun T, Kiessling F, et al. Sustained persistence of transplanted proangiogenic cells contributes to neovascularization and cardiac function after ischemia. [Internet]. Circulation research. 2008 ;103(11):1327-34.Available from: http://www.ncbi.nlm.nih.gov/pubmed/18927463

145. Damert A, Kusserow H. Generation of transgenic mice by pronuclear injection. [Internet]. Methods in molecular medicine. 2003 ;89513-28.Available from: http://www.springerlink.com/content/g4172kg20374037q

146. Saito M, Korsmeyer S, Schlesinger P. BAX-dependent transport of cytochrome c reconstituted in pure liposomes [Internet]. Nature cell biology. 2000 ;2(8):553–555.Available from: http://www.chantest.com/downloads/A25.pdf

147. Wolter K, Hsu Y, Smith C, Nechushtan A, Xi X, Youle R. Movement of Bax from the cytosol to mitochondria during apoptosis [Internet]. Journal of Cell Biology. 1997 ;139(5):1281.Available from: http://jcb.rupress.org/cgi/content/abstract/139/5/1281

148. Antonsson B, Conti F, Ciavatta A, Montessuit S, Lewis S, Martinou I, et al. Inhibition of Bax channel-forming activity by Bcl-2 [Internet]. Science. 1997 ;277(5324):370.Available from: http://www.sciencemag.org/cgi/content/abstract/sci;277/5324/370

149. Mahajan N, Linder K, Berry G, Gordon G, Heim R, Herman B. Bcl-2 and Bax interactions in mitochondria probed with green fluorescent protein and fluorescence resonance energy transfer [Internet]. Nature biotechnology. 1998 ;16(6):547–552.Available from: http://www.nature.com/nbt/journal/v16/n6/abs/nbt0698-547.html

150. Zha H, Aimé-Sempé C, Sato T, Reed J. Proapoptotic protein Bax heterodimerizes with Bcl-2 and homodimerizes with Bax via a novel domain (BH3) distinct from BH1 and BH2 [Internet]. Journal of Biological Chemistry. 1996 ;271(13):7440.Available from: http://www.jbc.org/content/271/13/7440.full

151. Usui K, Saijo Y, Narumi K, Koyama S, Maemondo M, Kikuchi T, et al. N-terminal deletion augments the cell-death-inducing activity of BAX in adenoviral gene delivery to nonsmall cell lung cancers [Internet]. Oncogene. 2003 ;22(17):2655–2663.Available from: http://www.nature.com/onc/journal/v22/n17/abs/1206331a.html

152. Ishibashi Y, Nishimaki K, Asoh S, Nanbu-wakao R, Yamada T, Ohta S. Pore Formation Domain of Human Pro-apoptotic Bax Induces Mammalian Apoptosis as well as Bacterial Death without Antagonizing Anti-apoptotic Factors. Biochemical and Biophysical Research Communications. 1998 ;616(243):609-616.

153. Nechushtan A, Smith C, Hsu Y, Youle R. Conformation of the Bax C-terminus regulates subcellular location and cell death. [Internet]. The EMBO journal. 1999 ;18(9):2330.Available from: http://www.pubmedcentral.nih.gov/articlerender.fcgi?artid=1171316

154. Suzuki M, Youle R, Tjandra N. Structure of Bax Coregulation of Dimer Formation and Intracellular Localization [Internet]. Cell. 2000 ;103(4):645–654.Available from: http://linkinghub.elsevier.com/retrieve/pii/S0092867400001677

155. Muchmore S, Sattler M, Liang H, Meadows R, Harlan J, Yoon H, et al. X-ray and NMR structure of human Bcl-xL, an inhibitor of programmed cell death [Internet]. Nature. 1996 ;381335-341.Available from: http://www.nature.com/nature/journal/v381/n6580/abs/381335a0.html

156. SUZUKI M, YOULE R, TJANDRA N. Structure of BaxCoregulation of Dimer Formation and Intracellular Localization [Internet]. Cell. 2000 ;103(4):645-654.Available from: http://dx.doi.org/10.1016/S0092-8674(00)00167-7

157. Goping I, Gross A, Lavoie J, Nguyen M, Jemmerson R, Roth K, et al. Regulated targeting of BAX to mitochondria [Internet]. Journal of Cell Biology. 1998 ;143(1):207.Available from: http://jcb.rupress.org/cgi/content/abstract/143/1/207

158. Dewson G, Kratina T, Sim HW, Puthalakath H, Adams JM, Colman PM, et al. To trigger apoptosis, Bak exposes its BH3 domain and homodimerizes via BH3:groove interactions. [Internet]. Molecular cell. 2008 ;30(3):369-80.Available from: http://www.ncbi.nlm.nih.gov/pubmed/18471982

159. George NM, Evans JJ, Luo X. A three-helix homo-oligomerization domain containing BH3 and BH1 is responsible for the apoptotic activity of Bax. [Internet]. Genes & development. 2007 ;21(15):1937-48.Available from: http://www.ncbi.nlm.nih.gov/pubmed/17671092

160. Parikh N, Koshy C, Dhayabaran V, Perumalsamy LR, Sowdhamini R, Sarin A. The N-terminus and alpha-5, alpha-6 helices of the pro-apoptotic protein Bax, modulate functional interactions with the anti-apoptotic protein Bcl-xL. [Internet]. BMC cell biology. 2007 ;816.Available from: http://www.ncbi.nlm.nih.gov/pubmed/17519046

161. Yu M, Liu F, Newland AC, Jia L. The alpha-5 helix of Bax is sensitive to ubiquitin-dependent degradation. [Internet]. Biochemical and biophysical research communications. 2008 ;371(1):10-5.Available from: http://www.ncbi.nlm.nih.gov/pubmed/18395515

162. Kalka C, Masuda H, Takahashi T, Kalka-Moll WM, Silver M, Kearney M, et al. Transplantation of ex vivo expanded endothelial progenitor cells for therapeutic neovascularization. [Internet]. Proceedings of the National Academy of Sciences of the United States of America. 2000 ;97(7):3422-7.Available from: http://www.ncbi.nlm.nih.gov/pubmed/10725398

163. De Palma M, Naldini L. Tie2-expressing monocytes (TEMs): novel targets and vehicles of anticancer therapy? [Internet]. Biochimica et biophysica acta. 2009 ;1796(1):5-10.Available from: http://www.ncbi.nlm.nih.gov/pubmed/19362584

164. Murdoch C, Muthana M, Coffelt SB, Lewis CE. The role of myeloid cells in the promotion of tumour angioenesis. Nature Reviews Cancer. 2008 ;8618-631.

165. Shojaei F, Wu X, Malik AK, Zhong C, Baldwin ME, Schanz S, et al. Tumor refractoriness to anti-VEGF treatment is mediated by CD11b+Gr1+ myeloid cells. Nat. Biotechnol. 2007 ;25911-920.

166. Lambiase PD, Edwards RJ, Anthopoulos P, Rahman S, Meng YG, Bucknall Ca, et al. Circulating humoral factors and endothelial progenitor cells in patients with differing coronary collateral support. [Internet]. Circulation. 2004 ;109(24):2986-92.Available from: http://www.ncbi.nlm.nih.gov/pubmed/15184289

167. Engelhardt M, Lübbert M, Guo Y. CD34(+) or CD34(-): which is the more primitive? [Internet]. Leukemia : official journal of the Leukemia Society of America, Leukemia Research Fund, U.K. 2002 ;16(9):1603-8.Available from: http://www.ncbi.nlm.nih.gov/pubmed/12200670

168. Guo Y, Lubbert M, Engelhardt M. CD34- Hematopoietic Stem Cells: Current Concepts and Controversies. Stem Cells. 2003 ;(21):15-20.

169. Krutzik PO, Nolan GP. Intracellular phospho-protein staining techniques for flow cytometry: monitoring single cell signaling events. [Internet]. Cytometry. Part A : the journal of the International Society for Analytical Cytology. 2003 ;55(2):61-70.Available from: http://www.ncbi.nlm.nih.gov/pubmed/14505311

170. Gory S, Vernet M, Laurent M, Dejana E, Dalmon J, Huber P. The vascular endothelial-cadherin promoter directs endothelial-specific expression in transgenic mice. [Internet]. Blood. 1999 ;93(1):184-92.Available from: http://www.ncbi.nlm.nih.gov/pubmed/9864160

171. Lang R, Rutschman RL, Greaves DR, Murray PJ. Autocrine deactivation of macrophages in transgenic mice constitutively overexpressing IL-10 under control of the human CD68 promoter. [Internet]. Journal of immunology (Baltimore, Md. : 1950). 2002 ;168(7):3402-11.Available from: http://www.jimmunol.org/cgi/content/abstract/168/7/3402

172. Koshikawa N, Takenaga K, Tagawa M, Sakiyama S. Therapeutic efficacy of the suicide gene driven by the promoter of vascular endothelial growth factor gene against hypoxic tumor cells. [Internet]. Cancer research. 2000 ;60(11):2936-41.Available from: http://cancerres.aacrjournals.org/cgi/content/abstract/60/11/2936

173. TEICHERT A, KARANTZOULISFEGARAS F, WANG Y, MAWJI I, BEI X, GNANAPANDITHEN K, et al. Characterization of the murine endothelial nitric oxide synthase promoter [Internet]. Biochimica et Biophysica Acta (BBA) - Gene Structure and Expression. 1998 ;1443(3):352-357.Available from: http://dx.doi.org/10.1016/S0167-4781(98)00236-X

174. Shaul PW. REGULATION OF ENDOTHELIAL NITRIC OXIDE SYNTHASE: Location, Location, Location [Internet]. Annual Review of Physiology. 2002 ;64(1):749-774.Available from: http://www.ncbi.nlm.nih.gov/pubmed/11826287

175. Huang P, McKee TD, Jain RK, Fukumura D. Green fluorescent protein (GFP)-expressing tumor model derived from a spontaneous osteosarcoma in a vascular endothelial growth factor (VEGF)-GFP transgenic mouse. [Internet]. Comparative medicine. 2005 ;55(3):236-43.Available from: http://www.ncbi.nlm.nih.gov/pubmed/16089171

176. Fukumura D, Xavier R, Sugiura T, Chen Y, Park EC, Lu N, et al. Tumor induction of VEGF promoter activity in stromal cells. [Internet]. Cell. 1998 ;94(6):715-25.Available from: http://www.ncbi.nlm.nih.gov/pubmed/9753319

177. Teichert A, Scott Ja, Robb GB, Zhou Y, Zhu S, Lem M, et al. Endothelial nitric oxide synthase gene expression during murine embryogenesis: commencement of expression in the embryo occurs with the establishment of a unidirectional circulatory system. [Internet]. Circulation research. 2008 ;103(1):24-33.Available from: http://www.ncbi.nlm.nih.gov/pubmed/18556578

178. Teichert aM, Miller TL, Tai SC, Wang Y, Bei X, Robb GB, et al. In vivo expression profile of an endothelial nitric oxide synthase promoter-reporter transgene. [Internet]. American journal of physiology. Heart and circulatory physiology. 2000 ;278(4):H1352-61.Available from: http://www.ncbi.nlm.nih.gov/pubmed/10749733

179. Alva JA, Zovein AC, Monvoisin A, Murphy T, Salazar A, Harvey NL, et al. VE-Cadherin-Cre-Recombinase Transgenic Mouse: A Tool for Lineage Analysis and Gene Deletion in Endothelial Cells. Molecular Biology. 2006 ;(January):759 -767.

180. Monvoisin A, Alva Ja, Hofmann JJ, Zovein AC, Lane TF, Iruela-Arispe ML. VE-cadherin-CreERT2 transgenic mouse: a model for inducible recombination in the endothelium. [Internet]. Developmental dynamics : an official publication of the American Association of Anatomists. 2006 ;235(12):3413-22.Available from: http://www.ncbi.nlm.nih.gov/pubmed/17072878

181. Loomans CJ, Wan H, de Crom R, van Haperen R, de Boer HC, Leenen PJ, et al. Angiogenic murine endothelial progenitor cells are derived from a myeloid bone marrow fraction and can be identified by endothelial NO synthase expression. [Internet]. Arteriosclerosis, thrombosis, and vascular biology. 2006 ;26(8):1760-7.Available from: http://www.ncbi.nlm.nih.gov/pubmed/16728651

182. Murohara T, Asahara T, Silver M, Bauters C, Masuda H, Kalka C, et al. Nitric oxide synthase modulates angiogenesis in response to tissue ischemia. [Internet]. The Journal of clinical investigation. 1998 ;101(11):2567-78.Available from: http://www.ncbi.nlm.nih.gov/pubmed/9616228

183. Aicher A, Heeschen C, Mildner-Rihm C, Urbich C, Ihling C, Technau-Ihling K, et al. Essential role of endothelial nitric oxide synthase for mobilization of stem and progenitor cells [Internet]. Nature medicine. 2003 ;9(11):1370–1376.Available from: http://www.nature.com/nm/journal/v9/n11/abs/nm948.html

184. Minamikawa T, Sriratana A, Williams DA, Bowser DN, Hill JS, Nagley P. Chloromethyl-X-rosamine (MitoTracker Red) photosensitises mitochondria and induces apoptosis in intact human cells. Journal of Cell Science. 1999 ;24302419-2430.

185. Kishimoto J, Ehama R, Ge Y, Kobayashi T, Nishiyama T, Detmar M, et al. In vivo detection of human vascular endothelial growth factor promoter activity in transgenic mouse skin. [Internet]. The American journal of pathology. 2000 ;157(1):103-10.Available from: http://www.ncbi.nlm.nih.gov/pubmed/10880381

186. Guillot PV, Liu L, Kuivenhoven Ja, Guan J, Rosenberg RD, Aird WC. Targeting of human eNOS promoter to the Hprt locus of mice leads to tissue-restricted transgene expression. [Internet]. Physiological genomics. 2000 ;2(2):77-83.Available from: http://www.ncbi.nlm.nih.gov/pubmed/11015585

187. Curiel TJ. Regulatory T-cell development: is Foxp3 the decider? [Internet]. Nature medicine. 2007 ;13(3):250-3.Available from: http://dx.doi.org/10.1038/nm0307-250

188. Lin W, Haribhai D, Relland LM, Truong N, Carlson MR, Williams CB, et al. Regulatory T cell development in the absence of functional Foxp3. [Internet]. Nature immunology. 2007 ;8(4):359-68.Available from: http://dx.doi.org/10.1038/ni1445

189. Hotta A, Ellis J. Cellular Biochemistry. Discovery. 2008 ;948(August):940-948.

190. Lee C. Morphological Analysis and Lentiviral Transduction of Fetal Monkey Bone Marrow-Derived Mesenchymal Stem Cells [Internet]. Molecular Therapy. 2004 ;9(1):112-123.Available from: http://dx.doi.org/10.1016/j.ymthe.2003.09.019

191. Mao X, Fujiwara Y, Chapdelaine A, Yang H, Orkin S. Activation of EGFP expression by Cre-mediated excision in a new ROSA26 reporter mouse strain [Internet]. Blood. 2001 ;97(1):324.Available from: http://bloodjournal.hematologylibrary.org/cgi/content/abstract/97/1/324

192. Sternberg N, Sauer B, Hoess R, Abremski K. Bacteriophage P1 cre gene and its regulatory region. Evidence for multiple promoters and for regulation by DNA methylation. [Internet]. Journal of molecular biology. 1986 ;187(2):197-212.Available from: http://www.ncbi.nlm.nih.gov/pubmed/3486297

193. Robbins PD, Ghivizzani SC. Viral vectors for gene therapy. [Internet]. Pharmacology & therapeutics. 1998 ;80(1):35-47.Available from: http://www.ncbi.nlm.nih.gov/pubmed/9804053

194. Koller R, Krall M, Mock B, Bies J, Nazarov V, Wolff L. Mml1, a new common integration site in murine leukemia virus-induced promonocytic leukemias maps to mouse chromosome 10. [Internet]. Virology. 1996 ;224(1):224-34.Available from: http://dx.doi.org/10.1006/viro.1996.0524

195. Mukhopadhyaya R, Wolff L. New sites of proviral integration associated with murine promonocytic leukemias and evidence for alternate modes of c-myb activation. [Internet]. Journal of virology. 1992 ;66(10):6035-44.Available from: http://www.ncbi.nlm.nih.gov/pubmed/1527851

196. Zovein AC, Hofmann JJ, Lynch M, French WJ, Turlo KA, Yang Y, et al. Fate tracing reveals the endothelial origin of hematopoietic stem cells. [Internet]. Cell stem cell. 2008 ;3(6):625-36.Available from: http://www.ncbi.nlm.nih.gov/pubmed/19041779

197. Abrahamsen B, Zhao J, Asante CO, Cendan CM, Marsh S, Martinez-Barbera JP, et al. The cell and molecular basis of mechanical, cold, and inflammatory pain. [Internet]. Science (New York, N.Y.). 2008 ;321(5889):702-5.Available from: http://www.ncbi.nlm.nih.gov/pubmed/18669863

198. Duvall CL, Taylor WR, Weiss D, Guldberg RE. Quantitative microcomputed tomography analysis of collateral vessel development after ischemic injury. [Internet]. American journal of physiology. Heart and circulatory physiology. 2004 ;287(1):H302-10.Available from: http://www.ncbi.nlm.nih.gov/pubmed/15016633

199. Kernick DP, Shore AC. Characteristics of laser Doppler perfusion imaging in vitro and in vivo. [Internet]. Physiological measurement. 2000 ;21(2):333-40.Available from: http://www.ncbi.nlm.nih.gov/pubmed/10847199